Ontogenetic niche shifts in megaherbivorous dinosaurs of Late Cretaceous North America and their ecological implications

by

Taia Wyenberg-Henzler

A thesis submitted to the Faculty of Graduate and Postdoctoral Affairs in partial fulfillment of the requirements for the degree of

Master of Science

in

Earth Sciences

Carleton University
Ottawa, Ontario

Abstract

Despite megaherbivore ontogeny being relatively well-studied, little research has been conducted on the ecological implications of growth stages. Using ecomorphological dietary correlates, investigations into potential ecological differences between mature and immature ceratopsids and hadrosaurids were undertaken. The results suggest that juvenile megaherbivores selectively consumed softer, lower-growing vegetation than their adult counterparts, which likely reduced intra-specific competition. Ecomorphological investigations into the potential for competition between juvenile megaherbivores and small ornithischians, and investigations into relative abundances, were conducted to test the competition and taphonomic hypotheses. An overlap in results indicated a potential for competition between juvenile megaherbivores and leptoceratopsids, and as predicted by the competition hypothesis small ornithischians were generally less abundant than megaherbivores. Other groups showed separation in the ecomorphospace and some distributions showed similar abundances between groups as predicted by the taphonomic hypothesis. Thus, size differences were important for resource partitioning, and competition and taphonomy both influenced observed Late Cretaceous size distributions.

Acknowledgements

I would like to than Dr. Jordan Mallon and Dr. Tim Patterson for their supervision and guidance throughout this project, and Dr. Gabriel Blouin-Demers, Dr. Michael Ryan and Dr. Andrew Simons for their feedback. I would also like to thank Dr. Danielle Fraser and Dr. Nicolas Campione for their help and suggestions with R. Thanks to staff and students of Carleton University, especially my colleagues in the Carleton University Palaeontology program, for their support and encouragement. I would like to acknowledge NSERC, the Dinosaur Research Institute and Jurassic Foundation as funding sources that made the travel necessary for the completion of this project possible.

My thanks also goes to the curators and assistants at the American Museum of Natural History, Museum of the Rockies, Royal Ontario Museum, Royal Tyrrell Museum of Palaeontology, Smithsonian National Museum of Natural History and University of Alberta Laboratory for Vertebrate Palaeontology for providing access to their collections. I thank Dr. Corwin Sullivan, Dr. David Evans, Amanda Millhouse and David Trexler for providing and/or facilitating access to restricted-access specimens. Thanks to Andrew Knapp for providing CT data on AMNH 5401 and AMNH 5402, Dr. Michael Ryan for photos of the MNHCM *Prenoceratops* from which measurements were taken, and staff at the Canadian Museum of Nature, Dr. Michael Ryan and Dr. Frank Varriale for providing help and suggestions on methods to remove bubbles from epoxy casts. Special thanks goes to my family who helped and supported me throughout this entire process.

Institutional Abbreviations

ACM, Beneski Museum of Natural History, Amherst College, Amherst; AMNH, American Museum of Natural History, New York, New York; ANSP, Academy of Natural Sciences of Philadelphia, Philadelphia, Pennsylvania; BHI, Black Hills Institute, Hill City, South Dakota; BMNH, British Museum of Natural History, London, U.K.; CMN, Canadian Museum of Nature, Ottawa, Ontario; CM, Carnegie Museum of Natural History, Pittsburgh, Pennsylvania; CCM, Carter County Museum, Ekalaka, Montana; DMNH, Denver Museum of Nature and Science, Denver, Colorado; FMNH, Field Museum of Natural History, Chicago, Illinois; GPDM, Great Plains Dinosaur Museum, Malta, Montana; IMNH, Idaho Museum of Natural History, Pocatello, Idaho; LACM, Natural History Museum of Los Angeles County, Los Angeles, California; MNHCM, Mokpo Natural History and Culture Museum, Mokpo, Korea; MCSNM, Museo Civico di Storia Naturale di Milano, Milan, Italy; MOR, Museum of the Rockies, Bozeman, Montana; NCSM, North Carolina Museum of Natural Sciences, Raleigh, North Carolina; NHMUK and NHM Natural History Museum, London, U.K; NMMNH, New Mexico Museum of Natural History, Albuquerque, New Mexico; NSM PV and NMST, National Museum of Nature and Science, Tokyo, Japan; OTM, Old Trail Museum, Choteau, Montana; RAM, Raymond M. Alf Museum of Paleontology, Claremont, California; ROM, Royal Ontario Museum, Toronto, Ontario; RSM, Royal Saskatchewan Museum, Regina, Saskatchewan; SM – Senckenberg Museum, Frankfurt, Germany; TMM, Texas Memorial Museum, Austin, Texas; TMP, Royal Tyrrell Museum of Palaeontology, Drumheller, Alberta; TLAM, Timber Lake and Area Museum, Timber Lake, South Dakota; TCMI, The Children's Museum of Indianapolis, Indianapolis, Indiana; UALVP,

University of Alberta, Edmonton, Alberta; UC, University of Calgary, Calgary, Alberta; UCMP, University of California Museum of Paleontology, Berkeley, California; UMMP, University of Michigan Museum of Paleontology, Ann Arbor, Michigan; USNM, Smithsonian Institution, National Museum of Natural History, Washington, D.C.; UTEP, University of Texas, El Paso, Texas; YPM, Peabody Museum of Natural History, Yale University, New Haven, Connecticut; YPM PU, Peabody Museum of Natural History, Yale University, New Haven, Connecticut, Princeton University Collection.

Table of Contents

List of Tables

List of Illustrations

List of Appendices

Chapter 1: Introduction

1.1 Background

During the Late Cretaceous (100-66 Ma), the Western Interior Seaway ran through North America, extending from the Gulf of Mexico to the Arctic Ocean (Lucas et al., 2016). The coastal plains that dominated western North America at this time were broken up by rivers flowing eastwards towards the western shoreline of the seaway. These rivers were sourced from the west, which was an area of active mountain building. At this time, the North American climate was subtropical, and included primitive flowering plants, ferns, czekanowskialeans, bennettitaleans, conifers, and cycads (Coe et al., 1987). Of these plant varieties, ferns are thought to have been the most abundant and were responsible for the extensive fern savannas and prairies of the time. Coastal shrublands and interior forests were also key components of the landscape (Lucas et al., 2016).

These environments were home to a variety of megaherbivorous (≥1000 kg) dinosaurs, including armoured ankylosaurids, duck-billed hadrosaurids, and horned ceratopsids (Brown et al., 2012; Codron et al., 2012; Mallon et al., 2012; Brown et al., 2013a,b; Lucas et al., 2016; Strickson et al., 2016). Smaller-bodied dinosaurs, such as leptoceratopsids, thescelosaurids and the dome-headed pachycephalosaurids, also inhabited Late Cretaceous North America. The ecology of larger herbivorous dinosaurs has long been a subject of in-depth research (O'Gorman and Hone, 2012; Codron et al., 2012, 2013; Mallon et al., 2012, 2013; Brown et al.,2013a,b; Mallon and Anderson, 2014a,b, 2015), and forms the basis of my thesis.

1.2 Taxonomy

Hadrosauridae was a clade of abundant and diverse ornithischians commonly referred to as duck-billed dinosaurs (Figure 1.1). At adult size, these animals were 7-12 m in length and weighed over 3000 kg (Horner et al., 2004). The "bills" of these dinosaurs were edentulous and likely used to crop vegetation, which was then sliced and crushed by numerous teeth arranged in complex dental batteries. These animals possessed hollow or bony crests on top of their heads that were likely used for inter-species recognition or sexual display (Horner et al., 2004).

Ceratopsidae was another clade of large-bodied (4-8 m long; ~2500 kg) herbivores that existed during the Late Cretaceous of North America and China (Xu et al., 2002; Dodson et al., 2004; Lehman, 2006) (Figure 1.1). Ceratopsids, also known as horned dinosaurs, exhibited a wide variety of elaborate horn and frill morphologies that are theorized to also have been used for sexual display or inter-species recognition (Dodson et al., 2004). Ceratopsids possessed a parrot like beak that was covered in a keratinous sheath. These beaks were likely used to obtain foliage that was then sliced by teeth arranged into tooth batteries that worked in a scissor-like fashion.

Ankylosaurs were a clade of large (~ 1,000 – 5,000 kg), quadrupedal herbivores that existed from the Late Jurassic (~157.3 Ma) to the end of the Cretaceous (66.0 Ma) (Vickaryous et al., 2004; Arbour and Mallon, 2017; Benson et al., 2017) (Figure 1.1). Remains have been recovered from every continent with the possible exception of Africa. These animals are best known for the rows of osteoderms distributed across the dorsal surfaces of their bodies and osseous ornamentations on the head. The ankylosaurs can be divided into two clades: Ankylosauridae and Nodosauridae. Some members of

Ankylosauridae (e.g., *Ankylosaurus*) are famous for their possession of a tail club. To support this tail club, these animals evolved a rigid "handle" formed from the fusion of the distal caudal vertebrae. It has been proposed that this tail club was used in intraspecific combat, as a weapon against predators, or even as a lure mimicking the head (Vickaryous et al., 2004). Ankylosaurs possessed small denticulate teeth that, on the basis of microwear evidence, may have been used to process fruit and leaves (Mallon and Anderson, 2014b).

Leptoceratopsids (e.g., *Leptoceratops, Prenoceratops, Montanoceratops*) were a basal group of small-bodied (190-350 kg) neoceratopsians found in Asia and North America during the Cretaceous (Chinnery and Horner, 2007; Farke et al., 2014; Benson et al., 2017) (Figure 1.1). Like the better-known ceratopsids (e.g., *Triceratops*), leptoceratopsids possessed an edentulous beak and frill at the back of the skull (You and Dodson, 2004). This frill, however, was less ornamented compared to those of ceratopsids. Leptoceratopsids possessed leaf-shaped teeth arranged in loose tooth batteries with only one replacement tooth in each tooth position (Dodson et al., 2004; You and Dodson, 2004). Leptoceratopsids were facultatively bipedal (Senter, 2007).

Thescelosaurids (e.g., *Thescelosaurus, Parksosaurus*) existed during the Cretaceous, with remains recovered from North America, South America, Asia, Australia, Europe and Antarctica (Norman et al., 2004; Boyd et al., 2009) (Figure 1.1). Members of this clade possessed simple skulls that were small compared to the body. Unlike ceratopsids and hadrosaurids, teeth were present along the entire length of the jaw. Thescelosaurids were small (>4 m; 13-356 kg), bipedal herbivores that inhabited a

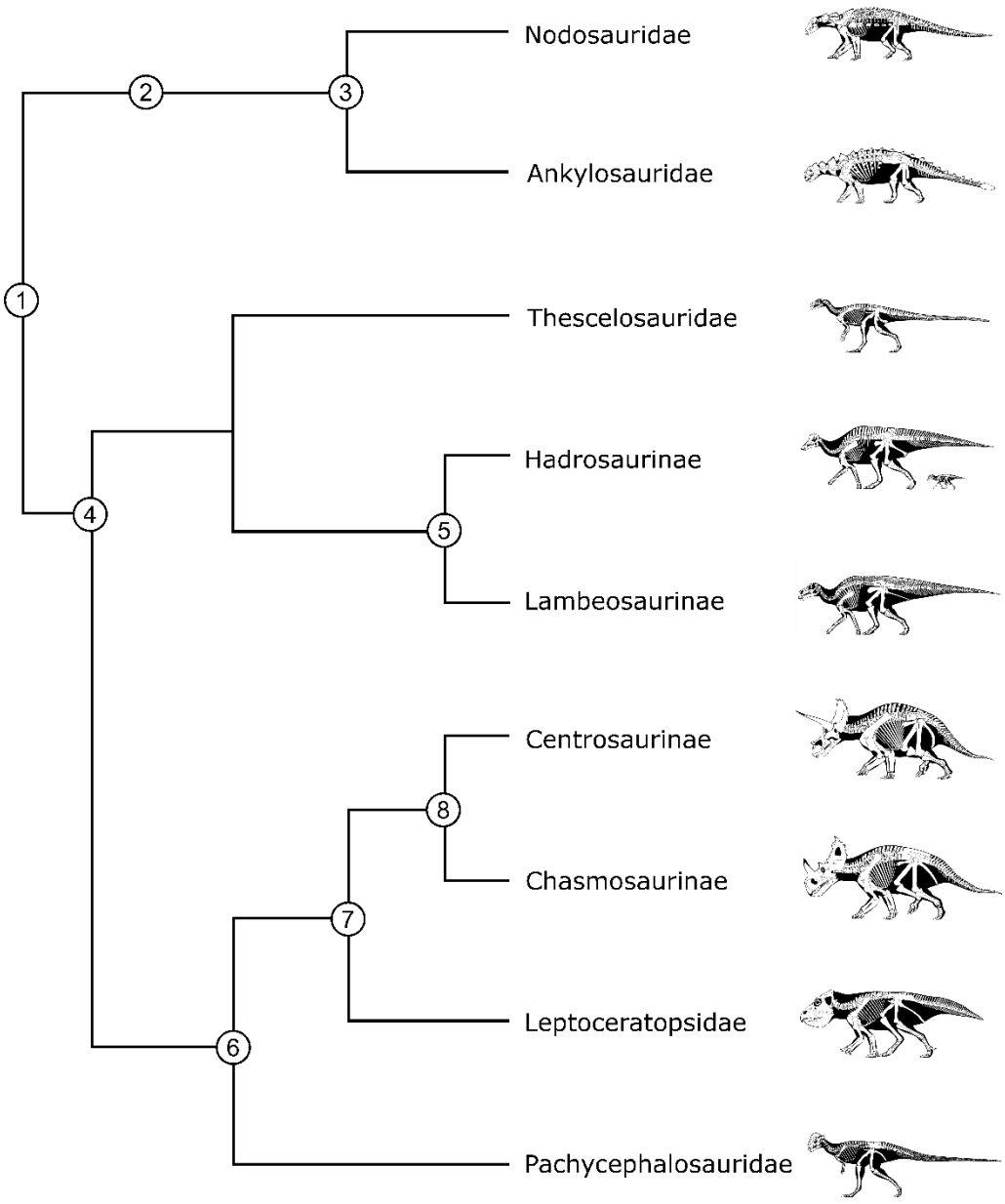

Figure 1.1: Phylogenetic relationships of herbivorous ornithischian dinosaurs from the Late Cretaceous of North America. Taxonomy: 1, Ornithischia; 2, Thyreophora; 3, Ankylosauria; 4, Ornithischia; 5, Hadrosauridae; 6, Marginocephalia; 7, Ceratopsia; 8, Ceratopsidae. After Butler et al., 2008, Dodson et al., 2004; Horner et al., 2004; Maryanska et al., 2004; Norman et al., 2004; Vickaryous et al., 2004; You and Dodson, 2004. Skeletal drawings (not to scale) by S. Hartman (used with permission).

wide variety of environments and climates (Norman et al., 2004; Brown et al., 2013b; Boyd, 2014; Campione et al., 2014).

Pachycephalosaurids (e.g., *Pachycephalosaurus, Stegoceras*) were small (16-370 kg) bipedal, dome-headed dinosaurs that were mainly restricted to the Late Cretaceous of North America and Asia (Maryanska et al., 2004; Brown et al., 2013b; Bensen et al., 2017) (Figure 1.1). The dome was formed by a well-ossified, thickened frontoparietal region of the skull (Galton and Sues, 1982; Maryanska et al., 2004). Similar to thescelosaurids, the entire length of the jaws were dentulous (Maryanska et al., 2004). Unlike many other ornithischians, this group exhibited heterodonty, with more peg-like teeth in the front of the mouth and more leaf-like teeth in the maxilla and dentary. Pachycephalosaurids are often reconstructed as low browsers (Maryanska et al., 2004).

Theropods like ornithomimids and caenagnathids (5-3000 kg) are not considered in this work as they were comparatively rare components of the Late Cretaceous ecosystem, and may have been omnivorous (Kobayashi et al., 1999; Barrett, 2005; Zanno and Makovicky, 2013; Bell et al., 2014; Lamanna et al., 2014).

1.3 Coexistence

Two hypotheses have been proposed to explain the coexistence of such a diverse Late Cretaceous herbivore fauna: 1) plant resources were not limiting because of factors such as lowered metabolic rates for herbivorous dinosaurs, elevated primary productivity, predation pressures and/or disease (Ostrom, 1964; Farlow et al., 1995; Lehman, 1997; Sampson, 2009), or, 2) plant resources were limiting and coexistence was achieved via dietary niche partitioning (Coe et al., 1987; Lehman, 2001; Sander et al., 2010 Mallon et

al., 2013; Mallon, 2019). Recent research into megaherbivorous dinosaurs of the middle to upper Campanian Dinosaur Park Formation suggests that plant resources may have been limiting based on evidence for dietary niche partitioning (Mallon and Anderson, 2013; Mallon et al., 2013; Mallon and Anderson, 2014a,b; Mallon and Anderson, 2015). However, multiple questions regarding Cretaceous dinosaur palaeoecology remain unanswered. For instance, did the ecological niches of megaherbivores change through ontogeny, and if so, how? Did young megaherbivores compete with small ornithischians? Codron et al. (2012, 2013) used population models to suggest that small ornithischian richness was limited as a result of competition with the young of larger herbivores. However, ecomorphology-based investigations into the competition hypothesis are lacking, and form the primary line of investigation for this thesis.

1.4 Ontogenetic Niche Shifts

Body size disparity has been cited as one of the primary mechanisms by which organisms avoid resource competition (Werner and Gilliam, 1984; ten Brink and de Roos, 2018). Differences in body size within a species can also vary enough to result in intraspecific niche partitioning. As a result, organisms undergo an ontogenetic niche shift (ONS) wherein different developmental stages occupy different ecological niches, requiring different foods, habitats, and/or being active at different times of day.

Ontogenetic niche shifts can increase a species' growth rate by reducing intraspecific competition (Werner and Gilliam, 1984; ten Brink and de Roos, 2018) (Figure 1.2). Decreased intraspecific competition means that more resources are potentially available to be exploited and available for growth, which results in higher

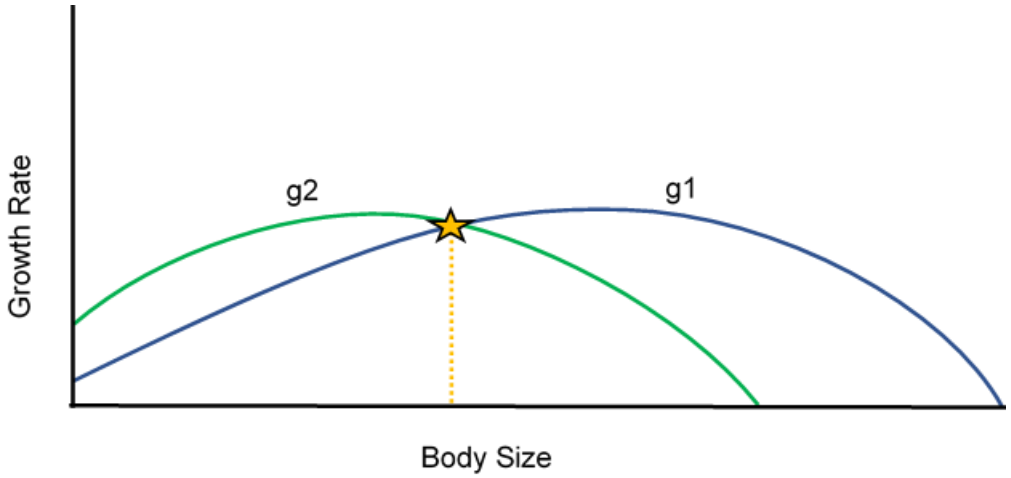

Figure 1.2: Absolute growth rates as a function of body size for a hypothetical species undergoing an ontogenetic habitat shift (this could presumably represent other resources (e.g., food), too). The blue curve (g1) is the growth rate in habitat 1 and the green curve (g2) is the growth rate for the same hypothetical species in habitat 2. The star marks the intersection between the two growth curves at which the habitat switch maximizes growth rate (modified from Werner and Gilliam, 1984).

growth rates. This, in turn, means that less time is spent at smaller, more vulnerable sizes, which can result in decreased predator-related mortality. Therefore, because organisms can impact resources differently during ontogeny (both in the type and amount of resource being consumed), it is important to consider ONSs when studying ecological interactions (Schellekens et al., 2010; Werner and Gilliam, 1984).

Ontogenetic niche shifts can be continuous or discrete (Werner and Gilliam, 1984). Continuous ONSs manifest in species that do not show distinct ecological stages and undergo constant changes in habitat and/or diet with growth. Discrete ONSs, on the other hand, involve a sudden change in habitat and/or diet as one developmental stage transitions to the next. This type of ONS is less common, and typically occurs in species that undergo metamorphosis, where the juvenile morphology is significantly different from that of the adult (Werner and Gilliam, 1984; Ebenman, 1992; Claessen and Diekmann, 2002).

1.4.1 Ontogenetic Niche Shifts in Extant Taxa

Ontogenetic niche shifts are reported in various extant taxa and can manifest in different ways. Continuous dietary ONSs occur in species that gradually incorporate larger prey items into their diet during maturation. Crocodilians generally experience a continuous dietary ONS in which there is a gradual increase in the consumption of fishes with maturity, until these comprise most of the diet. In this example, niche shifts occur in relation to what can be caught and overpowered. Thus, the changes that occur are mainly related to size, not morphology (Dodson, 1975a; Platt et al., 2006) (Figure 1.3). White sea catfish (*Genidens barbus*) and dwarf squeaker frogs (*Schoutedenella xenodactyloides*)

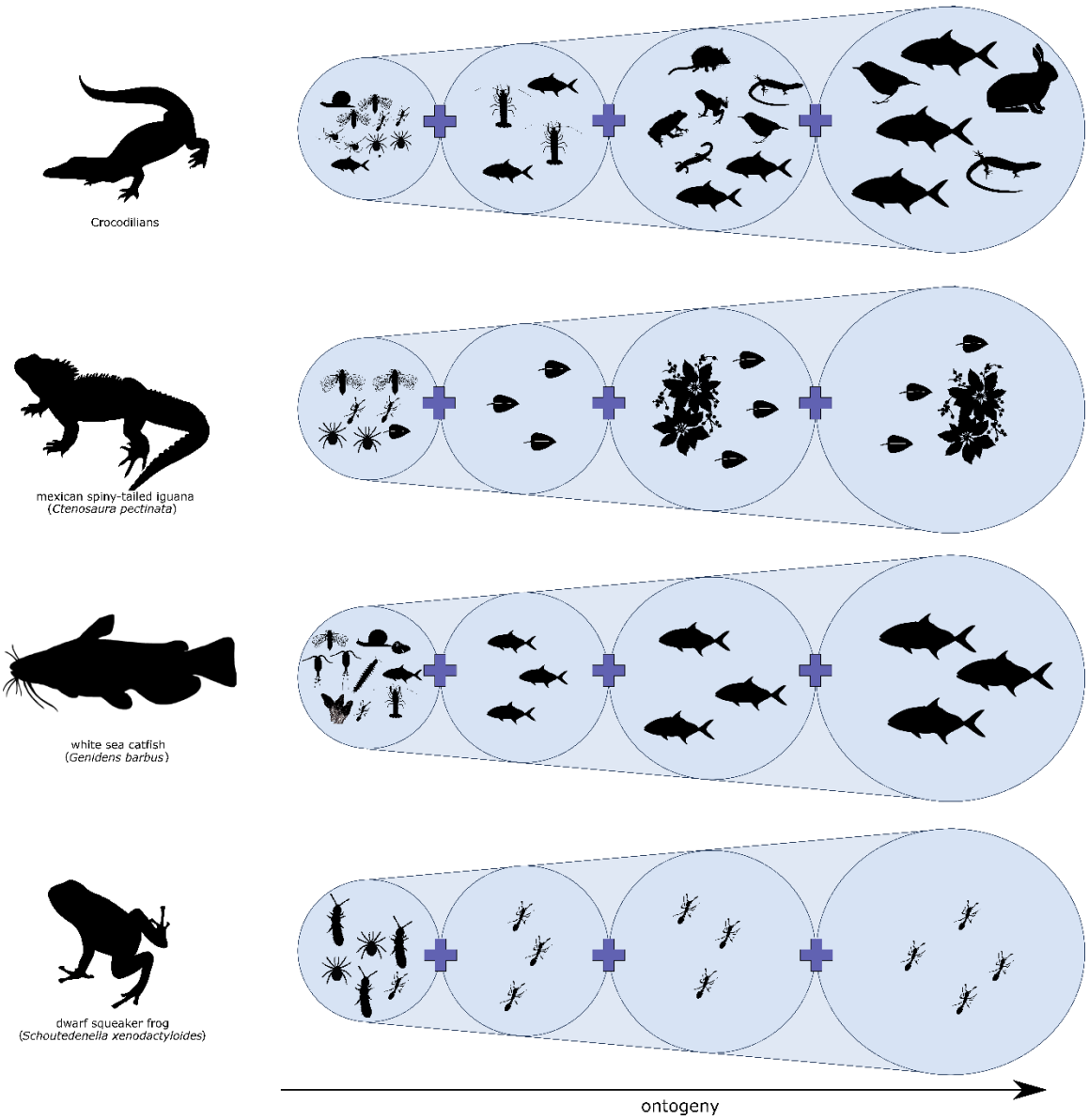

Figure 1.3: Continuous dietary ontogenetic niche shifts in select taxa (created based on information from Blackburn and Moreau, 2006; Durtsche, 2000; Dodson, 1974; Mendoza-Carranza and Paes Vieira, 2009; Platt et al., 2006). Silhouettes by B. Kimmel, F. Sayol, J. Wolfe, K. S. Jaron, K. S. Collins, L. Hughes, M. Ghazal, O. Griffith, R. Bishop-Taylor, S. Hartman, S. McCann, S. Traver, T.M. Keesey, and zoosnow (taken from phylopic.org).

experience a similar size-related niche shift (Mendoza-Carranza and Paes Vieira, 2009; Blackburn and Moreau, 2006) (Figure 1.3). Juvenile white sea catfish consume copepods and gradually shift to consume fishes as adults. Dwarf squeaker frogs consume collembolans and mites as juveniles, and then gradually incorporate a higher percentage of ants into their diet with maturation.

Ontogenetic niche shifts also occur in some lizards, such as the Mexican spiny-tailed iguana (*Ctenosaura pectinata*), which experience a more drastic change in diet during ontogeny (Durtsche, 2000) (Figure 1.3). Immature individuals primarily consume insects and some plant material, whereas adults primarily consume plants alone, especially legume flowers and leaves. Although juveniles are capable of consuming plants, insects may be preferentially consumed to avoid depletion in nitrogen which can cause slowed growth rates and reduce rates of protein synthesis.

Some dietary niche shifts are less permanent. For example, adult African elephant (*Loxodonta africana*) females tend to feed in lower portions of the canopy when juveniles are absent, and transition higher up in the canopy when juveniles are present (Woolley et al., 2011). Young elephants also tend to feed on more nutritious, less abundant plant parts, such as fruits, while adults tend to consume more abundant, less nutritious vegetation because these fruits are unavailable in quantities capable of sustaining them.

Dietary niche shifts are often associated with habitat changes (Werner and Gilliam, 1984). Eastern cottonmouth (*Agkistrodon piscivorous*) juveniles primarily consume salamanders, and occupy muddy, sparsely vegetated habitats, whereas adults exploit many different microhabitats and consume a greater variety of prey (Eskew et al., 2008). A change in coloration is also associated with this habitat shift, where juveniles

possess a yellow tail (used to lure prey) that is lost in free-ranging adults. During their first decade of life, loggerhead sea turtles (*Caretta caretta*) inhabit floating *Sargassum* matts, which they also feed upon, in addition to epipelagic prey items. They then transition to a neritic habitat and consume benthic prey. This shift is thought to relate to predation risk, which decreases with increasing body size. Alternatively, the patchy and narrow distribution of the algal mats, upon which loggerhead turtles feed and live during their first decade of life, may be unable to sustain larger turtles. Thus, the transition from one habitat to another may be required to optimize foraging strategy (Ramirez et al., 2017). Common chameleon (*Chamaeleo chamaeleon*) adults generally occupy trees and large bushes higher in the canopy, than juveniles which inhabit lower levels. This habitat shift decreases the occurrence of intraspecific aggression and cannibalism by reducing the amount of interaction between juveniles and adults (Karen-Rotem et al., 2006).

Increased risk of predation (including cannibalism) can also cause diel (nocturnal vs. diurnal) ontogenetic shifts. For example, young slimy sculpin (*Cottus cognatus*) restrict feeding to shallower depths at night to avoid diurnal predators until reaching maturity when they shift to a more continuous feeding style at greater depths (Brandt, 1986). Similarly, creek chub (*Semotilus atromaculatus*) juveniles exhibit opposing activity periods to the adults in order to avoid predation (Magnan and FitzGerald, 1984). However, unlike slimy sculpin, creek chub adults are nocturnal, and the juveniles are diurnal in order to avoid predation by brook charr (*Salvelinus fontinalis*), which are most active at dawn and dusk. Among cane toads (*Bufo marinus*), juveniles are diurnal to avoid being consumed by larger individuals, which are most active at night (Pizzatto et al., 2008).

1.4.2 Ontogenetic Niche Shifts in Dinosaurs

Unlike in modern taxa, behavioural observations cannot be used to identify t ONSs in dinosaurs. In such instances, the extant phylogenetic bracket approach is commonly recommended (Witmer, 1995), whereby some structure or behaviour is inferred in a fossil taxon based on its homologous presence in extant relatives (crocodilians and birds, in the case of dinosaurs). However, as it relates to the inference of ONSs, this approach is not readily applicable to dinosaurs because, with a few notable exceptions (Nakazawa and Yamamura, 2007; McLeay et al., 2009), ONSs are not commonly observed in birds; rather, birds mature quickly after leaving the nest and many consume the same food as their parents. This makes the presence of an ONS ambiguous in dinosaurs.

An alternative is to study ONSs in dinosaurs using an ecomorphological approach, which has been applied successfully in several studies. Ontogenetic niche shifts have been inferred in spinosaurids from the middle Cretaceous Kem Kem beds of Morocco (Lakin and Longrich, 2019). The remains of both juvenile and adult spinosaurids were found in the same semi-aquatic deposits, suggesting that growth stages were not separated geographically. Although juveniles and adults occupied the same habitat, they may have fed on slightly different food sources because of their size disparity. Young spinosaurids may have fed on small fish and other small prey, gradually incorporating larger prey into their diet as they grew (e.g., *Iguanodon*, *Lepidotes*), similar to extant crocodilians (Charig and Milner, 1997; Dodson, 1974). Further evidence of a

potential niche shift is the absence of hatchlings. While this absence of hatchling material may be related to taphonomic biases, it is also possible that hatchlings inhabited different environments than older individuals. Determining which of these two hypotheses is most likely requires further research. If hatchlings did occupy a different environment than more mature individuals, this would further suggest that spinosaurids behaved in a fashion similar to some modern crocodilians (Dodson, 1974; Platt et al., 2006). Ontogenetic niche shifts have also been proposed for the "toothless" (and potentially herbivorous) theropod *Limusaurus inextricabilis* (Wang et al., 2017) (Figure 1.4A). Several juvenile, subadult and adult specimens of *L. inextricabilis* have been recovered from the Upper Jurassic deposits of China. The most striking difference between ontogimorphs (different ontogenetic stages) is in the number of teeth. Young *L. inextricabilis* possessed fully toothed jaws, whereas progressively more mature individuals possessed fewer teeth until reaching the completely toothless "beaks" of adults. In addition, adult *L. inextricabilis* possessed gastroliths that were conspicuously absent in individuals from earlier ontogenetic stages. The progressive loss of teeth and introduction of gastroliths during ontogeny suggests that *L. inextricabilis* gradually shifted from an omnivorous to herbivorous lifestyle as it matured.

Ontogenetic differences in diplodicoids have also been used to suggest that this group underwent ONSs (Woodruff et al., 2018) (Figure 1.4B). When compared with the wide and square snouts of the adults, juveniles exhibited mediolaterally narrower snouts. This narrower snout suggests more selective feeding, possibly in forested environments, while a wider snout is believed to have enabled open ground-level browsing. The distribution of the teeth along the jaw, not only in terms of number but also of shape, also

changed during ontogeny (Figure 1.4B). Both juveniles and adults possessed peg-like teeth in the premaxilla; however, juveniles also possessed spatulate cheek teeth. In herbivorous taxa, spatulate teeth are efficient for coarse vegetation and/or bulk feeding, while non-spatulate teeth are inferred to be more efficient for softer foliage and/or concentrate feeding (Fiorillo, 1998). The presence of both peg-like and spatulate teeth in juveniles suggests that they may have fed on a greater variety of plants, and processed food differently compared to adults.

Erickson and Zelenitsky (2014) studied developmental differences in the dentition of *Hypacrosaurus*—one of the few studies to focus on how non-crest related structures developed in hadrosaurids (Figure 1.4C). They found that the occlusal surfaces of embryos and hatchlings were more horizontal compared to subadults and adults. Additionally, adults possessed dual planar occlusal surfaces, with a slicing edge at 56-60^{o}, and another more horizontal surface at 30^{o}. Embryos and hatchlings exhibited more mesiodistally elongate surfaces, while adults possessed labiolingually elongate surfaces, and subadults were intermediate. The number and topography of the teeth also showed ontogenetic variation (Figure 1.4C). These differences in morphology were inferred to represent dietary differences between different ontogenetic stages.

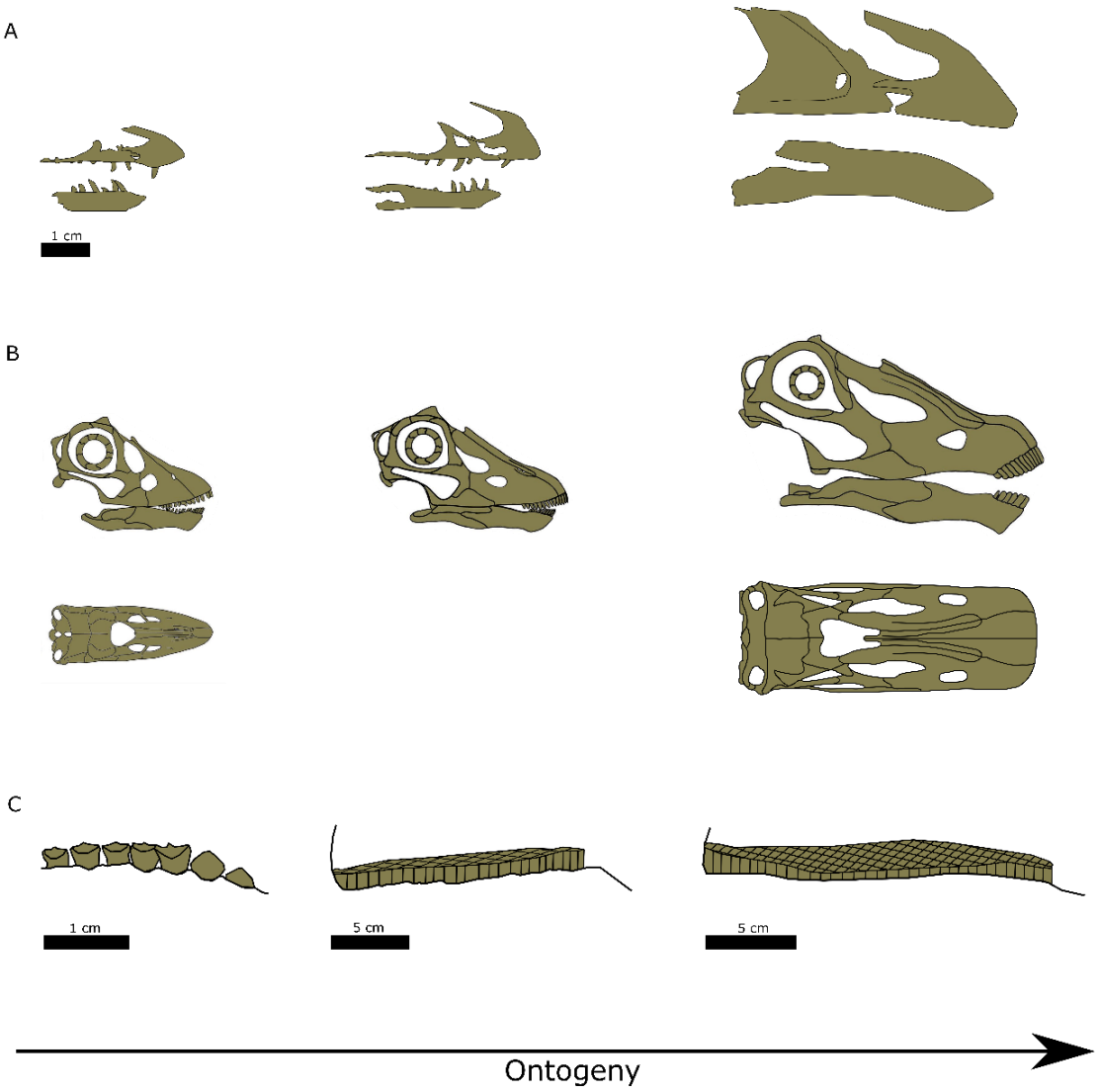

Figure 1.4: Ontogenetic niche shifts in select dinosaur species. A) Premaxilla, maxilla and dentary in the ceratosaur *Limusaurus inextricabilis* showing progressive tooth loss in ontogenetic stages I, II and IV (modified from Wang et al., 2017). B) Progressive tooth loss in *Diplodocus* sp. during ontogeny. Skulls of different ontogenetic stages are to proportionately scaled (modified from Woodruff et al., 2018; dorsal view of adult *Diplodocus* from Whitlock, 2011). C) Dentary teeth of neonate (TMP 1987.079.0241), subadult (CMN 2246) and adult (CMN 8501) *Hypacrosaurus* showing differences in wear surfaces that occur during ontogeny (neonate line drawing modified from Horner and Currie, 2016; information taken from Erickson and Zelenitsky, 2014).

1.5 Structure and Aims of Thesis

The research aims of this thesis are twofold: (1) to investigate what megaherbivorous dinosaur ONSs may have looked like, and (2) to determine how these niche shifts (if any) affected the structure of the contemporaneous herbivore community. The approach is primarily morphometric in nature, and focuses on aspects of skull and skeletal ecomorphology, and dental microwear.

Chapters 2 and 3 address the first aim, and centers on hadrosaurids and ceratopsids, respectively. These clades were chosen because they include reasonably known growth series. Despite numerous investigations into ontogenetic allometry in crest and limb proportions in these animals (Horner, 1983; Goodwin et al., 2006; Lehman, 2006; Evans, 2010; McGarrity et al., 2013; Farke et al., 2014; Frederickson and Tumarkin-Deratzian, 2014; Vanderveen et al., 2014; Konishi, 2015; Woodward et al., 2015; Wosik et al., 2018; Drysdale, 2019), most of this research has not explored the trophic implications of ontogenetic differences.

Chapter 4 will focus on identifying and quantifying ecomorphological overlap between ceratopsids, hadrosaurids and small ornithischians, and comment on how these results may have impacted overall community dynamics. Chapter 5 will provide a summary of the findings of chapter 2 through 4 and the implications these results had for dinosaur ecology. Topics for future research will also be identified and discussed in this chapter.

Chapter 2: Ontogenetic niche shifts in hadrosaurids of Late Cretaceous North America

2.1 Introduction

2.1.1 What is a hadrosaurid?

Hadrosauridae is a diverse family of herbivorous dinosaurs, colloquially known as duck-billed dinosaurs (Brett-Surman, 1997; Lucas et al., 2016). Hadrosaurids appeared in the Late Cretaceous (~80 Ma) and were mainly restricted to Laurasia, with the exception of several species also found in Gondwana.

Hadrosaurids consist of two subclades: Hadrosaurinae and Lambeosaurinae (Horner et al., 2004). Hadrosaurines had solid crests—or lacked bony crests altogether—whereas lambeosaurines possessed complex, hollow crests. These crests are thought to have been used for inter-species recognition, communication, and/or sexual display (Evans, 2010; Farke et al., 2013; McGarritty et al., 2013).

All hadrosaurids possessed multiple tooth rows that could be used for mastication of various types of plant matter (Erickson and Zelenitsky, 2014; Bramble et al., 2017). Their interlocking teeth were arranged in up to four vertical rows forming a complex dental battery, which have no equivalent in modern animals (Erickson and Zelenitsky, 2014; Bramble et al., 2017). These teeth were constantly replaced in a conveyor-belt like fashion. The beaks of these animals were covered in a horny sheath that likely served as a cropping device (Farke et al., 2013).

Similarities between hadrosaurids and modern ungulates have led some to postulate these groups occupied similar niches (Carrano et al., 1999). Both hadrosaurids and ungulates were/are terrestrial herbivores. Based on the distribution of fossil remains,

hadrosaurids are interpreted to have occupied both open and closed habitats similar to modern ungulates (Carrano et al., 1999). The complex dental batteries of hadrosaurids have also been interpreted as being analogous to the cheek teeth of ungulates, which are used to process coarse vegetation. However, unlike ungulates, hadrosaurids grew to much larger body sizes, with some reaching 20 m in length (Brett-Surman, 1997; Codron et al., 2012,2013; Lucas et al., 2016).

2.1.2 Hadrosaurids and ontogenetic niche shifts

In modern organisms, size disparity is a mechanism through which resources are partitioned, both inter- and intra-specifically (Werner and Gilliam, 1984; ten Brink and de Roos, 2018). Ontogenetic niche shifts (ONSs) occur when conspecific individuals of different ages occupy different ecological niches (Werner and Gilliam, 1984); individuals that pass through various sizes during growth often undergo such niche shifts to—potentially reducing competition within a species (Werner and Gilliam, 1984).

Ontogenetic niche shifts manifest throughout Vertebrata. In crocodilians, body size limits the size of prey that can be consumed (Dodson, 1975a; Platt et al., 2006). During ontogeny, isometric growth of the skull relative to body size and positive allometry of the snout, allow progressively larger prey items to be consumed. For approximately the first 10 years of life, loggerhead sea turtles (*Caretta caretta*) inhabit and consume *Sargassum* sea matts until they attain a certain size, at which point, they become free-roaming and consume benthic prey (Ramirez et al., 2017). This may in part be related to larger turtles being no longer able to sustain themselves on the *Sargassum* matts. Shifts observed in loggerhead sea turtles also result in the segregation of different

size classes; where smaller turtles inhabit oceanic habitats and larger turtles inhabit neritic habitats. Crested tern (*Sterna bergii*) adults primarily consume Degen's leatherjackets (*Thamnaconus degeni*) and barracoota (*Thyrsites atun*) while the chicks sustain mainly on clupeids fed to them by the adults (McLeay et al., 2009).

Like crocodilians, hadrosaurids are interpreted as having passed through a long growth trajectory with rapid growth occurring in the first few years of life, followed by slower growth in subsequent years (Dodson, 1975a; Carpenter, 1999; Varricchio, 2011; Codron et al., 2012, 2013; Vanderveen et al., 2014; Woodward et al., 2015). Similar to loggerhead turtles, changes in size and accompanying niche shifts may have also resulted in size-segregated aggregations of hadrosaurids. This phenomenon is evidenced by the presence of bonebeds where not all size classes are present (Table 2.1). Additionally, the potential for parental care and the oviparous nature of hadrosaurids would have facilitated the segregation of breeding from non-breeding individuals (Varricchio, 2011). This is because the needs of breeding individuals (e.g., nesting sites, potential territoriality during the breeding season) and non-breeding individuals (e.g., food resources for growth) would have conflicted, necessitating the formation of size/age-segregated groups and, potentially, niche shifts. Based on osteological evidence (see Horner, 2000), hadrosaurids may have undergone niche shifts similar to that of crested terns where adults select higher quality foodstuffs for their young than they themselves consumed. It is also possible that once hadrosaurids became independent from their parents they continued to forage for themselves on material different from that consumed by adults.

Table 2.1: Select Upper Cretaceous hadrosaur bonebed localities and their demographics. Abbreviations: Fm= Formation; BB= bonebed; MNI=minimum number of individuals.

Locality	Taxon/Taxa present	Ontogenetic stage(s) present	Reference(s)
Liscomb BB (Prince Creek Fm, Alaska)	*Edmontosaurus* sp.	Late juvenile (MNI=36)	Gangloff and Fiorillo, 2010
Standing Rock Hadrosaur Site (Hell Creek Fm, South Dakota)	*Edmontosaurus annectens*	Subadult to adult (MNI=4)	Bell et al., 2018
Danek BB (Horseshoe Canyon Fm, Alberta)	*Edmontosaurus regalis*	Subadult to adult (MNI=12)	Ullmann et al., 2017
West Hadrosaur BB (Two Medicine Fm, Montana)	*Maiasaura peeblesorum*	Adult (MNI=1) and juveniles (MNI=8)	Varricchio and Horner, 1983
Camposaur BB (Two Medicine Fm, Montana)	*Maiasaura peeblesorum*	Juvenile to subadult (MNI=20)	Varricchio and Horner, 1983
Wendy's BB (Oldman Fm, Alberta)	*Gryposaurus* sp.	Early and late juveniles (MNI=3)	Scott, 2015
Westside quarry (Two Medicine Fm, Montana)	*Prosaurolophus blackfeetensis*	Subadults and adults (MNI =5)	Varricchio and Horner, 1983
Jack's Birthday Site (Two Medicine Fm, Montana)	*Prosaurolophus blackfeetensis, Gryposaurus* sp., *Hypacrosaurus* sp.	Small juveniles and large subadults (MNI=17)	Varricchio and Horner, 1983
Sun River BB (Two Medicine Fm, Montana)	Lambeosaurinae indet.	Late juvenile (MNI=?)	Scherzer and Varricchio, 2010
Basturs Poble BB (Conques Fm, Spain)	Lambeosaurinae indet.	Juvenile to adult (MNI=?)	Fondevilla et al., 2018
Blagoveschensk locality (Udurchukan Fm, Russia)	*Amurosaurus* sp.	Late juvenile to early subadult (MNI=?)	Lauters et al., 2008
Quarry 11 (Dinosaur Park Fm, Alberta)	*Corythosaurus* sp.	Juvenile (MNI=4)	Eberth and Evans, 2011
Blacktail Creek North Assemblage (Two Medicine Fm, Montana)	*Hypacrosaurus* sp.	Juvenile (MNI=18)	Varricchio and Horner, 1983
Lambeosite (Two Medicine Fm, Montana)	*Hypacrosaurus* sp.	Large juveniles and adults (MNI=4)	Varricchio and Horner, 1983
"Dragon's Tomb" BB (Nemegt Fm, Mongolia)	*Saurolophus angustirostris*	Juvenile, subadult, large adult (MNI=100)	Bell et al., 2018

2.1.3 Chapter goals

Hadrosaurids have one of the most complete fossil records known among dinosaurs, with different growth stages (from embryos to adults) preserved (e.g., Campione and Evans, 2011; Erickson and Zelenitsky, 2014; Prieto-Marquez, 2014; Wosik et al., 2017). This makes them an ideal fossil group in which to investigate ONSs. Investigations into how cranial ecomorphology, snout shape and microwear may have changed during ontogeny, and the potential dietary implications of these potential differences, will be the focus of this chapter.

Despite multiple studies on hadrosaurid ontogeny, very few have focused on the implications that growth had on diet. Most studies have focused on cranial crest development, with some also investigating overall skull development (e.g., Dodson, 1975b; Evans, 2010; Campione and Evans, 2010; Farke et al., 2013; McGaritty et al., 2013). Despite predictions made regarding ONSs in hadrosaurids (e.g., Erickson and Zelenitsky, 2014), virtually none have been specifically tested from an ecomorphological perspective.

Changes in the cranium during growth have been a subject of interest for studies on both modern and extant taxa (e.g., Dodson, 1975a; Herrel, 2006; Evans, 2010; Campione and Evans, 2011). Classically, morphological traits have been defined as developing isometrically or allometrically (Gould, 1966). However, some more recent literature has defined isometry as a type of allometry (e.g., Klingenberg, 2016). For the purposes of my thesis, I will use the definitions originally put forth by Gould (1966) as these are the classical interpretations of how trait develop through ontogeny and are commonly used in the palaeontological literature (e.g., Evans, 2010; Campione and

Evans, 2011). Herein, isometry occurs when there is no change in the relative proportions of features with size and allometry is when there are disproportionate changes in the developing trait relative to size. If the trait disproportionately increases relative to size, this is positive allometry and if the trait disproportionately decreases, this is negative allometry.

Allometric growth is not required for an ONS to occur. Because size disparity is a mechanism through which resources can be partitioned (Werner and Gilliam, 1984; ten Brink and de Roos, 2018), ONSs can also occur in animals that experience isometric growth (e.g., loggerhead sea turtles) (Ramirez et al., 2017). Given hadrosaurids undergo a change in body size on the level of several orders of magnitude through growth (Carpenter, 1999; Varricchio, 2011; Vanderveen et al., 2014), it is likely that they also underwent ONSs. Dietary differences between juvenile and adult hadrosaurids, are uncertain. The aim of this chapter to provide some insight into hadrosaurid ONS using ecomorphological correlates of the skull, snout shape analysis and dental microwear analysis.

2.2 Methods

Skull morphology, snout shape and dental microwear have been used to quantify dietary differences in extant animals and their ancestors (Dodson, 1975a; Janis and Ehrhardt, 1988; Solounias et al., 1988; Janis, 1990; Spencer, 1995; Dompierre and Churcher, 1996; Erickson et al., 2003; Herrel et al., 2006). These ecomorphological correlates have also been used in investigations into dinosaur dietary preferences (e.g., Williams et al., 2000; Whitlock, 2011; Mallon and Anderson, 2013; Mallon, 2019). Thus,

changes in these ecomorphological correlates during growth can be used to infer the presence of, and interpret the nature of an ONS.

Investigations into hadrosaurid ONSs were conducted with reference to skull morphology, snout shape and microwear for species preserving relatively complete individuals from multiple ontogenetic stages. This includes the hadrosaurines *Maiasaura peeblesorum, Edmontosaurus annectens* and *E. regalis,* and the lambeosaurines *Hypacrosaurus stebingeri, H. altispinus, Hypacrosaurus* sp., *Lambeosaurus lambei, Lambeosaurus* sp., *Corythosaurus casuarius, C. intermedius,* and *Corythosaurus* sp. which have the best-preserved growth series among North American hadrosaurids to date (Dodson, 1975b; Evans, 2007; Campione and Evans, 2011; Prieto-Marquez, 2014; Wosik et al., 2017).

2.2.1 Skull allometry

Skull allometry was analyzed using twelve linear measurements previously considered by Mallon and Anderson (2013) and one size proxy (here quadrate height; see below for explanation) (Figure 2.1). In modern animals, including ungulates, the twelve linear measurements used are known reflect aspects such as plant quality, mechanical properties, and growth habit (Janis, 1990, 1995; Spencer, 1995; Mendoza et al., 2002). In instances where only half of a measurement could be taken across the midline (e.g., maximum beak width) due to damage, the measurement was doubled to produce a full value.

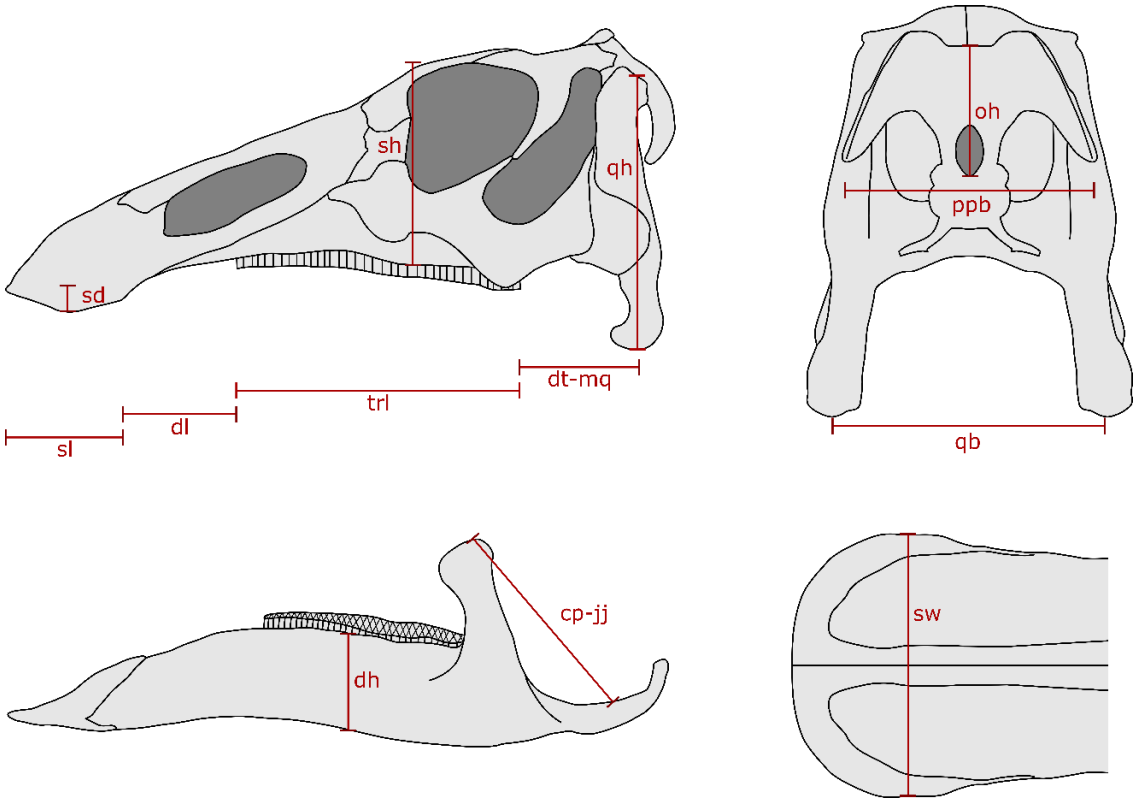

Figure 2.1: Linear measurements used for cranial morphometric analysis of hadrosaurid specimens (modified from Mallon and Anderson, 2013). Abbreviations – qh: quadrate height; sl: snout length; dl: diastema length; trl: tooth row length; dt-mq: distance from jaw joint to distal end of tooth row; sw: maximum beak width; dh: midpoint dentary height; ppb: paroccipital process breadth; oh: occiput height; cp-jj: distance from coronoid process apex to middle of jaw joint; sd: depression of snout below occlusal plane; sh: skull height; qb: quadrate breadth.

There are few examples of articulated juvenile hadrosaurids. Thus, it was necessary to include composite specimens constructed by scaling and combining elements from various individuals into a single skull. The use of such composites may therefore be a potential source of error in the dataset. They were, however, included because they were based on real material and deemed adequate representations of real individuals. To the extent that the reconstructions are erroneous, so too will be the functional interpolations.

Specimen maturity was gauged with reference to the degree of suture closure between the bones of the dermal skull roof (i.e., the frontals and the parietals, prefrontals and postorbitals), bone texture and size (Dodson, 1975b; Evans, 2010; Hone et al., 2016). In hadrosaurids (especially lambeosaurines), cranial crest development is another indicator of relative maturity (Dodson, 1975b; Evans, 2010; Brink et al., 2011; McGarrity et al., 2013). In this study, juveniles were defined as individuals that lacked a cranial crest (Figure 2.2), had little to no sutural closure between the bones of the dermal skull roof and lightly striated bone surface textures. Subadults possessed underdeveloped cranial crests, some sutural closure between the bones of the dermal skull roof and a mixture of lightly straited and rugose bone surface textures. Adults were identified by the possession of completely or almost completely developed cranial crests, fusion of the dermal skull roof and the presence of rugose bone surface textures. Because subadults and juveniles were the most difficult to distinguish, and due to small sample sizes, juveniles and subadults were grouped together to form an "immature" category in many of the analyses. In hadrosaurines, especially *Edmontosaurus*, relative cranial crest development cannot be used to reliably distinguish immature from mature individuals. Hadrosaurines,

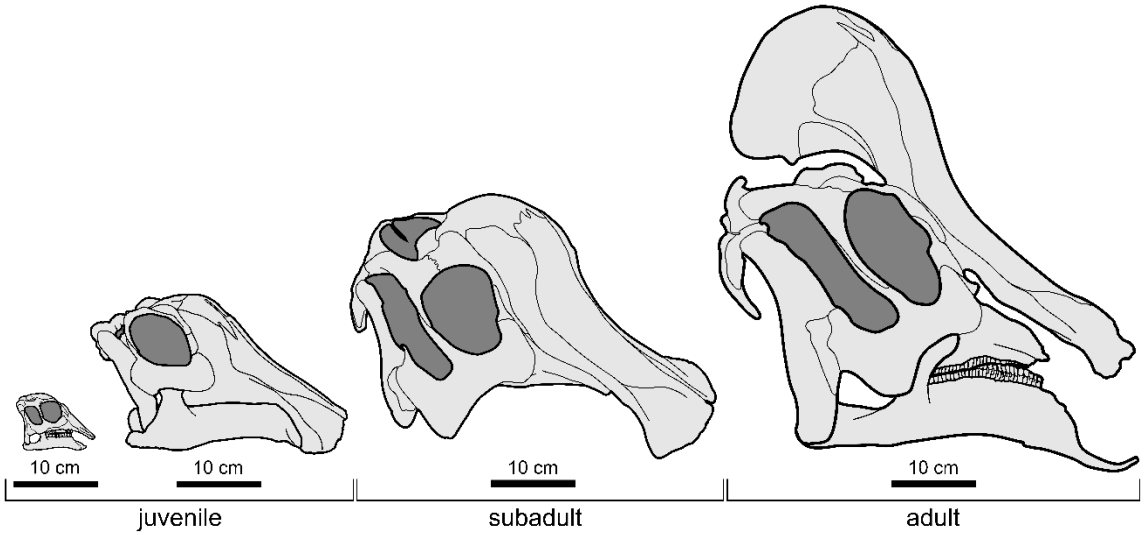

Figure 2.2: Determination of basic ontogenetic classifications in hadrosaurids based on cranial crest development and amount of sutural fusion. Specimen numbers for illustrated *Hypacrosaurus* specimens (from left-to-right): AMNH 28497, CMN 2247, CMN 2246 and CMN 8501.

therefore, were separated into these maturity groups using information provided by previous studies that aimed to identify growth trajectories. In *Edmontosaurus*, more immature specimens exhibit a thinner reflected premaxillary margin, decreased snout height, and shorter postorbital length (Campione and Evans, 2011). In *Prosaurolophus*, however, a small cranial crest is present and thus more useful in the determination of relative maturity (McGarrity et al., 2013).

To identify allometric trajectories, researchers often regress a morphological trait of interest against a size-related parameter. Isometry is then distinguished from allometry using the confidence intervals (CIs) for the slope of the regression line. If the CIs include values all above 1, then the relationship is positively allometric, and if the values are all below 1, then the relationship is negatively allometric (Klingenberg, 2016). If the CIs include 1 as a potential slope value, then the relationship is isometric. However, due to the nature of palaeontological research (e.g. small sample sizes, incomplete sampling), it can often be difficult to determine if the inclusion of 1 as a potential slope value is due to sampling or if the developmental trajectory is truly isometric. Brown and Vavrek (2015) suggested the use of "hard" and "soft" isometry. Hard isometry is when the slope is not statistically different from 1 and is unlikely to change with continued sampling (i.e., reflective of actual isometry). Soft isometry is when the slope is not statistically different from 1 but this result is likely due to small sample size or low statistical power. For the purposes of my thesis, I do not distinguish the two, but it should be stated that purported instances of isometry may be "soft" in the sense of Brown and Vavrek (2015).

Data were recorded in a Microsoft Excel file prior to being imported into R (v. 3.6.1; R Core Team, 2019) where subsequent data manipulation was conducted. To

identify potential allometry in ecomorphological correlates, skull measurements were initially log-transformed to linearize relationships between variables. Measurements were plotted against log-transformed quadrate height because it has been shown to scale isometrically with skull size and generally sustains little taphonomic distortion (Evans and Reiz, 2007; McGarrity et al., 2013; Lowi-Merri and Evans, 2019) (Figure 2.1). Quadrate height is also independent of the other measurements being used thereby decreasing the possibility of autocorrelation which can falsely produce "significant" regression values (McDonald, 2014; Appendix A).

Each cranial measurement was regressed against quadrate height using reduced major axis (RMA) regression with the "sma()" function from the "smatr" package (Warton et al., 2012). Reduced major axis regression was used instead of ordinary least squares (OLS) regression because RMA accounts for error in both the x and y variables (Hammer and Harper, 2006).

To identify potential differences in ontogenetic trajectories between lambeosaurines and hadrosaurines for each variable, tests for similarities in slopes were conducted using the "slope.com()" function from the "smatr" package (Warton et al., 2012). The "slope.com()" function tests for similarities in the slopes of two or more groups using log-likelihood (or simply likelihood) ratios. A likelihood test statistic is used instead of other test statistics because it is relatively robust to non-normality and does not assume (1) equal residual variances across groups, and (2) that the sum of squares of the numerator and denominator are independent (Warton et al., 2006).

If slopes were not significantly different between lambeosaurines and hadrosaurines, then tests for similarities in intercepts were conducted using the

"elev.com()" function (Warton et al., 2012). The "elev.com()" function uses a Wald test statistic because unlike other test statistics, it is not sensitive to (1) differences in mean x-values between groups, (2) unequal residual variances, and (3) unbalanced designs (Warton et al., 2006).

If slopes and intercepts were found to be significantly different ($p<0.05$) between lambeosaurines and hadrosaurines, then lambeosaurines and hadrosaurines were considered separately for that variable. If there were no significant differences in slope and intercept, then the regression line was calculated using lambeosaurine and hadrosaurine data combined together as a single hadrosaurid dataset. To control the inflation of familywise error rates, the resulting p-values were passed to the "p.adjust()" function from the "stats" package which calculated the adjusted p-values using the Holm-correction method (R Core Team, 2019). The Holm adjustment method was used instead of the classical Bonferroni method because the Holm method is less conservative and more powerful.

2.2.2 Snout shape

In extant ungulates, snout shape has been shown to correlate with dietary category, with more selective feeders possessing relatively narrower snouts compared to the broader, more rectangular snouts of bulk feeders (Janis and Ehrhardt, 1988). Modern animals that consume large quantities of low-nutrition vegetation (e.g. grasses) often possess wider snouts than animals that specialize on higher-quality vegetation (e.g., fruits, leaves). Thus, quantifying snout shape helps distinguish between potential bulk and selective feeders.

To determine if snout shape changed during ontogeny, it was quantified using a method similar to that of Dompierre and Churcher (1996). Photos of the snout in dorsal view were traced in InkScape v.0.92.3 (Harrington et al., 2004). The least distorted half of the snout was used to reduce the amount of taphonomically-related distortion. A vertical line was drawn at the midline to define the boundary between the two snout halves (Figure 2.3). The outer boundaries of the snout were defined by drawing lines at the widest point of the snout (vertical line) and at the anterior-most point of the snout (horizontal line) (Figure 2.3). Another line was drawn at 26^{o} from the midline, where it intersects the anterior part of the snout. The 26^{o} angle was arbitrary, but was used for comparability with other studies and because it adequately captures the shape of the snout. These intersecting lines together create a triangle that can be used to quantify the shape of the snout. In Dompierre and Churcher's (1996) method, the area of the snout contained within the triangle was used. For the purposes of this study, the area between the anterior margin of the snout contained within the triangle was used instead because, unlike ungulates, hadrosaurids possess snouts that curve back on themselves, and the negative space posterior to the widest point of the snout is thus uninformative.

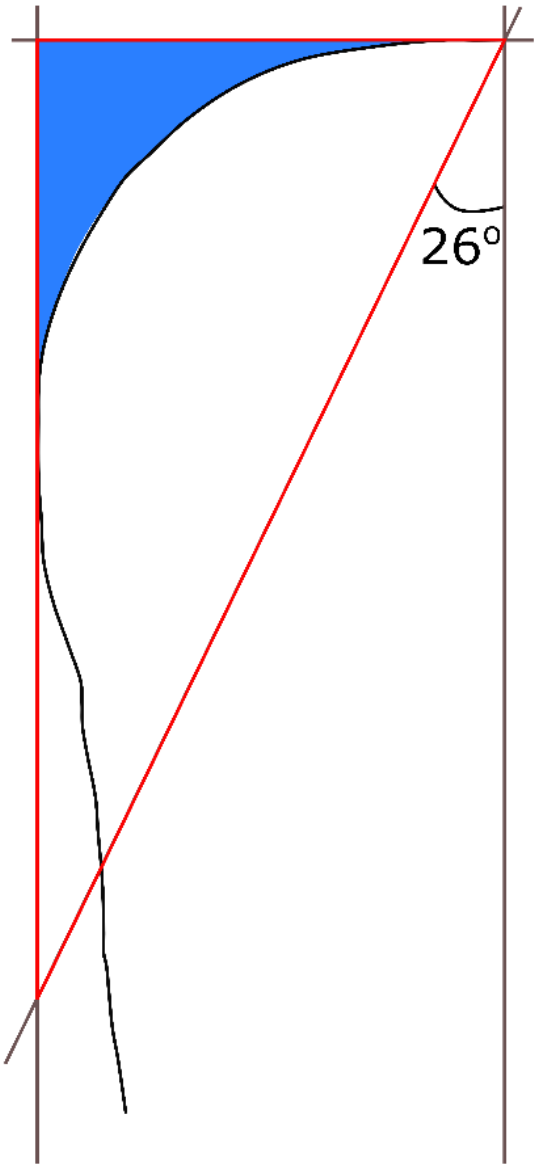

Figure 2.3: Snout shape analysis conducted for hadrosaurids based on Dompierre and Churcher (1996). Blue region denotes the area of negative space measured for analysis. Red triangle indicates the triangle area measured for analysis.

These areas were measured in ImageJ v.1.52a (Schneider et al., 2012) using the "Rectangle" and "Wand" tools. The ratio of the negative space area to the triangle area produces the snout shape index (SSI) (SSI= negative space area/triangle area) (Figure 2.3). The SSI will be higher (closer to 1) for narrower, more pointed snouts, and lower (closer to 0) for wider, more square snouts. Snout shape index was plotted against quadrate height to identify potential shape changes through ontogeny.

Comparisons between SSIs of immature and mature hadrosaurines and lambeosaurines were conducted using a Kruskal-Wallis test with the function "kruskal.test()" from the "stats" package (R Core Team, 2019). A Kruskal-Wallis test is a non-parametric test designed to determine if two or more independent samples were taken from populations with equal medians (Hammer and Harper, 2006). If the results of the Kruskal-Wallis test indicated significant differences between groups, then follow-up pairwise Mann-Whitney U comparisons with Holm-corrected p-values were conducted to identify which groups differed from one another.

2.2.3 Tooth wear analysis

Dental microwear is the damage inflicted on teeth during contact with various surfaces (Whitlock, 2011). In particular, microwear is formed during tooth-on-tooth, tooth-on-food and tooth-and-grit interactions. Tooth microwear is often separated into two categories: scratches and pits (Nelson et al., 2005). Scratches are defined as features with a length four or more times greater than the width, and pits are deep circular to ovate features.

Studying dental microwear provides useful insights into the diet of an organism, in particular, the last few meals consumed prior to death (Walker et al., 1978). Dental microwear is especially useful for fossil animals, such as hadrosaurids, that lack extant descendants that can be used for comparison of other ecomorphological correlates. Microwear has been used previously for various fossil animals including dinosaurs (e.g., Fiorillo, 1998; Williams et al., 2000; Goillot et al., 2009; Whitlock, 2011; Mallon and Anderson, 2014b; DeSantis, 2016).

Tooth wear was analyzed using in situ teeth to maximize taxonomic certainty, following the methods of Mallon and Anderson (2014b). Unlike Mallon and Anderson (2014b), teeth from both maxillae and dentaries were used to increase sample size, as juvenile specimens are relatively rare and microwear would otherwise be difficult to obtain from these early stages. Mallon and Anderson (2014b) indicated that the primary orientation of jaw feeding movements is best obtained by sampling the entire tooth row. Thus, the number of teeth from each individual and the number of individuals are important to obtain a representative sample.

Tooth wear facets were cleaned using cotton swabs and acetone to remove any surface contaminants. After cleaning, the tooth surfaces were molded using President regular body polyvinylsiloxane. These peels were then dammed using President soft two-part putty in preparation for casting.

Casts were constructed using Epotek 301 two-part epoxy. After mixing, the epoxy was put into a vacuum chamber to remove air bubbles that would obstruct the surface of the tooth. The epoxy was then poured into the dams and allowed to set for a minimum of 24 hours prior to being removed from the molds.

Casts with potential microwear were identified using an Olympus SZX12 stereo light microscope. These tooth casts were then sputter coated using a Denton Vacuum Desk II at 50 atm for 30 seconds under a 40-milliamp current. After sputter coating, specimens were loaded into an FEI Scanning Electron Microscope (SEM) for imaging at a chamber pressure of 50 Pa, voltage of 5.00 kV, and a beam current of 0.10 nA. Micrographs were taken at 100X magnification. When microwear features extended outside the field of view, multiple overlapping images were taken and then overlaid in InkScape v.0.92.3 (Harrington et al., 2004) to produce a composite image of the wear facet. Prior to being exported as png files, all teeth were rotated so that the apex of the tooth crown faced upwards. If teeth were taken from the left dentary or right maxilla, then the image was also mirrored along the vertical axis to standardize to the right dentary. Teeth were standardized to the right dentary to allow for direct comparison to previous work (Mallon and Anderson, 2014b).

Composite images were imported into ImageJ v.1.52a (Schneider et al., 2012) where a 0.4 X 0.4 mm bounding box was drawn on an area of the tooth with the best preserved microwear. Lengths, widths and orientations of microwear features observed in this box were taken using the "Straight" line segment tool and recorded in an Excel spreadsheet, which was then imported into R for further analysis. In some instances, data for multiple individuals from the same genus and relative ontogenetic stage (i.e., juvenile, subadult or adult) were combined and treated as a single individual for more complete sampling along the tooth row.

Previous research on extant ungulates and primates has highlighted the importance of scratch modality, average widths of scratches and average pit to scratch

count ratios in distinguishing between dietary categories (Solounias and Semprebon, 2002; Semprebon et al., 2004; Rivals and Semprebon, 2011). Therefore, to identify potential dietary differences between ontogenetic stages, scratch modality, average scratch width and average pit/scratch count ratios were compared between ontogenetic stages.

To investigate scratch modality, data were imported into R and plotted as rose diagrams using the "windRose()" function from the "openair" package (Carslaw and Ropkins, 2012). Rose diagrams were generated as pooled rose diagrams for each growth stage to identify overall modality.

Comparisons of microwear variables were made between stages at the subfamily level and, when more than two individuals were sampled for each stage, at the genus level. Non-parametric tests were used for these comparisons because sample sizes were small and the data were heteroscedastic and the residuals did not exhibit a normal distribution. Because there were up to three potential ontogenetic stages to compare, a Kruskal-Wallis test was used for all comparisons. If the p-value from a Kruskal-Wallis test with more than two ontogenetic stages was statistically significant, then a follow-up pairwise Mann-Whitney U test with Holm corrected p-values was used to identify which ontogenetic stages were statistically different.

In some instances, analysis of ratios can result in a variety of problems including violations of standard statistical assumptions and the potential for misinterpretation of results (Liermann et al., 2004). Ratios of particular concern include those where the expected ratio of the numerator and denominator is isometric or a ratio where the denominator is used as a standardization (e.g., 12 animals in $200m^2$). However, if the

ratio being analyzed is one where the numerator is independent of the denominator, then traditional types of analysis can be used. In the instance of pit/scratch ratio, there is no reason to presume that pit count would be dependent on scratch count and vice versa because there is no discernable relationship between average pit count and average scratch count.

2.3 Results

2.3.1 Skull allometry

Raw measurements used for skull morphometric analysis are provided in Appendix B. The number of specimens used for each stage (juvenile, subadult, adult) are given in Table 2.2. Analyses of regression lines showed that there was no statistical difference in slope between hadrosaurines and lambeosaurines for all variables considered (Table 2.3). Significant differences in intercepts were observed for skull and dentary height. Therefore, separate regression lines were plotted for hadrosaurines and lambeosaurines for this variable (Figure 2.4). Strong positive allometry (slope > 1.1) was observed in hadrosaurid snout depression, snout length, diastema length and occiput height (Table 2.4). All other measurements exhibited soft isometry.

Smaller individuals cluster together at one end of the regression with progressively larger (i.e., more mature) individuals spreading out along the regression line in a “fan” shape. Mature hadrosaurines also plotted higher up on the regression line than lambeosaurines due to their larger sizes (e.g., *Edmontosaurus*).

Table 2.2: Sample sizes for hadrosaurid specimens used in analyses. Note: for reduced major axis regression the numbers provided are maximum possible sample sizes as the actual sample size used varied based on what measurements could be obtained from each specimen.

Taxon	Stage	Sample size by analysis		
		Reduced major axis regression	Snout shape	Dental microwear
Hadrosauridae (overall)	Juvenile	3	3	0
	Subadult	10	5	2
	Adult	33	16	4
Brachylophosaurus	Adult	3	0	0
Edmontosaurus	Juvenile	1	1	0
	Subadult	6	4	1
	Adult	20	11	3
Gryposaurus	Subadult	1	1	0
	Adult	4	2	0
Maiasaura	Juvenile	2	2	0
	Subadult	1	0	0
	Adult	1	0	0
Prosaurolophus	Subadult	2	0	1
	Adult	5	3	1
Lambeosaurinae (overall)	Juvenile	11	9	3
	Subadult	8	8	7
	Adult	36	25	2
Lambsaurinae indet.	Juvenile	2	2	0
Lambeosaurus	Juvenile	2	1	0
	Subadult	2	2	0
	Adult	14	10	0
Corythosaurus	Juvenile	1	1	1
	Subadult	4	4	3
	Adult	18	12	2
Hypacrosaurus	Juvenile	5	5	2
	Subadult	1	1	4
	Adult	3	2	0
Parasaurolophus	Juvenile	1	0	0
	Subadult	1	1	2
	Adult	1	1	0

Table 2.3: Results for test of equivalent slopes and intercepts for regressions of various variables against quadrate height between hadrosaurines and lambeosaurines. Abbreviations: nHa- sample size for hadrosaurine specimens; nLa- sample size for lambeosaurine specimens; LR-likelihood ratio; SSI-snout shape index. All p-values reported are adjusted using the Holm correction method. Statistically significant p-values are in bold.

Log-transformed Y variables	nHa	nLa	LR statistic (slope)	p-value (slope)	Wald statistic (intercept)	p-value (intercept)
snout length	42	50	0.309	1	0.512	1
diastema length	42	48	1.991	1	0.023	1
tooth row length	45	52	0.325	1	3.167	0.661
distal end of tooth row to mid quadrate	42	53	1.595	1	3.204	0.661
snout width	31	41	0	1	0.033	1
height dentary	45	52	4.446	0.42	9.59	**0.025**
paroccipital process breadth	34	35	1.837	1	0.001	1
occiput height	28	27	6.712	0.124	6.936	0.089
coronoid process apex to mid jaw joint	43	49	2.325	1	2.887	0.661
snout depression	40	49	0.048	1	2.136	0.863
skull height	45	52	1.046	1	9.571	**0.025**
distance between quadrates	33	39	0.393	1	0.078	1
SSI	24	42	0.084	1	7.021	0.089

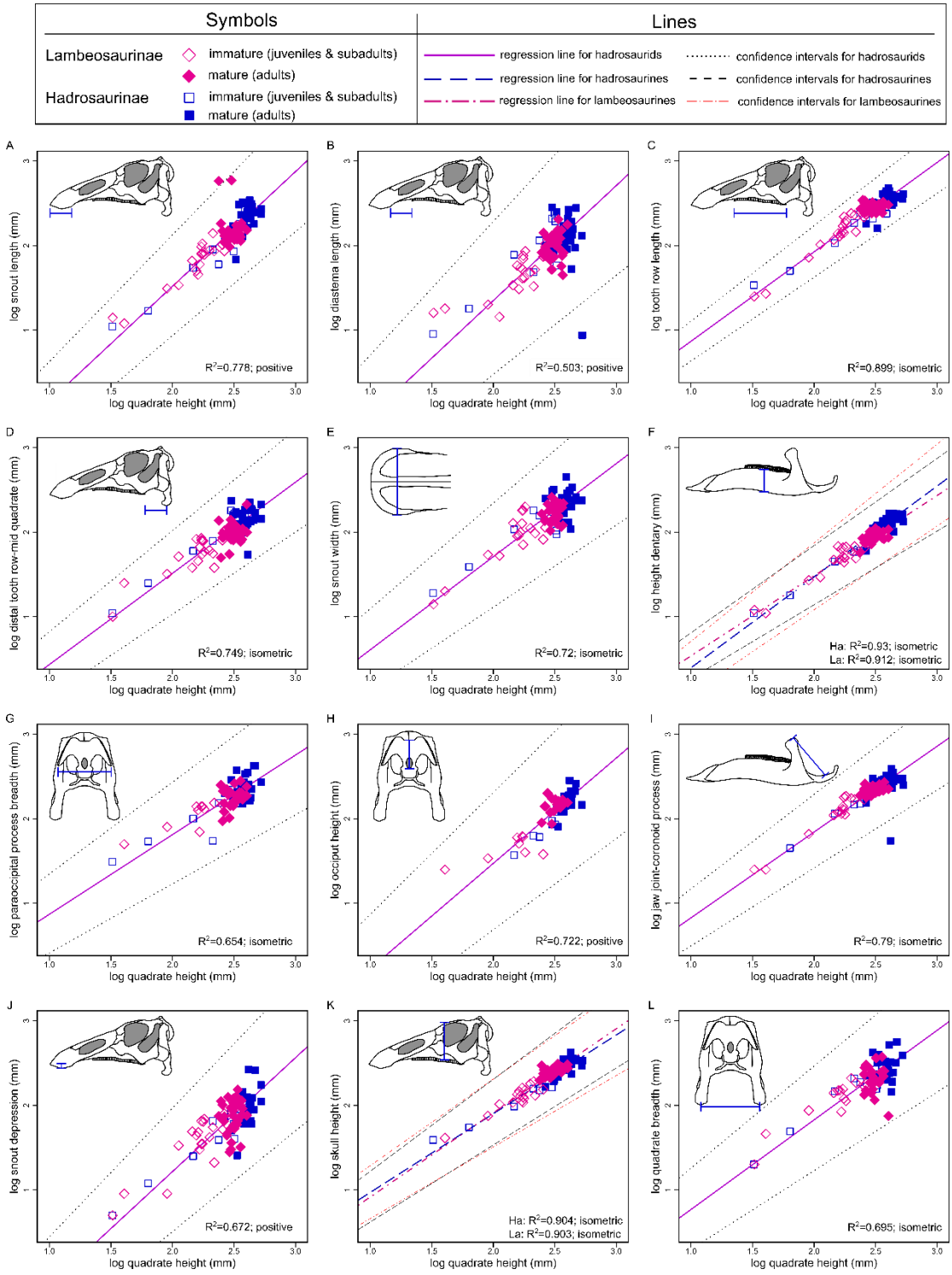

Figure 2.4: Bivariate allometric plots for reduced major axis regression of log-transformed hadrosaurid cranial variables. A) snout length, B) diastema length, C) tooth row length, D) distal tooth row to middle quadrate length, E) snout width, F) dentary height, G) paroccipital process breadth, H) occiput height, I) distance from coronoid process to jaw joint, J) snout depression below occlusal plane, K) skull height, L) distance between quadrates. Positive allometry is observed for hadrosaurids in A, B, H and J. In F and K two regression lines are plotted due to statistically significant differences in intercept (Table 2.2).

Table 2.4: Values obtained from reduced major axis regression of hadrosaurid variables against quadrate height. Reported p-values have been adjusted using the Holm-correction method. Abbreviations: grp-grouping; H-Hadrosauridae; Ha-Hadrosaurine; La-Lambeosaurinae; SSI-snout shape index; I-isometry; - negative allometry; + positive allometry; NS-non significant slope. Note: SSI does not show a slope significantly different from 0 and so it was not graphed with the other variables.

Log-transformed Y variables	grp	n	R^2	2-tailed p	intercept	95% CI intercept	slope	95% CI slope	trend
snout length	H	92	0.778	3.31E-30	-1.198	-1.526 to -0.87	1.358	1.23 to 1.498	+
diastema length	H	90	0.503	1.05E-14	-1.375	-1.873 to -0.877	1.362	1.174 to 1.581	+
tooth row	H	97	0.899	5.1E-48	-0.19	-0.358 to -0.022	1.058	0.992 to 1.129	i
distal tooth row-mid quadrate	H	95	0.749	8.9E-29	-0.645	-0.918 to -0.373	1.079	0.973 to 1.196	i
snout width	H	72	0.72	3.02E-20	-0.494	-0.832 to -0.157	1.102	0.972 to 1.25	i
height dentary	Ha	45	0.93	4.4E-25	-0.679	-0.9 to -0.458	1.075	0.991 to 1.166	i
	La	52	0.912	1.17E-26	-0.413	-0.604 to -0.222	0.949	0.872 to 1.032	i
paroccipital process breadth	H	69	0.654	1.78E-16	-0.072	-0.404 to 0.26	0.942	0.816 to 1.087	i
occiput height	H	55	0.722	6.85E-16	-1.022	-1.472 to -0.573	1.247	1.079 to 1.441	+
coronoid process apex-mid jaw joint	H	92	0.79	3.26E-31	-0.187	-0.427 to 0.053	1.015	0.922 to 1.117	i
snout depression	H	89	0.672	6.27E-22	-1.48	-1.882 to -1.078	1.348	1.194 to 1.523	+
skull height	Ha	45	0.904	3.78E-22	0.037	-0.188 to 0.261	0.932	0.847 to 1.025	i
	La	52	0.903	1.41E-25	-0.081	-0.293 to 0.131	0.996	0.912 to 1.088	i
quadrate breadth	H	72	0.695	4.77E-19	-0.292	-0.632 to 0.049	1.06	0.93 to 1.208	i
SSI	H	66	0.002	0.742532	1.483	0.945 to 2.021	-0.886	-1.135 to -0.692	NS

2.3.2 Snout shape

Raw snout shape data are provided in Appendix C and specimens used and their corresponding stages are provided in Table 2.2. There was no linear relationship between SSI and quadrate height (Table 2.4) and so a bivariate plot of SSI against quadrate height is shown (Figure 2.5). On the SSI axis, immature hadrosaurids appear to occupy the same range as mature hadrosaurids. Overlap is generally observed between lambeosaurines and hadrosaurines, and is supported by the results of the Kruskal-Wallis test ($p=0.94$). Lambeosaurines and hadrosaurines with quadrate heights <150 mm or >350 mm do not show complete overlap in the morphospace. This lack of overlap at the smallest and largest skull sizes is likely a result of reduced sampling of small individuals and the larger sizes attained by hadrosaurines.

2.3.3 Microwear

Dental microwear was recovered for juvenile and subadult *Hypacrosaurus*; juvenile, subadult and adult *Corythosaurus*; subadult *Parasaurolophus*; subadult and adult *Edmontosaurus*; and subadult and adult *Prosaurolophus* (Appendix D, E; Table 2.2, Figure 2.6).

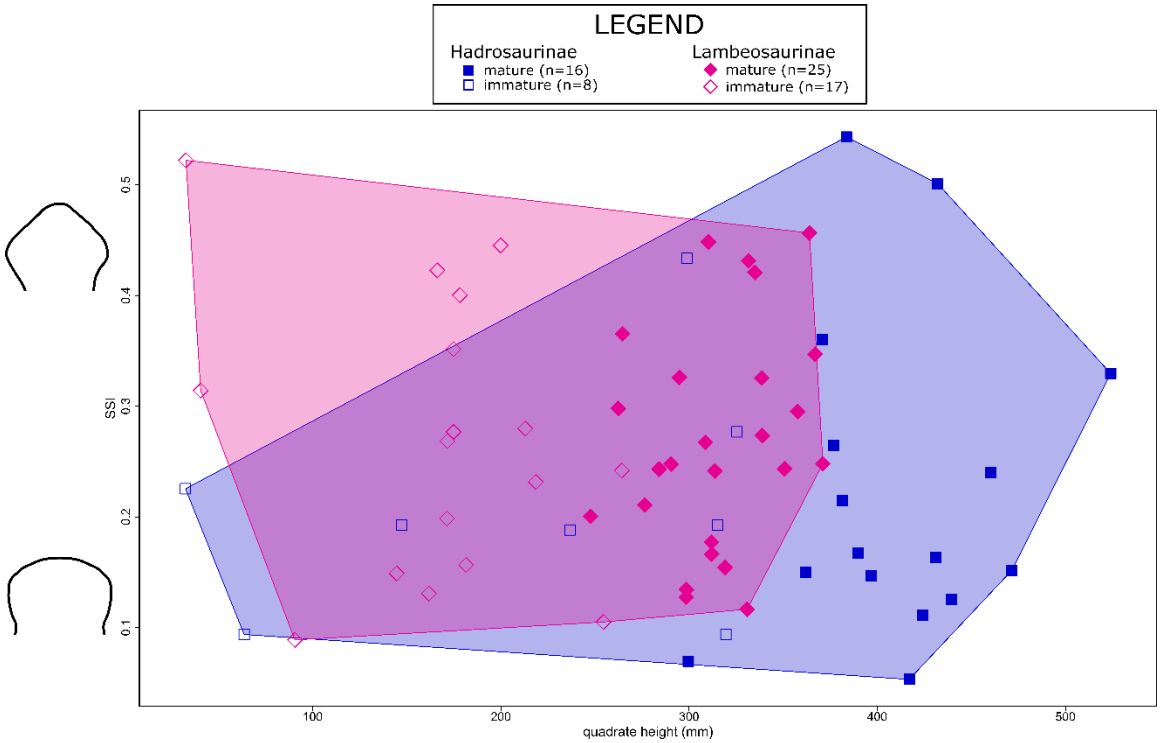

Figure 2.5: Snout shape plot for hadrosaurid specimens. Abbreviations: SSI-snout shape index.

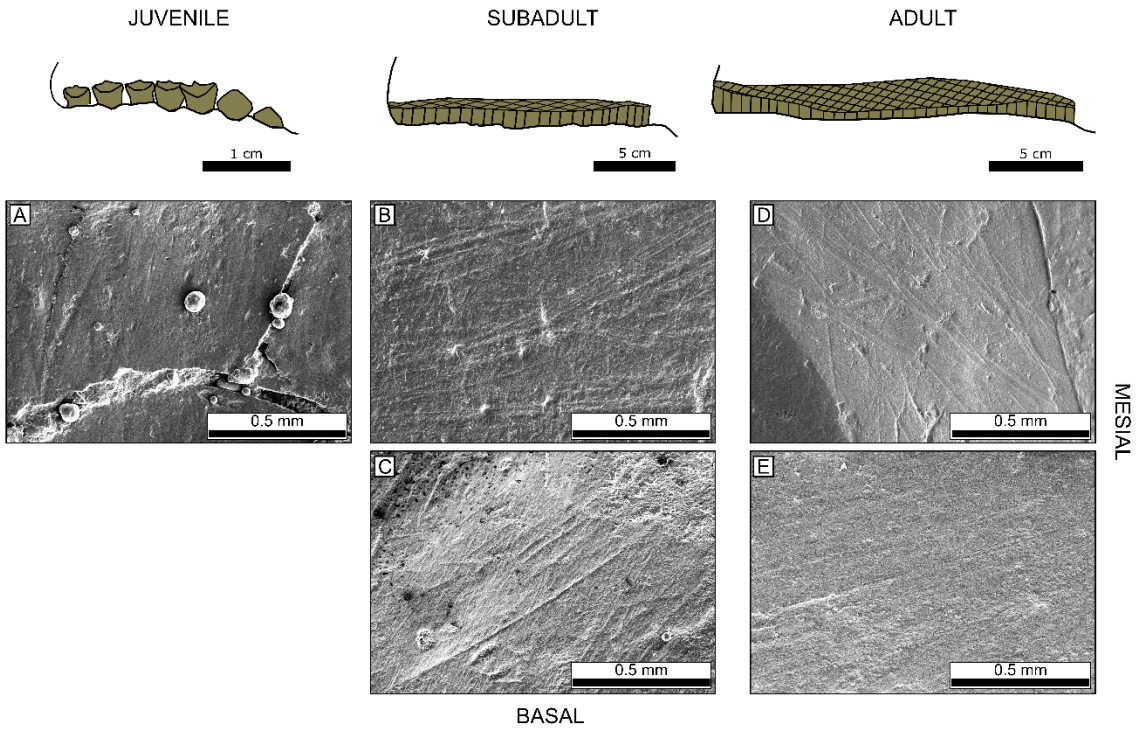

Figure 2.6: Microwear recovered from basic ontogenetic stages in hadrosaurines and lambeosaurines. All photos have been standardized to the right dentary and oriented so that the tooth apex is directed upwards. Microwear recovered from A) juvenile *Hypacrosaurus* (MOR 548 C, LD9), B) subadult *Hypacrosaurus* (TMP 1988.151.0005, LD8), C) subadult *Edmontosaurus* (CMN 8509, LD5), D) adult *Corythosaurus* (TMP 1982.037.0001, RD28), and E) adult *Edmontosaurus* (USNM 5389, LD48). Abbreviations: LD-left dentary.

2.3.3.1 Scratch orientation and distribution

In general, hadrosaurids exhibited dorsomesial-ventrodistal scratch orientations regardless of ontogenetic stage (Figure 2.7, 2.8). Unlike hadrosaurines, scratch orientation for lambeosaurines was more variable between ontogenetic stages and some specimens exhibited scratches generally oriented dorsodistally. Both hadrosaurines and lambeosaurines exhibited variability between stages in the angle of the scratches and in the modality of scratches. Rose diagrams for scratch orientations along the tooth row for select hadrosaurines and lambeosaurines are provided in Appendix E and not discussed here.

Scratches are commonly oriented dorsomesially in subadult and adult *Edmontosaurus*. Dorsodistal scratches are the next most common (Figure 2.7). Unlike adult *Edmontosaurus*, subadult *Edmontosaurus* exhibits fewer dorsodistal scratches relative to the number of dorsomesial scratches. Scratch orientations observed in *Prosaurolophus* are most similar between stages with both subadults and adults exhibiting a primary mode of dorsomesial scratches and a secondary mode of dorsodistal scratches. The main difference between subadult and adult *Prosaurolophus* is the angle of the main set of scratches. In subadult *Prosaurolophus*, dorsomesial scratches are directed more horizontally than those of adults which tend to be more vertically oriented.

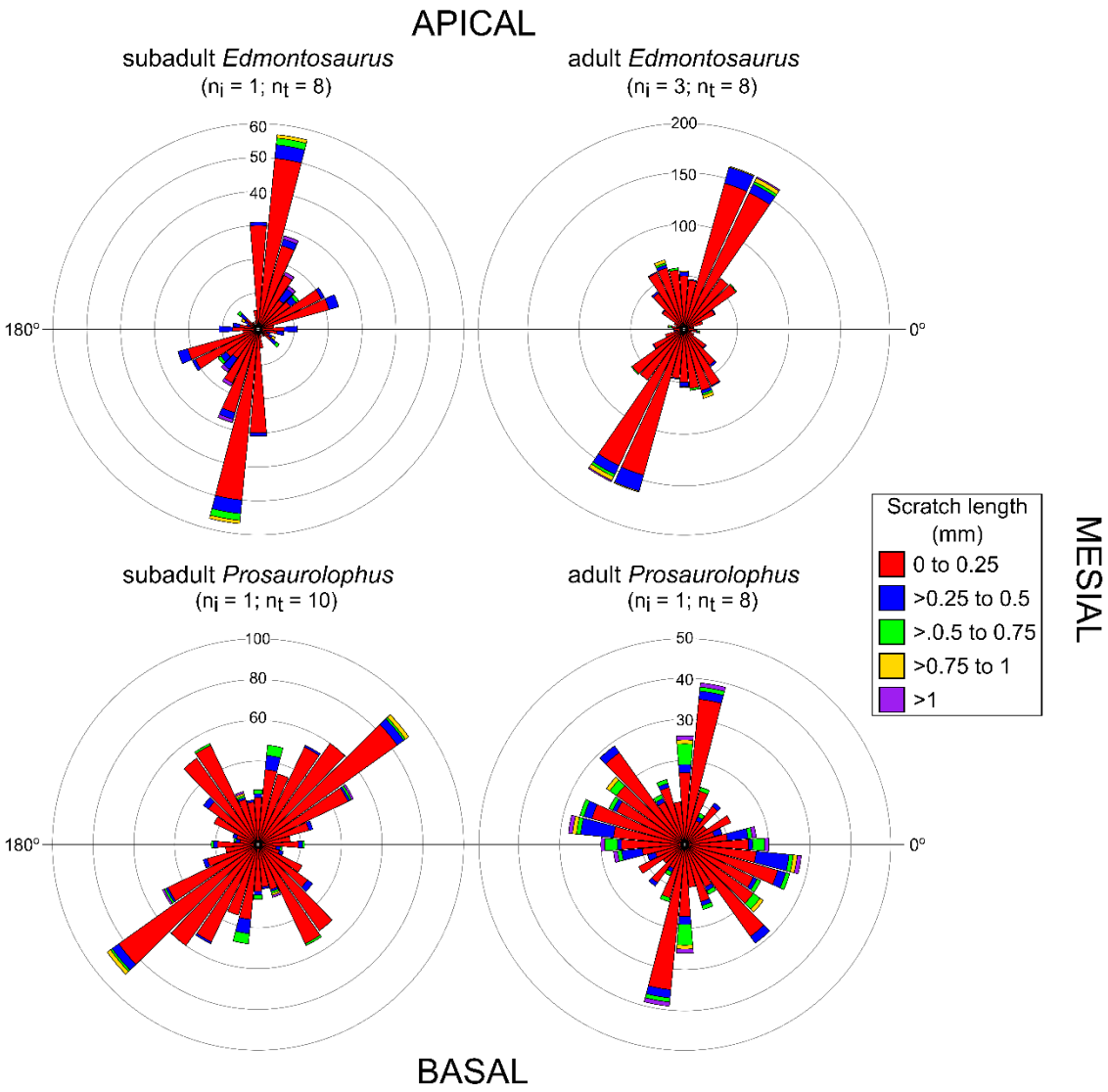

Figure 2.7: Rose diagrams for overall scratch orientation in subadult and adult hadrosaurines. All teeth are standardized to the right dentary. Abbreviations: n_i -total number of individuals used to construct diagram; n_t -total number of teeth used to construct each diagram. Mesial=0°, Apical/dorsal=90°, Distal= 180°, Basal/ventral= 270°.

The wear observed in juvenile *Corythosaurus* is distinct from the wear observed in the other specimens in that there is no clear directionality observed (Figure 2.8). The only possible sense of directionality indicated is by the orientation of the longest scratches which are generally directed dorsomesially. Wear in subadult *Corythosaurus* exhibits a primary mode of longer, dorsodistally oriented scratches and a secondary set of shorter, dorsomesial scratches. Wear in adult *Corythosaurus* is unimodal and oriented dorsomesially.

In juvenile *Hypacrosaurus*, wear is mainly oriented dorsomesially with a second mode of shorter scratches oriented dorsodistally (Figure 2.8). Wear in subadult *Hypacrosaurus* is generally oriented dorsomesially with a secondary set of is a second set of vertically oriented scratches which may correspond to the dorsodistal scratches observed in juveniles.

The wear observed between larger subadult (ROM 183; cf. *Parasaurolophus*) and smaller subadult (TMP 1990.036.0155) *Parasaurolophus* is very different (Figure 2.8). In the smaller subadult, scratches are oriented mesio-distally with only a few scratches in the dorsomesial-ventrodistal direction. In the larger subadult, however, the longest scratches are oriented dorsomesially with a second set of scratches in the dorsodistal direction.

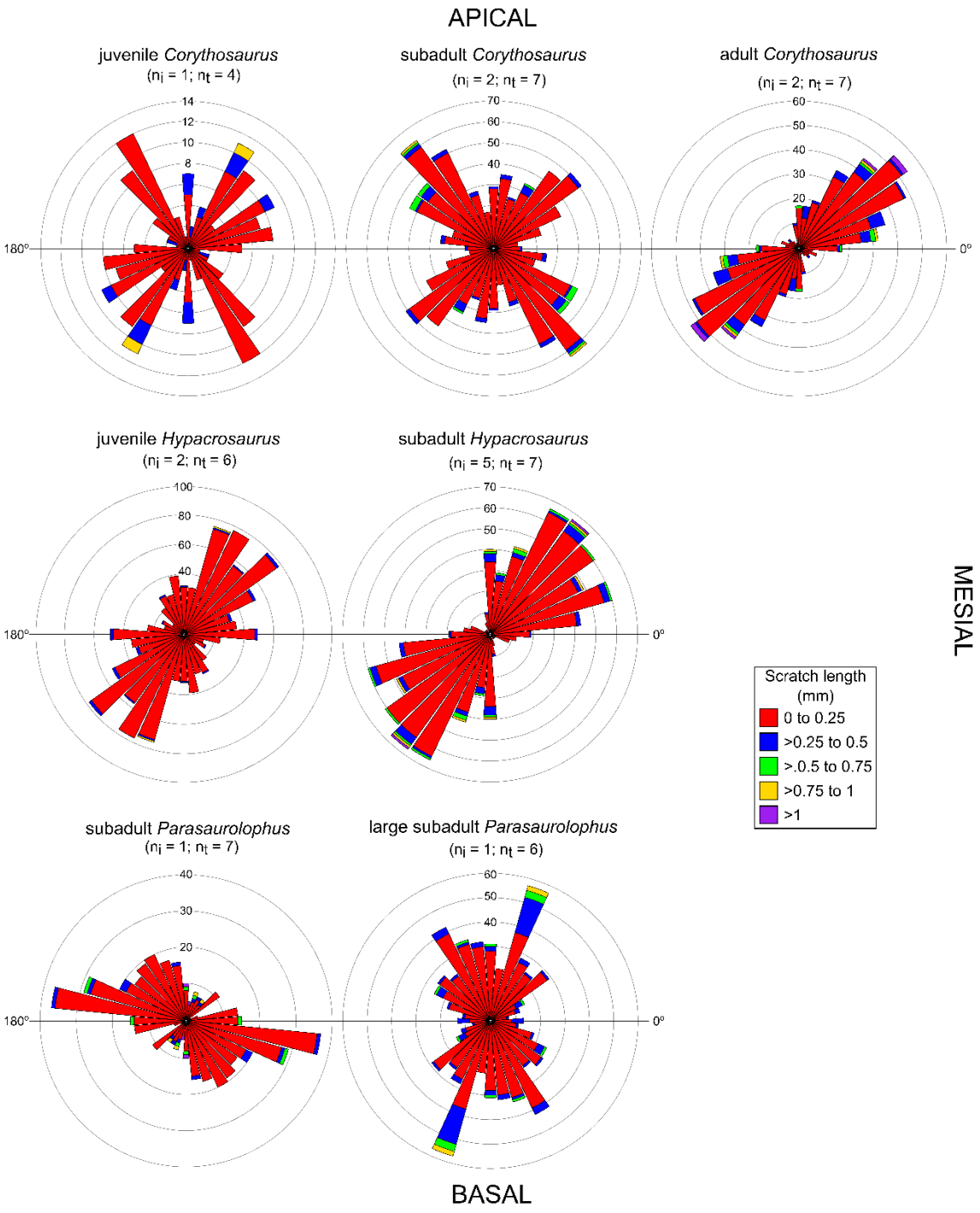

Figure 2.8: Rose diagrams for overall scratch orientation in juvenile, subadult and adult lambeosaurines. All teeth are standardized to the right dentary Abbreviations: n_i -total number of individuals used to construct diagram; n_t -total number of teeth used to construct each diagram. Mesial=0º, Apical/dorsal=90º, Distal= 180º, Basal/ventral= 270º.

2.3.3.2 Scratches and pits

Hadrosaurids generally exhibit fine scratches regardless of ontogenetic stage (Table 2.5). Statistical analysis of average scratch widths reveals no statistical difference between ontogenetic stages (Table 2.6). Boxplots of average pit/scratch counts do suggest that juveniles had higher ratios than subadults and adults (Figure 2.9). However, statistical comparisons do not indicate significant differences between ontogenetic stages, possibly due to small sample sizes (Table 2.7).

2.4 Discussion

2.4.1 Jaw mechanics

The matter of hadrosaurid feeding mechanics has long been contentious (e.g., Weishampel 1984, 1985; Williams et al., 2009; Cuthbertson et al., 2012; Mallon and Anderson, 2014b). Early work by Ostrom (1961) proposed that hadrosaurid skulls were mainly akinetic based on observations of a "sutural union" at every junction of the neurocranial and maxillary segments; the short, mesiodistally oriented scratches observed on teeth were thought to be produced during a propalinal power stroke.

Later studies (Weishampel, 1983, 1984; Norman and Weishampel, 1985) proposed a more complex, pleurokinetic model involving lateral flaring of the maxillae with occlusion, based on kinematic analysis of cranial joints. Subsequent work (e.g., Holliday and Witmer 2008; Rybczynski et al., 2008; Cuthbertson et al., 2012), however, indicated that pleurokinesis was impractical given the intracranial kinematic limitations of the skull, and Cuthbertson et al. (2012) advocated for a partially kinetic model where rotational and translational movement occurred predominately at the jaw joint. Williams et al. (2009) invoked a pleurokinetic hinge model to explain the formation of the four

Table 2.5: Average microwear feature information for hadrosaurids used in analysis by ontogenetic stage and genus. Classification (based on the categories provided by Mihlbachler et al., 2012) for scratches are provided with the value for average scratch width. Microwear data were combined for several specimens of the same stage to increase sample size. Abbreviations: n_i – number of individuals.

Genus	Stage & specimen number(s)	Avg scratch width (mm)	Avg pit/ scratch count
Corythosaurus	Juvenile (n_i= 1) (USNM 16600)	0.00282 (fine)	0.121
	Subadult (n_i= 3) (USNM 11839, ROM 1947 & 759)	0.00233 (fine)	0.267
	Adult (n_i= 2) (TMP 1982.037.0001, ROM 871)	0.00323 (fine)	0.250
Hypacrosaurus	Juvenile (n_i= 2) (MOR 548C & 548F)	0.00250 (fine)	0.525
	Subadult (n_i= 4) (ROM 61784, TMP 1985.036.0042 & 1988.151.0005, USNM 11950)	0.00240 (fine)	0.123
Parasaurolophus	Subadult (n_i= 1) (TMP 1990.036.0155)	0.00244 (fine)	0.058
	Large subadult (n_i= 1) (ROM 183)	0.00331 (fine)	0.177
Prosaurolophus	Subadult (n_i= 1) (TMP 2016.037.0001)	0.00314 (fine)	0.168
	Adult (n_i= 1) (CMN 2870)	0.00305 (fine)	0.078
Edmontosaurus	Subadult (n_i=1) (CMN 8509)	0.00369 (fine)	0.234
	Adult (n_i= 3) (USNM 4808 & 5389, MOR 003)	0.00242 (fine)	0.288

Table 2.6: Holm-corrected two-tailed p-values for Kruskal-Wallis tests of average scratch widths for hadrosaurids by ontogenetic stage. For average values and specimens used see Table 2.2, 2.5 and Appendix C. Abbreviations: J – juvenile, S – subadult, A –adult; df – degrees of freedom; n_i – number of individuals.

Comparison	df	Chi-square	Corrected p-value	Statistical Conclusion
Hypacrosaurus juvenile (n_i=2) vs subadult (n_i=4)	1	0.15	0.699	J = S
Corythosaurus subadult (n_i=3) vs adult (n_i=2)	1	2.4	0.121	S = A
Lambeosaurinae juvenile (n_i=3) vs subadult (n_i=7) vs adult (n_i=2)	2	1.723	0.422	J = S = A
Hadrosaurinae subadult (n_i=2) vs adult (n_i=4)	1	0.857	0.355	S = A
Hypacrosaurus juvenile (n_i=2) vs subadult (n_i=4)	1	0.15	0.699	J = S

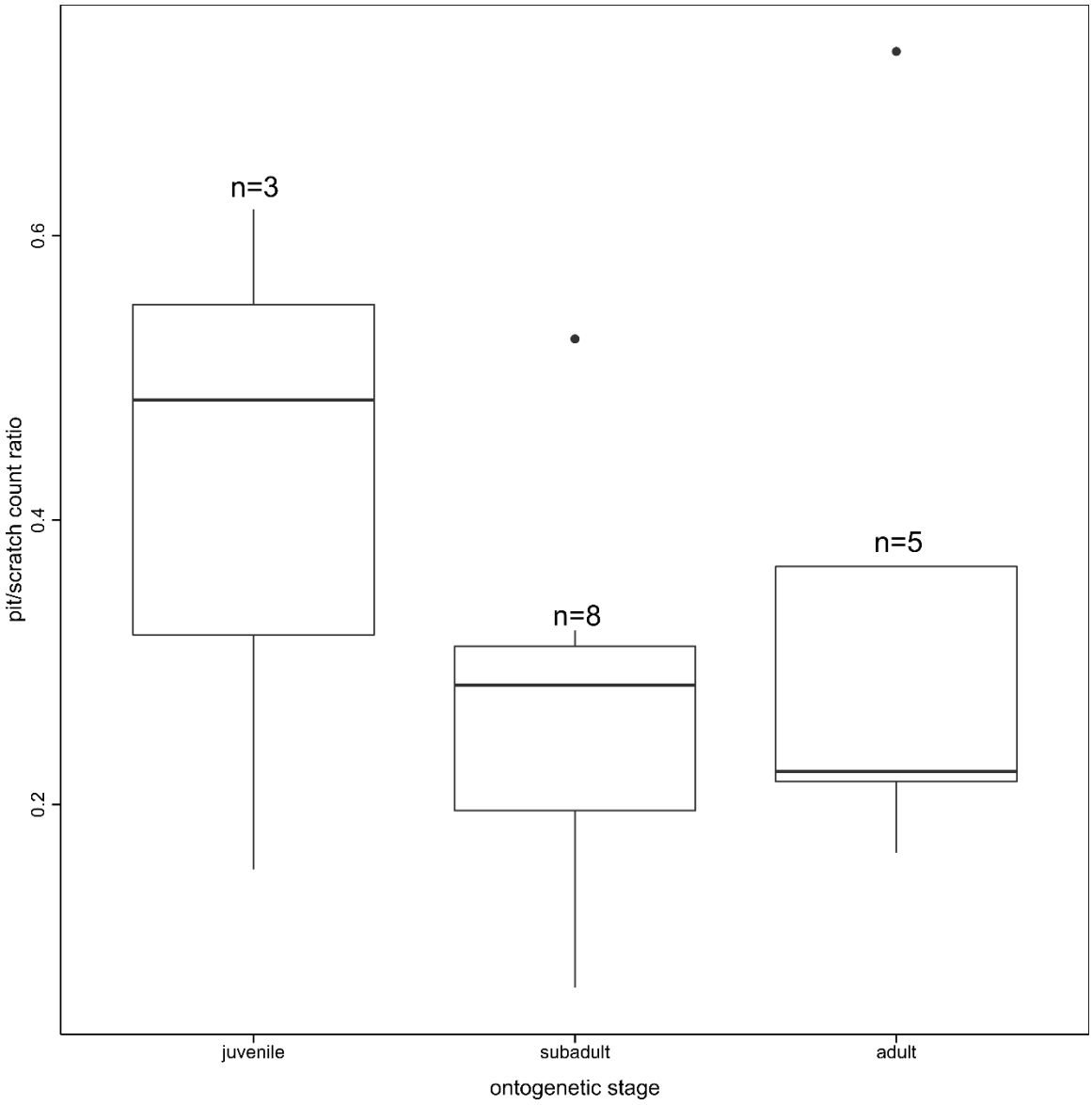

Figure 2.9: Boxplots of pit/scratch ratios for juvenile, subadult and adult hadrosaurids. Sample sizes for each stage are indicated above each boxplot.

Table 2.7: Holm-corrected two-tailed p-values for Kruskal-Wallis tests of pit/scratch count ratios for hadrosaurids by ontogenetic stage. Significant results are in bold. For average values and specimens used see Table 2.2, 2.4 and Appendix C. Abbreviations: J – juvenile, S – subadult, A – adult; df – degrees of freedom; ni – number of individuals.

Comparison	df	Chi-square	p-value	Statistical Conclusion
Hypacrosaurus juvenile (n_i=2) vs subadult (n_i=4)	1	3.429	0.064	J = S
Corythosaurus subadult (n_i=3) vs adult (n_i=2)	1	0	1	S = A
Lambeosaurinae juvenile (n_i=3) vs subadult (n_i=7) vs adult (n_i=2)	2	1.348	0.51	J = S = A
Hadrosaurinae subadult (n_i=2) vs adult (n_i=4)	1	0	1	S = A

main scratch modes that they observed (in order of most to least frequent): class 2 (steep dorsodistal), class 1 (shallow dorsodistal), class 4 (shallow dorsomesial) and class 3 (steep dorsomesial). More recent work by Mallon and Anderson (2014b) and Rivera-Sylva et al. (2019) also observed a dominant set of dorsodistal scratches with a secondary set of mesiodistal scratches. Dorsodistal scratches were interpreted as having formed during an orthopalinal power stroke while mesiodistal scratches were formed by supplemental propalinal motion of the mandible.

The primary dorsomesial and secondary dorsodistal scratch orientations identified in the present study, however, were rarely observed by several of the most recent studies (Williams et al., 2009; Mallon and Anderson; 2014b; Rivera-Sylva et al., 2019). It is likely that the difference in preferred scratch orientations between the current study and previous studies is a result of microwear quality (Teaford, 2007). At higher magnifications, post-mortem damage (e.g., acid etching) becomes more visible, resulting in the elimination of more specimens from analyses (Teaford, 2007; pers. obs.). Higher incidences of acid etching (which tend to occur at higher magnifications), can also obscure more of the tooth surface, making it harder to find multiple areas with wear of high enough quality for analysis. With decreasing sample sizes and reduction in the number of sampling areas on each tooth, obtaining data representative of the general population becomes more difficult. Incomplete sampling along the tooth row is likely the cause of this differential sampling as Mallon and Anderson (2014b) had shown that the preferred dorsodistal scratch orientation was best identified with complete sampling along the tooth row.

Despite differences in directionality, the observed bimodality in adults and larger subadults is consistent with that of Mallon and Anderson (2014b). By comparison, scratch distributions in juveniles and smaller subadults are more weakly constrained and higher modality than those of adults (e.g., juvenile and subadult *Corythosaurus* and *Hypacrosaurus*). Even when scratch orientations are pooled by individual rather than stage, juveniles still appear to exhibit greater variability than adults suggesting that this result is a reflection of an ontogenetic pattern rather than due to individual variability (Appendix E). This greater variability in juvenile scratch orientation/modality may be related to the quality of microwear preserved (at higher magnifications acid etching became more visible and obscured more of the tooth surface), sample size, diet and/or the amount of sutural fusion between the bones comprising the dermal skull roof (Evans, 2007). In more immature individuals, parts of the skull roof are unfused and joints are more cartilaginous permitting greater kinesis within the skull and potentially resulting in greater variability in scratch orientation (Hone et al., 2016).

2.4.2 Diet

Previous work on juvenile hadrosaurids (Erickson and Zelenitsky, 2014) noted cup-shaped occlusal surfaces that appear to have been well-suited for crushing fruits and seeds. This work also noted that subadults exhibited near-vertical occlusal surfaces and adults exhibited a combination of horizontal crushing and vertical shearing surfaces that were hypothesized to have been indicators of folivory and mixed feeding, respectively. From this, significant differences in pit/scratch ratios between juveniles and adults would be expected. However, statistical comparisons at select genus and subfamily levels

indicate no statistically significant differences between ontogenetic stages. Given the small sample sizes (<10 individuals/stage), the lack of statistical significance is likely due to lack of power. Until more specimens are found so that more microwear data can be obtained, it is currently not possible to infer dietary differences between hadrosaurid ontogimorphs based on dental microwear.

Differences in the skull through ontogeny strongly suggests that juveniles subsisted on softer vegetation (such as fruits) than adults. In modern browsers, the anterior portion of the snout is relatively short and positioned above the occlusal plane, the occiput is relatively taller and the width of the snout is relatively narrower than in modern grazers (Janis 1990, 1995; Spencer, 1995; Mendoza, 2002). The less depressed snouts, and shorter faces of juvenile hadrosaurids are shared with modern browsers. The shorter occiputs observed in juveniles suggests that they did not use sharp backward/upward motions of the head to strip plants. Potentially, juvenile hadrosaurids fed on softer vegetation that required minimal effort to pluck. Relatively shorter snouts would have increased mechanical efficiency and increased relative bite forces at the tip of the snout making it easier to pluck softer low-growing vegetation. However, smaller sizes would have meant less muscle mass and, as a result, lower absolute bite forces in juveniles, restricting them to softer vegetation (Mallon and Anderson, 2015). Conversely, the greater absolute bite forces observed in adults in combination with taller occiputs and longer, more depressed snouts would have enabled them to access vegetation of various mechanical resistances growing at different levels.

Although the longer faces of adults would have been useful for the exploitation of a wide variety of plant matter, the underlying cause for the development of this feature

may be related to a conserved evolutionary allometry which has been described in mammals (Cardini and Polly, 2013; Cardini et al., 2015). This research suggests that facial length is strongly constrained by adult size wherein larger animals experience facial lengthening (i.e., positive allometry of the face) and smaller animals are typically more brachycephalic. This trend could also be observed in hadrosaurids (Figure 2.10). The dwarf hadrosaur, *Telmatosaurus* exhibits a relatively shorter face compared to larger, more derived hadrosaurids such as *Edmontosaurus* (Weishampel et al., 1993). Regardless as to why, differences in facial length may have contributed to differences in niche breadth between hadrosaurid ontogimorphs.

Snout shape and width also likely contributed to ontogenetic changes in niche breadth by influencing relative selectivity. Even though no difference in snout shapes or relative snout widths were observed, because of absolute differences in size, the snouts of juvenile and subadult hadrosaurids would have been narrower than those of adults. Thus, changes in overall size of the animal would have resulted in relatively more selective feeding behaviour in juveniles and subadults, and less selective behaviour in adults without necessitating a change in snout shape.

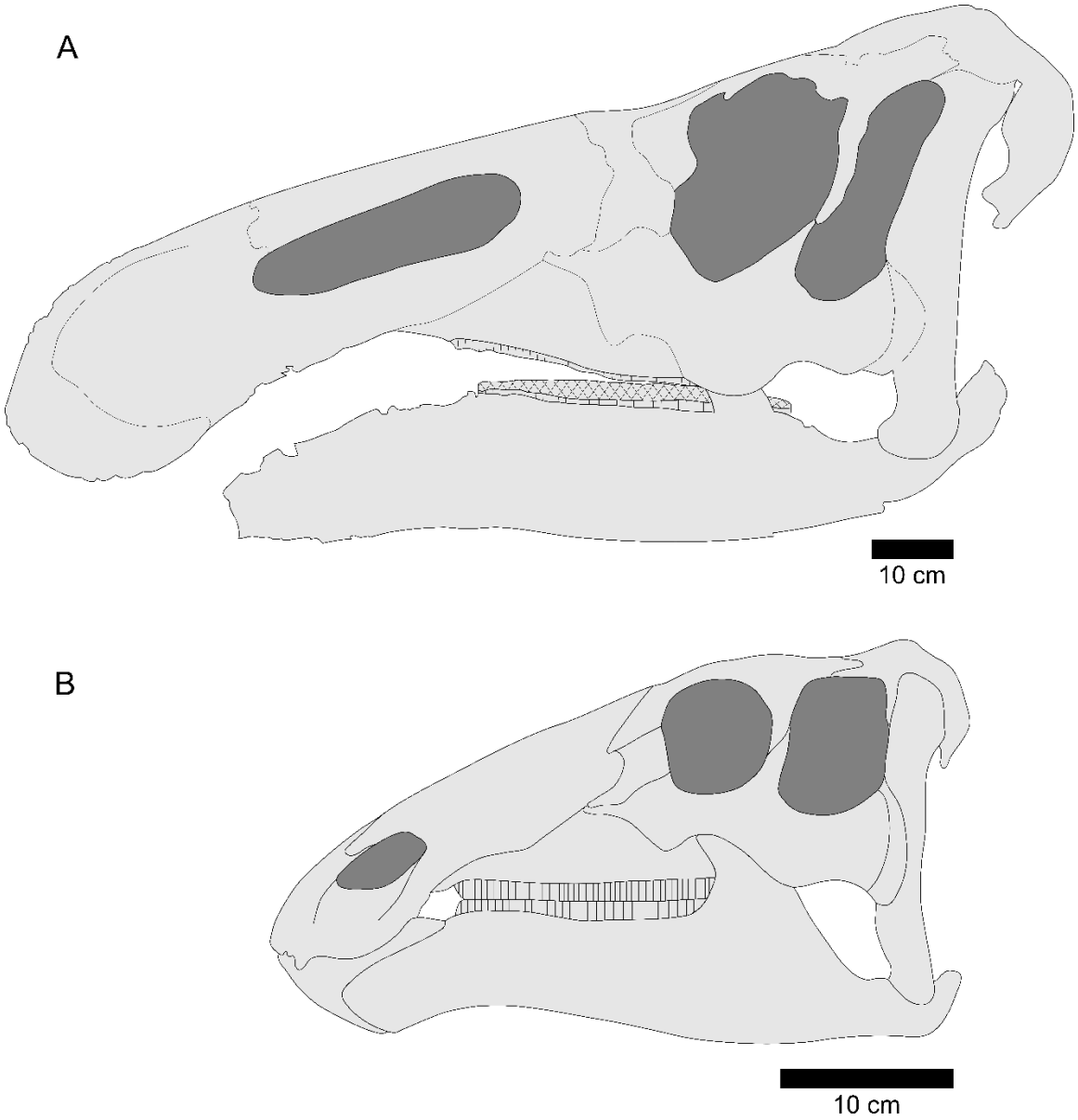

Figure 2.10: Differences in relative facial length between *Edmontosaurus* and *Telmatosaurus*. A) Large adult *Edmontosaurus* skull (MOR 003) (jugal, quadratojugal, distal end of the quadrate and parts of the orbit and postorbital fenestra have been drawn in). B) *Telmatosaurus* composite reconstruction modified from Weishampel et al. (1993). Note: drawings have been scaled so that the distance between the anterior edge of the orbit to the middle of the quadrate is the same to facilitate easier comparison between facial length.

2.5 Conclusions

Many investigations into hadrosaurid ontogeny have been conducted focusing on cranial crest and overall skull development (e.g., Dodson, 1975b; Evans, 2010; Campione and Evans, 2010; Farke et al., 2013; McGarrity et al., 2013) but very few studies have considered the potential dietary implications of growth (Erickson and Zelenitsky, 2014). The present study explored the dietary implications of growth in hadrosaurids by investigating differences in ecomorphological correlates between ontogenetic stages.

Hadrosaurid skull allometry and snout shape are consistent with ONSs in hadrosaurids. However, these results may be under or over representing actual trends observed in the overall population due to reduced sampling at small body sizes as some variability within the population is left unaccounted for. Pending the discovery of more juvenile specimens, the present work is currently the best available estimate of what hadrosaurid ontogenetic niche shifts may have looked like in Late Cretaceous North America. After more juvenile material is recovered, future work involving a greater number of immature individuals, and more complete sampling of microwear along the tooth row, will be needed to determine if the interpretations of the present study are supported at larger sample sizes. Additionally, investigations aimed at quantifying differences in the occlusal morphology of the tooth row between ontogenetic stages could be conducted to further support the potential for ONSs and better distinguish dietary habits of different ontogimorphs (Melstrom, 2012).

Multimodality of scratch orientations in juvenile specimens may also have important biomechanical implications. Earlier work on hadrosaurids proposed a pleurokinetic chewing model in hadrosaurids on the basis of occlusal morphology

(Weishampel, 1983, 1984; Norman and Weishampel, 1985). More recent work rejected this pleurokinetic model based on the relative immobility of cranial joints (Holliday and Witmer 2008; Rybczynski et al., 2008; Cuthbertson et al., 2012. However, all work has focused on kinesis in adult skulls with little consideration of the kinematics of juveniles. The multimodality of scratch orientations as well as lack of sutural fusion of the dermal skull roof (Evans, 2007) may indicate that juvenile skulls were more kinetic than their adult counterparts.

Future investigations into evolutionary allometry of facial length may also prove interesting. In modern placental mammals and macropodids, taxa with small adult body sizes have been shown to have shorter faces and taxa with large adult body sizes to have longer faces as part of a conserved evolutionary allometry across all mammalian clades (Cardini and Polly, 2013; Cardini et al., 2015). Thus, the positive allometry observed in hadrosaurid facial length, and the relatively shorter faces in smaller hadrosauroids such as *Telmatosaurus* (Weishampel et al., 1993), raises the question as to whether this is a broader evolutionary constraint that is observed in ornithopods, or even amniotes as a whole.

Evidence supporting the potential for an ONS in hadrosaurids has important implications for the structuring of Late Cretaceous ecosystems. Previous work showed that competition between adult hadrosaurines and lambeosaurines was mediated by ecomorphological differences (Mallon, 2019). The findings of this chapter suggest that intra-specific competition in hadrosaurids was also mediated by ecomorphological differences. Because different ontogenetic stages occupied different roles, and body size is one of the main mechanisms through which resources are partitioned (Werner and

Gilliam, 1984), juvenile hadrosaurids may have instead potentially competed with other similar-sized dinosaurs including juvenile ceratopsids, and adult small ornithischians such as leptoceratopsids, pachycephalosaurids and thescelosaurids. The potential impacts that hadrosaurid ONSs had in Late Cretaceous ecosystems will be further explored in chapter 4.

Chapter 3: Ontogenetic niche shifts in ceratopsids of Late Cretaceous North America

3.1 Introduction

3.1.1 What is a ceratopsid?

Ceratopsids (also known as horned dinosaurs) were a clade of quadrupedal, herbivorous dinosaurs that inhabited Late Cretaceous North America and Asia (Dodson et al., 2004; Chinnery-Allgeier and Kirkland, 2010; Xu et al., 2010). Well-known for their elaborate frill and horn morphologies, these dinosaurs grew to large sizes (~2500 kg) with some reaching lengths of 8 m. Ceratopsids are reported from the Turonian (~91 Ma) through to the end of the Cretaceous (~65.5 Ma) and have been collected in North America from localities from Alaska through to Mexico.

There are two ceratopsid subclades: Centrosaurinae and Chasmosaurinae (Dodson et al., 2004). Most chasmosaurines (e.g., *Anchiceratops, Pentaceratops*) have a frill that is more elongate than that of the centrosaurines (e.g., *Centrosaurus*). The frills and nasal horns of ceratopsids are thought to serve one or more purposes including predator defense (Sternberg, 1917), body temperature regulation (Wheeler, 1978), species recognition and sexual display (Sampson, 1997). The frills of ceratopsids are extremely large and ranges from 60% to just over 100% basal skull length.

Ceratopsids possessed dental batteries that were used for the mastication of tough and fibrous plant matter (Ostrom, 1966; Mallon and Anderson, 2014b). Ceratopsid dental batteries are relatively simple compared to those observed in hadrosaurids in that only a single functional tooth is observed in each tooth family. Beneath each functional tooth are three to five replacement teeth. These teeth are arranged so that the crown of a tooth

nestles into the split root of the tooth above it, forming a dental battery. Such an arrangement is thought to have provided stability, ensured continuous tooth replacement and provided a single, continuous cutting surface (Ostrom, 1966).

3.1.1.1 Ceratopsids and ontogenetic niche shifts

In modern ecosystems, resource partitioning can be facilitated by differences in body size (Werner and Gilliam, 1984; ten Brink and de Roos, 2018). Resources can be partitioned intra-specifically when different ontogenetic stages occupy different ecological niches (commonly called an ontogenetic niche shift or ONS) (Werner and Gilliam, 1984). These differences in diet and/or habitat through ontogeny can be facilitated by changes in body size and/or morphology.

Many extant vertebrates, including those comprising the extant phylogenetic bracket for ceratopsids, undergo ONSs. In crocodilians, isometric growth of the skull and positive allometry of the snout facilitate ONSs by allowing progressively larger prey items to be consumed (Dodson, 1975a; Platt et al., 2006). Changes in body size also facilitate ONSs in loggerhead sea turtles (*Caretta caretta*) (Ramirez et al., 2017). For the first 10 years of life, loggerhead sea turtles inhabit and consume *Sargassum* sea matts until they attain a certain size (Ramirez et al., 2017) At this size, loggerhead turtles become free-roaming and consume benthic prey. This may be partly related to larger turtles being unable to sustain themselves on the *Sargassum* matts. These shifts also facilitate the segregation of different size classes; where smaller turtles inhabit oceanic habitats and larger turtles inhabit neritic habitats. Some birds also exhibit ONSs. In the crested tern (*Sterna bergii*), for example, adults primarily consume Degen's

leatherjackets (*Thamnaconus degeni*) and barracoota (*Thyrsites atun*) while the chicks sustain mainly on clupeids fed to them by the adults (McLeay et al., 2009).

Similar to crocodilians, ceratopsids may have experienced long growth trajectories where rapid growth occurred in the first few years and was followed by several years of slower growth (Sampson, 1997; Lehman, 2006; Reizner and Horner, 2006; Erickson and Druckenmiller, 2011). Most studies indicate that ceratopsids attained a near-adult body size from anywhere between six and 20 years of age (Currie and Dodson, 1984; Reizner and Horner, 2006; Erickson and Druckenmiller, 2011; Mallon et al., 2016). The different body sizes and needs of sexually immature (e.g., food) and mature (e.g., nesting sites, territory, food) animals may have also led to the formation of size-segregated aggregations in ceratopsids. This formation is evidenced by the recovery of many large ceratopsid specimens—meaning that these individuals were at or near full adult size at death—and the relative scarcity of juvenile individuals (Lehman, 2006; Table 3.1). This could be partially attributed to taphonomic biases. However, there have been instances where the disarticulated remains of multiple juvenile individuals have been preserved (e.g., Triceratops sp. Hell Creek Homer site, collection of Brachyceratops montanensis from the Two Medicine formation) and lack any indications that extraordinary preservational processes were occurring (Gilmore 1914; Hunt and Farke, 2010; Mathews et al., 2012).

Table 3.1: Select ceratopsid bonebeds from Late Cretaceous North America. Abbreviations: Fm-Formation, BB-bonebed, MNI-minimum number of individuals.

Locality	Ceratopsid Taxon/Taxa present	Ontogenetic stage(s) present	Reference(s)
Homer Site (Hell Creek Fm, Montana)	*Triceratops* sp.	Juvenile (MNI=3)	Mathews et al., 2012
Quitten Time BB (Hell Creek Fm, Montana)	*Triceratops* sp.	Juvenile to young adult (MNI=?)	Keenan and Scannella, 2014
"South Side Ceratopsian" BB (Oldman Fm, Alberta)	*Wendiceratops pinhornensis*	Juvenile and adult (MNI=4)	Evans and Ryan, 2015
Kikak-Tegoseak Quarry (Prince Creek Fm, Alaska)	*Pachyrhinosaurus perotorum*	Subadult (MNI=9)	Fiorillo et al., 2010; Fiorillo and Tykoski, 2012
Pipestone Creek BB (Wapiti Fm, Alberta)	*Pachyrhinosaurus lakustai*	Juvenile to adult (MNI=27)	Currie et al., 2008
Scabby Butte (St. Mary River Fm, Alberta)	*Pachyhrinosaurus canadensis*	?- adult (MNI=27)	Hunt and Farke, 2010
Centrosaurus BB 43/ Quarry 143 (Dinosaur Park Fm, Alberta)	*Centrosaurus apertus*	Juvenile to adult (MNI=47)	Ryan and Russell, 2001
? (Judith River Fm, Montana)	*"Brachyceratops montanensis"*	subadult (MNI=5)	Gilmore 1914; Hunt and Farke, 2010
TMM 41361 (Javelina Fm, Texas)	*Torosaurus utahensis*	Juvenile and adult (MNI=3)	Hunt and Lehman, 2008
Mansfield BB (Judith River Fm, Montana)	*Medusaceratops lokii*	?- adult (MNI=?)	Ryan et al., 2010
Bluewash BB	*Utahceratops gettyi*	Juvenile to adult (MNI=3)	Levitt, 2013
WPA-1 BB (Aguja Fm, Texas)	*Agujaceratops mariscalensis*	Juvenile to adult (MNI=20)	Lehman, 2006

3.1.1.2 Chapter goals

Some ceratopsid genera (e.g., *Triceratops*) have multiple growth stages (from juveniles to adults) preserved (e.g., Goodwin et al., 2006; Horner and Goodwin, 2006, 2008; Campbell et al., 2016). This makes them a suitable fossil group in which to investigate ONSs. Investigations into how cranial ecomorphology, snout shape and dental microwear may have changed during ontogeny will be the focus of this chapter.

Despite multiple studies on ceratopsid ontogeny, none have focused on the implications that growth had on diet. Most studies have focused on frill and horn development, with some also investigating overall skull development (e.g., Sampson, 1997; Goodwin et al., 2006; Tumarkin-Deratzian, 2009; Longrich and Field, 2012; Frederickson and Tumarkin-Deratzian, 2014; Konishi, 2015; Mallon et al. 2015; Campbell et al., 2016). No predictions have been made regarding ONSs in ceratopsids, and none have tested this specifically from an ecomorphological perspective.

Like the hadrosaurids investigated in Chapter 2, ceratopsids also underwent a change in body size spanning several orders of magnitude through growth (Reizner and Horner, 2006; Erickson and Druckenmiller, 2011; Mallon et al., 2016), and so likely exhibited ONSs. Using concepts, definitions and methods previously discussed in Chapter 2, this chapter aims to investigate ceratopsid ONS using ecomorphological correlates of the skull, snout shape analysis and dental microwear analysis.

3.2 Methods

The ecomorphological correlates used in Chapter 2 for hadrosaurids were also used for ceratopsids. For this reason, only deviations from the methodologies established

in Chapter 2 will be noted. Species preserving relatively complete individuals from multiple ontogenetic stages were used to investigate ceratopsid ONSs. This includes the chasmosaurines *Chasmosaurus belli, Ch. russelli, Chasmosaurus* sp. *Triceratops horridus, T. prorsus* and *Triceratops* sp., and the centrosaurine *Centrosaurus apertus* (Sampson, 1997; Goodwin et al., 2006; Lehman, 2006; Frederickson, and Tumarkin-Deratzian, 2014; Campbell et al., 2016; Currie et al., 2016).

3.2.1 Skull allometry

Skull allometry was analyzed using the same twelve linear measurements in Chapter 2 (Figure 3.1). However, unlike for hadrosaurids, snout to mid-quadrate length (herein referred to as skull length) was used as a proxy for skull size because it is unknown how quadrate height scales with skull size in ceratopsids.

There are few examples of intact juvenile ceratopsids. Thus, it was necessary to include composite specimens constructed by scaling and combining elements from various individuals into a single skull. The inclusion of such composites may therefore be a potential source of error in the dataset. However, these composites were included because they were based on real material and deemed adequate representations of real individuals. To the extent that the reconstructions are erroneous, so too will be my functional interpolations.

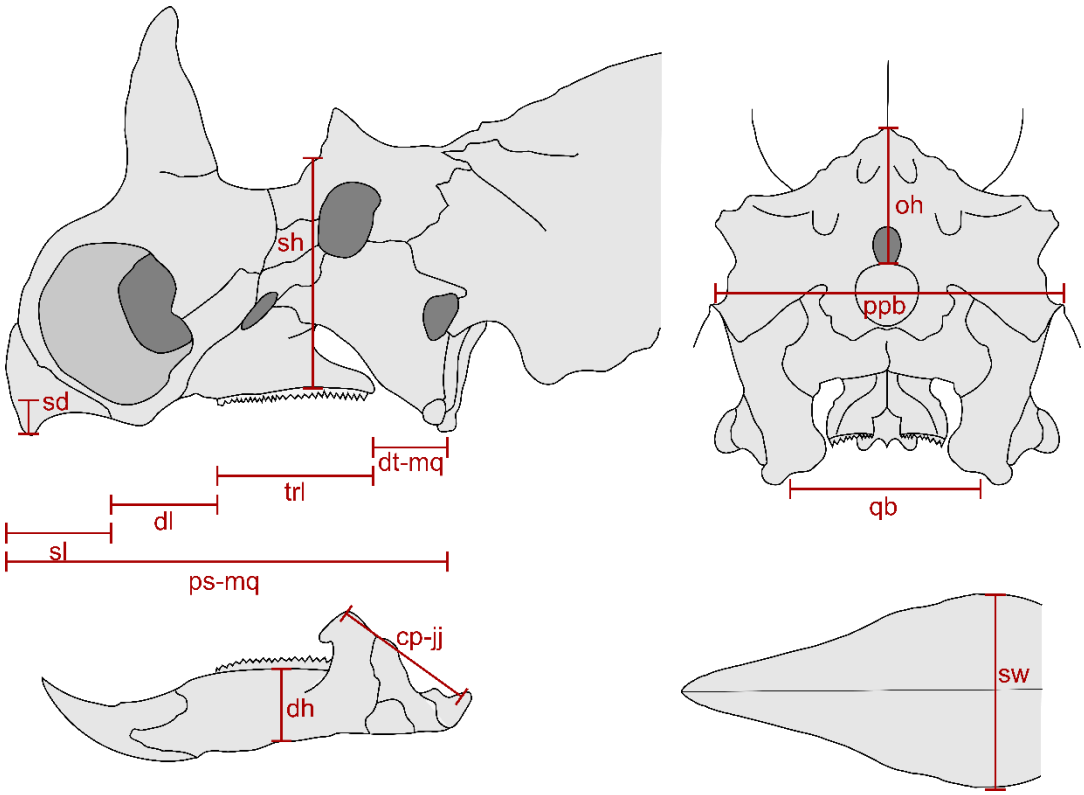

Figure 3.1: Linear measurements used for cranial morphometric analysis of ceratopsid specimens (modified from Mallon and Anderson, 2013). Abbreviations – ps-mq: distance from jaw joint to rostral beak tip referred to as skull length in text; sl: snout length; dl: diastema length; trl: tooth row length; dt-mq: distance from distal end of tooth row to middle ; sw: maximum beak width; dh: midpoint dentary height; ppb: paroccipital process breadth; oh: occiput height; cp-jj: distance apex of coronoid process to middle of jaw joint; sd: depression of snout below occlusal plane; sh: skull height; qb: distance between quadrates.

Specimen maturity was gauged with reference to bone texture, size, and degree of suture closure (Sampson, 1997; Goodwin et al., 2006; Tumarkin-Deratzian, 2009; Longrich and Field, 2012; Frederickson and Tumarkin-Deratzian, 2014; Konishi, 2015; Campbell et al., 2016). In ceratopsids, the fusion of epijugal to the jugal and quadratojugal, fusion of the nasals, and the articulation of epiossicifications to the posterior margin of the frill occurs at the subadult stage. The contacts between epijugal to the jugal and quadratojugal, the two nasals, and the epiossicifications and posterior margin of the frill are obliterated in adults. Contacts between the frontals, and the frontals and postorbitals are also closed in adults and then later obliterated later in life. The degree of development of cranial ornamentation (especially frill ornamentation) was another indicator of relative immaturity used to distinguish between ontogenetic stages in the present study.

Juveniles were defined as individuals that possessed short, underdeveloped frills and horns (Figure 3.2), and had little to no sutural closure. Subadults possessed moderately developed frills and horns and some sutural closure. Adults were identified by the possession of almost completely or completely developed frills and horns/partially resorbed horns and sutural fusion. Because subadults and juveniles were the most difficult to distinguish, and due to small sample sizes, juveniles and subadults were grouped together to form an “immature” category in many of the analyses.

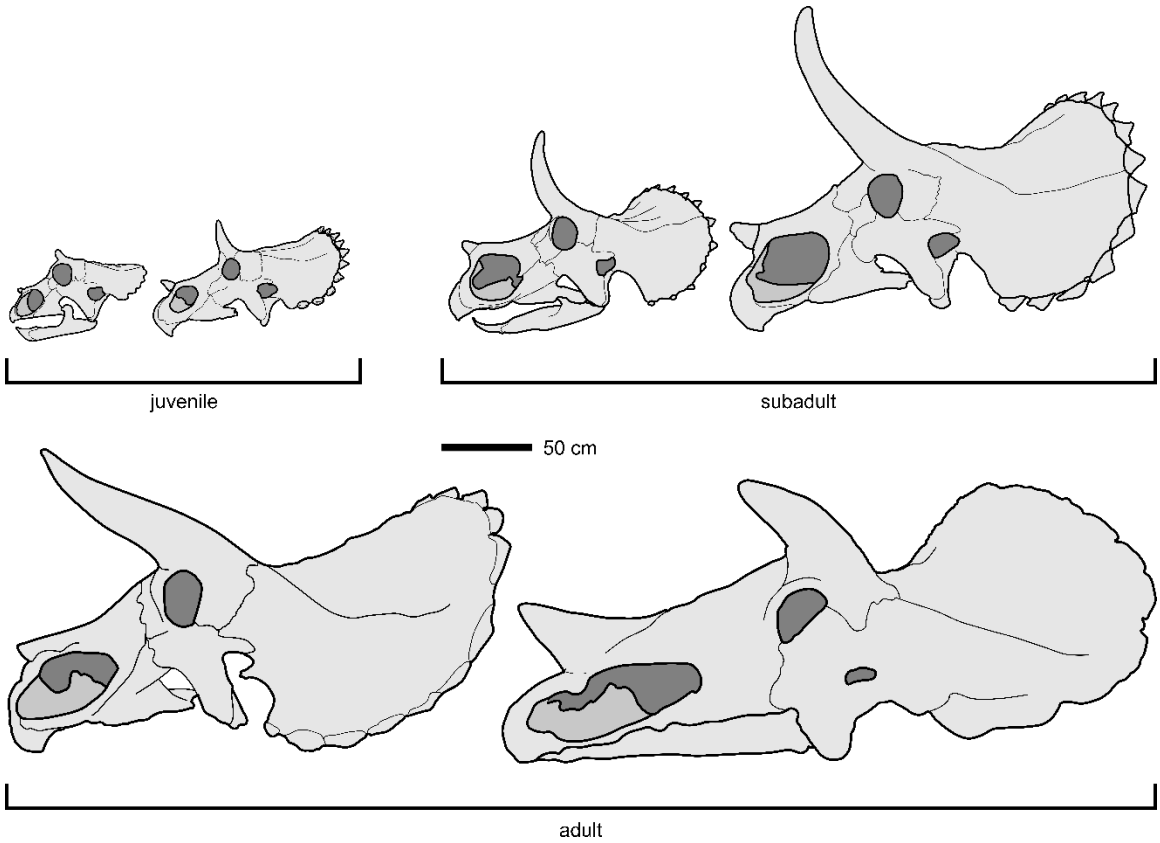

Figure 3.2: Determination of basic ontogenetic classifications in ceratopsids based on sutural fusion, relative frill development and relative development of the nasal and orbital horns. Specimen numbers for illustrated *Triceratops* specimens (from left-to-right, top-to bottom): UCMP 154452, MOR 2569, MOR 2951, MOR 1110, MOR 1120, and MOR 004.

After measurements were collected in a Microsoft Excel file, data were imported into the programming platform R to conduct subsequent data manipulation (R Core Team, 2019). For reduced major axis regressions (RMA), log-transformed values of the linear measurements of interest were plotted against log-transformed skull length, a proxy for body size, to identify positively allometric, negatively allometric and (softly) isometric trends using the exclusion/inclusion of 1 in confidence intervals as in the previous chapter (see Chapter 2 for details). Because some variables such as snout, diastema and tooth row length are measured along the same axis of the skull as the size parameter (skull length), there is potential for autocorrelation. To investigate this, Holm-corrected Durbin-Watson tests were conducted and the results are discussed below.

Slopes and intercepts of regressions between centrosaurines and chasmosaurines were also compared to determine if separate regressions should be used for centrosaurines and chasmosaurines, or if these subfamilies could be lumped together for an overall regression of a larger ceratopsid dataset.

3.2.2 Snout shape

To investigate potential changes in snout shape through ontogeny, the snout shape analysis method used in Chapter 2 was also employed for ceratopsids (Figure 3.3).

Snout shape index was regressed against skull length to identify potential shape changes through ontogeny. A Kruskal Wallis test was also conducted to compare snout shape between immature and mature ceratopsids and post-hoc pairwise comparisons were conducted using Mann-Whitney U tests with Holm-corrections as needed (see Chapter 2 for details).

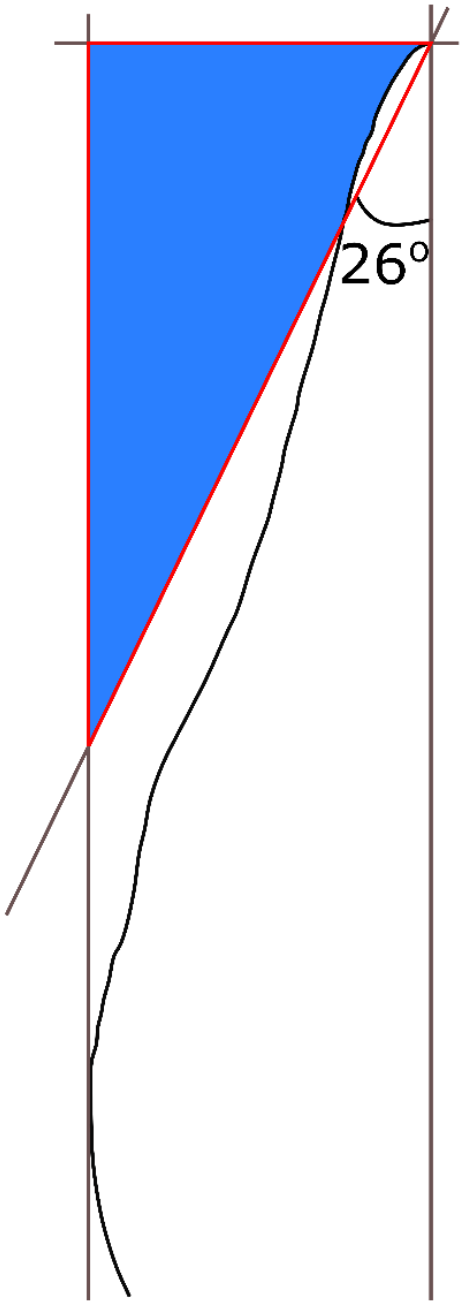

Figure 3.3: Snout shape analysis conducted for ceratopsids based on Dompierre and Churcher (1996). Blue region denotes the area of negative space measured for analysis. Red triangle indicates the triangle area measured for analysis.

3.2.3 Tooth wear analysis

Dental microwear was also quantified for ceratopsids at different ontogenetic stages to identify potential dietary differences through ontogeny. Intact teeth from both the maxillae and dentaries were sampled to increase possible sample size using the methodology previously discussed in Chapter 2. However, unlike hadrosaurids, small ceratopsids, especially those with teeth are rare and sample sizes are relatively small. Only scratch modality could be qualitatively compared as statistical comparisons between ontogenetic stages could not be conducted due to small sample sizes.

3.3 Results

3.3.1 Skull allometry

Raw measurements used for the skull morphometric analysis are provided in Appendix F. Sample sizes for the three ontogenetic stages previously discussed are provided in Table 3.2. Holm-corrected Durbin-Watson tests also indicate no significant autocorrelation for any of the variables tested (Appendix G). There were no statistical differences in slope or intercept between chasmosaurines and centrosaurines for all variables considered (Table 3.3). Positive allometry was observed for snout depression, paroccipital process breadth, snout length, diastema length, quadrate breadth and distance from the distal end of the tooth row to middle of the quadrate (Table 3.4; Figure 3.4). Negative allometry was observed in the distance from the jaw joint to coronoid process apex in both chasmosaurines and centrosaurines. Isometry could not be rejected for all other variables.

Table 3.2: Sample sizes for ceratopsid specimens used in analyses. Note: for reduced major axis regression analysis the numbers provided are maximum possible sample sizes as the actual sample size used varied based on what measurements could be obtained from each specimen.

Classification	Stage	Analysis		
		Reduced major axis regression	Snout shape	Dental microwear
Ceratopsidae indet.	Juvenile	0	0	1
Centrosaurinae (overall)	Juvenile	1	1	0
	Subadult	1	1	1
	Adult	13	10	1
Brachyceratops	Juvenile	1	1	0
Centrosaurus	Subadult	1	1	1
	Adult	11	8	1
"pachyrhinosaur"	Adult	1	1	0
Pachyrhinosaurus	Adult	1	1	0
Anchiceratops	Adult	1	1	0
Chasmosaurinae (overall)	Juvenile	3	5	0
	Subadult	4	2	0
	Adult	23	17	1
Chasmosaurus	Juvenile	1	1	0
	Subadult	0	0	0
	Adult	7	7	1
Triceratops	Juvenile	2	4	0
	Subadult	4	2	0
	Adult	12	8	0
Torosaurus	Adult	1	0	0

Table 3.3: Results for test of equivalent slopes and intercepts for regressions of various variables against skull length between centrosaurines and chasmosaurines. Abbreviations: nCe-number of centrosaurines; nCh- number of chasmosaurines; LR-likelihood ratio; SSI-snout shape index. Statistically significant p-values are in bold. Reported p-values have been adjusted for multiple comparisons using the Holm-method.

Log-transformed Y variables	nCe	nCh	LR statistic (slope)	p-value slope	Wald statistic (intercept)	p-value intercept
snout length	15	30	0.04	1	8.129	0.052
diastema length	15	30	1.138	1	0.026	1
tooth row length	15	28	1.619	1	2.547	0.773
distal end tooth row to mid quadrate	14	30	2.381	1	4.13	0.421
snout width	15	28	3.047	0.971	0.827	1
height dentary	12	15	0.924	1	3.094	0.638
paroccipital process breadth	11	22	0.22	1	8.326	0.051
occiput height	10	16	4.07	0.568	3.261	0.638
distance jaw joint to coronoid process	10	14	0.648	1	0.061	1
snout depression	15	25	0.067	1	4.406	0.394
skull height	15	30	0.054	1	1.818	1
distance between quadrates	13	23	0.018	1	0.964	1
SSI	12	24	0.243	1	0.101	1

Table 3.4: Values obtained from reduced major axis regression of ceratopsid variables against skull length. Abbreviations: grp-grouping; C-Ceratopsidae; SSI-snout shape index; i-isometry; - negative allometry; + positive allometry; NS-non significant slope. Note: SSI does not show a slope significantly different from 0 and so it was not graphed with the other variables. Reported p-values have been adjusted for multiple comparisons using the Holm-method.

Log-transformed Y variables	grp	n	R^2	2-tailed p	intercept	95% CI intercept	slope	95% CI slope	trend
snout length	C	45	0.766	4.55E-14	-1.448	-1.985 to -0.91	1.269	1.095 to 1.472	+
diastema length	C	45	0.561	1.96E-08	-2.538	-3.506 to -1.57	1.669	1.363 to 2.043	+
Tooth row	C	43	0.86	5.65E-18	-0.345	-0.678 to -0.013	0.99	0.88 to 1.114	i
distal tooth row-mid quadrate	C	44	0.338	1.39E-04	-2.137	-3.174 to -1.1	1.437	1.118 to 1.846	+
snout width	C	43	0.645	6.35E-10	-0.996	-1.567 to -0.424	1.072	0.89 to 1.292	i
height dentary	C	27	0.841	1.4E-10	-0.676	-1.118 to -0.234	0.95	0.807 to 1.119	i
paroccipital process breadth	C	33	0.667	3.39E-08	-0.943	-1.684 to -0.203	1.245	1.009 to 1.536	+
occiput height	C	26	0.232	0.026	-1.433	-2.726 to -0.139	1.24	0.864 to 1.78	i
coronoid process apex - mid jaw joint	C	24	0.94	7.38E-14	-0.081	-0.334 to 0.173	0.825	0.741 to 0.92	-
snout depression	C	40	0.202	0.011	-4.575	-6.374 to -2.776	2.151	1.61 to 2.872	+
skull height	C	45	0.703	6.8E-12	-0.372	-0.86 to 0.115	1.022	0.865 to 1.207	i
quadrate breadth	C	36	0.758	4.77E-11	-1.173	-1.801 to -0.544	1.3	1.096 to 1.542	+
SSI	C	36	0.064	0.137	-1.38	-1.811 to -0.948	0.452	0.325 to 0.629	NS

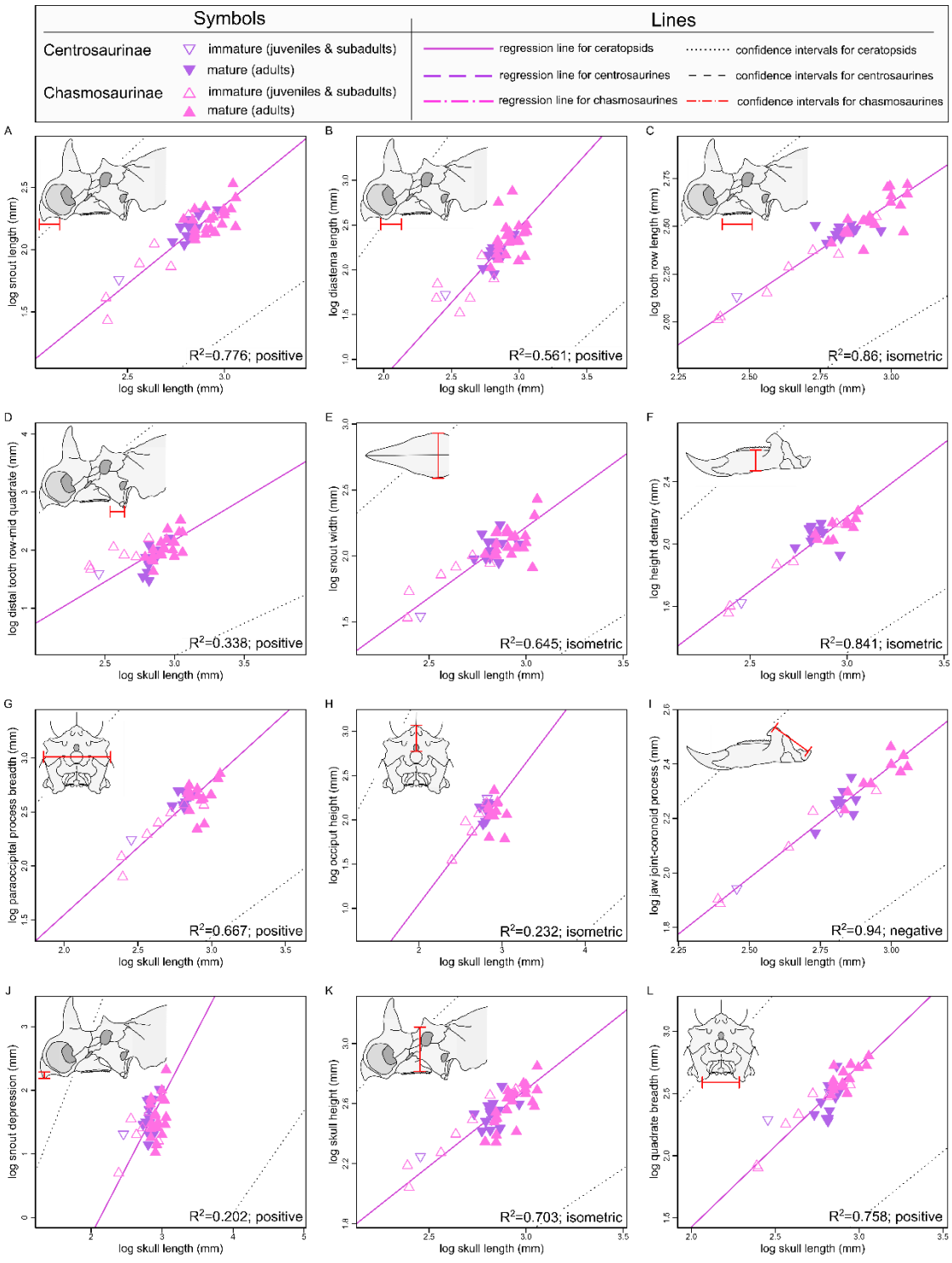

Figure 3.4: Bivariate allometric plots for reduced major axis regression of log-transformed ceratopsid cranial variables. A) snout length, B) diastema length, C) tooth row length, D) distal tooth row to middle quadrate length, E) snout width, F) dentary height, G) paroccipital process breadth, H) occiput height, I) distance from coronoid process to jaw joint, J) snout depression below occlusal plane, K) skull height, L) distance between quadrates. Positive allometry is observed for variables in plots A, B, D, G, J, and L. Negative allometry observed for variables in plot I.

3.3.2 Snout shape

Raw snout shape data are provided in Appendix H. Sample sizes are provided in Table 3.2. There is no linear relationship between SSI and skull length (Table 3.4) and so a bivariate plot of SSI against skull length is shown (Figure 3.5). On the SSI axis, immature ceratopsids appear to occupy the same range as mature ceratopsids. Overlap is generally observed between centrosaurines and chasmosaurines, and is supported by the results of the Kruskal-Wallis ($p=0.1465$). Centrosaurines and chasmosaurines with skull lengths <300 mm or >950 mm do not show complete overlap in the morphospace. This lack of overlap at the smallest and largest skull sizes is likely a result of reduced sampling of small individuals and the larger sizes attained by chasmosaurines, respectively.

3.3.3 Microwear

Dental microwear was recovered for an indeterminate juvenile ceratopsid (n=1), subadult (n=1) and adult *Centrosaurus* (n=1), and an adult *Chasmosaurus* (n=1) (Appendix I; Figure 3.6; Table 3.2). *Chasmosaurus* and *Centrosaurus* were used because the stratigraphic and temporal position of the juvenile ceratopsid specimen (upper Campanian Dinosaur Park Formation, Alberta) was similar to these two species and therefore these species were the most likely adult candidate of this juvenile specimen. Other small ceratopsid jaws are known; however, they either lack intact dentitions (UCMP 154452, *Triceratops*), have dentitions with inaccessible occlusal surfaces (UALVP 526342, *Chasmosaurus*) or have no preserved microwear (MOR 1999, *Triceratops*).

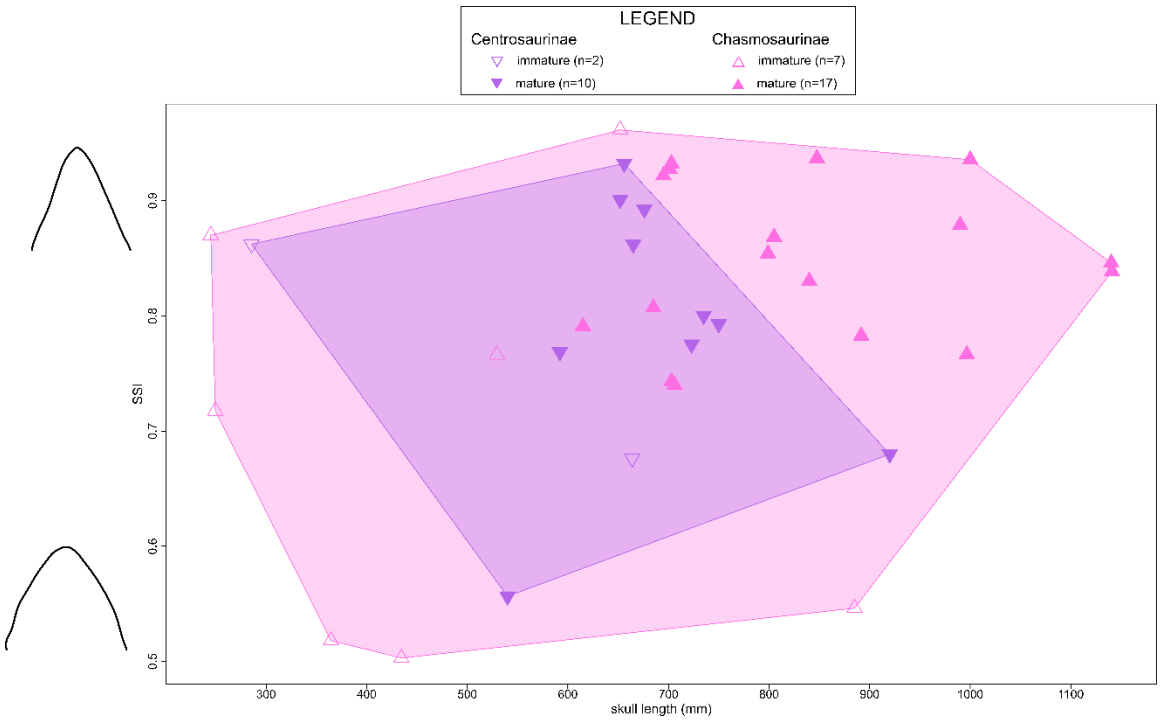

Figure 3.5: Snout shape plot for ceratopsid specimens. Snout outlines indicate relative differences in snout shape corresponding to different SSI values at opposite ends of the y-axis. Abbreviations: SSI-snout shape index.

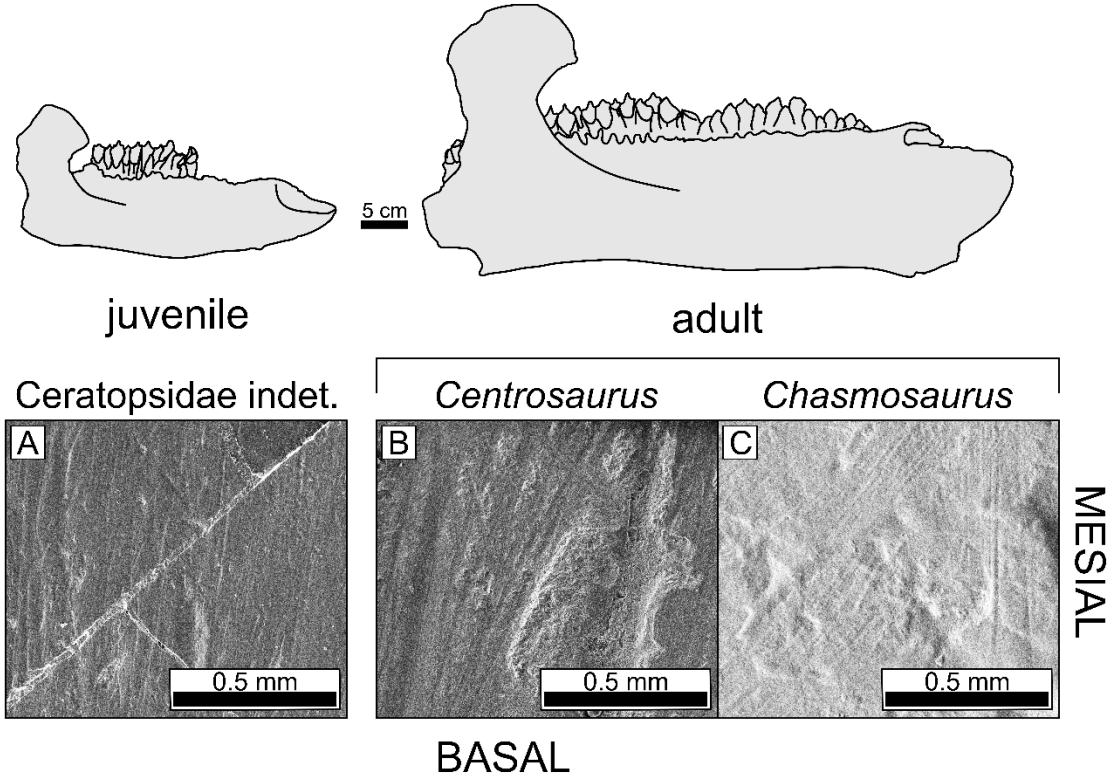

Figure 3.6: Microwear recovered from juvenile and adult ceratopsids. All photos have been standardized to the right dentary and oriented so that the tooth apex is directed upwards. Microwear recovered from A) juvenile ceratopsid (UC 16624 LD5), B) adult *Centrosaurus* (TMP 1997.085.0001 RD24), C) adult *Chasmosaurus* (CMN 8801 RD11). Line drawings for juvenile and adult ceratopsids jaws are based off of the *Triceratops* dentaries (from left to right) MOR 1199 and MOR 2574.

The pooled results in the juvenile ceratopsid are multimodal, and bimodal in subadult and adult ceratopsids (Figure 3.7). Each pooled rose diagram represents the scratch distributions for a single individual and therefore any variability observed is not due to the variability between individuals. It is also possible that there will be more variability in specimens where more teeth from along the row have been sampled. The greater distribution observed between adults and juveniles is likely a real signal because scratch variability (especially for scratches longer than 0.5 mm) is greater in the juvenile ceratopsid compared to the adult *Chasmosaurus*, even though there are more teeth sampled for the adult *Chasmosaurus* (n_t=7) than the juvenile (n_t=4). If the greater variability in juveniles was entirely due to variation as a result of more teeth being sampled in a given specimen, then the juvenile should have less variability when compared to the adult *Chasmosaurus* which has more teeth from along the tooth row sampled. Rose diagrams for individual teeth along the tooth row for the ceratopsid specimens considered are provided in Appendix J and not discussed here.

In the juvenile ceratopsid, steeply inclined dorsodistally oriented scratches are the longest (> 1 mm) and most common, followed by shallower dorsodistal scratches (≤0.75 mm) and steeper dorsomesial scratches (≤0.75 mm). Short scratches (≤0.25 mm) are recovered from all angles. In subadult *Centrosaurus*, longer (> 1 mm), dorsodistal scratches are present in similar proportions to shorter (≤0.75 mm) dorsomesial scratches. Scratches in adult *Centrosaurus* are long (> 1mm) and primarily mesiodistally oriented with a secondary set of equally long, but less frequent dorsodistal scratches. In adult *Chasmosaurus*, the longest scratches are oriented dorsomesially (>1 mm) while the

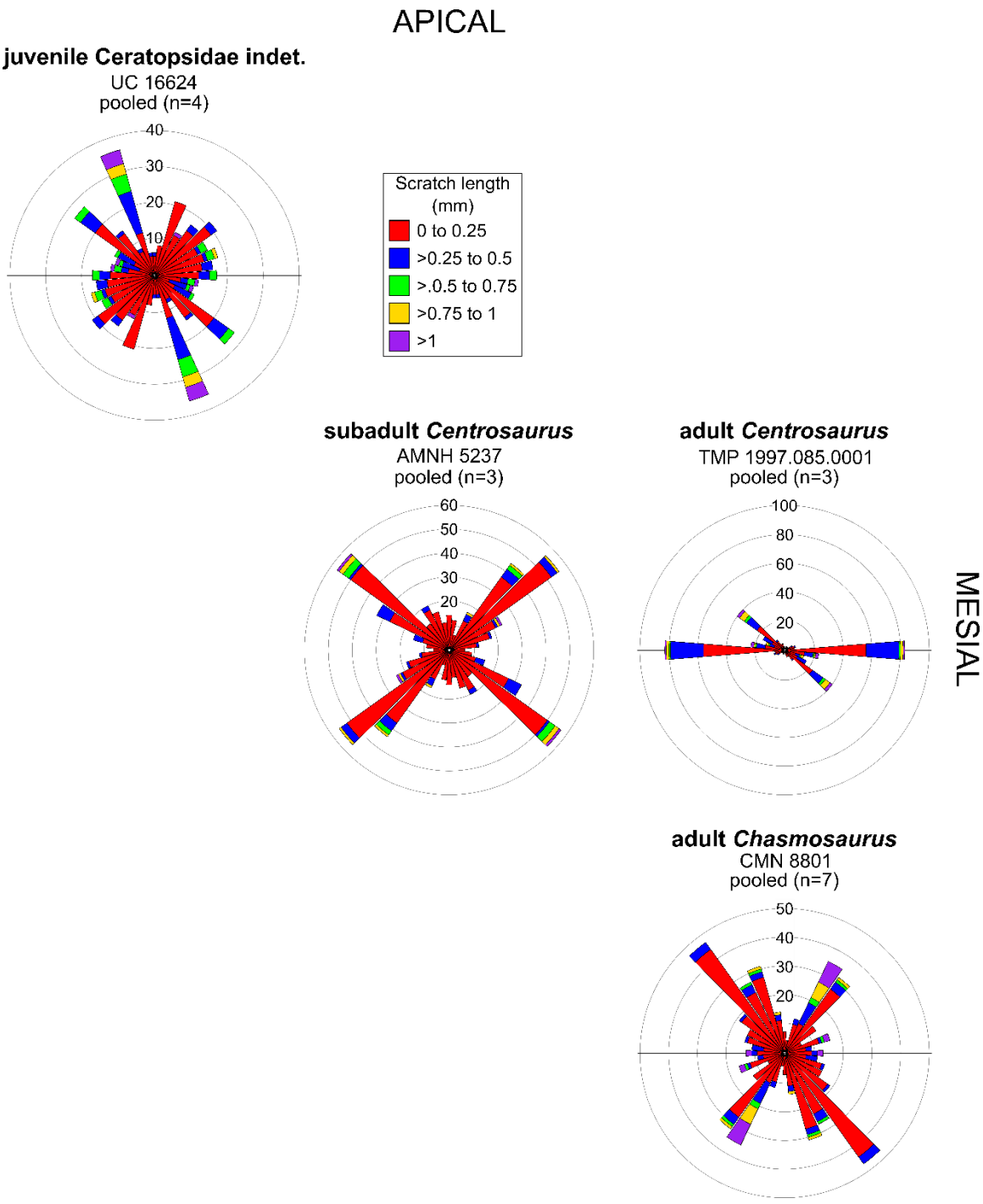

Figure 3.7: Rose diagrams for overall scratch orientation for individual juvenile, subadult and adult ceratopsids. All teeth are standardized to the right dentary. Number of teeth used to construct each rose diagram is indicated by "n=". Mesial= 0º, distal=180º, Apical/dorsal=90º, Basal/ventral=270º.

greatest number of scratches are steeply inclined and oriented dorsodistally (≤0.5 mm). A few longer (> 1mm) mesiodistal scratches are also present.

3.4 Discussion

3.4.1 Jaw mechanics

Microwear has previously been used to infer feeding motion of the jaws in ceratopsids (e.g., Varriale, 2011; Mallon and Anderson, 2014b). Early work by Ostrom (1966) proposed that ceratopsids were only capable of simple orthal jaw motions based on the presence of vertically oriented occlusal surfaces which were argued to have prevented any lateral motion of the fully adducted mandibles.

Subsequent studies (Varriale, 2011; Mallon and Anderson, 2014b), however, suggested on the basis of dental microwear analysis that ceratopsids were in fact capable of more complex jaw movements than the simple orthal motions proposed by Ostrom (1966) based on dental microwear analyses. Work conducted by Varriale (2011) identified four main scratch orientations (in order of most to least frequent): class 1 (dorsodistal), class 2 (shallow dorsodistal to mesiodistal), class 3 (shallow dorsomesial to mesiodistal) and class 4 (dorsomesial). Mallon and Anderson (2014b) also observed a dominant dorsodistal scratch mode and, like Varriale (2011), proposed that the high frequency and overall greater length of dorsodistal scratches were indicative of an orthopalinal power stroke. Both studies also agreed in the interpretation of the infrequent, typically shorter, dorsomesial scratches as disengagement scratches. However, Mallon and Anderson (2014b) alternatively suggested that these scratches may have been formed during the repositioning of the jaws between power strokes. Mallon and Anderson

(2014b) also differed from Varriale (2011) in their interpretation of mesiodistal scratches. In their study, Mallon and Anderson (2014b) observed a single set of more tightly constrained mesiodistal scratches rather than the two distinct sets observed by Varriale (2011). Two models were suggested to explain the formation of these more tightly constrained mesiodistal scratches: 1) a passive mechanism occurring during adduction in which the mandible is pushed palinally as the predentary traces a dorsocaudal arc defined by its contact with the inner surface of the rostral bone; or 2) occasional propalinal movements accompanying mandible adduction with influences of complementary actions of the pterygoideus and posterior adductor musculature. Mallon and Anderson (2014b) advocated for the second mechanism, given that the first is highly unlikely because it predicts the presence of correspondingly curved scratches that are almost never seen.

The generally polymodal scratch distributions with dominant dorsodistal scratch modes observed in this study are consistent with the findings of Mallon and Anderson (2014b), supporting previous interpretations of an orthopalinal power stroke with occasional propalinal movements during adduction and the repositioning of food within the mouth between power strokes. Juveniles also exhibit a dominant dorsodistal set of scratches but, unlike subadults and adults, juveniles exhibit scratch distributions that apparently are more weakly constrained (see juvenile ceratopsid in Figure 3.7). The apparent multimodality observed in juveniles is consistent with more flexibility in the skull but the results are not statistically robust and require further testing.

3.4.2 Diet

3.4.2.1 Ceratopsid ontogeny

Both juvenile and adult ceratopsids possess vertical occlusal surfaces (Figure 3.6; pers. obs.), suggesting that all ontogenetic stages used their teeth for shearing plant matter. Mallon and Anderson (2014b) proposed that adult ceratopsids were tough browse specialists. Based on overall similarities in occlusal surface between different ontogenetic stages, it is possible that juveniles were also tough browse specialists. However, because of small sample sizes, statistical comparisons of dental microwear between ontogenetic stages to confirm this inference will have to wait until more juvenile ceratopsids with preserved dentitions can be sampled.

In modern ungulates, cervical musculature responsible for elevating the head attach to the paroccipital processes (Janis, 1990). Increases in the breadth of the paroccipital processes, and subsequently the cervical musculature that elevate the head, may have been necessary to lift the heavier, more ornamented heads of adults. Differences in snout morphology, however, do seem to suggest differences in feeding ecology between ontogenetic stages. Even though relative snout width and shape did not change through ontogeny, absolute size differences would have had implications for relative selectivity of different ontogenetic stages. The absolutely larger size of adult rostra would have made adults relatively less selective than juveniles. The longer snouts observed in adults may have also made them less selective as they would have been able to access vegetation growing at various different levels (i.e., their niche breadth would have increased). However, it is also possible that the reduced cranial ornamentation of juvenile ceratopsids may have meant that they were capable of rearing up on their hind

legs to feed. Rearing up on the hind legs to feed has previously proposed for less derived ceratopsians such as leptoceratopsids which also lack heavy and complex cranial ornamentation (Mallon et al., 2013). Certain aspects of immature ceratopsid postcranial morphology (e.g., laterally narrow glenoid) have also been shown to share similarities with more basal, bipedal ceratopsians (e.g. *Psittacosaurus*) (Slowiak et al., 2019). Whether or not juvenile ceratopsids could actually rear up on their hind legs to feed is uncertain and would require further investigations that is beyond the scope of the present research.

Changes in the length and depression of the snout tip, the distance from the apex of the coronoid process to the jaw joint, and width of the quadrates may have also had important dietary implications (Janis 1990, 1995; Spencer, 1995; Mendoza, 2002). For juveniles, relatively shorter muzzles and increased distance from the coronoid process apex to the jaw joint would have resulted in greater mechanical efficiency and so generated greater relative bite forces (Ostrom, 1966; Henderson, 2010; Mariano et al., 2015; Mitchell et al., 2018). However, the relatively narrower quadrate breadths and less depressed snout tips observed in juvenile ceratopsids are suggestive of reduced relative bite forces.

The reason for this conflicting signal may be related to the implications of overall body size. Mallon and Anderson (2015) suggested that the absolute bite forces were lower in juveniles because overall muscle mass was smaller due to the smaller overall size of juveniles themselves. Presumably, as in modern lizards and finches, narrowing at the back of the skull (i.e., narrower quadrate breadth) would have meant that the jaw adductors were also smaller in juveniles producing reduced bite forces (Meyers et al.,

2002; Herrel et al., 2006). In addition to increased area for musculature, greater quadrate breadth is also proposed to be correlated to increases in relative bite force because wider skulls are better able to resist torsional forces that are generated during biting (Greaves, 1997). Thus, lower overall bite forces due to reduced musculature would have also meant that torsional forces within the skull would be lessened and so the skull would not need to be as effective at resisting these forces in juveniles.

Similarly, the association of higher bite forces with greater ventral deflection of the snout in adults (Figure 3.8) (Bowman, 1961; van der Meij and Bout, 2008) may be less related to the generation of those bite forces and more to stress accommodation. During vertical biting, forces exerted on the snout can be resolved into two parts: 1) fracture-risk components which must be resisted by the strength of materials comprising the beak, and 2) pressure components that act tangentially to beak curvature and are taken up by bone and subsequently dissipated (Bowman, 1961; Soons et al., 2010). With increasing ventral deflection of the snout, more of the overall force is taken up as pressure. This is because the fracture-risk component decreases as the angle between the direction of the overall force and the slope of the beak decreases (see Figure 39 in Bowman, 1961). At the very tip of the snout, the pressure component is eliminated, and the overall force is resolved into the fracture-risk component. Lengthening of the snout, and perpendicular orientation of the beak to the mandible, steepens the slope of the beak further reducing the magnitude of the fracture-risk component because the upper mandible is brought into better alignment with the orientation of the main biting forces. The more ventrally deflected and longer snouts in adult ceratopsids would therefore serve to allow higher bite forces to be exerted without exceeding the maximum strength of the

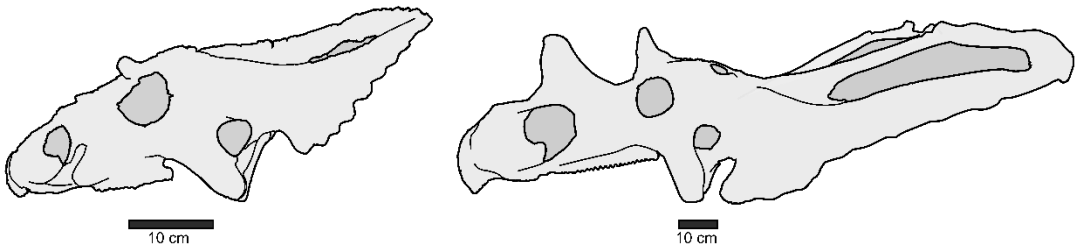

Figure 3.8: Differences in relative snout length and deflection of the snout tip between juvenile and adult ceratopsids. Left: juvenile *Chasmosaurus* (UALVP 52613). Right: adult *Chasmosaurus* (CMN 2245). Note: skulls have been scaled to have the same snout tip to mid-quadrate length.

materials comprising the rostra and the rest of the skull. Based on the above information, the shorter snouts and increased distance between the coronoid apex and jaw joint in juvenile ceratopsids would have served to increase relative bite forces by increasing mechanical advantage but due to differences in absolute size and head width, adults would have possessed larger muscles and been capable of producing higher bite forces. These differences in morphology would therefore suggest that juveniles selectively fed on softer, lower growing vegetation than adults which may have fed on larger quantities of tougher, slightly higher growing vegetation.

As in hadrosaurids, the longer faces of adult ceratopsids would have been useful for the exploitation of a wide variety of plant matter and may indicate conserved evolutionary allometry (see Chapter 2 discussion). Smaller bodied ceratopsians, such as *Leptoceratops*, possess relatively shorter faces compared to more derived ceratopsians such as *Chasmosaurus* and *Triceratops* (Figure 3.9). Further, comparison between more derived ceratopsids such as *Chasmosaurus* and *Triceratops* (both from the subfamily Chasmosaurinae) shows that the larger *Triceratops* possesses a relatively longer face than *Chasmosaurus*, as would be expected if ceratopsians experienced evolutionary facial allometry. The potential for conserved evolutionary allometry in both hadrosaurids and ceratopsids may be related to broader evolutionary trends within the Dinosauria or, alternatively, related to related to the possession of a dental battery by members of both clades (see section 3.4.3).

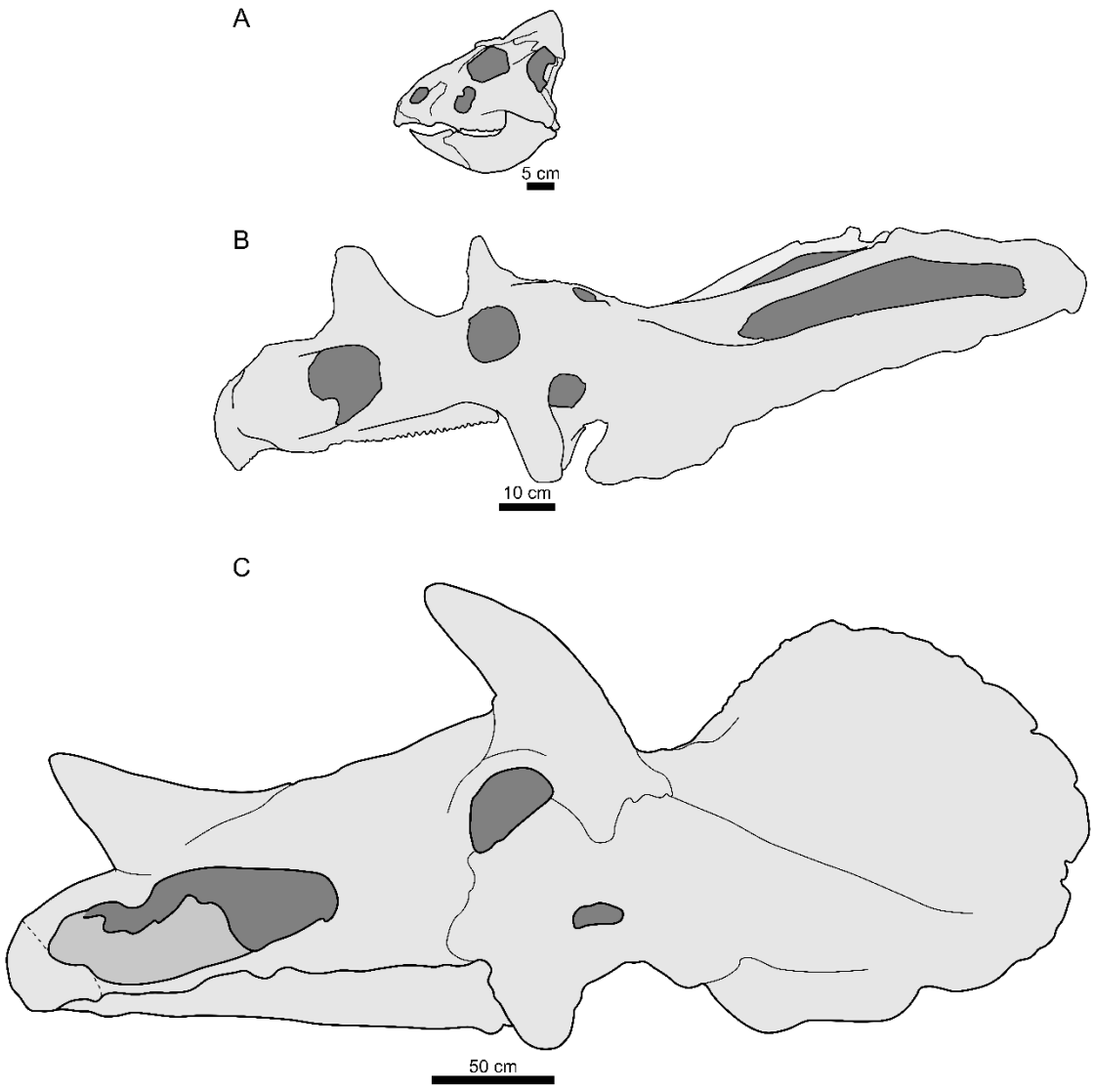

Figure 3.9: Differences in relative facial length between *Leptoceratops, Chasmosaurus* and *Triceratops*. A) *Leptoceratops* skull (CMN 8887). B) Adult *Chasmosaurus* skull (CMN 2245). C) Large adult *Triceratops* skull (MOR 004) (dashed line indicates the inferred location of the end of the rostrum). Note: drawings have been scaled so that the distance from the anterior edge of the orbit to middle of the quadrate are the same.

3.4.2.2 Subfamily differences

Previous work on adult centrosaurines and chasmosaurines indicated that centrosaurines possessed relatively shorter faces, and suggested that centrosaurines were capable of generating greater bite forces (Henderson, 2010). More recent geometric morphometric work by Maiorino et al. (2017) also found that chasmosaurines possessed relatively longer faces than centrosaurines. Results of the NPMANOVA conducted by Mallon and Anderson (2013) for the same linear measurements used in the present study also suggested that there were significant differences in relative skull proportions between ceratopsids subfamilies but small samples sizes reduced certainty in the reliability of these results. In the present study, results do not indicate statistically significant differences between ceratopsid subfamilies. Perhaps the allometric trajectories of both subfamilies are the same even though there are differences in the overall skull length. If this were the case, then the results of the ANCOVA would not be expected to be statistically significant. However, it is also possible that because relatively few small individuals are available for study, estimates of the slopes being made for these groups are inaccurate and there are actual differences in allometric trajectories that cannot be detected. Like the work of Mallon and Anderson (2013), sample sizes are presently too small to tease out potential differences between the allometric trajectories and further research will be warranted once more specimens are found.

3.4.3 Comparison with hadrosaurids

Both hadrosaurids and ceratopsids are characterized by independently evolved tooth batteries. Despite differences in the adult number of functional teeth in each tooth

family (ceratopsids have one functional tooth and hadrosaurids have three to four function teeth in each tooth family), both groups experience an increase in the number of tooth families through ontogeny (Erickson and Zelenitsky, 2014; Godfrey and Holmes, 1995; Currie et al., 2016). Investigations into cranial allometry have suggested that both groups experienced positive allometric growth in the lengths of the snout and diastema (see chapter 2 and results and discussion this chapter). Potentially, this shared ontogenetic trend is related to the development of the dental battery, where the addition of tooth families along the dental battery also results in lengthening of the face. However, positive allometric growth does appear to occur in the sauropod *Diplodocus* and theropod *Limusaurus* which both undergo a reduction in the number of teeth during ontogeny (Woodruff et al., 2017; Wang et al., 2017). Until further quantitative investigations into ontogenetic development of facial length in other dinosaurian clades can be conducted, whether positive allometry of the snout in ceratopsids and hadrosaurid is due to development of the dental battery or not, remains uncertain. However, if facial elongation is confirmed to be unrelated to tooth count, this may provide further evidence for evolutionary cranial allometry in ornithopods, or even dinosaurs in general.

3.5 Conclusions

Despite several studies previously conducted on ceratopsid ontogeny (Sampson, 1997; Goodwin et al., 2006; Tumarkin-Deratzian, 2009; Longrich and Field, 2012; Frederickson and Tumarkin-Deratzian, 2014; Konishi, 2015; Campbell et al., 2016), the implications that growth had on ceratopsid diet were previously not investigated. Work on ontogeny and diet interpreted the presence of ONSs in spinosaurids (Lakin and

Longrich, 2019), diplodocids (Woodruff et al. 2018), *Limusaurus inextricabilis* (Wang et al., 2017) and in hadrosaurids (Erickson and Zelenitsky, 2014; chapter 2) based on changes in body size as well as differences in skull morphology. Observations of these potential ONSs in multiple dinosaurian taxa would appear to suggest that, as in modern reptiles and some birds, ONSs are the rule rather than the exception in animals that experience long growth trajectories

Facial lengthening observed in ceratopsids and in hadrosaurids may have been related to the lengthening of the dental battery. However, preliminary comparisons between photos of juvenile and adult material for *Limusaurus* and *Diplodocus* suggests that these dinosaurs also experienced positive allometric growth despite a reduction in the number of teeth in the skull during ontogeny. Future investigations into the prospect of positive facial allometry during ontogeny for other dinosaurian taxa will help to further elucidate whether or not the evolution and development of the hadrosaurid and ceratopsid dental battery influenced development of the rest of the skull. Statistical support for positive allometric growth of the length of the snout, if found in other dinosaurs such as *Limusaurus* and *Diplodocus*, could potentially suggest that other factors (e.g., developmental constraint, ecology) are responsible for controlling development of the skull.

Based on investigations of ceratopsid skull allometry and snout shape conducted in the present study, it would appear that ceratopsids also underwent ONSs. However, these results may be under or over representing actual trends observed in the overall population due to reduced sampling at small body sizes as some variability within the population is left unaccounted for. In addition, quantitative analysis of dental microwear

features could not be conducted due to small sample sizes. Pending the discovery of more juvenile specimens, the present work is currently the best available estimate of what ceratopsid ONSs may have looked like. After more juvenile material is recovered, future work involving a greater number of immature individuals, and more complete sampling of microwear between stages and along the tooth row, will be needed to determine if the interpretations of the present study are supported at larger sample sizes.

Multimodality of scratch orientations in juvenile specimens may also have important biomechanical implications. Earlier work on ceratopsids had previously proposed a simple scissor-like motion for ceratopsid chewing on the basis of occlusal morphology (Ostrom, 1966). More recent work using dental microwear, however, suggested that ceratopsids may have been capable of more complex jaw motions, invoking an orthopalinal power stroke with supplementary propalinal motion of the mandible (Mallon and Anderson, 2014b). The multimodality of scratch orientations as well as lack of sutural fusion within the skull and more cartilaginous joints (Frederickson and Tumarkin-Deratzian, 2014; Campbell et al., 2016**;** Hone et al., 2016) may indicate that juvenile skulls were more kinetic than their adult counterparts. However, investigations into how kinesis may have changed through ontogeny have yet to be conducted.

Future investigations into evolutionary allometry of facial length may also prove interesting. In modern placental mammals, taxa with small adult body sizes have been shown to have shorter faces and taxa with large adult body sizes to have longer faces as part of a conserved evolutionary allometry across all mammalian clades (Cardini and Polly, 2013; Cardini et al., 2015). The positive allometry observed in ceratopsid and

hadrosaurid (see chapter 2) facial length and the relatively shorter faces in smaller ceratopsians such as *Leptoceratops* (and hadrosauroids such as *Telmatosaurus;* Weishampel et al., 1993) raises the question as to whether this is a broader evolutionary constraint that is observed in ornithischians, or even amniotes as a whole.

Evidence supporting the potential for an ONS in ceratopsids has important implications of the structuring of Late Cretaceous ecosystems. Previous work suggested that competition between adult chasmosaurines and centrosaurines was mediated by ecomorphological differences (Mallon, 2019). The findings of this chapter suggests that intra-specific competition in ceratopsids may have also been mediated by ecomorphological differences. Because different ontogenetic stages potentially occupied different roles, and body size is one of the main mechanisms through which resources are partitioned (Werner and Gilliam, 1984), juvenile ceratopsids may have instead potentially competed with other similar sized dinosaurs including juvenile hadrosaurids, particularly the closely related leptoceratopsids. The potential impacts that ceratopsid ONSs had in Late Cretaceous ecosystems will be explored in Chapter 4.

Chapter 4: Juvenile megaherbivores versus small ornithischians

4.1 Introduction

4.1.1 Community structure and the fossil record

Body size distributions of both fossil and modern mammalian communities are positively-skewed and relatively consistent through time and space (Damuth, 1982; Peters and Wassenberg, 1983; Siemann and Brown, 1999; Kozlowski and Gawelcyzk, 2002; Smith and Lyons, 2011) (Figure 4.1). Some authors have proposed that mammals exhibit positively-skewed distributions because smaller taxa can more easily subdivide a habitat, enabling them to coexist in larger numbers (Damuth, 1982; Peters and Wassenberg, 1983; Siemann and Brown, 1999). If this were more generally applicable to non-mammalian communities, the smallest body sizes should always be the most abundant (Kozlowski and Gawelcyzk, 2002). However, the relationship between habitat subdivision and body size cannot explain why some avian distributions are negatively-skewed.

A more broadly applicable explanation may be related to energy acquisition (Smith and Lyons, 2011). Metabolic theory suggests that many individual, population, community and ecosystem level attributes scale with body size and temperature in a manner similar to mass-specific metabolic rate (Brown and Sibly, 2006). These relationships have been shown to hold true within and between species. With metabolic rate, mass-specific production rate (i.e., the rate of energy assimilation minus the rate of respiration) is lower in larger animals compared to smaller ones (Gaston and Blackburn, 2000; Brown and Sibly, 2006). Assuming Darwinian fitness (=birth rate-death rate), natural selection will favour reduced body sizes because production is increased as long

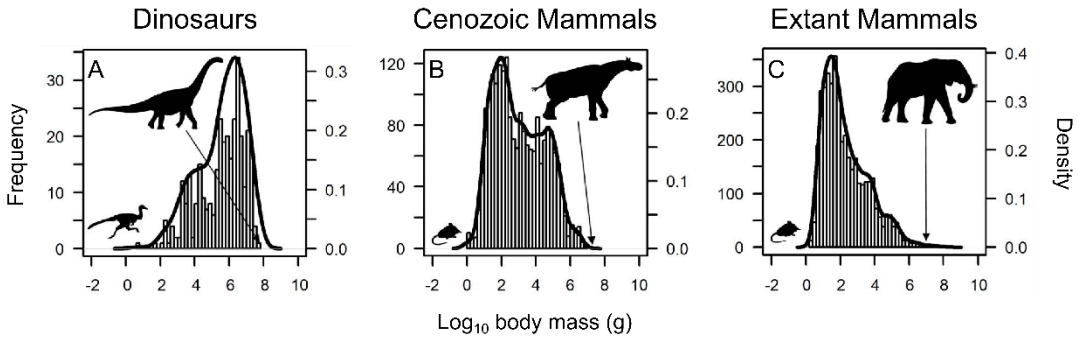

Figure 4.1: Body size frequency distributions for dinosaurs (A), Cenozoic mammals (B), and modern mammals (C) taken from O'Gorman and Hone (2012). Distributions for Cenozoic and extant mammals are positively skewed and distributions for dinosaurs are negatively skewed (modified from O'Gorman and Hone, 2012).

as mortality is unaffected (Brown and Sibly, 2006). If mortality is affected, then body size increases are favoured as long as these increases reduce mortality or enhance reproductive success enough to sufficiently overcome the production constraint. Larger body sizes may also involve morphological/physiological innovations which overcome pre-existing constraints making new food sources available. For instance, larger body sizes may be favoured in mammalian herbivores that consume high quantities of low-quality vegetation because gut capacity is greater at larger body sizes. A larger gut increases passage time allowing harder-to-digest plant materials to be broken down increasing nutrition and productivity. Complex processes at the community level such as competition may also be important in the shaping of size distributions, as this can influence food availability especially if some food resources are only accessible to organisms of a certain size range (Kozlowski and Gawelcyzk, 2002).

In contrast to mammalian communities, North American Jurassic and Cretaceous herbivorous dinosaur communities appear to have consisted of diverse and abundant large-bodied taxa, and relatively fewer small taxa (Figure 4.1) (O'Gorman and Hone, 2012; Codron et al., 2012, 2013; Brown et al., 2013b). The Jurassic Morrison Formation, for example, preserves a higher diversity and abundance of large-bodied dinosaur remains (e.g., sauropods) compared to smaller ornithischian taxa (Dodson et al., 1980; Foster, 2003; Noto and Grossman, 2010). The Upper Cretaceous Dinosaur Park Formation also shows low small herbivore diversity and abundance (Brown et al., 2013b).

Codron et al. (2012, 2013) proposed that the low diversity of small-bodied taxa was due to competition between the young of large herbivores and similar-sized adults of

small ornithischians. Intuitively, the larger adult:offspring mass ratios observed in dinosaurs relative to similar sized mammals and differences in reproductive strategy (dinosaurs are oviparous and mammals viviparous) would have led to more pronounced changes in diet during ontogeny. Because of this more complex life history, Codron et al. (2013) hypothesized that there would be more overlap in body size and niche occupation and a higher frequency of density dependent ecological interactions in dinosaurian ecosystems. To investigate how competition between similar-sized taxa influenced the relative abundances of dinosaurian size classes, the authors ran size-structured, mathematical models, assuming the presence of size-induced competition. Their results suggested that competition between juvenile megaherbivores and small ornithischians would have also reduced the relative abundances of the latter.

Brown et al. (2013b) alternatively reasoned that taphonomic biases were at least partly, if not completely, responsible for the patterns described above (Figure 4.2; Figure 4.3). They found that, with the Campanian Dinosaur Park Formation of Alberta, taxa with estimated adult body masses less than 60 kg were generally < 41% complete, and only five of the smaller-bodied taxa (most of which were carnivores) were known from more than 10% of the skeleton (Figure 4.4A). Plots of taphonomic mode (i.e., preservation as articulated skeleton, associated skeleton, isolated skeleton) against body size showed small-bodied taxa are also most commonly represented by isolated elements (Figure 4.4B). The same preferential preservation of larger-bodied animals is also observed within large-bodied dinosaur clades. Trends within Hadrosauridae and Ceratopsidae showed that juvenile specimens were less likely than adults to be preserved as complete specimens, and are more often represented by isolated elements. Taphonomic biases may

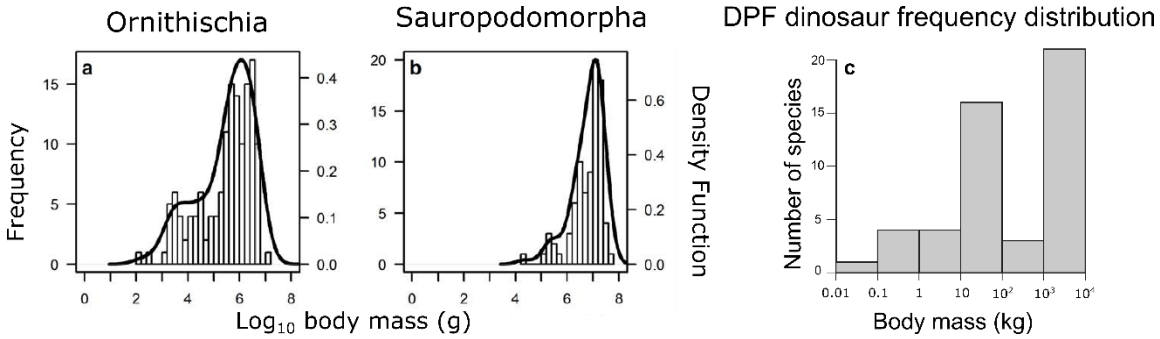

Figure 4.2: Body size distribution results from O'Gorman and Hone (2012) and Brown et al. (2013b). A) and B) Body size vs. frequency (number of species) and density function for ornithischian taxa (A) and sauropod taxa (B), showing negatively skewed distribution (modified from O'Gorman and Hone, 2012). C) Body size vs. number of species for dinosaur taxa from the Campanian Dinosaur Park Formation showing bias against small bodied taxa (modified from Brown et al., 2013b).

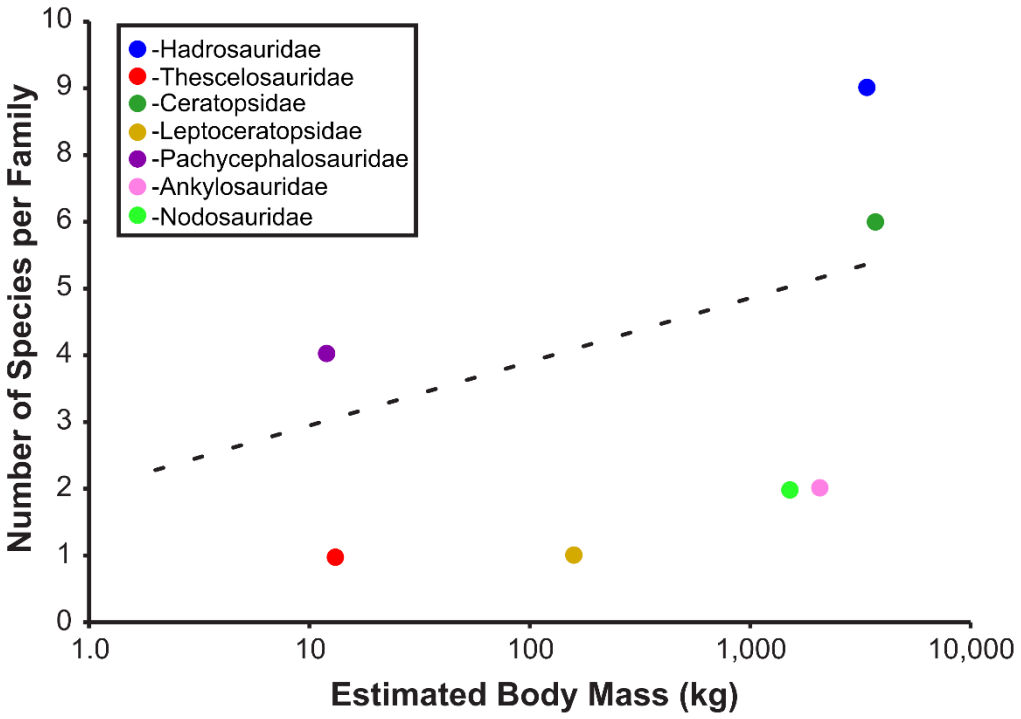

Figure 4.3: Correlation between mean estimated body mass of each ornithischian dinosaur family and number of species per family (modified from Brown et al., 2013b). The relationship between diversity and body mass is reported as being both positive, with diversity increasing with body mass, and significant (Brown et al., 2013b).

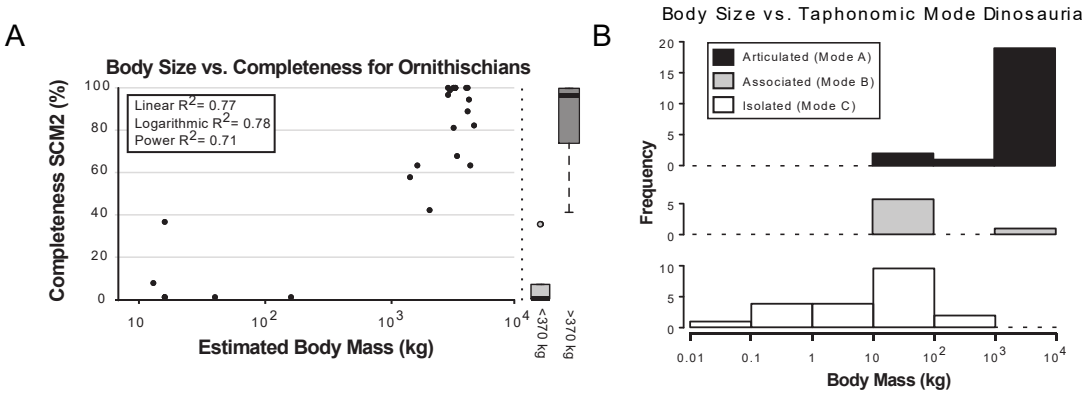

Figure 4.4: Results for taphonomic analyses conducted by Brown et al. (2013b). A) Plot of skeletal completeness (SCM2) as a function of estimated adult body mass for ornithischian taxa showing an increase in skeletal completeness as body mass increases (modified from Brown et al., 2013b). Boxplots to the right demonstrate significant dichotomy of completeness when samples are divided into large and small body size classes (Brown et al., 2013b). B) Size distributions (log mass) of Dinosaur Park Formation dinosaur species for the three taphonomic modes used by Brown et al. (2013b) (modified from Brown et al., 2013b).

thus be at least partly responsible for the limited diversity and abundance of small ornithischian taxa.

4.1.2 Hypotheses and Predictions

Thus, there exist two alternative (but not mutually exclusive) hypotheses (ecological competition vs. taphonomic artifact) that purport to explain the unusual size distribution of dinosaur assemblages. But while the evidence for a taphonomic size bias seems unassailable, some predictions that follow from the competition hypothesis remain untested. For instance, if left-skewed richness distributions resulted from competition at smaller body sizes, then this competition should have resulted in niche partitioning between remaining species. This prediction has never been tested and so will form the first line of investigation for this chapter.

Under the taphonomy hypothesis, it has also been argued that small ornithischians were not only more diverse than is currently reflected in the fossil record, but that they were also more abundant and that this signal is biased by taphonomic processes (Brown et al., 2013a,b). If this were true, then, all else being equal, small ornithischians should be relatively more abundant than similar-sized immature megaherbivores (Figure 4.6). The second part of this chapter will test this prediction to attain a better understanding of herbivore community structure during the Late Cretaceous.

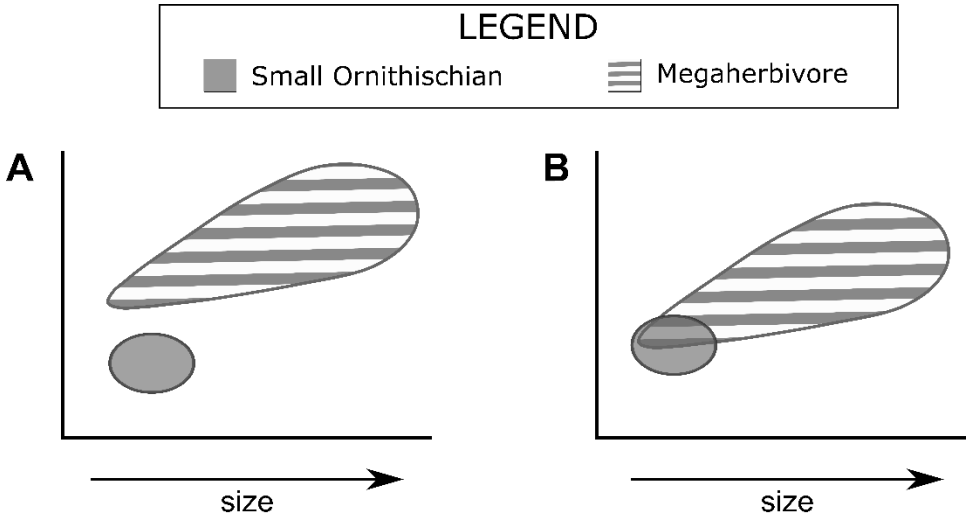

Figure 4.5: Hypothetical ecomorphospaces for one megaherbivore clade and one small ornithischian clade. A) Expected model for ecomorphospace resulting from prolonged ecological competition between species. B) Expected model for ecomorphospace where resources are non-limiting and there is no competition between species.

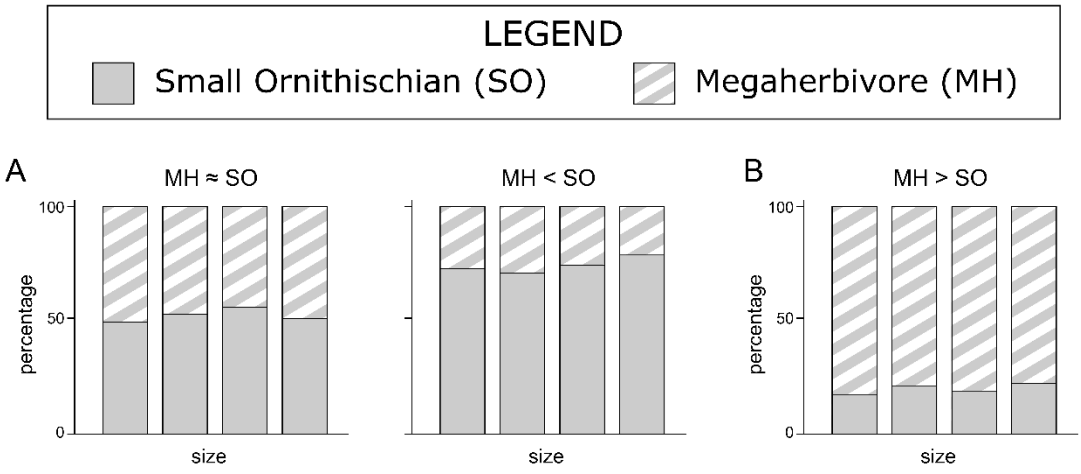

Figure 4.6: Hypothetical femoral distributions for young megaherbivores and small ornithischians. A) Expected models under the taphonomic hypothesis where small ornithischians are predicted to be equally or more abundant than megaherbivores. B) Expected model under the competition hypothesis where small ornithischians are predicted to relatively less abundant than megaherbivores.

4.2 Methods

During the Late Cretaceous (~65.5 – 80.0 Ma), the Western Interior Seaway extended from the Gulf of Mexico to the Arctic Ocean and divided North America in two (Laramidia in the west and Appalachia in the east) (Gates et al., 2012; Lucas et al., 2016). Fluctuations in sea-levels as a result of pulses of orogenic activity along the western edge of Laramidia likely contributed to the high rates of dinosaur turnover that occurred at this time, especially during the Campanian (Horner et al., 1992; Gates et al., 2012). This orogenic activity was also the source of eastward flowing rivers which connected to the western shoreline of the seaway and formed extensive alluvial and coastal plains across the landscape that were home to a diverse array of large (i.e., hadrosaurids, ceratopsids, ankylosaurs) and small (i.e., thescelosaurids, pachycephalosaurids, leptoceratopsids) ornithischians (Gates et al., 2012; Mallon, 2019). Of these taxa, hadrosaurids and ceratopsids appear to have dominated the landscape, with the remains of various ontogenetic stages being recovered for these taxa. Small ornithischians (thescelosaurids, pachycephalosaurids and leptoceratopsids) were relatively more dispersed across the landscape. Ankylosaurs were also rarer than hadrosaurids and ceratopsids, and very little juvenile material has been recovered from North America. For this reason, I consider only hadrosaurids, ceratopsids and small ornithischians below (Table 4.1). It is also worthy of mention that the taxa considered represent a time span of ~10 Myr and thus do not comprise a "true" ecological community. However, because members of these clades are present throughout the Cretaceous, these taxa likely co-occurred and therefore, time-averaging is unlikely to have appreciably influenced ecological relationships between these taxa.

Table 4.1: Late Cretaceous North American taxa used in ecological analyses. Asterisk (*) indicates temporal ranges for the given species. Otherwise, the ranges provided are for the specified time period, formation(s) or genus.

Classification	Formation & time range	Reference(s)
Hadrosauridae		
Hadrosaurinae		
Maiasaura peeblesorum	Two Medicine (74.0 – 82.6 Ma)	Dilkes, 2001
Edmontosaurus annectens	Hell Creek/ Lance/ Frenchman (65.5 – 66.7 Ma)*	Campione and Evans, 2011; Eberth et al., 2013
Edmontosaurus regalis	Horseshoe Canyon (71.0 – 72.5 Ma)*	Eberth et al., 2013
Edmontosaurus sp.	St. Mary River (71.0 Ma)	Eberth et al., 2013
Edmontosaurus sp. (= "*Ugrunaaluk kuukpikensis*")	Prince Creek (68.4 – 73.4 Ma)*	Fowler, 2017
Brachylophosaurus canadensis	Oldman/ Judith River/ Kaiparowits (76.5 – 77.5 Ma)*	Fowler, 2017; Lowi-Merri and Evans, 2019
Prosaurolophus maximus	Dinosaur Park/ Two Medicine (74.1 – 75.7 Ma)*	McGarrity et al., 2013
Gryposaurus notabilis/ Gryposaurus incurvimanus	Kaiparowits/ Dinosaur Park (74.0 – 76.6 Ma)	Gates and Sampson, 2007; Lowi-Merri and Evans, 2019
Gryposaurus latidens	Two Medicine (80.0 Ma)*	Gates and Sampson, 2007
Gryposaurus monumentensis	Kaiparowits (74.0 – 76.1 Ma)	Lowi-Merri and Evans, 2019
Lambeosaurinae		
Hypacrosaurus stebingeri	Oldman/ Two Medicine (71.0 – 74.0 Ma)*	Eberth et al., 2013
Hypacrosaurus altispinus	Horseshoe Canyon (68.4 – 71.0 Ma)*	Eberth et al., 2013; Fowler, 2017
Lambeosaurus lambei	Dinosaur Park (75.5 – 76.3 Ma)*	Mallon et al., 2012; Eberth et al., 2013
Lambeosaurus magnicristatus	Dinosaur Park (75.5 – 75.7 Ma)*	Mallon et al., 2012; Eberth et al., 2013
Lambeosaurus sp.	Dinosaur Park (75.5 – 77.0 Ma)	Evans, 2007; Fowler, 2017
Corythosaurus casuarius	Dinosaur Park (76.2 – 76.5 Ma)*	Mallon et al., 2012; Eberth et al., 2013
Corythosaurus intermedius	Dinosaur Park (76.0 – 76.2 Ma)*	Mallon et al., 2012; Eberth et al., 2013

Corythosaurus sp.	Dinosaur Park (75.5 – 77.0 Ma)	Evans, 2007; Fowler, 2017
Ceratopsidae		
Chasmosaurinae		
Chasmosaurus belli	Dinosaur Park (75.7 – 76.0 Ma)*	Mallon et al., 2012; Eberth et al., 2013
Chasmosaurus irvinensis	Dinosaur Park (75.5 – 75.7 Ma)*	Mallon et al., 2012; Eberth et al., 2013
Chasmosaurus russelli	Dinosaur Park (76.0 – 76.5 Ma)*	Mallon et al., 2012; Eberth et al., 2013
Triceratops horridus	Lance/ Hell Creek/Scollard (65.5 – 65.7 Ma)	Eberth et al., 2013
Triceratops prorsus	Lance/ Hell Creek/Scollard (65.5 – 65.7 Ma)	Eberth et al., 2013
Centrosaurinae		
Centrosaurus apertus	Dinosaur Park (76.5 – 76.9 Ma)*	Fowler, 2017
Styracosaurus albetensis	Dinosaur Park (76.2 – 76.4 Ma)*	Fowler, 2017
Brachyceratops montanensis	Two Medicine (74.0 – 75.0 Ma)*	McDonald, 2011
Leptoceratopsidae		
Leptoceratops gracilis	Scollard/ Lance/ Hell Creek (65.5 – 66.7 Ma)*	Eberth et al., 2013; Fowler, 2017
Montanoceratops cerorhynchus	St. Mary River/ Horseshoe Canyon (69.5 – 71.0 Ma)*	Eberth et al., 2013
Pachycephalosauridae		
Pachycephalosaurus wyomingensis/ *Pachycephalosaurus* sp.	Lance/ Hell Creek (65.5 – 66.8 Ma)	Maryanska et al., 2004; Williamson and Carr, 2006; Sullivan, 2006
Stygimoloch spinifer/ *Stygimoloch* sp.	Lance/ Hell Creek/ Ferris (65.0 – 77.0 Ma)	Maryanska et al., 2004; Williamson and Carr, 2006; Russell and Manabe, 2002
Stegoceras validum	Dinosaur Park/ Horseshoe Canyon/ Judith River (74.0 – 81.0 Ma)	Fowler, 2017; Maryanska et al., 2004; Williamson and Carr, 2006; Russell and Manabe, 2002
Thescelosauridae		
Parksosaurus warreni	Horseshoe Canyon (68.4 – 70.4 Ma)*	Eberth et al., 2013

Thescelosaurus neglectus/ Thescelosaurus garbanii	Lance/ Hell Creek/ Scollard/ Frenchman (65.5 – 70.6 Ma)	Brown, 2009; Boyd et al., 2009
Oryctodromeus cubicularis	Blackleaf/ Wayan (95.0 – 100.0 Ma)	Brown, 2009; Krumenacker, 2017
Orodromeus makelai	Two Medicine/ Judith River (71.3 – 83.5 Ma)	Brown, 2009

4.2.1 Skull morphometrics

4.2.1.1 Selection and collection of measurements

From the competition hypothesis of Codron et al. (2012,2013), it is predicted that, within a size-structured assemblage such as that considered here, small ornithischians and similar-sized young megaherbivores would occupy different niches. To investigate this. niche relationships were approximated by examining ecomorphospace occupation for the assemblage as this has been previously done in other palaeontological investigations (e.g., Mallon, 2019). To evaluate the distribution of small ornithischians and megaherbivores in ecomorphospace, two lines of investigation were explored. The first included size as a factor because this is an ecologically important variable. The second controlled for size and addressed shape alone.

Twelve linear measurements previously considered by Mallon and Anderson (2013) and snout shape index (SSI) were used, following the methods previously established in chapters 2 and 3 (Figure 4.7, 4.8). Only specimens preserving more than 50% of these measurements were used in the analysis. In modern animals, including ungulates, these parameters have been shown to reflect aspects such as plant quality, mechanical properties, growth habit and feeding selectivity (Janis and Ehrhardt, 1988; Janis, 1990, 1995; Spencer, 1995; Mendoza et al., 2002).

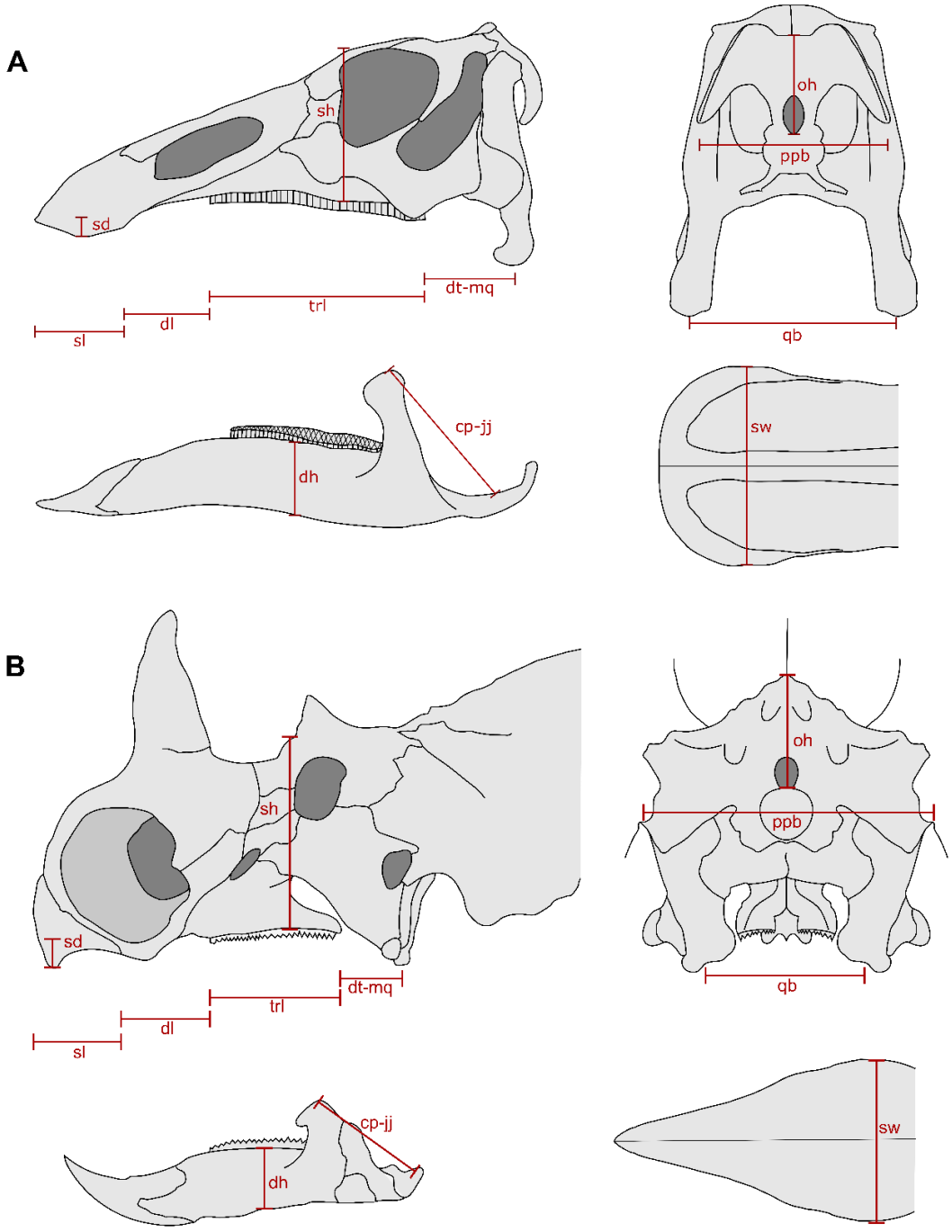

Figure 4.7: Linear measurements used for cranial morphometric analysis (modified from Mallon and Anderson, 2013). A) Hadrosaurid skull, and B) ceratopsid skull. Measurements: sl: snout length, dl: diastema length, trl: tooth row length, dt-mq: distance from jaw joint to distal end of tooth row, sw: maximum beak width, dh: midpoint dentary height, ppb: paroccipital process breadth, oh: occiput height, cp-jj: distance from coronoid process apex to middle of jaw joint, sd: depression of snout below occlusal plane, sh: skull height, qb: quadrate breadth.

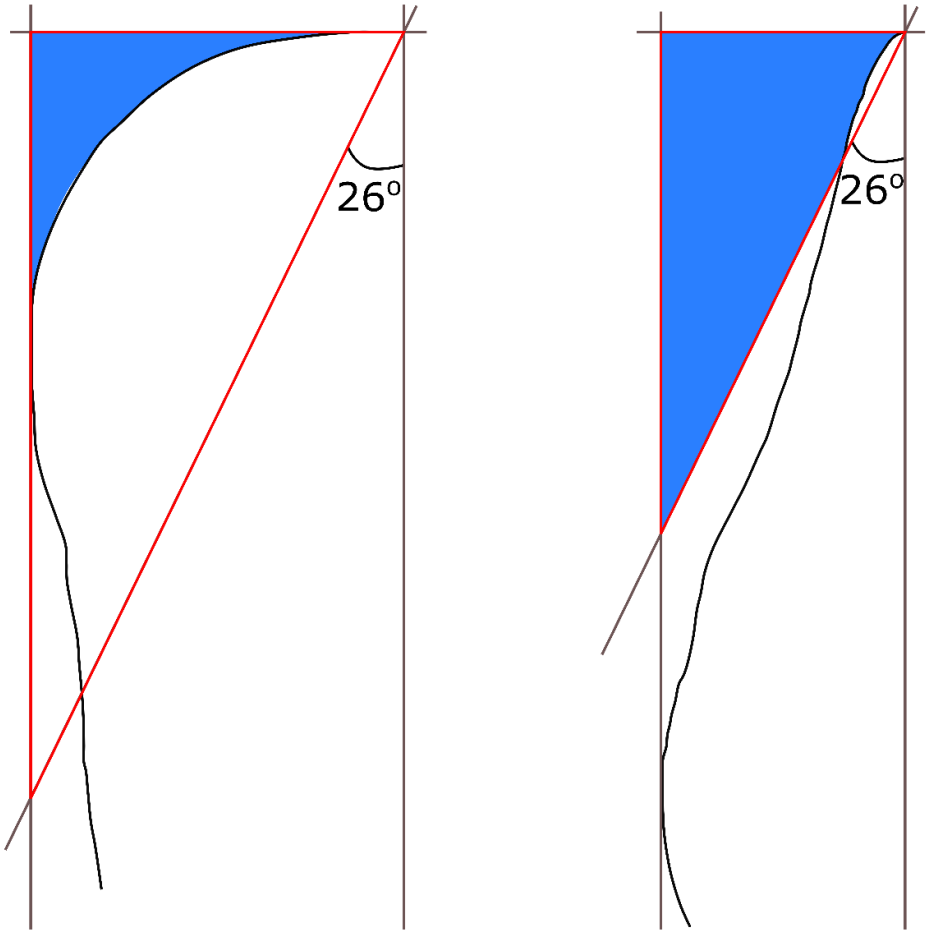

Figure 4.8: Snout shape analysis conducted based on Dompierre and Churcher (1996). Blue region denotes the area of negative space measured for analysis. Red triangle indicates the triangle area measured for analysis.

4.2.1.2 Ontogenetic considerations

Immature megaherbivores were identified using their relatively smaller size, degree of suture closure, bone texture and relative development of cranial ornamentation, as in chapters 2 and 3 (Goodwin et al., 2006; Tumarkin-Deratzian, 2009; Evans, 2010; Frederickson and Tumarkin-Deratzian, 2014; Campbell et al., 2016; Hone et al., 2016) (Figure 4.9). Because subadults and juveniles were rare and the most difficult to distinguish, they were grouped together to form an "immature" category in many of the analyses.

There are few examples of articulated juvenile megaherbivores and small ornithischian taxa. This necessitated the inclusion of composite specimens constructed from the scaling and combination of elements from various individuals into a single skull (e.g., hatchling and nestling-sized *Maiasaura* and *Hypacrosaurus*, composite reconstruction of *Oryctodromeus*). Inclusion of these composites into the dataset may therefore be a potential source of error. These composites were included because here they were mostly based on real material and deemed adequate representations of real individuals. To the extent that the reconstructions are erroneous, so too will be my functional interpolations.

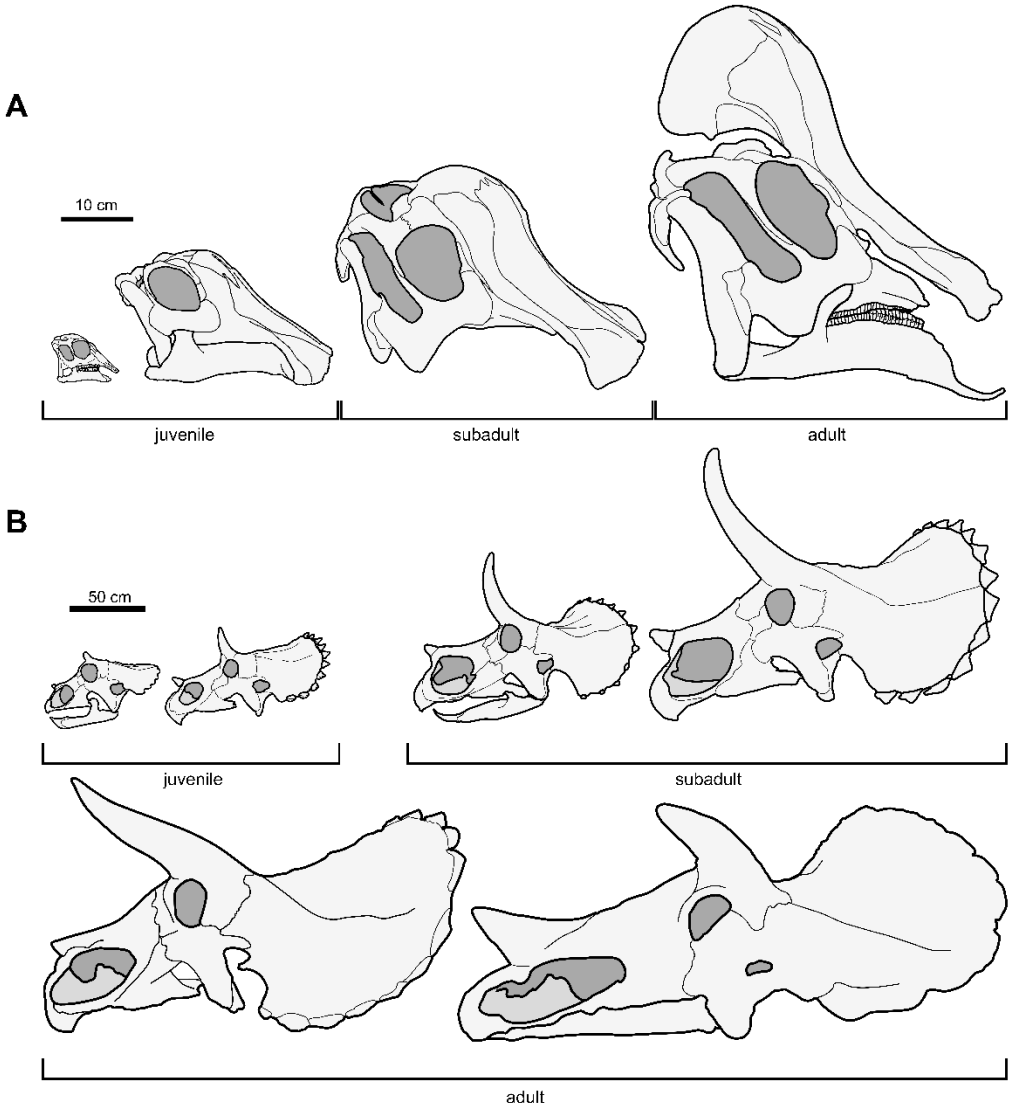

Figure 4.9: Basic ontogenetic classifications in megaherbivorous dinosaurs. A) Basic ontogenetic stages for hadrosaurids based on cranial crest development and amount of sutural fusion. B) Basic ontogenetic stages for ceratopsids based on sutural fusion, relative frill development and relative development of the nasal and orbital horns.

4.2.1.3 Ordination and comparisons

Data were recorded in a Microsoft Excel file prior to being imported into R v. 3.6.1 (R Core Team, 2019) where subsequent data manipulation was conducted. Prior to any further analysis, cranial measurements were log-transformed to linearize relationships between the variables (Hammer and Harper, 2006). I performed two analyses: the first on a size-included dataset containing measurements from megaherbivores of various ontogenetic stages (including adults) and small ornithischians, and a second on a size-corrected dataset containing measurements from similar-sized megaherbivores and small ornithischians. It was necessary to conduct a size-corrected analysis because the potential shape differences at small sizes was of particular interest to investigate if small ornithischians overlapped with immature megaherbivores in the ecomorphospace as a result of similarities in shape. To reduce the amount of size-related variation in cranial measurements I regressed my cranial measurements against a size proxy and used the residuals from these regressions in subsequent analyses. To produce the size-corrected dataset, cranial measurements from all specimens (including adult megaherbivores) were regressed against anterior snout to mid-quadrate length (my size proxy, herein referred to as skull length) using reduced major axis regression (see Chapter 2 methods for details). Residuals for specimens with a skull length shorter than or equal to the skull length of the largest small ornithischian (CMN 40602; *Pachycephalosaurus* sp.; skull length= 375 mm) were then selected for use in subsequent size-corrected analyses.

Given the multivariate nature of the dataset and the complexities associated with trying to identify relationships within such a multi-dimensional space, both size-included

and size-corrected datasets were subjected to principal component analysis (PCA). The goal of PCA is to reduce multidimensional space down to a few variables of maximal variance to make trends/groupings in the data easier to identify (Hammer and Harper, 2006). Because not all variables shared the same units, the PCAs used the correlation matrix rather than the typical variance-covariance matrix to calculate principal component (PC) scores (Hammer and Harper, 2006; Jolliffe and Cadima, 2016).

Like many other multivariate morphometric procedures, PCAs can only be conducted on complete datasets (Strauss et al., 2003). The often-incomplete nature of fossil specimens means that palaeontological datasets typically contain missing values that have to be addressed prior to analysis. Missing values were iteratively calculated using an uncentered Bayesian PCA (BPCA) with the "pca()" function in the "pcaMethods" package (Strauss et al., 2003; Stacklies et al., 2019). The BPCA method was used because, unlike other substitution methods (e.g., Gower's distance matrix, substitution of mean, correlated variable regression), Brown et al. (2012) found that BPCA introduced the least amount of error. Bayesian PCA uses existing values within the dataset to calculate values for the missing data, individual BPCAs were run on family or subfamily level subsets to reduce potential taxonomic biases from influencing the imputed values. A separate imputation was also run for a dataset containing the log-transformed skull lengths in order to decrease the amount influence size had on the dataset. After the incorporation of imputed values into the individual data subsets, these subsets were combined into a single dinosaur dataset. Following the imputation of missing values, RMA was conducted to obtain the size-corrected dataset. Both the size-included and size-corrected datasets were then independently subjected to a PCA using

the “princomp()” function (R Core Team, 2019). Only PCs representing ≥5% of the total variation in the dataset were considered.

A non-parametric analysis of variance (NPMANOVA) was then conducted on PC scores of the size-corrected dataset to test if taxa differed significantly from one another. The PC scores for the size-uncorrected dataset were not analyzed further. An NPMANOVA is a non-parametric test for significant differences in means between two or more groups in a multivariate dataset (Hammer and Harper, 2006). Unfortunately, the number of specimens in each group are different, thus necessitating the implementation of rarefaction. Rarefying the data removes influences caused by sample size differences between compared datasets (Hammer and Harper, 2006). Because chapters 2 and 3 indicated little difference between megaherbivore subfamilies (especially at small body sizes), and to increase overall sample size, comparisons were conducted at the family level. To rarefy the data, hadrosaurids, ceratopsids, thescelosaurids, pachycephalosaurids, and leptoceratopsids were first separated into different data subsets so that an equal number of representatives could be selected from each family. The maximum number of individuals that could be selected from and used for all subsets was then determined by finding the number of rows in the smallest dataset. Using the “sample_n()” function in the package “dplyr” (Wickham et al., 2018), the same number of randomly selected specimens from the other, larger data subsets was selected and combined to produce a single data frame. The NPMANOVA omnibus test was then conducted using the “adonis2()” function from the “vegan” package (Oksanen et al., 2019) using the Mahalanobis distance metric and 1000 permutations. This process was repeated 1000 times and the results were averaged over these intervals. The Mahalanobis distance

metric was used for similarity/dissimilarity values (sim.method) because it can handle correlated multidimensional variables (Lewicki and Hill, 2006).

If the averaged omnibus p-value was <0.05, then follow-up post-hoc comparisons were conducted on rarified datasets using the "pairwise.adonis()" function from the "funfuns" package (Trachsel, 2019) over 1000 permutations using the Mahalanobis distance metric. This was repeated and p-values were averaged over 1000 iterations. The "pairwise.adonis()" function also allows the user to implement a correction method to obtain adjusted p-values when multiple comparisons are being made. For the purpose of this analysis, p-values were adjusted using Holm correction because it is less conservative and more powerful than the Bonferroni method (Holm, 1978). To increase the rigour of the statistical tests, rarefaction and subsequent NPMANOVAs were conducted over 1000 iterations.

4.2.2 Maximum feeding height estimates

Maximum feeding height was calculated to determine the height at which immature megaherbivores were able to extend beyond the reach of small ornithischian taxa. Maximum feeding height was determined following the methods of Mallon et al. (2013). The feeding heights of quadrupedal ceratopsids was calculated by summing the lengths of the humerus, radius (or ulna if the radius is unavailable), and metacarpal III (Figure 4.10). This is based on the assumption that the large parieto-squamosal frill observed in ceratopsids would have prevented the beak from being elevated much higher than the shoulders.

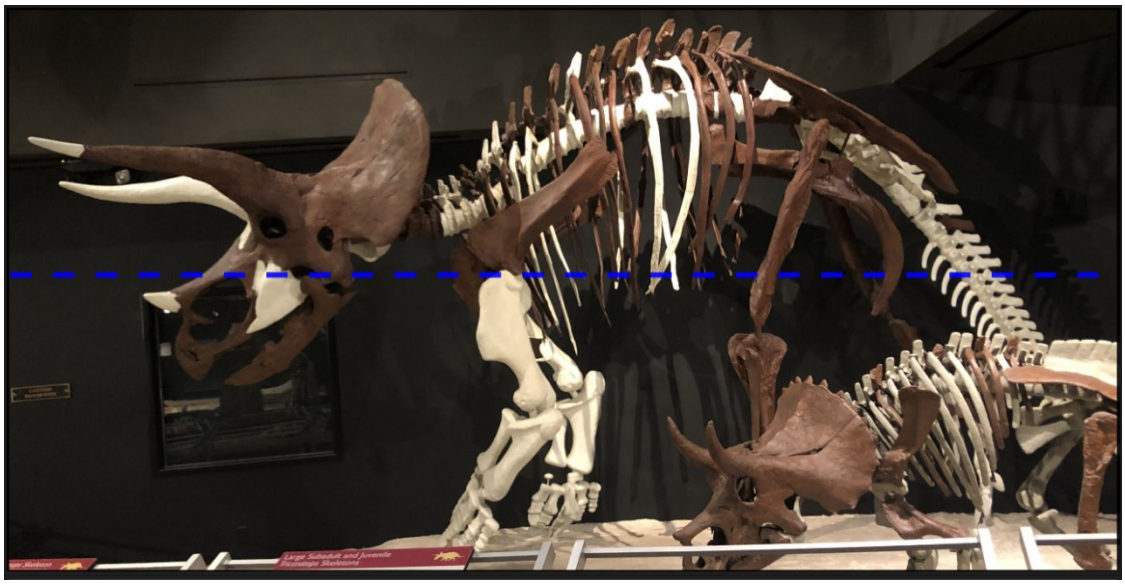

Figure 4.10: Quadrupedal maximum feeding height proxies used. Shoulder height (calculated from the summation of humerus, radius/ulna and metacarpal III lengths) used to approximate the maximum feeding height for ceratopsids.

Hadrosaurs, leptoceratopsids, pachycephalosaurs and thescelosaurids are assumed to be bipedal or facultatively bipedal. Because this analysis is focused on determining the maximum feeding height for these animals, only the bipedal feeding heights were calculated. Calculating bipedal feeding height requires estimations of hip height, tail length and trunk length because these calculations assume that, when the animal reared up on its hind legs, it could only do so until the distal tip of its tail touched the ground (Figure 4.11). Hip height was obtained by summing the lengths of the femur, tibia (or fibula if the tibia is unavailable), and metatarsal III. Tail and trunk length was measured by draping a tailor's measuring tape along the length of the vertebral column, and the boundary between tail and trunk was considered to be the middle of the acetabulum.

Using the hip height (vertical side) and tail length (hypotenuse), a small right-angle triangle can be constructed (Figure 4.11). From this triangle, an angle, Θ, can be calculated: $\Theta = \sin^{-1}(\text{hip height/tail length})$. The hypotenuse of this small triangle can be extended by adding neck and torso length to tail length. The vertical side of this larger triangle is the maximum feeding height, and can be calculated using the angle of the smaller triangle with the equation $(\sin \Theta)\cdot(\text{body length})$. Barplots for quadrupedal and bipedal feeding heights for each family were then generated.

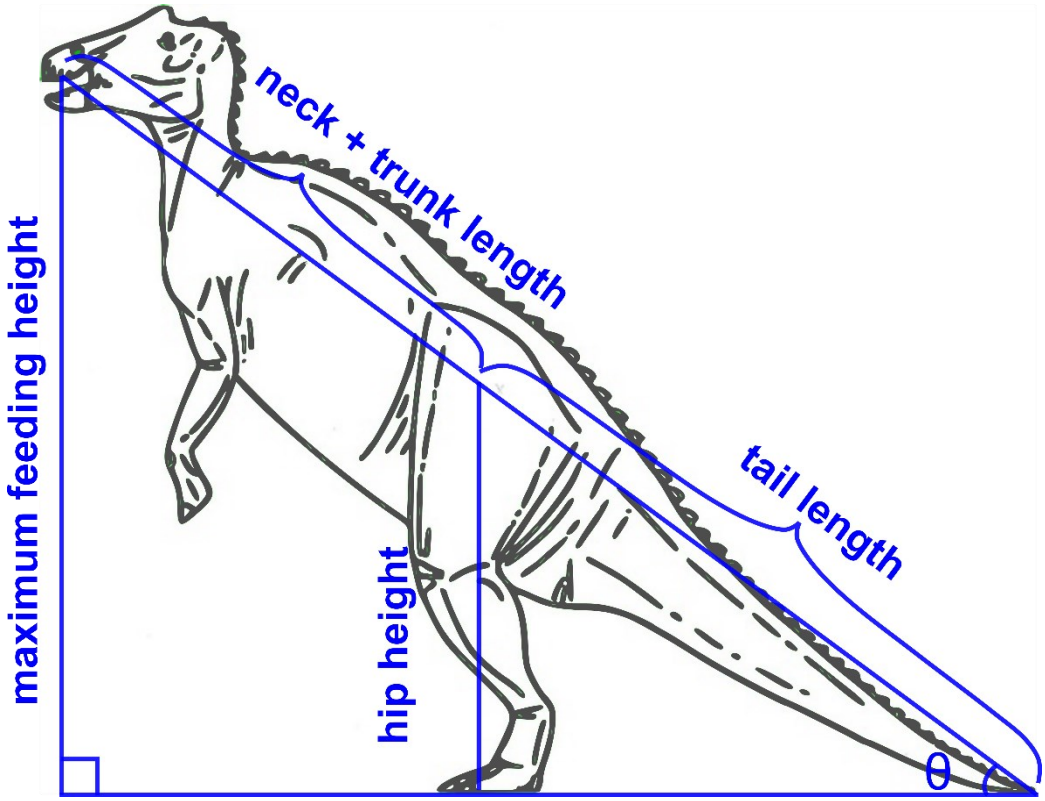

Figure 4.11: Trigonometric model used to estimate bipedal maximum feeding heights for hadrosaurids, thescelosaurids, leptoceratopsids, and pachycephalosaurids (modified from Mallon et al., 2013). See text for details.

The "QE()" function in the R package "MASSTIMATE" (Campione, 2019) was used to estimate the body masses at which hadrosaurids and ceratopsids would have surpassed the maximum feeding heights of small ornithischian taxa. This function takes advantage of the universal and highly conserved relationship between proximal weight-bearing limb bone circumferences and body mass observed in extant terrestrial mammalian and reptilian quadrupeds to construct a bivariate regression from which body masses of dinosaurs can be calculated from humeral and femoral circumferences (Campione and Evans, 2012).

4.2.3 Relative abundances

Taphonomic processes are important to consider because they can impact how likely (or unlikely) a specimen is to enter the fossil record. For example, bonebeds often originate due to flooding events, which involve rapid burial of skeletal elements, causing the preservational potential to be higher than 'normal' conditions (Rogers and Kidwell, 2007). Many bonebeds represent mass death assemblages comprised of several to thousands of individuals of a single species. Unlike small ornithischians, many megaherbivore clades (e.g., centrosaurines, lambeosaurines, hadrosaurines) were likely gregarious for at least part of the year (Varricchio and Horner, 1993; Farlow et al., 1995; Ryan and Russell, 2001; Varricchio, 2011), and so comprise the majority of such monodominant bonebeds (e.g., *Centrosaurus* bonebeds from Dinosaur Provincial Park); small ornithischians are more often preserved as isolated individuals. By including these monodominant bonebeds in the dataset, there is a risk of potentially biasing the results towards higher proportions of megaherbivores because it requires less effort to recover

the remains of multiple individuals from a single site than it does to recover multiple individuals from multiple sites (conversely, the very existence of these assemblages likely attests to the dominance of their constituent species on the landscape). The same can be said for the inclusion of nesting sites, as many more megaherbivore nesting sites have been recovered (Rogers and Kidwell, 2007). Microsites on the other hand, often contain small elements from a variety of taxa which, in some instances, have been concentrated by physical processes. Because microsites, bonebeds and nests are instances where multiple individuals can be preserved, it is important to take steps to prevent artificial inflation in the number of individuals represented at each site due potential 'duplication'. To reduce the potential for such 'duplication', femora of similar sizes originating from different sides of the body were removed from the dataset (i.e., the minimum number of individuals were counted based on femora).

Differences in lithology are also important to consider due to the relationship between grain size and flow energy (Wilson and Moore, 2016). Small bones can be transported at lower flow velocities and over greater distances (i.e., they have higher transportation potential) than larger elements (Martin, 1999; Wilson and Moore, 2016). The farther an element is transported from its source, the more likely it is to be destroyed (Wilson and Moore, 2016). This means that smaller elements are less likely to be preserved in the fossil record, even if they were actually more common than larger elements, especially in river channel settings (Martin, 1999).

To control for these biases while investigating relative abundances of small ornithischians and megaherbivores, femoral lengths (in mm) were measured (both directly and from the literature) and information regarding taphonomic mode (i.e., found

in bonebed/microsite/nest or not) and lithology (i.e., found in sandstone, mudstone or other lithology) was collected. Femoral length was used because it is known to scale isometrically with body size in terrestrial vertebrates (O'Gorman and Hone, 2012; Campione and Evans, 2012) and because femoral shapes are robust, easy to identify and broadly similar between ornithischian taxa, making their transportation potential at equal lengths comparable (Moore and Norman, 2009). Only ceratopsian and hadrosaur femora that were of the same length or shorter than the largest small ornithischian femur (468 mm; *Thescelosaurus*, MOR 1158) were included in the dataset to compare abundances at small body sizes. For simplicity, ceratopsid and hadrosaurid femora were grouped together under a "megaherbivore" category while leptoceratopsid, thescelosaurid, and pachycephalosaurid femora were grouped under a "small ornithischian" category.

After importing the data into R v. 3.6.1 (R Core Team, 2019), the specimens were plotted on a histogram using the "geom_histogram()" function in the "ggplot" package (Wickham, 2016) and bins were set for 100 mm increments, with the relative proportion of counts in each bin displayed as percentages. Expressing counts as percentages allows visual comparisons of relative abundance to be made more easily by removing differences in overall sample size at each bin. Horner et al. (2000) identified early nestling, late nesting, early juvenile, and late juvenile stages at femoral lengths of approximately 70, 120, 180 and 500 mm, respectively, in *Maiasaura* (Wosik et al., 2017 and references therein). Similarly, late nestling and late juvenile stages for *Edmontosaurus* have been established for femora of lengths of 148 and 567 mm, respectively. In *Hypacrosaurus*, however, embryonic, nestling and juvenile stages were identified at femoral lengths of approximately 80, 168–255, and 600 mm. Setting bins at

100, 200, 300, 400, and 500 mm increments allows for abundance differences at various life stages in hadrosaurs to be investigated while accounting for variability between species. Bin increments cannot be related to ceratopsid growth data because relatively few femora were recovered for ceratopsids at femoral lengths <300 mm. A chi-square test was used to determine if the counts observed for each subset (i.e., all, bonebed, isolated, sandstone, mudstone) and bin were significantly different from a 50:50 distribution (i.e., assuming equal distributions for megaherbivore and small ornithischians). The resulting p-values from all of these tests were adjusted for multiple comparisons using the Holm-correction method.

4.3 Results

4.3.1 Skull morphometrics

4.3.1.1 Size-included PCA

The raw data are provided in Appendix K and sample sizes are provided in Table 4.2. The first two PC axes account for 81.5% of the total variation within the dataset (PC1= 68.4%, PC2=13.1%). Loading plots for these axes are provided in Appendix L. Immature megaherbivores and all small ornithischians are separated from mature megaherbivores along PC1 due to their overall smaller sizes (Figure 4.12). Along PC2, a large amount of overlap occurs between leptoceratopsids and juvenile ceratopsids, and thescelosaurids and juvenile hadrosaurids (Figure 4.12). Pachycephalosaurids show some overlap between immature hadrosaurids (especially lambeosaurines), leptoceratopsids and immature ceratopsids. Snout shape index loads heavily and negatively along PC2, followed by paroccipital process breadth (Appendix L). Snout depression, distance from

Table 4.2: Sample sizes for principal components analysis of size-included and size-corrected datasets.

Classification	Stage	Size-included	Size-corrected
Hadrosauridae	Juvenile	15	4
	Subadult	21	3
	Adult	70	0
Ceratopsidae	Juvenile	4	4
	Subadult	8	0
	Adult	42	0
Pachycephalosauridae	Adult	5	5
Thescelosauridae	Adult	5	5
Leptoceratopsidae	Adult	4	4

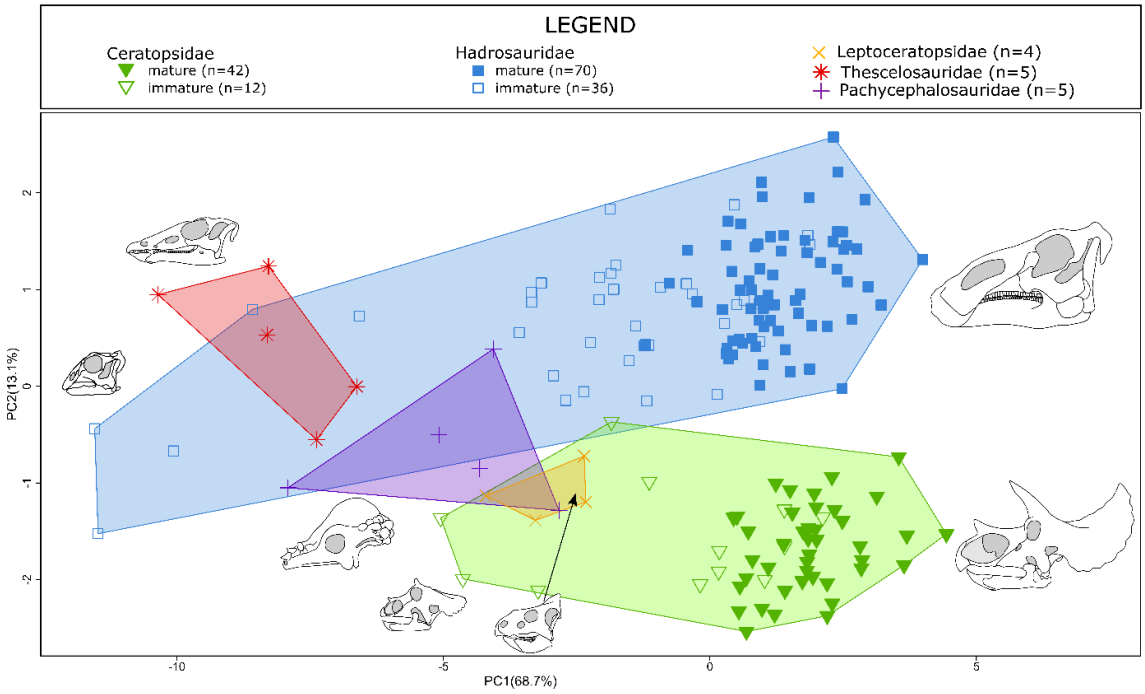

Figure 4.12: Principal component analysis of megaherbivores and small ornithischians showing the plot of PC2 against PC1 for the non-sized corrected dataset.

the distal end of the tooth row to middle quadrate, and snout width load positively along PC2.

4.3.1.2 Size corrected PCA

Sample sizes are provided in Table 4.2. The first six PC axes account for 87.3% of the total variation within the dataset (PC1= 33.6%, PC2=17.9%, PC3= 12%, PC4=10.2%, PC5= 6%, PC6=5.5%). Loading plots for these axes are provided in Appendix M. Thescelosaurids are separated from other taxa along PC1 due to their narrower snouts and paroccipital processes, shorter snout lengths anterior the diastema, and squatter skulls, occiputs and dentaries (Figure 4.13). Pachycephalosaurids have intermediate values for these variables and show slight overlap with leptoceratopsids, hadrosaurids, ceratopsids and thescelosaurids. Pachycephalosaurids are separated from other taxa along PC2, distinguished by their longer tooth rows, less depressed snouts, and shorter diastema lengths (Figure 4.13).

Most taxa show overlap along PC3 except for ceratopsids, which do not exhibit any overlap with pachycephalosaurids (Figure 4.13). Overlap between juvenile ceratopsids and hadrosaurids along PC3 is minimal. The lack of overlap between ceratopsids and pachycephalosaurids and the minimal amount of overlap between ceratopsids and hadrosaurids may be due to small sample sizes for juvenile ceratopsids, as there is likely variation within the population unaccounted for. However, because a wide range of sizes have been sampled, this overlap will likely remain relatively minimal—even with increased sample sizes. Along PC3, SSI, occiput height, skull height and distance from the distal end of the tooth row to the middle of the quadrate load

negatively, and snout width, snout length and the distance from the coronoid apex to the middle jaw joint load positively (Appendix M). Overlap is observed for all taxa along PC4, PC5 and PC6 (Figure 4.13; Appendix N).

The omnibus tests for the rarified NPMANOVA indicate statistically significant differences ($p=0.001$) between some of the small ornithischians and juvenile megaherbivores considered in the size-corrected dataset (Table 4.3). To increase the power of post-hoc pairwise tests, comparisons were made between thescelosaurids, pachycephalosaurids and juvenile megaherbivores because, based on the results of the PCA, thescelosaurids and pachycephalosaurids showed the most separation between each other and with juvenile megaherbivores. Leptoceratopsids were not considered because this group exhibited some overlap with other small ornithischian taxa and overlap with juvenile megaherbivores along all PCs. Even though significant differences were detected by the omnibus test, post-hoc pairwise NPMANOVAs were unable to identify groups that significantly differed from one-another (Table 44). From the results of these post-hoc comparisons, it is expected that pachycephalosaurids would be significantly different from all other taxa, as these comparisons yielded the least significant p-values.

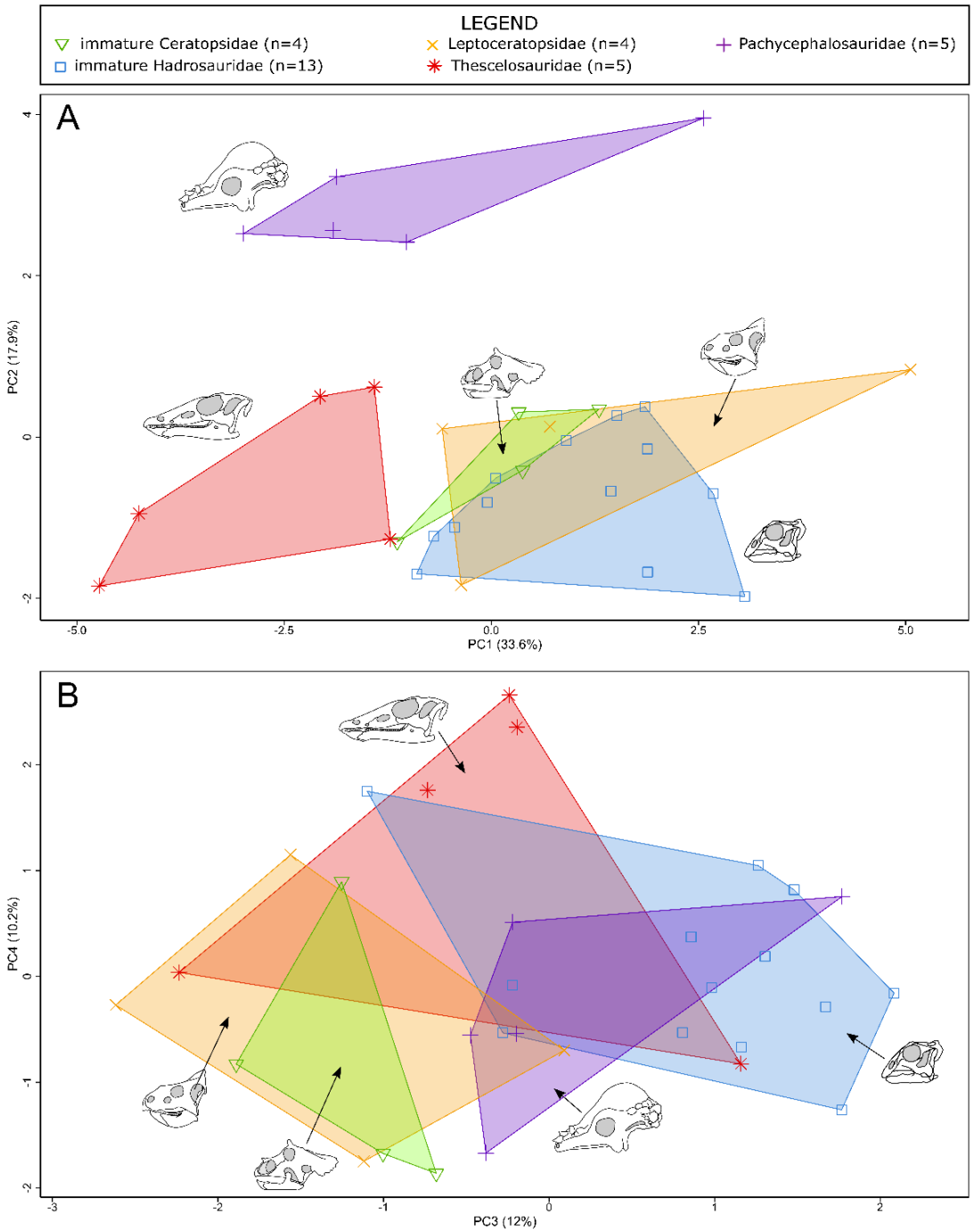

Figure 4.13: Principal component analysis of similar-sized megaherbivores and small ornithischians showing the plot of the first four PCs for the size-corrected dataset. A) Plot of PC1 vs. PC2. B) PC3 vs. PC4. The plot of PC5 vs. PC6 is available in Appendix N.

Table 4.3: Average omnibus values for NPMANOVA tests conducted on rarified size-corrected small ornithischian and juvenile megaherbivore datasets. Abbreviations: Df- degrees of freedom, SS- sum of squares. Sample sizes are provided in Table 4.2.

	Df	SS	R^2	F	Pr(>F)
Model	4	45.063	0.395	2.459	0.001
Residual	15	68.937	0.605		
Total	19	114.000	1.000		

Table 4.4: Average values for select post-hoc pairwise NPMANOVAs conducted on rarified size-corrected small ornithischian and juvenile megaherbivore data. Sample sizes are provided in Table 4.2.

Pairwise comparison	F statistic (of model)	R^2	Uncorrected p-value	Holm-corrected p-value
Hadrosauridae vs. Ceratopsidae	1.162	0.162	0.272	0.748
Hadrosauridae vs. Thescelosauridae	1.167	0.163	0.249	0.724
Hadrosauridae vs. Pachycephalosauridae	1.191	0.166	0.146	0.624
Ceratopsidae vs. Thescelosauridae	1.125	0.158	0.377	0.816
Ceratopsidae vs. Pachycephalosauridae	1.192	0.166	0.162	0.674
Thescelosauridae vs. Pachycephalosauridae	1.183	0.165	0.188	0.685

4.3.2 Maximum feeding height estimates

Raw postcranial data and feeding height estimates are provided in Appendix O.1. The estimated feeding heights for all specimens from the five ornithischian families are depicted in Figure 4.14 and given in Appendix O.2. Of the small ornithischian taxa, leptoceratopsids were the most restricted and unable to reach much higher than 1 m, even when assuming a bipedal feeding posture. Most pachycephalosaurids and thescelosaurids were also restricted feeding at or below ~1.5 m, with the exception of a single large *Thescelosaurus* (MOR 979R), which has a feeding height of ~2 m.

Hadrosaurids would have surpassed the feeding heights of all small ornithischians when they reached a bipedal feeding height of ~2.3 m. Ceratopsids would have fed within the same height ranges as most small ornithischians, as the maximum ceratopsid feeding height is estimated at around ~ 1.3 m (Figure 4.14). The only small ornithischians that ceratopsids surpassed in feeding height were the leptoceratopsids, and this only occurred at very large adult body sizes (~4,400 kg).

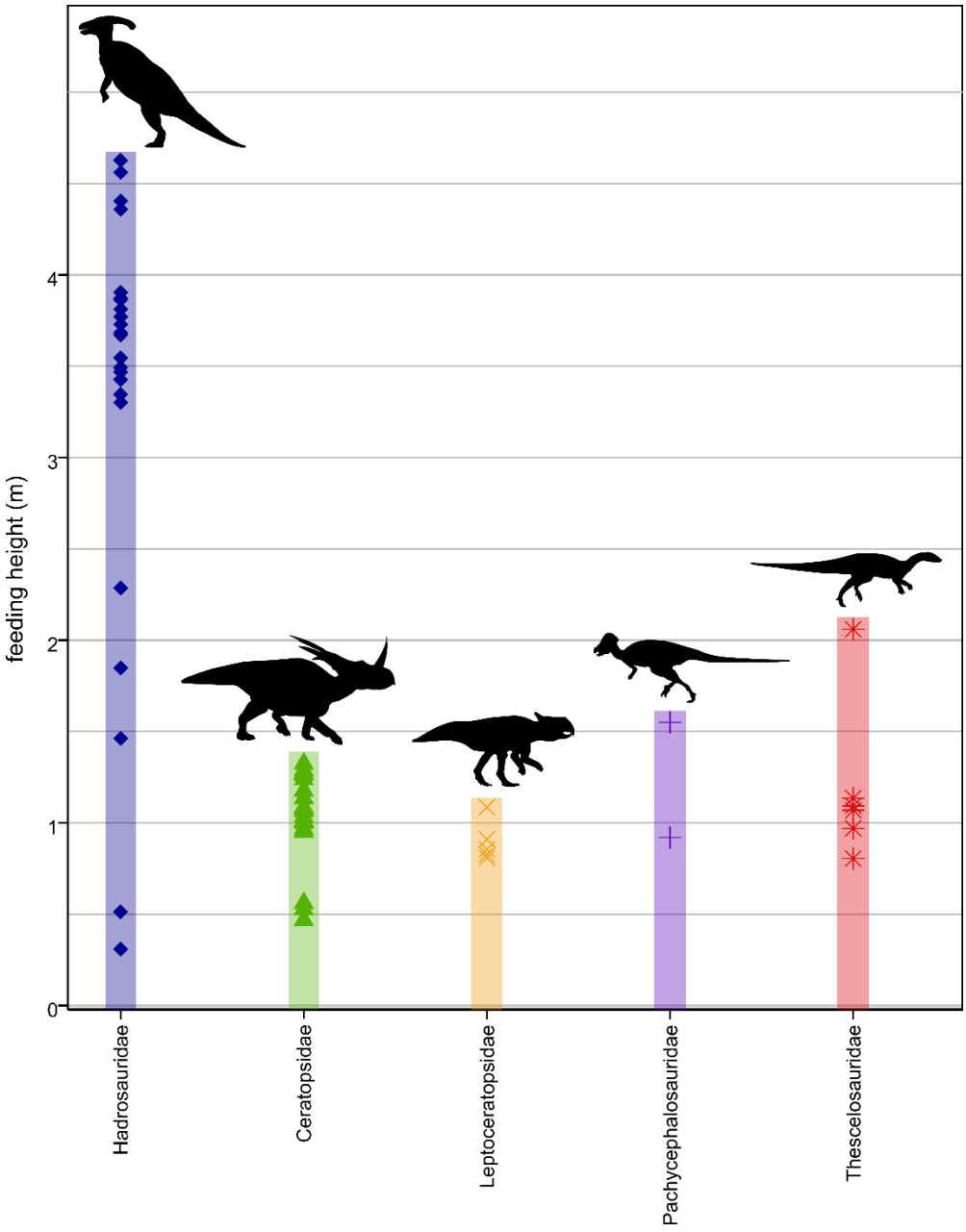

Figure 4.14: Maximum feeding heights calculated for megaherbivores throughout ontogeny and adult small ornithischian taxa. Each point represents a feeding height calculated for a single specimen (see Appendix for raw data and calculated maximum feeding heights for each group). Note: estimates provided for ceratopsids are quadrupedal feeding heights and the estimates for all other taxa are bipedal feeding heights. *Styracosaurus* silhouette modified from C. Dylke (taken from phylopic.org). Hadrosaur silhouette created based on drawing of bipedal hadrosaur from Mallon et al. (2013) and *Parasaurolophus* silhouette by J.M. Wood (taken from phylopic.org). *Thescelosaurus* silhouette constructed from drawings in Boyd et al., 2009; leptoceratopsid silhouette constructed from artwork taken from paleofile.com; *Pacycephalosaurus* silhouette constructed based on artwork by S.A. Vega.

4.3.3 Relative abundances

The raw femoral dataset is provided in Appendix P. Young megaherbivore femora generally outnumber those of small ornithischians (Table 4.5; Figure 4.15). This is particularly true for bonebed- and mudstone-hosted occurrences. Isolated and sandstone-hosted occurrences exhibit no significant differences in abundance. Within the combined dataset, megaherbivores significantly outnumbered small ornithischians for femora <100 mm, and between 400 and 600 mm (Table 4.6; Figure 4.15). Megaherbivores outnumber small ornithischians in mudstone deposits for femora between 200 and 500 mm in length. In the bonebed dataset, megaherbivores also outnumber small ornithischians for femora <100 mm in length and between 300 and 500 mm. No significant differences were observed otherwise.

The above results include specimens from multiple sedimentary formations, time-averaged over a period of approximately 10 Myr. To reduce the effects of time-averaging, comparisons of relative abundances were also made for the Two Medicine (n=43) and Dinosaur Park (n=30) formations, as these formations are the best sampled. The Dinosaur Park and Two Medicine formations contain significantly greater numbers of young megaherbivores—likely due to the number of bonebeds found in these formations (Table 4.5; Figure 4.15). Within the three formations, most comparisons at the bin-level did not indicate significant differences with the exception of the 400-500 mm bin in the Two Medicine Formation, which indicated significantly higher proportions of megaherbivores (Table 4.6; Figure 4.15).

Table 4.5: Results for chi-squared tests conducted on femoral dataset and sub-sets. Significant p-values are given in bold. Abbreviations: Fm-formation; MH- megaherbivore (ceratopsids, hadrosaurids); SO- small ornithischians (leptoceratopsids, pachycephalosaurids, thescelosaurids).

comparison	Observed count		Expected count	χ^2 statistic	p-value
	MH	SO			
complete	116	56	86	20.930	**4.76E-06**
sandstone	16	15	15.5	0.032	0.857
mudstone	49	9	29	27.586	**1.50E-07**
isolated	11	26	18.5	6.081	**0.014**
bonebed	76	17	46.5	37.430	**9.47E-10**
Dinosaur Park Fm	24	6	15	10.800	**0.001**
Two Medicine Fm	41	12	26.5	15.868	**6.79E-05**

Table 4.6: Bin-level chi-squared comparisons. Significant p-values are given in bold. Abbreviations: MH- megaherbivore (ceratopsids, hadrosaurids); SO- small ornithischians (leptoceratopsids, pachycephalosaurids, thescelosaurids).

comparison	Observed count		Expected count	χ^2 statistic	Un-adjusted p-value	Holm-adjusted p-value
	MH	SO				
Complete Dataset						
[0,100]	24	5	14.5	12.448	**4.18E-04**	**0.002**
(100,200]	26	20	23	0.783	0.376	0.753
(200,300]	20	17	18.5	0.243	0.622	0.753
(300,400]	21	8	14.5	5.828	**0.016**	**0.047**
(400,500]	25	6	15.5	11.645	**0.001**	**0.003**
Sandstone subset						
[0,100]	1	0	0.5	1.000	0.317	1.000
(100,200]	5	5	5	0.000	1.000	1.000
(200,300]	2	6	4	2.000	0.157	0.786
(300,400]	5	2	3.5	1.286	0.257	1.000
(400,500]	3	2	2.5	0.200	0.655	1.000
Mudstone subset						
[0,100]	7	1	4	4.500	**0.034**	0.068
(100,200]	12	5	8.5	2.882	0.090	0.090
(200,300]	12	2	7	7.143	**0.008**	**0.027**
(300,400]	10	1	5.5	7.364	**0.007**	**0.027**
(400,500]	8	0	4	8.000	**0.005**	**0.023**
Isolated subset						
[0,100]	2	0	1	2.000	0.157	0.472
(100,200]	1	7	4	4.500	**0.034**	0.136
(200,300]	2	11	6.5	6.231	**0.013**	0.063
(300,400]	3	6	4.5	1.000	0.317	0.635
(400,500]	3	2	2.5	0.200	0.655	0.655
Bonebed subset						
[0,100]	16	4	10	7.200	**0.007**	**0.022**
(100,200]	17	10	13.5	1.815	0.178	0.178
(200,300]	12	3	7.5	5.400	**0.020**	**0.040**
(300,400]	13	0	6.5	13.000	**3.11E-04**	**0.001**
(400,500]	18	0	9	18.000	**2.21E-05**	**1.10E-04**
Dinosaur Park Formation subset						
[0,100]	3	0	1.5	3.000	0.083	0.354
(100,200]	11	4	7.5	3.267	0.071	0.354
(200,300]	4	2	3	0.667	0.414	0.414
(300,400]	3	0	1.5	3.000	0.083	0.354
(400,500]	3	0	1.5	3.000	0.083	0.354
Two Medicine Formation subset						
[0,100]	6	3	4.5	1.000	0.317	0.635

(100,200]	13	7	10	1.800	0.180	0.539
(200,300]	6	1	3.5	3.571	0.059	0.235
(300,400]	3	1	2	1.000	0.317	0.635
(400,500]	13	0	6.5	13.000	**3.11E-04**	**0.002**

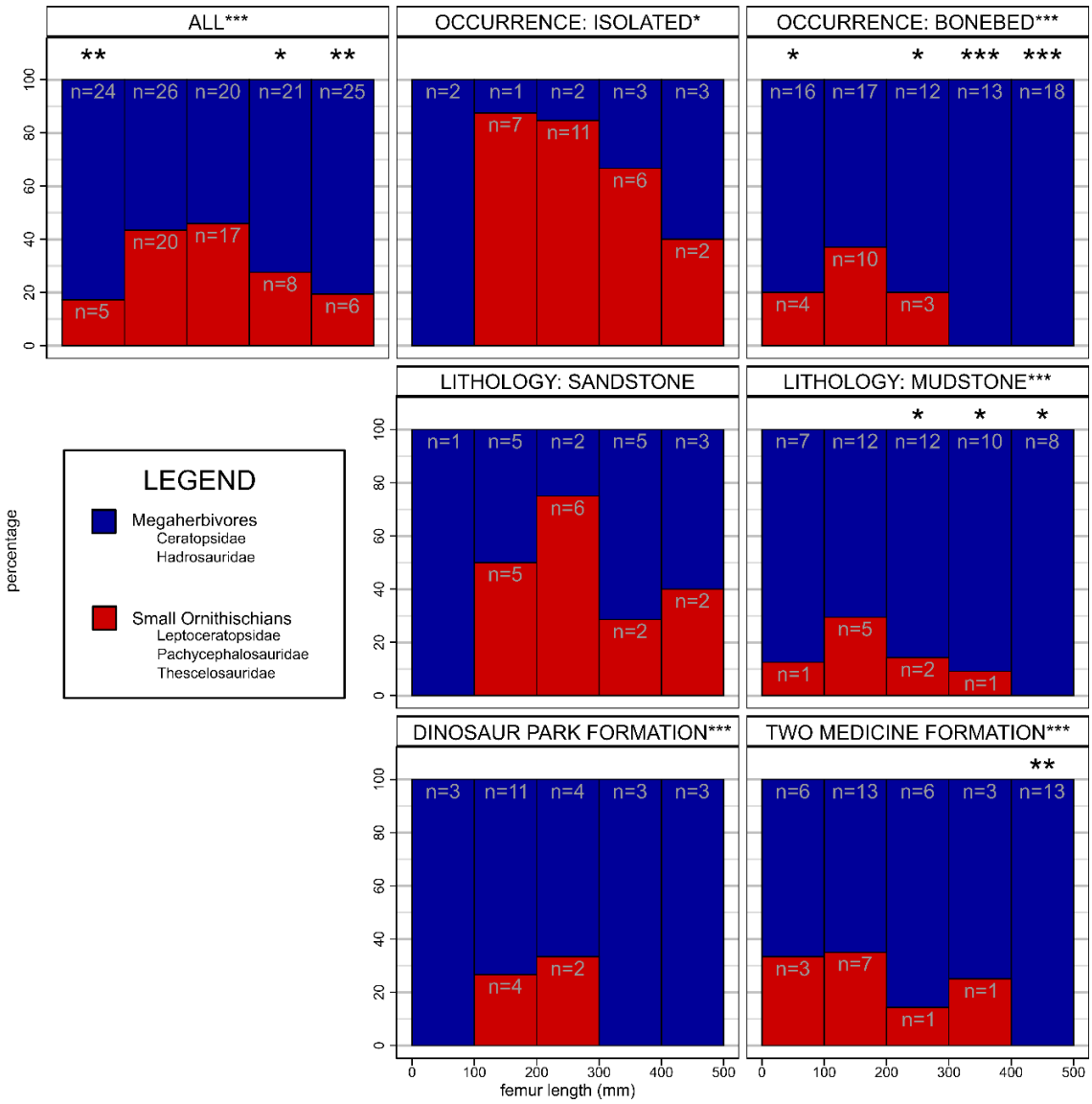

Figure 4.15: Femoral count distributions for the overall dataset and select data subsets. Note: total number of counts have been normalized to 100%. Asterisks indicate statistically significant results where: * if p<0.05, ** if p<0.01, and *** if p<0.001. At the bin level significance is based on Holm-corrected p-values.

4.4 Discussion

4.4.1 Potential for competition at small body sizes

It was predicted that, if competition at small body sizes led to the left-skewed body size distributions observed for Late Cretaceous North American herbivorous dinosaurs, then small ornithischians should have been isolated from similar-sized megaherbivores within the ecomorphospace. Overlap is not observed between some similar-sized ornithischians in both the size-corrected and size-included ecomorphospaces, and is generally consistent with the predictions made by the competition hypothesis. In the size-corrected ecomorphospace, some separation is also observed between juvenile megaherbivores and pachycephalosaurids and thescelosaurids. Even though the rarified omnibus NPMANOVA results did indicate that there were at least some significant differences between groups, post-hoc tests could not identify which groups differed – likely due to low power. Despite being unable to detect statistical differences between groups, there were likely differences between small ornithischian taxa as well as between pachycephalosaurids (and possibly thescelosaurids) and juvenile megaherbivores based on separation along the first two PCs in the size-corrected ecomorphospace. The inability to detect significant differences between groups in post-hoc tests and distributions in the ecomorphospace indicates that, despite some results being consistent with the competition hypothesis, there are further considerations to be made regarding sample sizes and potential deviations from the predictions made regarding separation.

In the size-corrected dataset, the maximum number of individuals that could be selected from each group is small (n=5). Despite this limitation, a large amount of

variance was accounted for especially in the thescelosaurid, pachycephalosaurid, and hadrosaurid subsets, as individuals from a variety of different sizes are included. In addition, the data were rarified and permuted to make statistical comparisons more robust. Given that all currently available and usable juvenile megaherbivores and small ornithischians from the Late Cretaceous of North America were sampled, the results presented here are the best estimates currently available for investigations into potential for competition at small body sizes. When more specimens are found that are suitable for ecomorphological investigations, it will be important to conduct a follow-up study to determine how and if the results presented here change with larger sample sizes. Post-hoc power tests suggest that at least six more specimens per family would be needed, based on the effect size of the current dataset (Appendix Q).

The ecomorphological overlap between leptoceratopsids and juvenile megaherbivores also demands some attention as it does not necessarily follow from the competition hypothesis. One possibility is that these taxa were still experiencing some competitive process on the palaeolandscape. Another possibility is that they were separated along some other niche dimension that was not or could not be considered here (e.g., diel activity, preferred habitat). Given that leptoceratopsids and ceratopsids coexisted throughout the Late Cretaceous – a duration of ~10 million years – separation along another niche dimension is quite probable.

4.4.2 Diet and Ecology

It is also important to consider how these morphological differences may have impacted feeding ecology. Two organisms may feed on the same resource but possess

different morphological features (e.g., due to phylogeny) that would allow them to feed on this resource. Because the taxa investigated here belong to different families, it is likely that there are phylogenetic and/or behavioural differences that could contribute to the differences in morphology detected along PC1 and 2 in the size-corrected ecomorphospace.

Absolute size differences have implications for feeding selectivity, bite forces and feeding height. The absolutely greater sizes of adult megaherbivores compared to small ornithischians would have meant that adult megaherbivores could feed on large quantities of mechanically resistant vegetation growing at different heights. Juvenile megaherbivores and small ornithischians would have selectively fed on softer/more easily cropped vegetation that grew close to the ground.

Within the size-corrected ecomorphospace, separation of thescelosaurids and pachycephalosaurids suggests there may have been some differences in feeding behaviour despite overall size similarities. The narrower snouts of these taxa would have made them more selective compared to juvenile hadrosaurids.

The deeper mandibles and taller skulls in leptoceratopsids and juvenile megaherbivores would have provided better resistance against bending stresses generated during biting of mechanically resistant materials (Janis, 1990, 1995; Spencer, 1995; Mendoza, 2002; Henderson, 2010). The greater distance between the coronoid process apex and jaw joint observed in leptoceratopsids and juvenile megaherbivores would have also enabled them to process more mechanically resistant materials by positioning the coronoid apex more anteriorly relative to the distal end of the tooth row, increasing mechanical advantage, and consequently, bite force (Ostrom, 1966; Henderson, 2010).

Taxonomic differences in overall snout length and depression would have had consequences for feeding behaviour due to differences in relative bite forces generated at the snout tip. Shortening of the snout and/or increases in ventral deflection of the snout would increase bite forces generated at the cropping mechanism by moving the bite point caudally (Greaves, 1974, 1991; Spencer, 1995; van der Meij and Bout, 2008; Mitchell et al. 2018). A more caudally located bite point shortens the moment arm of the applied force (the length of the snout anterior the tooth row) relative to the moment arm of the resistance force (length of the lower jaw anterior the jaw joint) (Mallon and Anderson, 2015). Because vertebrate jaws generally behave like third-class levers, by decreasing the length of the moment arm relative to the resistance force, the leverage increases and, as a result, so does relative bite force. A more ventrally deflected beak tip may have also facilitated the consumption of lower-growing vegetation as the cropping mechanism would have been positioned closer to ground-level. The longer tooth rows and less ventrally deflected snouts in pachycephalosaurids would have reduced relative bite forces at the snout tip and assisted with the cropping of higher-growing vegetation while the shorter length of the snout increased relative bite forces. The shortened length of the snout anterior the diastema observed in thescelosaurids compared to other forms (especially leptoceratopsids and juvenile megaherbivores) would have increased relative bite forces at the snout tip.

In modern bovids, differences in paroccipital process breadth and occiput height are correlated with differences in feeding behaviour (Janis, 1990; Spencer, 1995; Mendoza, 2002). Unlike browsers, which use their tongues and lips to pluck vegetation off of branches, grazers use sharp head motions to sever vegetation gripped between the

incisors. Because the paroccipital and occipital areas are areas for the insertion of cervical musculature, increases in the width of the paroccipital processes and height of the occiput correspond to increases in the size of this musculature. Hadrosaurs, ceratopsians and thescelosaurids would have lacked lips altogether, instead possessing a hard, keratinous sheath over the rostral bone/premaxilla, and would have therefore had to rely on head movements or increased forces at the snout tip to sever vegetation (Morris, 1970; Dodson et al., 2004; Boyd, 2014). The wider paroccipital processes and taller occiputs in juvenile megaherbivores and leptoceratopsids may be reflective of the relatively more important role of sharp head movements made during feeding as bite forces generated at the snout tip may have not been enough to sever vegetation. The narrower paroccipital processes in thescelosaurids and pachycephalosaurids, on the other hand, may indicate that these taxa relied on higher relative bite forces at the tip of the snout to sever vegetation, rather than sharp head movements.

4.4.3 Ecological Release

Increasing size would have been especially important for hadrosaurids as it relates to feeding height. Feeding height and body mass estimates indicate that hadrosaurid feeding height would have exceeded that of the largest small ornithischian specimen (*Thescelosaurus*) at ~335 kg. Based on the calculated growth curves for *Maiasaura* (Woodward, 2015), this means that hadrosaurids would have outgrown their small ornithischian competitors within the first year of life. This ‘escape’ from competition with small ornithischians is known as competitive release (Begon et al., 2006), which occurs when the niche of an organism expands in the absence of a competitor. Thus,

when hadrosaurids were able to outreach and process more mechanically resistant food than their small-bodied ornithischian competitors, they were able to expand their niche as suggested by the fanning of megaherbivore data within the size-included ecomorphospace.

Competitive release may have also occurred in ceratopsids; however, this release would have only been a result of niche expansion due to increasing bite forces. Feeding height would not have helped to alleviate competition because ceratopsids would have only exceeded the maximum feeding height of leptoceratopsids by ~4400 kg—a size that, for most ceratopsids (with the exception of *Triceratops*) would have been attained sometime during adulthood. In addition, even the largest ceratopsids were unable to outreach thescelosaurids and pachycephalosaurids as the maximum feeding heights for these taxa are greater than the maximum 1.3 m feeding height attained by ceratopsids.

In animals undergoing ONSs, ecological release from resource competition may be accelerated by higher intrinsic growth rates at sizes where competitive pressure is highest (Werner and Gilliam, 1984; Arendt and Wilson, 1997). With this "optimistic growth" strategy, these higher intrinsic growth rates mean that individuals spend less time in size classes where competition for resources are relatively high. However, the trade-off is that the probability of surviving to larger size classes is reduced due to a competitive juvenile bottleneck. "Optimistic growth" strategies also have implications for the competitor. In situations where the other competitor species does not shift its niche with size, lower intrinsic growth rates are expected because the non-shifting species experiences competition (i.e., poor resource conditions) for their entire life cycles. It is possible that hadrosaurids and ceratopsids also evolved an "optimistic growth" strategy

as there is high potential for ONSs in these groups and growth rates in the first couple years of life are known to be high (see Chapter 2 and 3 for details; Lehman, 2006; Reizner and Horner, 2006; Erickson and Druckenmiller, 2011; Varricchio, 2011; Vanderveen et al., 2014; Woodward et al., 2015). Small ornithischians (specifically orodromines) are also known to have secondarily developed slower growth rates compared to these larger dinosaurs – potentially due to competition (Padian et al., 2001). Future research investigating if higher growth rates observed in large-bodied dinosaurs (e.g., hadrosaurids, ceratopsids) secondarily evolved may provide further support for this concept of "optimistic growth".

4.4.4 Relative abundance

Interspecific competition is often highly asymmetric and stronger interspecific competitors will typically outcompete weak interspecific competitors (Begon, 2006). Because megaherbivores appeared to have been able to escape competition after a certain point in their development (for hadrosaurids, this would have been within the first year), this would have made them potentially better competitors than small ornithischians (see end of previous section). Competitive asymmetry is expected to influence the relative densities of the competing taxa where the better interspecific competitor is expected to be more abundant than the weak interspecific competitor. Thus, assuming interspecific competition was more important than intraspecific competition (which may be expected given the presence of ONSs in megaherbivores), and competitive asymmetry, juvenile megaherbivores should be relatively more abundant than small ornithischians under taphonomic equivalency.

Overall, the distributions and p-values for chi-squared tests match this prediction. Even though small ornithischians outnumber megaherbivores as isolated occurrences, this is not completely unexpected given that small ornithischians are commonly (though not exclusively) interpreted as having been solitary animals (Rogers, 1990; Farlow et al., 1995). Thus, it is more likely that they would be preserved as isolated individuals compared to the more gregarious megaherbivores.

Similarities in the relative number of small ornithischians and megaherbivores in sandstones may also be a result of transportation. As discussed previously, small elements have higher transportation potential. Thus, remains found in sandstones are less likely to represent true ecological assemblages. Dodson et al. (1998) proposed that small ornithischians preferred upland settings which have poor preservational potential compared to floodplain/fluvial settings. If small ornithischians did prefer, and were more abundant in, upland settings, then, potentially, rivers may have carried small ornithischian remains from the uplands and deposited them in the lowland areas where megaherbivores are typically found, thus producing a deposit with statistically similar proportions of megaherbivores and small ornithischians. Distinguishing this would require more taphonomic information (e.g., rounding/scouring or other evidence of long-distance transport). In short, there does appear to be some influence of competition and taphonomy in the observed body size distributions. It is also worth noting that there are no instances where small ornithischians significantly outnumber megaherbivores as may be expected if taphonomy were purely responsible for the shaping of these communities.

4.5 Conclusions

Dinosaur assemblages exhibit a bias towards larger-bodied herbivores, which runs contrary to modern mammal communities. Some workers proposed that dinosaur communities were so different because of competition between juvenile megaherbivores and small ornithischians, which limited the relative abundances (and diversity) of the latter (Codron et al., 2012, 2013). Other workers proposed that the negatively-skewed distributions may have been the result of taphonomic biases (Brown et al., 2013b).

The present study demonstrates, providing some evidence for the competition hypothesis. This is further attested by the generally greater abundances of the immature megaherbivores under taphonomic equivalency. However, some caution is needed with the interpretation of these results at face value as it is also possible that these taxa partitioned resources along other niche dimensions (e.g., diel activity, habitat preference) that were not/could not be accounted for in these analyses. Because niche partitioning is expected to originate under conditions of strong competitive pressure, it should be expected that ancestral assemblages should exhibit more overlap in ecomorphospace. Under the competition hypothesis, it also follows that these ancestral assemblages should also contain a greater diversity of small species. However, research to this end is required.

Given their larger adult body sizes and oviparous nature (Varricchio, 2011), megaherbivorous dinosaurs experienced more complex life histories than mammals, which would have resulted in differences in overall community structure. Results presented in chapters 2 and 3 provide evidence for changes in niche occupation through ontogeny which would have allowed megaherbivorous dinosaurs to occupy various roles

within the ecosystem. During ontogeny, ceratopsids and hadrosaurids experienced changes in size and shape would have enabled them to escape competition with small ornithischians and broaden their occupied niches. Expansion of these niches would have increased survivorship as there would have been less competition for resources at larger body sizes, resulting in their relatively higher observed abundances in the fossil record. Conversely, small ornithischians would have remained in these competitive bottlenecks and remained relatively limited in terms of diversity and abundance.

This study is the first to investigate if competition produced left-skewed body size-species richness distributions of herbivorous dinosaurs of Late Cretaceous North America from an ecomorphological perspective. Presently, only a handful of individuals from each family ($n<10$) have been collected and are available for study. These small sample sizes may not accurately reflect morphological variation within these groups despite the individuals included representing a range of body sizes (e.g., 16 kg *Stegoceras* vs. 370 kg *Pachycephalosaurus*; Brown et al., 2013; Bensen et al., 2017). Once more adequate specimens are found and made available for study, follow-up investigations will be prudent to test the findings presented here. Research into dental microwear may also prove useful as analyses of dental microwear in both extinct and extant animals have been shown to reflect dietary differences (Solounias and Semprebon, 2002; Semprebon et al., 2004; Rivals and Semprebon, 2011; Whitlock, 2011; Mallon and Anderson, 2014b). Again, caution should be used with the interpretation of competition based exclusively on overlap within reconstructed ecomorphospace as partitioning can occur along other dimensions which were not or cannot be accounted for. Future investigations into relative abundances will also be needed once more complete and detailed specimen locality

information can be obtained as this will increase the power of statistical tests conducted on lithological and taphonomic mode subsets allowing researchers to construct a more detailed picture of how these dinosaurs were distributed across the landscape. Given the incomplete nature of the fossil record and the complexity of dinosaur ecosystems, competition and taphonomy appear to have both played a role in shaping the observed distributions of dinosaur communities.

Chapter 5: Conclusions

Late Cretaceous North America hosted an array of large- (≥1000 kg) and small-bodied (<100 kg) herbivorous dinosaurs (O'Gorman and Hone, 2012; Codron et al., 2012, 2013; Mallon et al., 2012, 2013; Brown et al., 2013a,b; Mallon and Anderson, 2014a,b, 2015). Multiple questions have arisen regarding how so many herbivores could have occupied the same landmass at the same time. Megaherbivores comprised 75-82% of the total dinosaur fauna in terms of abundance, and in some instances up to six species of megaherbivores coexisted at one time (Dodson, 1983). Previous research has shown that adult megaherbivores were able to coexist via niche partitioning (Mallon, 2019). However, little is known about the roles juvenile megaherbivores and smaller-bodied ornithischians played in these communities. It was proposed that, because dinosaur life strategies were likely different from those of mammals (e.g., oviparity vs. viviparity, reproductive output, adult:neonate mass ratio), young megaherbivores occupied their own ecological roles and were potentially important competitors of small ornithischians (Codron et al., 2012, 2013; Mallon, 2019).

Unlike mammals, dinosaurs were oviparous and experienced multi-year growth, which likely meant that they had more complex life histories (i.e., experienced more niche changes during ontogeny) (Varricchio, 2011; Codron et al., 2012, 2013). Because many modern oviparous animals, such as crocodilians and some birds, undergo ONSs, it was proposed that megaherbivorous dinosaurs also underwent ONSs (Dodson, 1975a; Platt et al., 2006; McLeay et al., 2009). Investigations into the dietary implications of growth in hadrosaurids and ceratopsids (chapters 2 and 3) provided evidence for ONSs in these taxa. Results suggested that juvenile megaherbivores selectively fed on soft, low-

growing vegetation, while adults ate tougher, more mechanically resistant vegetation growing at various different heights. Thus, morphological differences would have not only mediated competition interspecifically, but also intraspecifically.

Differences in dietary requirements may have also helped facilitate the segregation of different age-classes, as implied by the existence of bonebeds lacking certain age-classes. These age-segregated groups may have been necessitated by differences in the needs of sexually mature and sexually immature individuals (Varricchio, 2011). Oviparity would have meant sexually mature individuals had to seek out suitable nesting sites and potentially even have had to defend territory to earn breeding rights and/or prime nesting sites. If dinosaurs were similar to modern archosaurs, the pre-hatching portion of the reproductive cycle may have taken 4 to 7 months to complete. If parental care was also provided, the reproductive cycle would have lasted even longer, potentially taking most of the year to complete. Parental care has been implicated for several different dinosaurs, including the hadrosaurid *Maiasaura*. In *Maiasaura* nestlings, the ends of the limb bones have an incomplete, spongy endochondral metaphysis which would have been unable to withstand prolonged locomotor activity (Horner, 2000). Thus, (at least some) dinosaurs would have been nest-bound and required parental care for some period of time after hatching, further extending the length of the breeding season and spatially and temporally restricting reproductively mature adults to nesting areas for most of the year (Varricchio, 2011). Non-breeding individuals, on the other hand, would have been mobile year-round and probably relied on resources farther away from nesting areas to reduce competition and/or because territorial breeders drove them away from the area. Thus, differences in

dietary requirements would have allowed breeding and non-breeding individuals to form separate aggregations and occupy different areas of the landscape (Varricchio, 2011).

The greater complexity of dinosaur life histories may have also meant that dinosaur ecosystems were controlled by different processes than mammalian ecosystems. In both modern and extinct mammalian ecosystems, smaller animals are more abundant and diverse compared to larger animals (Damuth, 1982; Peters and Wassenberg, 1983; Siemann and Brown, 1999; Kozlowski and Gawelcyzk, 2002; Smith and Lyons, 2011). In Late Cretaceous North American dinosaur ecosystems, however, smaller-bodied ornithischians, such as leptoceratopsids, thescelosaurids and pachycephalosaurids, were relatively less diverse and less abundant than larger taxa (e.g., hadrosaurids and ceratopsids) (O'Gorman and Hone, 2012; Codron et al., 2012, 2013; Brown et al., 2013a,b). This bias towards megaherbivores was proposed to be the result of competition between similar-sized juvenile megaherbivores and small ornithischians, which ultimately limited the diversity of the latter (Codron et al., 2012, 2013). Within a size-structured assemblage such as that of Late Cretaceous North America, small ornithischians and similar-sized young megaherbivores are expected to occupy different niches (i.e., different areas of the ecomorphospace) if the assemblage represented the result of strong competitive forces acting over evolutionary history. It would also be expected that this past competition would have limited the abundance and richness of small ornithischian species, especially if megaherbivores exhibited "optimistic growth" (see Chapter 4 end of section 4.4.3 for details). If taphonomic biases were responsible for the body size distributions observed in Late Cretaceous assemblages, then, when

accounting for these biases, small ornithischians are expected to be as or more abundant than megaherbivores.

Chapter 4 demonstrated potential competition between some juvenile megaherbivores and small ornithischians, specifically between leptoceratopsids and juvenile megaherbivores, as other small ornithischian clades (thescelosaurids, pachycephalosaurids) are separated from other groups within the ecomorphospace. However, this separation (i.e., niche partitioning) is also to be expected as an end-result under conditions of strong competition. Regardless of which groups of small ornithischians juvenile megaherbivores competed with, megaherbivores would have outgrown their competitors, undergoing ecological release and expanding their occupied niches (for hadrosaurids, this would have been within the first year of life). Codron et al. (2012,2013) also predicted that small ornithischians would be less abundant than juvenile megaherbivores as a result of their competitive disadvantage. The relative abundances of similar-sized megaherbivores and small ornithischians generally match this prediction. However, for isolated and sandstone occurrences, small ornithischians were present in statistically similar abundances as megaherbivores, as would be expected if taphonomic processes were responsible for the observed dinosaur body size distributions. Thus, both competition and taphonomy are likely responsible for the body size distributions observed in Late Cretaceous North American dinosaur assemblages.

5.1 Limitations

This study presents a first step in examining the potential influences ONSs had in the structuring of dinosaur communities; however, further research is needed. The

relative rarity of small dinosaur material means that sample sizes are low, and analyses inescapably rely on composite reconstructions. The analyses presented here will need to be repeated once more suitable specimens have been recovered and made available for study to see if they are supported.

There are other inherent difficulties associated with working on palaeontological dataset. With dental microwear analyses for example, obtaining useful data can be extremely difficult because wear is not always preserved on occlusal surfaces and, unlike with modern datasets, the pool of specimens to sample from is already limited to a small subset as teeth often fall out of the skull shortly after death (LeBlanc et al., 2016). Another issue that arises from working with dental microwear is that postmortem damage (e.g., acid etching, tool marks) can obscure wear potentially reducing samples sizes even further. How dental microwear is measured can also create issues of comparability with other studies because there can be variability not only in working magnification, but also in the numbers of features counted between observers (Mihlbachler et al., 2012; Mihlbachler and Beatty, 2012).

The inclusion of measurements taken from composite reconstructions is another important consideration that must be made. Composite reconstructions are typically produced by scaling and combining material belonging to multiple individuals into a single skull (Lautenschlager, 2016). This process makes assumptions regarding how these elements may have actually scaled with size. Sometimes these assumptions are not even made using material from the same genus. Other times assumptions regarding relative proportions are best guesses made using material from closely-related taxa. The inclusion of such composites can thus create a false representation of morphological variability

within a population. Attempts were made to reduce the amount of error associated with the use of such composites in my datasets by only selecting composite specimens produced from individuals of the same taxon from the same bonebed (e.g., MOR 548). While this makes fewer assumptions, there is still the opportunity for error to be introduced because variation across multiple individuals is being concentrated and treated as a "single" individual. Because samples sizes are especially limited for certain taxa (e.g., small ornithischians), it is necessary to use these constructions but acknowledge that these reconstructions can potentially introduce error into analyses.

There are also possible issues with using morphology as an ecological proxy. Even though anatomical features have been shown to be closely correlated with diet, habitat and feeding behaviours in modern animals (e.g., Spencer, 1995; Janis, 1990, 1995; Mendoza et al., 2002), there are some aspects of an organism's ecology that will not be accounted for in its skeletal morphology. Modern animals may have similar morphologies but not compete with each other due to differences in, for example, habitat preference, diel activity, and migration patterns (Begon et al., 2006). In ornithischian dinosaurs, this creates some difficulties because there are no extant descendants relative available to study. It is therefore impossible to know for certain if, for example, two taxa were active at the same times of day or if they occupied the same area at the same time. This means that, even though leptoceratopsids do overlap in ecomorphospace with juvenile megaherbivores (Chapter 4), they may have still partitioned resources along another niche dimension that was not or could not be accounted for.

Lastly, error can be introduced through the use of a time-averaged dataset. For competition to even potentially occur, taxa must overlap in both space and time (Begon et

al., 2006). In the case of the present study, it was necessary to include specimens from various formations to achieve a sample size large enough for analysis. However, because taxa were sampled from various formations, the datasets were time-averaged over ~10 Myr. This means that many specimens never overlapped in time and/or space and therefore did not comprise a "true" ecological community. However, because of the nature of the fossil record, there is no real way to study community-level interactions without time-averaging being present in the dataset. All than can be done is to acknowledge that the sample is time-averaged and how this time-averaging may influence the results. Therefore, the present analyses were still conducted even though the samples were time-averaged because the basic composition of Late Cretaceous communities remain broadly similar through time and space (i.e., pachycephalosaurids, thescelosaurids, leptoceratopsids, hadrosaurids and ceratopsids are all found together). Thus, the structuring of Late Cretaceous communities should be broadly similar. Additionally, if overlap does not occur at all even when there is time averaging then overlap will be absent even at finer temporal and spatial scales.

5.2 Future lines of inquiry

Research into ONSs in other taxa could provide further insight into factors influencing the structure of other dinosaur communities. Morphological changes have been shown to occur during *Diplodocus* ontogeny and have been cited as evidence for an ONS (Woodruff et al., 2018). As in Late Cretaceous communities, the Late Jurassic Morrison Formation also shows relatively higher abundances of large-bodied taxa (here sauropods such as *Diplodocus*, *Camarasaurus* and *Barosaurus*) compared to smaller-

bodied taxa (Dodson et al., 1980; Noto and Grossman, 2010). Potentially, the structuring of the Morrison palaeocommunities were influenced by sauropod ONSs in much the same way that hadrosaurid and ceratopsid ONSs appear to have influenced the structuring of Late Cretaceous North American communities.

Ontogenetic niche shifts may have also had important implications for the structuring of other palaeocommunities. Lakin and Longrich (2019) proposed that the piscivorous theropod, *Spinosaurus* also underwent ONSs based on size disparity through ontogeny and absence of any hatchling-sized material. This relative absence of juvenile material is likely not related to taphonomy because smaller theropods with similar preservation potential have been recovered from the Kem Kem beds. The Cretaceous Kem Kem beds from which many of these remains have been found, show unusually high abundances of spinosaurids compared to other theropod taxa (Benyoucef et al., 2015). Undergoing an ONS would have reduced intra-specific competition giving spinosaurids a competitive advantage over other theropods similar to how ONSs in North American megaherbivores gave them a competitive advantage over small ornithischians.

Ontogenetic niche shifts have also been proposed for other carnivorous dinosaur taxa (e.g., *Tyrannosaurus rex*) based on morphological differences observed through ontogeny (Carr, 1999). These ONSs may also explain negatively-skewed body size distributions observed in carnivorous taxa as well as why observed predator/prey proportions in some dinosaur communities are higher than predictions made using mammalian predator/prey proportions and relationships. For example, in the Hell Creek Formation, (with the exception of *Dakotaraptor*) medium-sized predators between 200 and 900 kg are virtually absent (Horner et al., 2011). Differences in the shape of the skull

(e.g., snout shape, skull height, tooth shape) may have allotted different ontogenetic stages different mechanical advantages, allowing different stages to consume different prey and potentially occupying all available niche space that would otherwise be occupied by other medium- to large-bodied predators. In *T. rex*, juvenile skulls are more gracile (e.g., snout is longer and narrower) and probably unable to withstand bending stresses generated by bite forces needed to process bone, thus restricting them to consuming softer animal materials. Other tyrannosaurids (e.g., *Albertosaurus*) exhibit a similar shift from a more gracile to more robust morphotype over ontogeny suggesting ONSs may have been prevalent within the tyrannosaurid clade. Investigations into the potential for ONSs in tyrannosaurids facilitated by these possible changes in bite forces and mechanical resistances using Finite Element Analysis may prove an interesting line of investigation.

When archosaur body mass-species richness distributions became negatively-skewed is also uncertain, although some distributions observed from the Middle Permian to Early Jurassic Beaufort Group of the Karoo Supergroup are negatively-skewed (Codron et al., 2016). Carnivore size distributions for the Middle Permian *Tapinocephalus* assemblage zone was positively-skewed, and negatively-skewed in the Late Permian *Tropidostoma* and *Cynognathus* assemblage zones, and the remaining assemblage zones could not be distinguished from normal (Figure 5.1). Most herbivore distributions from the Karoo Basin at this time were positively-skewed with the exception of the Middle Permian *Tapinocephalus* and Triassic *Lystrosaurus* assemblage zones, which could not be distinguished from normal. This would suggest that negatively-skewed size distributions were present in terrestrial ecosystems by the Triassic. However,

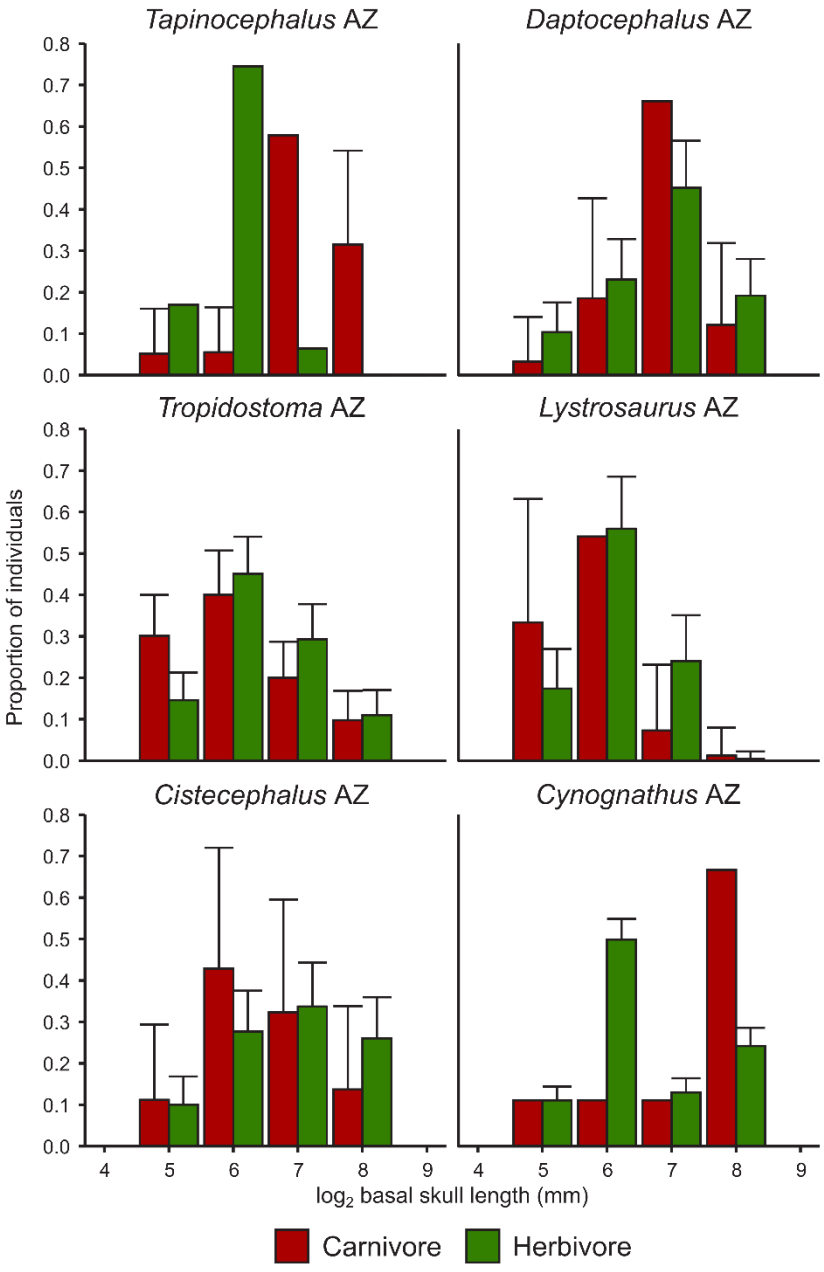

Figure 5.1: Log_2-transformed basal skull length distributions of carnivores and herbivores from six assemblages zones in the Karoo Permo-Triassic sequence (modified from Codron et al., 2016). The graphs show the means (bars) and 95% confidence intervals (whiskers) taken from 1000 random subsamples. Subsample sizes were equal to the smallest sample in the sequence. Abbreviations: AZ-assemblage zone.

in the Middle to Late Jurassic Yanliao Biota in Northeastern China, sauropodomorphs and other vertebrates larger than a few kg are completely absent from this fauna (Xu et al., 2016). The cause of this absence is uncertain but taphonomic and collection biases are at least partly responsible for these absences as most deposits are lacustrine (i.e., there is preferential preservation) and most excavations of this biota have been conducted commercially. What can be said for certain is that archosaur/dinosaur communities were dominated by larger-bodied taxa by the Late Jurassic of North America (Dodson et al., 1980; Foster, 2003; Noto and Grossman, 2010).

Palaeontologists have proposed a variety of different reasons to explain the structuring of dinosaurian communities (e.g., habitat preference, competition, taphonomy) (Farlow et al., 1995). The results of the present study provide some support the role of ONSs in community dynamics. Like North American assemblages, some assemblages from other parts of the world (e.g., Jurassic sediments of the Tremp Basin in Spain, Upper Cretaceous Sao Khua and Khok Kruat formations of northeastern Thailand) also show a bias towards larger bodied taxa (sauropods or ornithopods) (Buffetaut and Suteethorn, 1999; Buffetaut et al., 2005; Riera et al., 2009). However, other assemblages do not. For example, iguanodontids and *Hypsilophodon* are the most common taxa found in Early Cretaceous Wessex Formation assemblages (Insole and Hutt, 1994). A mixture of both large (titanosaurs, *Telmatosaurus*) and small (*Zalmoxes*) taxa also dominate various deposits throughout the Haţeg Basin of Late Cretaceous Romania (Csiki, 2010; Botfalvai et al., 2016). Other assemblages even exhibit a bias towards smaller-bodied taxa. The Lower Cretaceous Jehol Group in Liaoning, China the small ceratopsian *Psittacosaurus* is typically the most common herbivorous dinosaur recovered (Xing and

Norell, 2006). Small to medium-sized animals are also relatively more abundant than large animals within the arid eolian deposits of the Late Cretaceous Djadokhta Formation in Inner Mongolia (Jerzykiewicz et al., 1993). This is unexpected based on the research presented by Noto and Grossman (2010) which suggested small taxa were less common in more arid conditions due to relatively lower densities of low-lying groundcover to protect against predators and to support a vast array of herbivores. To gain insight into why dinosaur assemblages from other parts of the world are not always negatively-skewed, future research will need to consider how interactions between and within a species through ontogeny structured these communities and how taphonomy may have altered those distributions.

5.3 Final remarks

In modern oviparous non-mammalian animals, such as crocodilians, ONSs are more often the norm rather than the exception (Dodson, 1975a; Platt et al., 2006; McLeay et al., 2009). Given that animals comprising the extant phylogenetic bracket for dinosaurs undergo ONSs, and that many dinosaurs experience long growth trajectories (e.g., ceratopsids, hadrosaurids, sauropods), it is likely that ONSs occurred more commonly in dinosaurs than is presently known. While the results presented here represent a good first step in providing insight into other factors influencing the structuring of dinosaur communities, further research will be needed to better understand how the interactions between species as well as within a species through ontogeny structured dinosaur communities and how these interactions are masked by taphonomic processes to produce the archosaur body size distributions currently observed in the fossil record.

Appendices

Appendix A Holm-adjusted p-values for Durbin-Watson tests of regression of linear hadrosaurid cranial measurements against quadrate height.

Cranial measurement	Adjusted p-value DW (x= quadrate height)
Snout length	1.000
Diastema length	0.158
Tooth row length	0.445
Distance from distal end of tooth row to mid-quadrate	0.195
Snout width	0.097
Dentary height	**0.001**
Paroccipital process breadth	1.000
Occiput height	0.267
Distance from coronoid process apex to middle jaw joint	0.445
Depression of snout below occlusal plane	0.381
Skull height	1.000
Quadrate breadth	1.000

Appendix B Raw cranial data used for regression analysis of hadrosaurid dataset. Abbreviations: Subfam-subfamily, On.-ontogenetic description used, quad- quadrate height, sl- snout length, dl- diastema length, trl- tooth row length, dt-mq- distance from jaw joint to distal end of tooth row, sw- maximum beak width, dh- midpoint dentary height, ppb- paroccipital process breadth, oh- occiput height, cp-jj: distance apex of coronoid process to middle of jaw joint, sd- depression of snout below occlusal plane, sh- skull height, qb- quadrate breadth, La-Lambeosaurinae, Ha-Hadrosaurinae, Cory-*Corythosaurus*, Lamb-*Lambeosaurus*, Lamb indet.-Lambeosaurinae indet., Hyp-*Hypacrosaurus*, Para-*Parasaurolophus*, Gryp-*Gryposaurus*, Brachy-*Brachylophosaurus*, Maia-*Maiasaura*, Edm-*Edmontosaurus*, J-juvenile, S-subadult, A-adult; *cast, if the original specimen is known the number is provided; [†]composite; [§]measured original and reconstructed portions of specimen. [1]Campione and Evans, 2011; [2]Farke et al., 2013; [3]Gates and Sampson, 2007; [4]Lull and Wright, 1942; [5]Mallon and Anderson, 2013. All measurements are in mm. Empty cells denote missing data.

Subfam	Genus	Specimen	On.	quad	sl	dl	trl	dt-mq	sw	dh	ppb	oh	cp-jj	sd	sh	qb
La	Lamb indet.	TMP 1989.079.0052	J	32.7	14.0	16.0	25.0	10.0	14.0	12.0			25.0	5.0		20.0
La	Lamb indet.	UALVP 57103	J	171.6	97.0	41.0	170.0	80.0	180.0	66.0	140.0	62.0	130.0	65.0	112.0	156.0
La	Cory	TMP 1983.031.0003*[§] cast ROM 759	J	166.2	60.0	55.0	139.0	66.0	100.0	63.0	70.0		115.0	30.0	130.0	84.0
La	Cory	ROM 1947	S	174.9	106.0	76.0	220.0	80.0	182.0	50.0			180.0	35.0	125.0	
La	Cory	CMN 34825	S	199.9	88.0	48.0	241.0	61.0	112.0	60.0			175.0	42.0	180.0	210.0
La	Cory	USNM 16600	S	218.6	86.0	52.0	145.5	38.0	97.0	49.0	154.0			21.0	131.0	185.0
La	Cory	TMP 1997.012.0232[5]	S	213.0	140.0	33.0	231.0	56.0		68.0			170.0	55.0	192.0	
La	Cory	ROM 870[5]	A	256.2			242.0	97.0		75.0	94.0		195.0		212.0	134.0
La	Cory	TMP 1982.037.0001[5]	A	262.4	110.0	75.0	251.0	93.0	136.0	74.0	122.0	141.0	214.0	65.0	221.0	150.0
La	Cory	FMNH 1357[5]	A	312.6	127.0	73.0	287.0	102.0		97.0			235.0	120.0	255.0	
La	Cory	ROM 868[5]	A	331.6	156.0	129.0	294.0	112.0	124.0	96.0			226.0		292.0	190.0
La	Cory	UALVP 52826	A	247.8	182.0	83.0	345.0	50.0	165.0	84.3	250.0	90.0		112.0	295.0	
La	Cory	ROM 1933[5]	A	312.0	137.0	115.0	285.0	80.0	147.0	87.0	160.0	123.0	224.0	107.0	230.0	
La	Cory	TMM 40484-88	A	238.0	580.0		271.2	136.9		57.8			192.2	74.8	197.0	
La	Cory	AMNH 5338	A	308.7	132.6	130.1	299.6	118.8		89.4			238.9	86.3	248.6	
La	Cory	ROM 871[5]	A	402.5				100.0		108.0	188.0	156.0	225.0		275.0	75.0

La	Cory	TMP 1980.040.0001[5]	A	319.2	118.0	102.0	241.0	114.0	209.0	90.0	262.0	169.0	230.0	53.0	266.0	363.0
La	Cory	TMP 1984.121.0001[5]	A	276.5	123.0	123.0	285.0	99.0	215.0	92.0	222.0	200.0	235.0	44.0	260.0	285.0
La	Cory	TMP 1980.023.0004[5]	A	258.1			340.0	86.0			212.0		260.0		262.0	278.0
La	Cory	CMN 8676[5]	A	264.6	130.0	96.0	248.0	90.0	141.0	81.0	151.0	140.0	179.0	74.0	213.0	300.0
La	Cory	CMN 8704[5]	A	367.0	166.0	45.0	303.0	82.0	120.0	84.0		145.0	233.0	77.0	271.0	220.0
La	Cory	ROM 776[5]	A	371.1	168.0	82.0	298.0	109.0	220.0	83.0	170.0	160.0	271.0	91.0	270.0	256.0
La	Cory	ROM 777[5]	A	311.9	141.0	137.0	305.0	100.0	173.0	82.0			237.0	76.0	260.0	190.0
La	Cory	ROM 845[5]	A	350.7	139.0	122.0	269.0	100.0	220.0	90.0	205.0	135.0	230.0	100.0	273.0	247.0
La	Lamb	AMNH 5340[4]	J	178.3	84.7	41.5	185.6	79.3		49.6			112.3	64.0	119.8	
La	Lamb	TMP 1983.031.0002*§ cast ROM 758	J	156.3	50.0	58.0	139.0	83.0	90.0	68.0	140.0	60.0	120.0	44.0	135.0	150.0
La	Lamb	ROM 869[5]	S	264.2	86.0	104.0	236.0	104.0	114.0	75.0	120.0		212.0	80.0	218.0	180.0
La	Lamb	CMN 8633	S	254.5	102.0	74.0	216.0	80.0	82.0	64.0	148.0	38.0	168.0	52.0	154.0	168.0
La	Lamb	CMN 8503[5]	A	290.5	97.0	67.0	250.0	55.0	104.0	72.0	102.0	119.0	186.0	28.0	211.0	140.0
La	Lamb	NHMUK R9527[5]	A	301.7	591.0		304.0	100.0		87.0			245.0	36.0	271.0	
La	Lamb	USNM 10309	A	401.7	153.3	177.6	305.1	213.6		86.1	240.5			76.0	304.3	
La	Lamb	CMN 2869[5]	A	294.9	142.0	108.0	242.0	106.0	130.0	89.0	142.0		191.0	52.0	256.0	248.0
La	Lamb	FMNH 1479[5]	A	330.9	174.0	107.0	293.0	107.0	226.0	95.0	160.0	148.0	212.0	128.0	263.0	190.0
La	Lamb	ROM 1218[5]	A	364.0	184.0	76.0	327.0	95.0	196.0	101.0	205.0	168.0	216.0	114.0	282.0	257.0
La	Lamb	ROM 794[5]	A	338.9	136.0	205.0	269.0	95.0	182.0	99.0	174.0	162.0	210.0	153.0	290.0	185.0
La	Lamb	TMP 1982.038.0001[5]	A	357.7	114.0	57.0	244.0	77.0	215.0	85.0	280.0	140.0	238.0	98.0	247.0	375.0
La	Lamb	CMN 351[5]	A	357.9	127.0	152.0	295.0	105.0	116.0	89.0			235.0	32.0	279.0	
La	Lamb	CMN 8703[5]	A	335.0	119.0	153.0	309.0	90.0	160.0	94.0	186.0	160.0	216.0	59.0	310.0	190.0
La	Lamb	TMP 1981.037.0001[5]	A	298.4	124.0	131.0	327.0	82.0	202.0	92.0	205.0	175.0	227.0	93.0	258.0	155.0
La	Lamb	CMN 8705[5]	A	338.7	161.0	94.0	300.0	113.0	152.0	102.0	176.0	152.0	256.0	65.0	290.0	192.0
La	Lamb	TMP 1966.004.0001[5]	A	310.3	138.0	118.0	285.0	93.0	140.0	100.0	142.0		225.0	91.0	265.0	116.0
La	Hyp	CMN 2247	J	144.6	66.0	34.0	117.0	38.0	128.0	47.0			110.0	49.0	108.0	140.0
La	Hyp	AMNH 28497*	J	40.5	12.0	18.0	27.0	25.0	20.0	11.0	50.0	25.0	25.0	9.0	41.0	46.0

La	Hyp	TMP 1994.385.0001	J	174.8	80.0	70.0	141.0	55.0	71.0	44.0	140.0	61.0	127.0	35.0	107.5	120.0
La	Hyp	AMNH 5461	J	161.7	45.3	30.5	129.0	45.5	92.0	47.5	127.0	51.0	121.0	48.0	147.0	150.0
La	Hyp	MOR 548B[1]	J	90.5	31.0	20.0	72.0	32.0	54.0	27.0	80.0	34.0	66.0	9.0	75.0	87.0
La	Hyp	CMN 2246	S	181.5	78.0	86.0	196.0	59.0	200.0	67.0	130.0	40.0	185.0	69.0	152.0	112.0
La	Hyp	CMN 8501	A	298.6	128.0	52.0	250.0	140.0	260.0	102.0	204.0	87.0	245.0	30.0	245.0	220.0
La	Hyp	AMNH 5278	A	313.7	135.4	115.7	273.2	127.1		110.9			201.6	58.2	251.7	
La	Hyp	MOR 549	A	255.4	148.2	142.0	321.0	86.4		80.3			223.8	100.9	238.0	233.1
La	Para	RAM 14000[2]	J	112.3	34.0	14.4	102.6	51.4	52.7	29.3				33.4	103.1	
La	Para	TMP 1990.036.0155[5]	S	171.3	80.0	53.0	147.0	85.0	127.0	52.0			140.0	35.0	161.0	
La	Para	ROM 768[5]	A	284.1	151.0	82.0	291.0	113.0	180.0	102.0	192.0		235.0	125.0	229.0	185.0
Ha	Pro	ROM 1928[5]	S	334.4	162.0	94.0	314.0	93.0		96.0	152.0		247.0	76.0	218.0	
Ha	Pro	TMM 41262[5]	S	324.7	140.0	80.0	305.0	114.0	104.0	91.0			223.0	110.0	222.0	
Ha	Pro	CMN 2277[5]	A	370.7	129.0	172.0	382.0	116.0	130.0	131.0			254.0	62.0	296.0	235.0
Ha	Pro	CMN 2870[5]	A	381.5	180.0	111.0	414.0	98.0	221.0	129.0	270.0	142.0	258.0	67.0	295.0	330.0
Ha	Pro	ROM 787[5]	A	376.9	184.0	121.0	364.0	124.0	166.0	133.0	170.0	183.0	271.0	79.0	302.0	200.0
Ha	Pro	TMP 1984.001.0001[5]	A	403.4	250.0	115.0	395.0	140.0	248.0	139.0			294.0	125.0	280.0	
Ha	Pro	USNM 12712[5]	A	409.7	276.0	124.0	435.0	140.0	130.0	123.0		190.0	272.0	83.0	348.0	240.0
Ha	Gryp	TMP 1980.022.0001[5]	S	325.4	140.0	58.0	277.0	105.0	94.0	92.0	197.0	153.0	220.0	75.0	238.0	174.0
Ha	Gryp	RAM 6797[3]	A	528.5	271.7	8.7	408.7	143.5		132.6			248.6	110.9	339.2	
Ha	Gryp	CMN 2278[5]	A	460.2	181.0	94.0	381.0	140.0	238.0	142.0	423.0	211.0	289.0	89.0	337.0	318.0
Ha	Gryp	ROM 873[5]	A	432.1	208.0	53.0	396.0	134.0	201.0	125.0	176.0	146.0	284.0	107.0	305.0	190.0
Ha	Maia	MOR* cast YPM 22400	J	63.6	17.0	18.0	50.0	25.0	39.0	18.0	54.0		45.0	12.0	55.0	49.0
Ha	Maia	MOR-cast-090*	J	32.4	11.0	9.0	34.0	11.0	19.0	11.0	31.0			5.0	39.0	20.0
Ha	Maia	MOR cast 019*	S	212.3	90.0	48.5	186.0	78.5	181.5	58.5	55.0	63.0	146.5	65.5	158.0	209.0
Ha	Maia	MOR cast 089* of OTM F138	A	310.9	170.0	85.0	280.0	160.0	320.0	88.0	180.0		212.0	90.0	191.0	
Ha	Brachy	CMN 8893	A	335.0	156.0	95.0	320.0	100.0	220.0	98.0	210.0	81.0	243.0	25.5	260.0	401.0
Ha	Brachy	GPDM.115	A	265.7	125.0	100.0	180.0	95.0	252.0	60.0	200.0		155.0	70.0	165.0	224.0

Ha	Brachy	GPDM.200	A	327.9	69.0	251.0	160.0			105.0	170.0		249.0	104.0	218.0	322.0
Ha	Edm	CMN 58500*	J	147.1	55.0	78.0	107.0	60.0	108.0	45.0	100.0	37.0	115.0	25.0	97.0	148.0
Ha	Edm	CMN 40586* cast NHM R8927	S	319.6	120.0	194.0	253.0	168.0	190.0	115.0	155.0	86.0	270.0	40.0	216.0	156.0
Ha	Edm	CMN 8399	S	299.1	150.0	210.0	210.0	180.0	174.0	110.0	220.0	95.0	220.0	80.0	164.0	230.0
Ha	Edm	CM 26259[1]	S	353.0	180.8	113.3	289.3	164.7		118.4			285.3	115.0	279.1	
Ha	Edm	AMNH 5046	S	236.7	60.0	115.0	245.0		158.0	61.0	154.0	61.0	150.0	39.0	150.0	188.0
Ha	Edm	CMN 8509	S	315.1	85.0	240.0	285.0	110.0	210.0	112.0	190.0	120.0	255.0	60.0	200.0	266.0
Ha	Edm	SM R4050[1]	S	388.0	265.6	120.1	238.5	167.5		137.0			231.2	99.8	262.2	
Ha	Edm	CMN 2289	A	409.0	164.0	268.0	418.0	127.0		167.0	351.0	151.0	315.0			515.0
Ha	Edm	MOR 1626B	A	373.1			308.0	152.0		125.0	150.0	121.0	270.0		291.0	222.0
Ha	Edm	TMP 2017.014.0001	A	383.7	219.0	124.0	444.0		204.0	114.0	180.0		250.0	60.0	280.0	
Ha	Edm	TMP 1980.051.0001* cast AMNH 5730	A	299.6	132.0	283.0	325.0	235.0	306.0	110.0	290.0	85.0	302.0	50.0	210.0	420.0
Ha	Edm	ROM 801	A	439.5	310.0	135.0	360.0	190.0	340.0	168.0	224.0	198.0	355.0	60.0	360.0	245.0
Ha	Edm	AMNH 5254	A	385.6			365.0	185.0		144.0	248.0	143.0	325.0		340.0	256.0
Ha	Edm	CMN 2288	A	524.1	235.0	130.0	358.0	212.0	238.0	162.0	272.0	146.0	300.0	175.0	296.0	388.0
Ha	Edm	FMNH 15004	A	424.0	344.5	113.3	344.2	225.1	108.2	166.0	163.9	212.6	393.4	103.3	426.0	143.7
Ha	Edm	USNM 12711	A	396.7	315.0	91.0	444.0	120.0	290.0		206.0	151.0		65.0	336.0	315.0
Ha	Edm	MOR* cast DMNH 1493	A	362.1	230.5	141.0	410.0	99.0	255.0	135.5	245.0	120.0	257.0	122.0	260.0	326.0
Ha	Edm	MOR* cast UCMP 128374	A	390.0	209.0	146.0	339.0	180.0	450.0	130.0	340.0		255.0	89.0	285.0	215.0
Ha	Edm	USNM 2414	A	431.0	227.0	194.0	303.0	180.0	202.0	126.0		162.0	229.0	65.0	236.5	246.0
Ha	Edm	YPM 2182[1]	A	346.7	304.5	142.1	295.5	166.9		119.5				138.6	254.9	
Ha	Edm	ROM 57100	A	402.0	222.0	208.0	482.0			138.0	170.0	170.0	265.0	85.0	293.0	260.0
Ha	Edm	USNM 3814	A	417.0	225.0	189.0	316.0	190.0	310.0	167.0	256.0	284.0	55.0	265.0	324.0	324.0
Ha	Edm	MOR 003	A	471.4	248.0	280.0	369.0	171.0	262.0	165.0	424.0	259.0	300.0	259.0	351.0	564.0
Ha	Edm	UMMP 20000[1]	A	443.0	288.7	157.9	322.6	180.5		101.5			278.8	121.9	360.9	
Ha	Edm	NCSM 23119[1]	A	370.0	328.2	106.6	346.8	160.7		130.3			296.1	145.5	350.2	
Ha	Edm	CCM #[1]	A	410.0	286.5	245.9	442.1	54.1		150.0			293.6		261.7	

Ha	Edm	ROM 867	A	327.0			255.0	175.0		120.0	172.0	135.0	275.0		271.0	

Appendix C Raw snout shape index data used for hadrosaurid snout shape analysis. Abbreviations: Subfam- subfamily, On.- ontogenetic stage; SSI-snout shape index, quadrate-quadrate height, La-Lambeosaurinae, Ha-Hadrosaurinae, J-juvenile, S-subadult, A-adult; *cast, if the original specimen is known the number is provided; †composite, §measured original and reconstructed portions of specimen; Photos for measurements taken from: [1]Horner, 1983; [2]Lull and Wright, 1942. All measurements are in mm.

Subfam	Genus	Specimen	On.	quad	SSI
La	Lambeosaurinae indet.	TMP 1989.079.0052	J	32.7	0.522
La	Lambeosaurinae indet.	UALVP 57103	J	171.6	0.268
La	*Corythosaurus*	TMP 1983.031.0003*§ cast ROM 759	J	166.2	0.423
La	*Corythosaurus*	ROM 1947	S	174.9	0.351
La	*Corythosaurus*	CMN 34825	S	199.9	0.445
La	*Corythosaurus*	USNM 16600	S	218.6	0.231
La	*Corythosaurus*	TMP 1997.012.0232[4]	S	213.0	0.280
La	*Corythosaurus*	TMP 1982.037.0001[4]	A	262.4	0.298
La	*Corythosaurus*	ROM 868[4]	A	331.6	0.431
La	*Corythosaurus*	UALVP 52826	A	247.8	0.200
La	*Corythosaurus*	ROM 1933[4]	A	312.0	0.166
La	*Corythosaurus*	AMNH 5338	A	308.7	0.267
La	*Corythosaurus*	TMP 1980.040.0001[4]	A	319.2	0.154
La	*Corythosaurus*	TMP 1984.121.0001[4]	A	276.5	0.211
La	*Corythosaurus*	CMN 8676[4]	A	264.6	0.365
La	*Corythosaurus*	CMN 8704[4]	A	367.0	0.347
La	*Corythosaurus*	ROM 776[4]	A	371.1	0.248
La	*Corythosaurus*	ROM 777[4]	A	311.9	0.177
La	*Corythosaurus*	ROM 845[4]	A	350.7	0.243
La	*Lambeosaurus*	AMNH 5340[3]	J	178.3	0.400
La	*Lambeosaurus*	ROM 869[4]	S	264.2	0.242
La	*Lambeosaurus*	CMN 8633	S	254.5	0.105
La	*Lambeosaurus*	CMN 8503[4]	A	290.5	0.248
La	*Lambeosaurus*	CMN 2869[4]	A	294.9	0.326
La	*Lambeosaurus*	FMNH 1479[4]	A	330.9	0.117
La	*Lambeosaurus*	ROM 1218[4]	A	364.0	0.456
La	*Lambeosaurus*	ROM 794[4]	A	338.9	0.273
La	*Lambeosaurus*	TMP 1982.038.0001[4]	A	357.7	0.295
La	*Lambeosaurus*	CMN 8703[4]	A	335.0	0.421
La	*Lambeosaurus*	TMP 1981.037.0001[4]	A	298.4	0.127
La	*Lambeosaurus*	CMN 8705[4]	A	338.7	0.325

La	*Lambeosaurus*	TMP 1966.004.0001[4]	A	310.3	0.448
La	*Hypacrosaurus*	CMN 2247	J	144.6	0.149
La	*Hypacrosaurus*	AMNH 28497*	J	40.5	0.314
La	*Hypacrosaurus*	TMP 1994.385.0001	J	174.8	0.277
La	*Hypacrosaurus*	AMNH 5461	J	161.7	0.131
La	*Hypacrosaurus*	MOR 548B[t]	J	90.5	0.089
La	*Hypacrosaurus*	CMN 2246	S	181.5	0.156
La	*Hypacrosaurus*	CMN 8501	A	298.6	0.134
La	*Hypacrosaurus*	AMNH 5278	A	313.7	0.241
La	*Parasaurolophus*	TMP 1990.036.0155[4]	S	171.3	0.199
La	*Parasaurolophus*	ROM 768[4]	A	284.1	0.243
Ha	*Prosaurolophus*	CMN 2277[4]	A	370.7	0.360
Ha	*Prosaurolophus*	CMN 2870[4]	A	381.5	0.215
Ha	*Prosaurolophus*	ROM 787[4]	A	376.9	0.264
Ha	*Gryposaurus*	TMP 1980.022.0001[4]	S	325.4	0.277
Ha	*Gryposaurus*	CMN 2278[4]	A	460.2	0.240
Ha	*Gryposaurus*	ROM 873[4]	A	432.1	0.501
Ha	*Maiasaura*	MOR* cast YPM 22400	J	63.6	0.094
Ha	*Maiasaura*	MOR-cast-090*	J	32.4	0.225
Ha	*Edmontosaurus*	CMN 58500*	J	147.1	0.193
Ha	*Edmontosaurus*	CMN 40586* cast NHM R8927	S	319.6	0.094
Ha	*Edmontosaurus*	CMN 8399	S	299.1	0.433
Ha	*Edmontosaurus*	AMNH 5046	S	236.7	0.188
Ha	*Edmontosaurus*	CMN 8509	S	315.1	0.192
Ha	*Edmontosaurus*	TMP 2017.014.0001	A	383.7	0.543
Ha	*Edmontosaurus*	TMP 1980.051.0001* cast AMNH 5730	A	299.6	0.070
Ha	*Edmontosaurus*	ROM 801	A	439.5	0.126
Ha	*Edmontosaurus*	CMN 2288	A	524.1	0.330
Ha	*Edmontosaurus*	FMNH 15004	A	424.0	0.111
Ha	*Edmontosaurus*	USNM 12711	A	396.7	0.147
Ha	*Edmontosaurus*	MOR* cast DMNH 1493	A	362.1	0.150
Ha	*Edmontosaurus*	MOR* cast UCMP 128374	A	390.0	0.167
Ha	*Edmontosaurus*	USNM 2414	A	431.0	0.163
Ha	*Edmontosaurus*	USNM 3814	A	417.0	0.053
Ha	*Edmontosaurus*	MOR 003	A	471.4	0.151

Appendix D Table of hadrosaurid specimens with microwear used in this study. Abbreviations: Ed-*Edmontosaurus*, Pro-*Prosaurolophus*, Hyp-*Hypacrosaurus*, Par-*Parasaurolophus*, Cor-*Corythosaurus*; J-juvenile, S-subadult, A-adult; LD-left dentary, RD-right dentary, LM-left maxilla, RM-right maxilla.

Genus	Stage	Specimen number	Teeth with measured microwear
Ed	S	CMN 8509	LD 5, 6, 7, 8, 10, 11, 12, 18
Ed	A	USNM 4808	LD 5,8
Ed	A	USNM 5389	LD 33, 46, 49
Ed	A	MOR 003	RD 27, 33, 41
Pro	S	TMP 2016.037.0001	RM 6, 12, 14, 18, 22, 24, 27 LM 16, 31, 34 RD 20
Pro	A	CMN 2870	LD 8, 9, 26 RD 11, 20, 22, 23, 29
Hyp	J	MOR 548 C	LD 5, 7, 9, 11
Hyp	J	MOR 548 F	LM 11, 13, 18
Hyp	S	ROM 61784	LD 10
Hyp	S	TMP 1985.036.0042	RD 2
Hyp	S	TMP 1988.151.0005	LD 4, 9
Hyp	S	USNM 11950	LD 31, 35
Par	S	TMP 1990.036.0155	RD 1, 2, 7, 8, 12 LD 18, 19, 25
cf.Par	S	ROM 183	RD 9, 11, 14, 17, 19, 23, 26
Cor	J	USNM 16600	RM 18, 19, 20, 21
Cor	S	USNM 11839	RD 10, 11, 15, 16 LD 14
Cor	S	ROM 1947	RD 12, 21
Cor	S	ROM 759	RD 3, 11
Cor	A	TMP 1982.037.0001	RD 28, 32
Cor	A	ROM 871	LD 13, 17, 19, 21, 24

Appendix E Scratch distributions along the tooth row for select hadrosaurids.

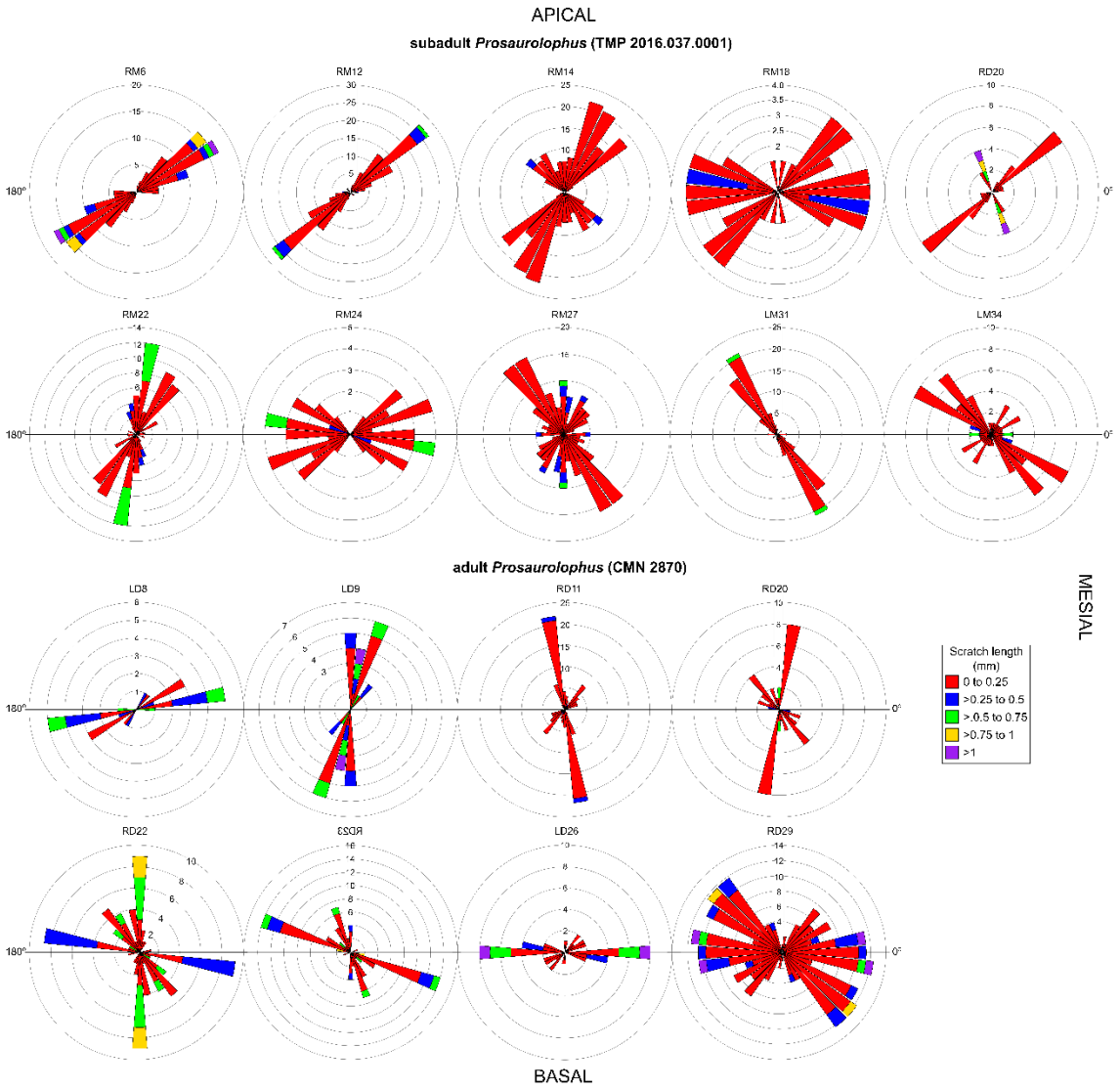

E.1 Scratch distributions along the tooth row for hadrosaurines. All teeth are standardized to the right dentary. Mesial=0º, Apical/dorsal=90º, Distal= 180º, Basal/ventral= 270º.

E.2 Scratch distributions along the tooth row for lambeosaurines. All teeth are standardized to the right dentary. Mesial=0º, Apical/dorsal=90º, Distal= 180º, Basal/ventral= 270º (see p. 190).

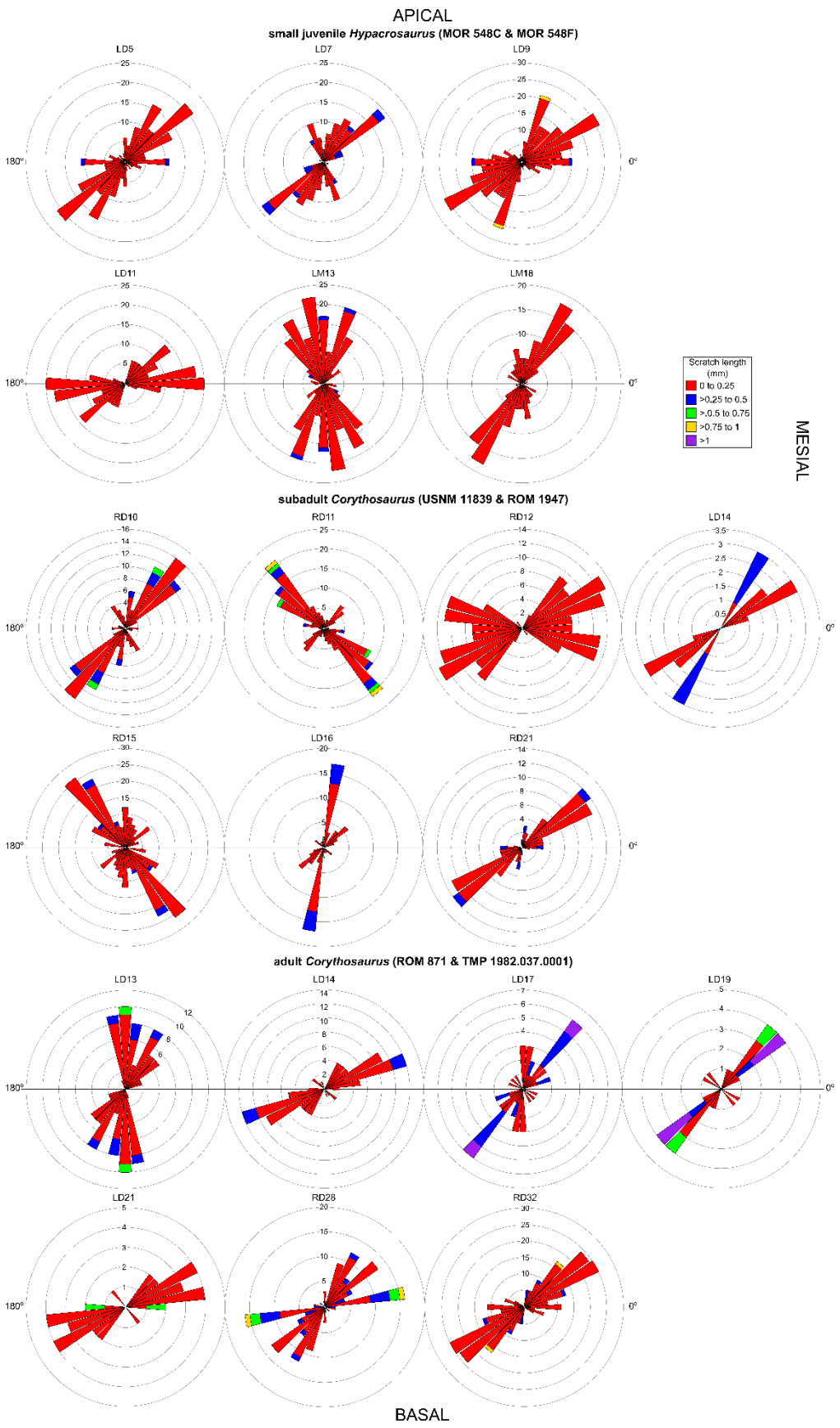
APICAL
small juvenile Hypacrosaurus (MOR 548C & MOR 548F)
LD5
LD7
LD9
LD11
LM13
LM18
180°
0°
Scratch length (mm)
0 to 0.25
>0.25 to 0.5
>0.5 to 0.75
>0.75 to 1
>1
MESIAL
subadult Corythosaurus (USNM 11839 & ROM 1947)
RD10
RD11
RD12
LD14
RD15
LD16
RD21
adult Corythosaurus (ROM 871 & TMP 1982.037.0001)
LD13
LD14
LD17
LD19
LD21
RD28
RD32
BASAL

Appendix F Raw cranial data used for regression analysis of ceratopsid dataset. Abbreviations: Subfam.-subfamily, gen-genus, On-ontogenetic description used, ps-mq- distance from jaw joint to rostral beak tip (skull length), sl- snout length, dl- diastema length, trl- tooth row length, dt-mq- distance from jaw joint to distal end of tooth row, sw- maximum beak width, dh- midpoint dentary height, ppb- paroccipital process breadth, oh- occiput height, cp-jj: distance apex of coronoid process to middle of jaw joint, sd- depression of snout below occlusal plane, sh- skull height, qb- quadrate breadth, Ce-Centrosaurinae, Ch-Chasmosaurinae, Br-*Brachyceratops*, Sty-*Styracosaurus*, Pa-*Pachyrhinosaurus*, "pa"-"pachyrhinosaur", Cen-*Centrosaurus*, An-*Anchiceratops*, Cha-*Chasmosaurus*, Tri-*Triceratops*, Tor-*Torosaurus*, J-juvenile, S-subadult, A-adult; *cast, if the original specimen is known the number is provided; [†]composite; [††]composite constructed using material from USNM 14765, 8023, 7951, 7953, 7957, 7958, 8076, 8077, 8078, 8079; [§]measured original and reconstructed portions of specimen. [1]Hatcher et al. 1907, Forster, 1996; [2]Mallon and Anderson, 2013; [3]Measured using digital models provided by A. Knapp. All measurements are in mm. Empty cells denote missing data.

Sub fam.	Gen	Specimen	On	ps-mq	sl	dl	trl	dt-mq	sw	dh	ppb	oh	cp-jj	sd	sh	qb
Ce	Br	USNM ID# 289[††]	J	285.5	57.5	53.0	135.5	39.5	35.0	42.0	175.0		87.5	20.5	177.0	195.0
Ce	Sty	CMN 344[2]	A				254.0	53.0		116.0	564.0	98.0	203.0		319.0	409.0
Ce	Pa	TMP 1993.003.0001	A	920.0	210.0	250.0	300.0	160.0	124.0	85.0				103.0	395.0	
Ce	"pa"	TMP 2002.076.0001[2]	A	750.0	202.0	142.0	306.0	100.0	125.0	119.0			186.0	20.0	519.0	320.0
Ce	Cen	CMN 8790[2]	S				253.0	60.0			431.0	63.0			247.0	
Ce	Cen	CMN 8795[2]	S	664.0	160.0	148.0	296.0	60.0	120.0	115.0	489.0	175.0	168.0	40.0	310.0	322.0
Ce	Cen	AMNH 5351[2]	A	637.0	130.0	177.0	288.0	42.0	128.0	126.0	371.0	96.0	180.0	14.0	385.0	199.0
Ce	Cen	AMNH 5377[2]	A				425.0	50.0		102.0	390.0	193.0	187.0		511.0	310.0
Ce	Cen	CMN 348[2]	A	723.0	150.0	164.0	324.0	85.0	89.0	124.0	448.0	151.0	225.0	63.0	361.0	295.0
Ce	Cen	NHMUK R4859[2]	A	656.0	161.0	150.0	315.0	30.0	110.0		480.0	127.0		20.0	340.0	200.0
Ce	Cen	ROM 767[2]	A	652.0	154.0	145.0	297.0	56.0	97.0	105.0	352.0	127.0	186.0	37.0	352.0	190.0
Ce	Cen	TMP 1997.085.0001[2]	A	735.0	191.0	173.0	297.0	74.0	173.0	136.0			164.0	72.0	273.0	525.0
Ce	Cen	UALVP 11735[2]	A	592.0	152.0	147.0	258.0	35.0	147.0		499.0	90.0		32.0	261.0	270.0
Ce	Cen	UALVP 16248[2]	A	540.0	116.0	104.0	320.0		95.0	95.0	360.0	140.0	140.0	29.0	340.0	214.0
Ce	Cen	USNM 8897[2]	A	665.0	174.0	155.0	275.0	61.0	101.0	108.0	392.0	147.0	181.0	31.0	384.0	230.0

Ce	Cen	YPM 2015[2]	A	676.0	153.0	158.0	291.0	74.0	129.0	113.0	451.0	158.0	199.0	73.0	400.0	325.0
Ce	Cen	TMP 2006.003.0001	A	654.0	124.0	90.0	315.0	125.0	108.0	130.0	340.0	135.0		50.0	265.0	368.0
Ce	Cen	TMP 1992.082.0001	A	620.0	110.0	165.0	269.0	76.0	96.0					69.0	303.0	
Ch	An	TMP 1983.001.0001	A	700.0	130.0	170.0	300.0	100.0	150.0		470.0			75.0	350.0	360.0
Ch	An	CMN 56354	A	615.0	175.0	105.0	259.0	76.0	103.0						222.0	
Ch	An	CMN 8535	A	701.0	211.0	131.0	294.0	65.0	111.0		430.0	63.0		30.0	220.0	400.0
Ch	Cha	UALVP 52613[2]	J	249.5	27.0	69.5	106.5	46.5	54.0	40.0	79.0	35.0	77.0		110.0	80.0
Ch	Cha	ROM 839[2]	S				349.0	49.0		133.0	430.0	120.0	218.0		346.0	186.0
Ch	Cha	UALVP 40[2]	S				276.0	39.0		99.0	350.0	104.0			261.0	180.0
Ch	Cha	CMN 8801[2]	A	840.0	174.0	201.0	356.0	109.0	103.0	137.0				14.0	453.0	
Ch	Cha	TMP 1981.019.0175[2]	A	695.0	125.0	212.0	289.0	69.0	101.0		502.0	131.0		18.0	313.0	360.0
Ch	Cha	CMN 2280[2]	A	685.0	173.0	148.0	294.0	70.0	102.0	116.0	470.0	140.0	170.0	60.0	300.0	306.0
Ch	Cha	AMNH 5401[3]	A	706.2	119.8	192.6	293.2	100.6	153.7		324.8				318.9	528.8
Ch	Cha	AMNH 5402[3]	A	891.6	137.4	754.2		230.1	116.6		242.9				258.9	542.5
Ch	Cha	CMN 2245[2]	A					105.0		128.0	508.0	150.0	195.0		305.0	317.0
Ch	Cha	ROM 843[2]	A				356.0	68.0		140.0	645.0	80.0	200.0		313.0	530.0
Ch	Cha	YPM 2016[2]	A	703.0	145.0	172.0	343.0	43.0	101.0		558.0	110.0		25.0	246.0	375.0
Ch	Cha	CMN 41357	A	703.0	135.0	568.0		79.0	124.0	107.0			198.0	72.0	319.0	340.0
Ch	Tri	AMNH 30609*[§] (cast UCMP 154452)	J	245.0	41.0	48.0	103.0	53.0	34.0	36.0	122.0		80.0	5.0	154.0	83.0
Ch	Tri	MOR 2569	J	364.5	77.0	33.0	142.0	112.5	72.0		196.0	95.0		35.5	187.5	179.0
Ch	Tri	ROM 55380	S	885.0	189.0	206.0	355.0	135.0	115.0	135.0	365.0	159.0	200.0	16.0	495.0	372.0
Ch	Tri	MOR 1110	S	652.0	189.0	79.0	225.0	159.0	88.0		370.0	155.5		45.0	452.0	298.5
Ch	Tri	MOR 2951	S	529.5	73.0	143.5	236.5	76.5	101.0	77.0	311.0	118.0	168.0	25.5	311.0	315.0
Ch	Tri	MOR 1199	S	434.5	110.5	48.0	193.3	82.8	82.5	73.5	250.0	73.0	124.5	20.0	249.0	215.0

Ch	Tri	YPM 1823[1]	A	996.6	189.9	307.0	421.5	78.1		132.7			290.2		463.2	
Ch	Tri	YPM 1822[1]	A	847.6	147.0	263.8	333.0	103.8	138.6	105.9	403.9	125.6	212.5	25.9	413.0	316.8
Ch	Tri	USNM 1201[1]	A	990.0	210.0	126.0	513.0	141.0	142.0		456.0			100.0	499.0	510.0
Ch	Tri	USNM 4928[1]	A	1140.9	260.8	267.3	521.5	91.3						208.6	704.1	
Ch	Tri	YPM 1834[1]	A	798.9	132.6	293.7	236.8	135.8	158.7	104.2	515.0		212.9	42.1	432.6	359.1
Ch	Tri	MOR 1604	A	970.0	160.0	206.0	504.0	100.0	115.0					75.0	543.0	
Ch	Tri	MOR 1122	A	1140.3	152.8	318.3	466.8	202.5	270.0	163.3	715.0	114.5	244.8	37.5	489.8	632.5
Ch	Tri	MOR 2999	A	805.0	145.3	239.3	338.0	82.5	116.5		449.0	215.0		10.5	483.0	471.0
Ch	Tri	MOR 004	A	1079.0	211.5	257.5	407.0	203.0	82.0	127.0		61.0	235.0	70.0	407.0	
Ch	Tri	MOR 1120	A	876.0	181.5	218.0	324.0	152.5	141.0		420.0	155.0		31.0	466.3	415.0
Ch	Tri	MOR 3027	A	1000.0	200.5	208.5	456.0	135.0	126.0	140.0			250.0	20.0	530.0	
Ch	Tri	TMP 1982.006.0001*	A	1105.0	337.5	141.5	296.0	330.0	203.0	146.0	640.0		270.0	29.0	380.0	530.0
Ch	Tri	USNM 1205	A				412.0	30.0			352.0	165.0	420.0			422.0
Ch	Tri	USNM 2414	A				542.0	78.0			650.0	190.0			448.5	560.0
Ch	Tor	TMP 1985.010.0013*	A	796.0	221.0	147.5	337.5	90.0	150.0		220.0	110.0		40.0	362.0	381.0

Appendix G Holm-adjusted p-values for Durbin-Watson and Breusch-Pagan tests of regression of linear cranial measurements against skull length and principal component 1 for the ceratopsid cranial dataset. Instances of significant autocorrelation or heteroscedasticity are in bold. Asterisks indicate variables measured along same axis of the skull as skull length. Abbreviations: DW-Durbin Watson test; BP-Breusch-Pagan test; PC1-principal component 1.

Cranial measurement	Adjusted p-value DW (x = skull length)	Adjusted p-value BP (x = skull length)	Adjusted p-value DW (x = PC1)	Adjusted p-value BP (x = PC1)
Snout length	0.617	1.000	1.000	**4.91E-04**
Diastema length	1.000	1.000	1.000	**0.003**
Tooth row length	1.000	1.000	1.000	1.000
Distance from distal end of tooth row to mid-quadrate	0.954	**0.008**	1.000	**3.10E-06**
Snout width	1.000	1.000	1.000	0.252
Dentary height	0.257	1.000	1.000	1.000
Paroccipital process breadth	1.000	1.000	0.576	1.000
Occiput height	1.000	0.741	1.000	1.000
Distance from coronoid process apex to middle jaw joint	1.000	0.955	0.370	1.000
Depression of snout below occlusal plane	0.954	1.000	0.372	0.823
Skull height	0.368	1.000	0.576	0.105
Quadrate breadth	1.000	1.000	0.576	0.064

Appendix H Raw snout shape index data used for ceratopsid snout shape analysis. Abbreviations: SSI-snout shape index, ps-mq- distance from jaw joint to rostral beak tip (skull length), Ce-Centrosaurinae, Ch-Chasmosaurinae, Br-*Brachyceratops*, Sty-*Styracosaurus*, Pa-*Pachyrhinosaurus*, "pa"-"pachyrhinosaur", Cen-*Centrosaurus*, An-*Anchiceratops*, Cha-*Chasmosaurus*, Tri-*Triceratops*, Tor-*Torosaurus*, J-juvenile, S-subadult, A-adult; *cast, if the original specimen is known the number is provided; [†]composite, [††]composite mount from USNM 14765, 8023, 7951, 7953, 7957, 7958, 8076, 8077, 8078, 8079; [§]measured original and reconstructed portions of specimen; [1]Photos for measurements taken from Hatcher et al., 1907; [2]Measured using digital models provided by A. Knapp. All measurements are in mm.

subfamily	Genus	Specimen	On	SSI	ps-mq
Ce	Br	USNM ID# 289[††]	J	0.862	285.5
Ce	Pa	TMP 1993.003.0001	A	0.680	920.0
Ce	"pa"	TMP 2002.076.0001	A	0.793	750.0
Ce	Cen	CMN 8795	S	0.676	664.0
Ce	Cen	CMN 348	A	0.775	723.0
Ce	Cen	NHMUK R4859	A	0.932	656.0
Ce	Cen	ROM 767	A	0.901	652.0
Ce	Cen	TMP 1997.085.0001	A	0.800	735.0
Ce	Cen	UALVP 11735	A	0.769	592.0
Ce	Cen	UALVP 16248	A	0.557	540.0
Ce	Cen	USNM 8897	A	0.862	665.0
Ce	Cen	YPM 2015	A	0.893	676.0
Ch	An	CMN 56354	A	0.791	615.0
Ch	An	CMN 8535	A	0.928	701.0
Ch	Cha	UALVP 52613	J	0.718	249.5
Ch	Cha	CMN 8801	A	0.830	840.0
Ch	Cha	TMP 1981.019.0175	A	0.922	695.0
Ch	Cha	CMN 2280	A	0.807	685.0
Ch	Cha	AMNH 5401[2]	A	0.740	706.2
Ch	Cha	AMNH 5402[2]	A	0.783	891.6
Ch	Cha	YPM 2016	A	0.743	703.0
Ch	Cha	CMN 41357	A	0.932	703.0
Ch	Tri	AMNH 30609*[§] (cast UCMP 154452)	J	0.870	245.0
Ch	Tri	MOR 2951	J	0.766	529.5
Ch	Tri	MOR 1199	J	0.503	434.5
Ch	Tri	MOR 2569	J	0.518	364.5
Ch	Tri	ROM 55380	S	0.546	885.0
Ch	Tri	MOR 1110	S	0.961	652.0
Ch	Tri	YPM 1823[1]	A	0.767	996.6
Ch	Tri	YPM 1822[1]	A	0.937	847.6
Ch	Tri	USNM 1201	A	0.879	990.0

Ch	Tri	USNM 4928[1]	A	0.839	1140.9
Ch	Tri	YPM 1834[1]	A	0.854	798.9
Ch	Tri	MOR 1122	A	0.846	1140.3
Ch	Tri	MOR 2999	A	0.868	805.0
Ch	Tri	MOR 3027	A	0.936	1000.0

Appendix I Table of ceratopsid specimens with microwear used in this study.
Abbreviations: LD-left dentary, RD-right dentary, LM-left maxilla, RM-right maxilla.

Genus	Ontogenetic classification	Specimen number	Teeth with measured microwear
Ceratopsidae indet.	juvenile	UC 16624	LD 1, 5 RM 6, 11
Centrosaurus	large subadult	AMNH 5237	RD 11, 18, 20
Centrosaurus	adult	TMP 1997.085.0001	RD 18, 24, 'posterior'
Chasmosaurus	adult	CMN 8801	RD 2, 4, 6, 9, 11, 19, 24

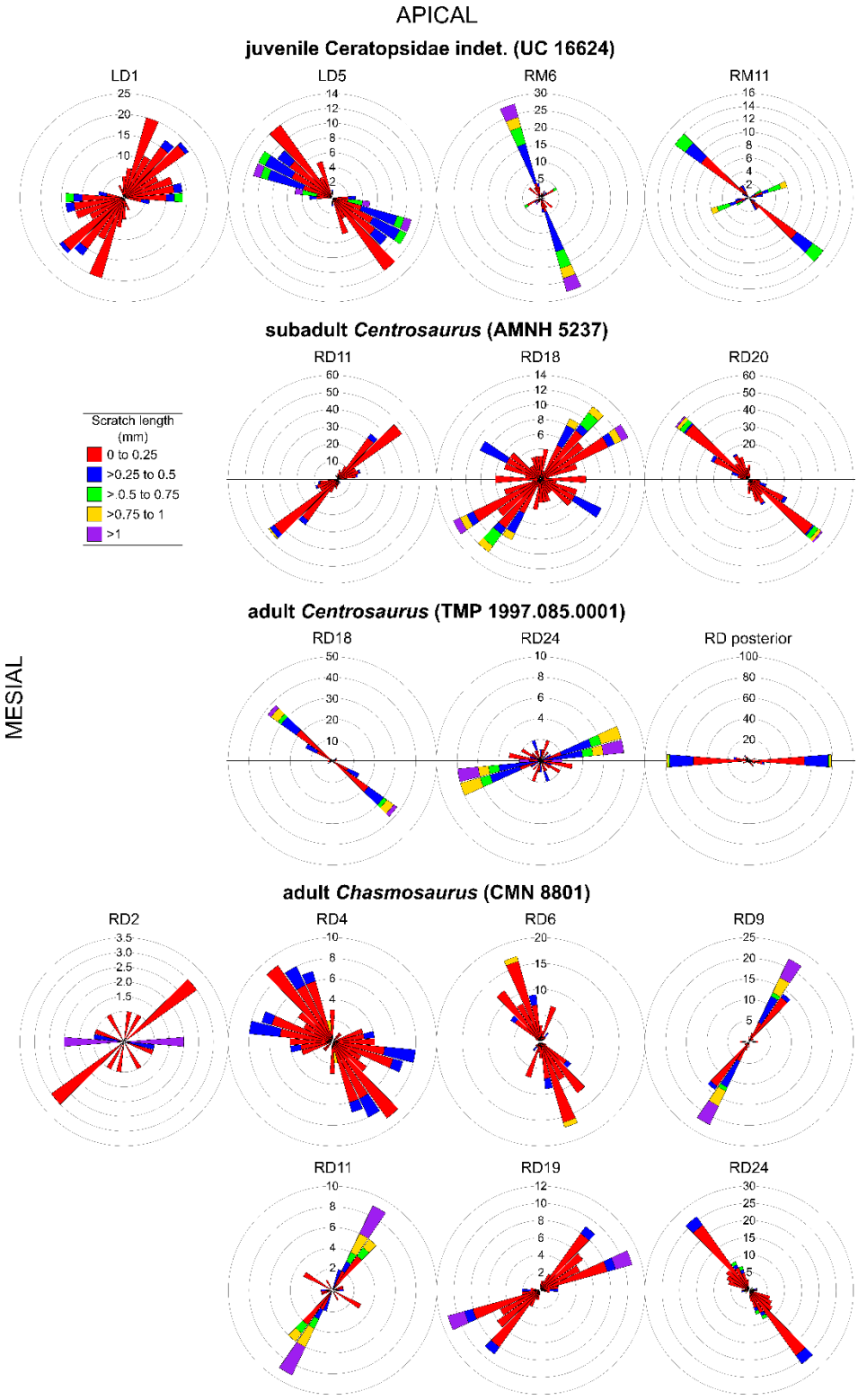

Appendix J Scratch distributions along the tooth row for ceratopsid specimens. All teeth are standardized to the right dentary. Mesial=0º, Apical/dorsal=90º, Distal= 180º, Basal/ventral= 270º.

Appendix K Raw cranial data used for principal component analysis. Abbreviations: Fam/subfam-family/subfamily, On.-ontogenetic description used, sl-snout length, dl-diastema length, trl-tooth row length, dt-mq- distance from jaw joint to distal end of tooth row, sw- maximum beak width, dh- midpoint dentary height, ppb- paroccipital process breadth, oh- occiput height, cp-jj- distance apex of coronoid process to middle of jaw joint, sd- depression of snout below occlusal plane, sh- skull height, qb- quadrate breadth, SSI- snout shape index, skl- skull length, La-Lambeosaurinae, Ha-Hadrosaurinae, Le-Leptoceratopsidae, Th-Thescelosauridae, Pa-Pachycephalosauridae, Ce-Centrosaurinae, Ch-Chasmosaurinae, Cory-*Corythosaurus*, Lamb-*Lambeosaurus*, Lamb indet.-Lambeosaurinae indet., Hyp-*Hypacrosaurus*, Para-*Parasaurolophus*, Gryp-*Gryposaurus*, Brachy-*Brachylophosaurus*, Maia-*Maiasaura*, Edm-*Edmontosaurus*, Lepto-*Leptoceratops*, Preno-*Prenoceratops*, Park-*Parksosaurus*, Thesc-*Thescelosaurus*, Oro-*Orodromeus*, Ory-*Oryctodromeus*, Steg-*Stegoceras*, Pachy-*Pachycephalosaurus*, Draco-*Dracorex*, Br-*Brachyceratops*, Sty-*Styracosaurus*, Pa-*Pachyrhinosaurus*, "pa"-"pachyrhinosaur", Cen-*Centrosaurus*, An-*Anchiceratops*, Cha-*Chasmosaurus*, Tri-*Triceratops*, Tor-*Torosaurus*, J-juvenile, S-subadult, A-adult; *cast, if the original specimen is known the number is provided; **measured from composite cast and measurements taken from photos provided in Boyd, 2014; [†]composite; [§]measured original and reconstructed portions of specimen; blank cells denote missing data. [††]composite constructed using material from USNM 14765, 8023, 7951, 7953, 7957, 7958, 8076, 8077, 8078, 8079; [1]Campione and Evans, 2011; [2]Gates and Sampson, 2007; [3]Hatcher et al. 1907, Forster, 1996; [4]Lull and Wright, 1942; [5]Mallon and Anderson, 2013. [6]Measured using digital models provided by A. Knapp; [7]Measured using photos provided by M.J. Ryan. All measurements are in mm. Empty cells denote missing data.

Fam/ Subfam.	Genus	Specimen	On	sl	dl	trl	dt-mq	sw	dh	ppb	oh	cp-jj	sd	sh	qb	SSI	skl
Ce	"pa"	TMP 2002.076.0001[5]	A	202.0	142.0	306.0	100.0	125.0	119.0			186.0	20.0	519.0	320.0	0.793	750.0
Ce	Br	USNM ID# 289[††]	J	57.5	53.0	135.5	39.5	35.0	42.0	175.0		87.5	20.5	177.0	195.0	0.862	285.5
Ce	Cen	AMNH 5351[5]	A	130.0	177.0	288.0	42.0	128.0	126.0	371.0	96.0	180.0	14.0	385.0	199.0		637.0
Ce	Cen	AMNH 5377[5]	A			425.0	50.0		102.0	390.0	193.0	187.0		511.0	310.0		
Ce	Cen	CMN 348[5]	A	150.0	164.0	324.0	85.0	89.0	124.0	448.0	151.0	225.0	63.0	361.0	295.0	0.775	723.0
Ce	Cen	CMN 8790[5]	S			253.0	60.0			431.0	63.0			247.0			
Ce	Cen	CMN 8795[5]	S	160.0	148.0	296.0	60.0	120.0	115.0	489.0	175.0	168.0	40.0	310.0	322.0	0.676	664.0
Ce	Cen	NHMUK R4859[5]	A	161.0	150.0	315.0	30.0	110.0		480.0	127.0		20.0	340.0	200.0	0.932	656.0
Ce	Cen	ROM 767[5]	A	154.0	145.0	297.0	56.0	97.0	105.0	352.0	127.0	186.0	37.0	352.0	190.0	0.901	652.0
Ce	Cen	TMP 1992.082.0001	A	110.0	165.0	269.0	76.0	96.0					69.0	303.0			620.0

Ce	Cen	TMP 1997.085.0001[5]	A	191.0	173.0	297.0	74.0	173.0	136.0			164.0	72.0	273.0	525.0	0.800	735.0
Ce	Cen	TMP 2006.003.0001	A	124.0	90.0	315.0	125.0	108.0	130.0	340.0	135.0		50.0	265.0	368.0		654.0
Ce	Cen	UALVP 11735[5]	A	152.0	147.0	258.0	35.0	147.0		499.0	90.0		32.0	261.0	270.0	0.769	592.0
Ce	Cen	UALVP 16248[5]	A	116.0	104.0	320.0		95.0	95.0	360.0	140.0	140.0	29.0	340.0	214.0	0.557	540.0
Ce	Cen	USNM 8897[5]	A	174.0	155.0	275.0	61.0	101.0	108.0	392.0	147.0	181.0	31.0	384.0	230.0	0.862	665.0
Ce	Cen	YPM 2015[5]	A	153.0	158.0	291.0	74.0	129.0	113.0	451.0	158.0	199.0	73.0	400.0	325.0	0.893	676.0
Ce	Pa	TMP 1993.003.0001	A	210.0	250.0	300.0	160.0	124.0	85.0				103.0	395.0		0.680	920.0
Ce	Sty	CMN 344[5]	A			254.0	53.0		116.0	564.0	98.0	203.0		319.0	409.0		
Ch	An	CMN 56354	A	175.0	105.0	259.0	76.0	103.0						222.0		0.791	615.0
Ch	An	CMN 8535	A	211.0	131.0	294.0	65.0	111.0		430.0	63.0		30.0	220.0	400.0	0.928	701.0
Ch	An	TMP 1983.001.0001	A		170.0	300.0	100.0	150.0		470.0			75.0	350.0	360.0		700.0
Ch	Cha	AMNH 5401[6]	A	119.8	192.6	293.2	100.6	153.7		324.8				318.9	528.8	0.740	706.2
Ch	Cha	AMNH 5402[6]	A	137.4	754.2		230.1	116.6		242.9				258.9	542.5	0.783	891.6
Ch	Cha	CMN 2245[5]	A				105.0		128.0	508.0	150.0	195.0		305.0	317.0		
Ch	Cha	CMN 2280[5]	A	173.0	148.0	294.0	70.0	102.0	116.0	470.0	140.0	170.0	60.0	300.0	306.0	0.807	685.0
Ch	Cha	CMN 41357	A	135.0	568.0		79.0	124.0	107.0			198.0	72.0	319.0	340.0	0.932	703.0
Ch	Cha	CMN 8801[5]	A	174.0	201.0	356.0	109.0	103.0	137.0				14.0	453.0		0.830	840.0
Ch	Cha	ROM 839[5]	S			349.0	49.0		133.0	430.0	120.0	218.0		346.0	186.0		
Ch	Cha	ROM 843[5]	A			356.0	68.0		140.0	645.0	80.0	200.0		313.0	530.0		
Ch	Cha	TMP 1981.019.0175[5]	A	125.0	212.0	289.0	69.0	101.0		502.0	131.0		18.0	313.0	360.0	0.922	695.0
Ch	Cha	UALVP 40[5]	S			276.0	39.0		99.0	350.0	104.0			261.0	180.0		
Ch	Cha	UALVP 52613[5]	J	27.0	69.5	106.5	46.5	54.0	40.0	79.0	35.0	77.0		110.0	80.0	0.718	249.5
Ch	Cha	YPM 2016[5]	A	145.0	172.0	343.0	43.0	101.0		558.0	110.0		25.0	246.0	375.0	0.743	703.0
Ch	Tor	TMP 1985.010.0013*	A	221.0	147.5	337.5	90.0	150.0		220.0	110.0		40.0	362.0	381.0		796.0
Ch	Tri	AMNH 30609*[§] (cast UCMP 154452)	J	41.0	48.0	103.0	53.0	34.0	36.0	122.0		80.0	5.0	154.0	83.0	0.870	245.0
Ch	Tri	MOR 004	A	211.5	257.5	407.0	203.0	82.0	127.0		61.0	235.0	70.0	407.0			1079.0

Ch	Tri	MOR 1110	S	189.0	79.0	225.0	159.0	88.0		370.0	155.5		45.0	452.0	298.5	0.961	652.0
Ch	Tri	MOR 1120	A	181.5	218.0	324.0	152.5	141.0		420.0	155.0		31.0	466.3	415.0		876.0
Ch	Tri	MOR 1122	A	152.8	318.3	466.8	202.5	270.0	163.3	715.0	114.5	244.8	37.5	489.8	632.5	0.846	1140.3
Ch	Tri	MOR 1199	S	110.5	48.0	193.3	82.8	82.5	73.5	250.0	73.0	124.5	20.0	249.0	215.0	0.503	434.5
Ch	Tri	MOR 1604	A	160.0	206.0	504.0	100.0	115.0					75.0	543.0			970.0
Ch	Tri	MOR 2569	J	77.0	33.0	142.0	112.5	72.0		196.0	95.0		35.5	187.5	179.0	0.518	364.5
Ch	Tri	MOR 2951	S	73.0	143.5	236.5	76.5	101.0	77.0	311.0	118.0	168.0	25.5	311.0	315.0	0.766	529.5
Ch	Tri	MOR 2999	A	145.3	239.3	338.0	82.5	116.5		449.0	215.0		10.5	483.0	471.0	0.868	805.0
Ch	Tri	MOR 3027	A	200.5	208.5	456.0	135.0	126.0	140.0			250.0	20.0	530.0		0.936	1000.0
Ch	Tri	ROM 55380	S	189.0	206.0	355.0	135.0	115.0	135.0	365.0	159.0	200.0	16.0	495.0	372.0	0.546	885.0
Ch	Tri	TMP 1982.006.0001*	A	337.5	141.5	296.0	330.0	203.0	146.0	640.0		270.0	29.0	380.0	530.0		1105.0
Ch	Tri	USNM 12011	A	210.0	126.0	513.0	141.0	142.0		456.0			100.0	499.0	510.0	0.879	990.0
Ch	Tri	USNM 1205	A			412.0	30.0			352.0	165.0	420.0			422.0		
Ch	Tri	USNM 2414	A			542.0	78.0			650.0	190.0			448.5	560.0		
Ch	Tri	USNM 49281	A	260.8	267.3	521.5	91.3						208.6	704.1		0.839	1140.9
Ch	Tri	YPM 18221	A	147.0	263.8	333.0	103.8	138.6	105.9	403.9	125.6	212.5	25.9	413.0	316.8	0.937	847.6
Ch	Tri	YPM 18231	A	189.9	307.0	421.5	78.1		132.7			290.2		463.2		0.767	996.6
Ch	Tri	YPM 18341	A	132.6	293.7	236.8	135.8	158.7	104.2	515.0		212.9	42.1	432.6	359.1	0.854	798.9
Ha	Brachy	CMN 8893	A	156.0	95.0	320.0	100.0	220.0	98.0	210.0	81.0	243.0	25.5	260.0	401.0		671.0
Ha	Brachy	GPDM.115	A	125.0	100.0	180.0	95.0	252.0	60.0	200.0		155.0	70.0	165.0	224.0		500.0
Ha	Brachy	GPDM.200	A	69.0	251.0	160.0			105.0	170.0		249.0	104.0	218.0	322.0		480.0
Ha	Edm	AMNH 5046	S	60.0	115.0	245.0		158.0	61.0	154.0	61.0	150.0	39.0	150.0	188.0	0.188	420.0
Ha	Edm	AMNH 5254	A			365.0	185.0		144.0	248.0	143.0	325.0		340.0	256.0		
Ha	Edm	CCM #[1]	A	286.5	245.9	442.1	54.1		150.0			293.6		261.7			1028.6

Ha	Edm	CM 26259[1]	S	180.8	113.3	289.3	164.7		118.4			285.3	115.0	279.1			748.1
Ha	Edm	CMN 2288	A	235.0	130.0	358.0	212.0	238.0	162.0	272.0	146.0	300.0	175.0	296.0	388.0	0.330	935.0
Ha	Edm	CMN 2289	A			418.0	127.0		167.0	351.0	151.0	315.0			515.0		977.0
Ha	Edm	CMN 40586* cast NHM R8927	S	120.0	194.0	253.0	168.0	190.0	115.0	155.0	86.0	270.0	40.0	216.0	156.0	0.094	735.0
Ha	Edm	CMN 58500	J	55.0	78.0	107.0	60.0	108.0	45.0	100.0	37.0	115.0	25.0	97.0	148.0	0.193	300.0
Ha	Edm	CMN 8399	S	150.0	210.0	210.0	180.0	174.0	110.0	220.0	95.0	220.0	80.0	164.0	230.0	0.433	750.0
Ha	Edm	CMN 8509	S	85.0	240.0	285.0	110.0	210.0	112.0	190.0	120.0	255.0	60.0	200.0	266.0	0.192	720.0
Ha	Edm	FMNH 15004	A	344.5	113.3	344.2	225.1	108.2	166.0	163.9	212.6	393.4	103.3	426.0	143.7	0.111	1027.1
Ha	Edm	MOR 003	A	248.0	280.0	369.0	171.0	262.0	165.0	424.0	259.0	300.0	259.0	351.0	564.0	0.151	1068.0
Ha	Edm	MOR 1626B	A			308.0	152.0		125.0	150.0	121.0	270.0		291.0	222.0		
Ha	Edm	MOR* cast DMNH 1493	A	230.5	141.0	410.0	99.0	255.0	135.5	245.0	120.0	257.0	122.0	260.0	326.0	0.150	880.5
Ha	Edm	MOR* cast UCMP 128374	A	209.0	146.0	339.0	180.0	450.0	130.0	340.0		255.0	89.0	285.0	215.0	0.167	874.0
Ha	Edm	NCSM 23119[1]	A	328.2	106.6	346.8	160.7		130.3			296.1	145.5	350.2			942.3
Ha	Edm	ROM 57100	A	222.0	208.0	482.0			138.0	170.0	170.0	265.0	85.0	293.0	260.0		912.0
Ha	Edm	ROM 801	A	310.0	135.0	360.0	190.0	340.0	168.0	224.0	198.0	355.0	60.0	360.0	245.0	0.126	995.0
Ha	Edm	ROM 867	A			255.0	175.0		120.0	172.0	135.0	275.0		271.0			
Ha	Edm	SM R4050[1]	S	265.6	120.1	238.5	167.5		137.0			231.2	99.8	262.2			791.7
Ha	Edm	TMP 1980.051.0001* cast AMNH 5730	A	132.0	283.0	325.0	235.0	306.0	110.0	290.0	85.0	302.0	50.0	210.0	420.0	0.070	975.0
Ha	Edm	TMP 2017.014.0001	A	219.0	124.0	444.0		204.0	114.0	180.0		250.0	60.0	280.0		0.543	787.0
Ha	Edm	UMMP 20000[1]	A	288.7	157.9	322.6	180.5		101.5			278.8	121.9	360.9			949.6
Ha	Edm	USNM 12711	A	315.0	91.0	444.0	120.0	290.0		206.0	151.0		65.0	336.0	315.0	0.147	970.0
Ha	Edm	USNM 2414	A	227.0	194.0	303.0	180.0	202.0	126.0		162.0	229.0	65.0	236.5	246.0	0.163	904.0
Ha	Edm	USNM 3814	A	225.0	189.0	316.0	190.0	310.0	167.0	256.0	284.0	55.0	265.0	324.0	324.0	0.053	920.0
Ha	Edm	YPM 2182[1]	A	304.5	142.1	295.5	166.9		119.5				138.6	254.9			909.0

Ha	Grypp	CMN 2278[5]	A	181.0	94.0	381.0	140.0	238.0	142.0	423.0	211.0	289.0	89.0	337.0	318.0	0.240	796.0
Ha	Grypp	CMN 8784	J	156.0	31.0	163.0	82.0		60.0		62.0	131.0		149.0	130.0		432.0
Ha	Grypp	RAM 6797[2]	A	271.7	8.7	408.7	143.5		132.6			248.6	110.9	339.2			832.6
Ha	Grypp	ROM 764[5]	A				125.0		105.0	376.0	148.0	245.0		223.0	236.0		
Ha	Grypp	ROM 873[5]	A	208.0	53.0	396.0	134.0	201.0	125.0	176.0	146.0	284.0	107.0	305.0	190.0	0.501	791.0
Ha	Grypp	TMP 1980.022.0001[5]	S	140.0	58.0	277.0	105.0	94.0	92.0	197.0	153.0	220.0	75.0	238.0	174.0	0.277	580.0
Ha	Grypp	TMP 1991.081.0001[5]	S	150.0	55.0	300.0	55.0		91.0	150.0		217.0	97.0	243.0		0.569	560.0
Ha	Maia	MOR-cast-090*	J	11.0	9.0	34.0	11.0	19.0	11.0	31.0			5.0	39.0	20.0	0.225	65.0
Ha	Maia	MOR cast 019*	S	90.0	48.5	186.0	78.5	181.5	58.5	55.0	63.0	146.5	65.5	158.0	209.0		403.0
Ha	Maia	MOR cast 089* of OTM F138	A	170.0	85.0	280.0	160.0	320.0	88.0	180.0		212.0	90.0	191.0			695.0
Ha	Maia	MOR* cast YPM 22400	J	17.0	18.0	50.0	25.0	39.0	18.0	54.0		45.0	12.0	55.0	49.0	0.094	110.0
Ha	Maia	ROM 44770	A	125.0	75.0	260.0	170.0	215.0	97.0	208.0	168.0	249.5	65.0	205.0	204.0	0.203	630.0
Ha	Maia	ROM 66207	J	69.0	94.0	174.0	65.0	178.0	59.0			138.0	30.0		230.0	0.238	402.0
Ha	Maia	TMP 1989.019.0002* cast YPM 22405	A	92.0	145.0	295.0	151.0	318.0	75.0	220.0	125.0	235.0	35.0	201.0	115.0	0.125	683.0
Ha	Pro	CMN 2277[5]	A	129.0	172.0	382.0	116.0	130.0	131.0			254.0	62.0	296.0	235.0	0.360	799.0
Ha	Pro	CMN 2870[5]	A	180.0	111.0	414.0	98.0	221.0	129.0	270.0	142.0	258.0	67.0	295.0	330.0	0.215	803.0
Ha	Pro	ROM 1928[5]	S	162.0	94.0	314.0	93.0		96.0	152.0		247.0	76.0	218.0			663.0
Ha	Pro	ROM 787[5]	A	184.0	121.0	364.0	124.0	166.0	133.0	170.0	183.0	271.0	79.0	302.0	200.0	0.264	793.0
Ha	Pro	TMM 41262[5]	S	140.0	80.0	305.0	114.0	104.0	91.0			223.0	110.0	222.0			639.0
Ha	Pro	TMP 1984.001.0001[5]	A	250.0	115.0	395.0	140.0	248.0	139.0			294.0	125.0	280.0		0.278	900.0
Ha	Pro	USNM 12712[5]	A	276.0	124.0	435.0	140.0	130.0	123.0		190.0	272.0	83.0	348.0	240.0		975.0
La	Cory	AMNH 5338	A	132.6	130.1	299.6	118.8		89.4			238.9	86.3	248.6		0.267	681.2
La	Cory	CMN 34825	S	88.0	48.0	241.0	61.0	112.0	60.0			175.0	42.0	180.0	210.0	0.445	438.0
La	Cory	CMN 8676[5]	A	130.0	96.0	248.0	90.0	141.0	81.0	151.0	140.0	179.0	74.0	213.0	300.0	0.365	564.0
La	Cory	CMN 8704[5]	A	166.0	45.0	303.0	82.0	120.0	84.0		145.0	233.0	77.0	271.0	220.0	0.347	596.0
La	Cory	FMNH 1357[5]	A	127.0	73.0	287.0	102.0		97.0			235.0	120.0	255.0			589.0

La	Cory	ROM 1933[5]	A	137.0	115.0	285.0	80.0	147.0	87.0	160.0	123.0	224.0	107.0	230.0		0.166	617.0
La	Cory	ROM 1947	S	106.0	76.0	220.0	80.0	182.0	50.0			180.0	35.0	125.0		0.351	482.0
La	Cory	ROM 776[5]	A	168.0	82.0	298.0	109.0	220.0	83.0	170.0	160.0	271.0	91.0	270.0	256.0	0.248	657.0
La	Cory	ROM 777[5]	A	141.0	137.0	305.0	100.0	173.0	82.0			237.0	76.0	260.0	190.0	0.177	683.0
La	Cory	ROM 845[5]	A	139.0	122.0	269.0	100.0	220.0	90.0	205.0	135.0	230.0	100.0	273.0	247.0	0.243	630.0
La	Cory	ROM 868[5]	A	156.0	129.0	294.0	112.0	124.0	96.0			226.0		292.0	190.0	0.431	691.0
La	Cory	ROM 870[5]	A			242.0	97.0		75.0	94.0		195.0		212.0	134.0		
La	Cory	ROM 871[5]	A				100.0		108.0	188.0	156.0	225.0		275.0	75.0		
La	Cory	TMM 40484-88	A	580.0		271.2	136.9		57.8			192.2	74.8	197.0			580.0
La	Cory	TMP 1980.023.0004[5]	A			340.0	86.0			212.0		260.0		262.0	278.0		
La	Cory	TMP 1980.040.0001[5]	A	118.0	102.0	241.0	114.0	209.0	90.0	262.0	169.0	230.0	53.0	266.0	363.0	0.154	575.0
La	Cory	TMP 1982.037.0001[5]	A	110.0	75.0	251.0	93.0	136.0	74.0	122.0	141.0	214.0	65.0	221.0	150.0	0.298	529.0
La	Cory	TMP 1983.031.0003* § cast ROM 759	J	60.0	55.0	139.0	66.0	100.0	63.0	70.0		115.0	30.0	130.0	84.0		320.0
La	Cory	TMP 1984.121.0001[5]	A	123.0	123.0	285.0	99.0	215.0	92.0	222.0	200.0	235.0	44.0	260.0	285.0	0.211	630.0
La	Cory	TMP 1997.012.0232[5]	S	140.0	33.0	231.0	56.0		68.0			170.0	55.0	192.0			460.0
La	Cory	UALVP 52826	A	182.0	83.0	345.0	50.0	165.0	84.3	250.0	90.0		112.0	295.0		0.200	660.0
La	Cory	USNM 16600	S	86.0	52.0	145.5	38.0	97.0	49.0	154.0			21.0	131.0	185.0	0.231	321.5
La	Hyp	AMNH 28497*	J	12.0	18.0	27.0	25.0	20.0	11.0	50.0	25.0	25.0	9.0	41.0	46.0	0.314	82.0
La	Hyp	AMNH 5278	A	135.4	115.7	273.2	127.1		110.9			201.6	58.2	251.7		0.241	651.3
La	Hyp	AMNH 5461	J	45.3	30.5	129.0	45.5	92.0	47.5	127.0	51.0	121.0	48.0	147.0	150.0	0.131	250.3
La	Hyp	CMN 2246	J	78.0	86.0	196.0	59.0	200.0	67.0	130.0	40.0	185.0	69.0	152.0	112.0	0.156	419.0
La	Hyp	CMN 2247	S	66.0	34.0	117.0	38.0	128.0	47.0			110.0	49.0	108.0	140.0	0.149	255.0
La	Hyp	CMN 8501	A	128.0	52.0	250.0	140.0	260.0	102.0	204.0	87.0	245.0	30.0	245.0	220.0	0.134	570.0
La	Hyp	MOR 548†	J	31.0	20.0	72.0	32.0	54.0	27.0	80.0	34.0	66.0	9.0	75.0	87.0	0.089	155.0
La	Hyp	MOR 549	A	148.2	142.0	321.0	86.4		80.3			223.8	100.9	238.0	233.1		697.6
La	Hyp	TMP 1982.010.0001	S	90.0	65.0	215.0	140.0	110.0	80.0				73.0	222.0		0.237	510.0

La	Hyp	TMP 1994.385.0001	J	80.0	70.0	141.0	55.0	71.0	44.0	140.0	61.0	127.0	35.0	107.5	120.0	0.277	346.0
La	Hyp	TMP 2006.015.0001	S			180.0	100.0		71.5	152.0		135.0		172.0	220.0		
La	Lamb indet.	TMP 1989.079.0052	J	14.0	16.0	25.0	10.0	14.0	12.0			25.0	5.0		20.0	0.522	65.0
La	Lamb indet.	UALVP 57103	J	97.0	41.0	170.0	80.0	180.0	66.0	140.0	62.0	130.0	65.0	112.0	156.0	0.268	388.0
La	Lamb	AMNH 5340[4]	J	84.7	41.5	185.6	79.3		49.6			112.3	64.0	119.8		0.400	391.1
La	Lamb	CMN 2869[5]	A	142.0	108.0	242.0	106.0	130.0	89.0	142.0		191.0	52.0	256.0	248.0	0.326	598.0
La	Lamb	CMN 351[5]	A	127.0	152.0	295.0	105.0	116.0	89.0			235.0	32.0	279.0			679.0
La	Lamb	CMN 8503[5]	A	97.0	67.0	250.0	55.0	104.0	72.0	102.0	119.0	186.0	28.0	211.0	140.0	0.248	469.0
La	Lamb	CMN 8633	S	102.0	74.0	216.0	80.0	82.0	64.0	148.0	38.0	168.0	52.0	154.0	168.0	0.105	472.0
La	Lamb	CMN 8703[5]	A	119.0	153.0	309.0	90.0	160.0	94.0	186.0	160.0	216.0	59.0	310.0	190.0	0.421	671.0
La	Lamb	CMN 8705[5]	A	161.0	94.0	300.0	113.0	152.0	102.0	176.0	152.0	256.0	65.0	290.0	192.0	0.325	668.0
La	Lamb	FMNH 1479[5]	A	174.0	107.0	293.0	107.0	226.0	95.0	160.0	148.0	212.0	128.0	263.0	190.0	0.117	681.0
La	Lamb	NHMUK R9527[5]	A	591.0		304.0	100.0		87.0			245.0	36.0	271.0			591.0
La	Lamb	ROM 1218[5]	A	184.0	76.0	327.0	95.0	196.0	101.0	205.0	168.0	216.0	114.0	282.0	257.0	0.456	682.0
La	Lamb	ROM 794[5]	A	136.0	205.0	269.0	95.0	182.0	99.0	174.0	162.0	210.0	153.0	290.0	185.0	0.273	705.0
La	Lamb	ROM 869[5]	S	86.0	104.0	236.0	104.0	114.0	75.0	120.0		212.0	80.0	218.0	180.0	0.242	530.0
La	Lamb	TMP 1966.004.0001[5]	A	138.0	118.0	285.0	93.0	140.0	100.0	142.0		225.0	91.0	265.0	116.0	0.448	634.0
La	Lamb	TMP 1981.037.0001[5]	A	124.0	131.0	327.0	82.0	202.0	92.0	205.0	175.0	227.0	93.0	258.0	155.0	0.127	664.0
La	Lamb	TMP 1982.038.0001[5]	A	114.0	57.0	244.0	77.0	215.0	85.0	280.0	140.0	238.0	98.0	247.0	375.0	0.295	492.0
La	Lamb	TMP 1983.031.0002* [§]cast ROM 758	J	50.0	58.0	139.0	83.0	90.0	68.0	140.0	60.0	120.0	44.0	135.0	150.0	0.423	330.0
La	Lamb	TMP 1997.012.0128[5]	A	133.0	122.0	283.0	67.0	110.0	100.0			207.0	90.0	271.0		0.280	605.0
La	Lamb	USNM 10309	A	153.3	177.6	305.1	213.6		86.1	240.5			76.0	304.3			849.5
La	Para	ROM 768[5]	A	151.0	82.0	291.0	113.0	180.0	102.0	192.0		235.0	125.0	229.0	185.0	0.243	637.0
La	Para	TMP 1990.036.0155[5]	S	80.0	53.0	147.0	85.0	127.0	52.0			140.0	35.0	161.0		0.199	365.0

Le	Lepto	CMN 8887	A	39.0	72.0	96.0	68.0	30.0	57.0	108.0	65.0	84.0	15.0	151.0	48.0	0.669	275.0
Le	Lepto	CMN 8889	A	88.0	58.0	154.0	70.0	46.0	65.0	225.0	55.0	112.0	30.0	114.0	195.0	0.629	370.0
Le	Lepto	TMP 2013.024.0001	A			112.0	68.0	70.0	66.0	190.0	82.0	80.0	77.0		135.0		205.0
Le	Preno	MNHCM #[7]	A	55.4	57.6	118.9	56.8	58.0	82.0	72.7		84.5	7.1	156.9	179.4	0.736	288.7
Pa	Draco	ROM 53579	A	61.0	23.5	161.0	74.5	66.0	64.5	170.0	58.0	55.0	1.0	118.0	110.0	0.207	320.0
Pa	Draco	ROM 53580* cast TCMI 2004.17.1	A			154.0	86.0	40.0	48.0	156.0	55.0	45.0		85.0	126.0		
Pa	Pachy	CMN 40602	A	65.0	45.0	208.0	57.0	65.0		205.0	84.0		5.0	161.0	275.0	0.286	375.0
Pa	Pachy	ROM 55378 cast of NSM PV 20423	A	61.0	10.0	160.0	110.0	74.0	43.0	142.0	36.0	80.0	4.0	111.0	296.0	0.134	341.0
Pa	Steg	UALVP 2	A	20.0	6.0	74.0	20.0	22.0	55.0	77.0	42.0	29.0	2.0	66.0	106.0	0.170	120.0
Th	Oro	MOR 294	A				30.0		11.0	20.0	24.0	21.0		44.0	20.0		
Th	Ory	MOR[1] (1636+1642)	A	34.0	8.0	60.0	63.0	10.0	20.5	80.0	31.0	35.0	5.0	66.5	62.0	0.078	165.0
Th	Park	TMP 1980.051.0003	A	21.0	13.0	60.0	56.0	22.0	24.0			62.0	8.0	59.0	17.0		150.0
Th	Thesc	MOR 979	A			85.0	66.5		29.3	112.0		67.0		93.8	96.0		
Th	Thesc	NCSM 15728**	A	19.0	67.0	89.0	55.0	9.2	25.0	88.0	45.3	27.0		72.0	55.5	0.126	230.0

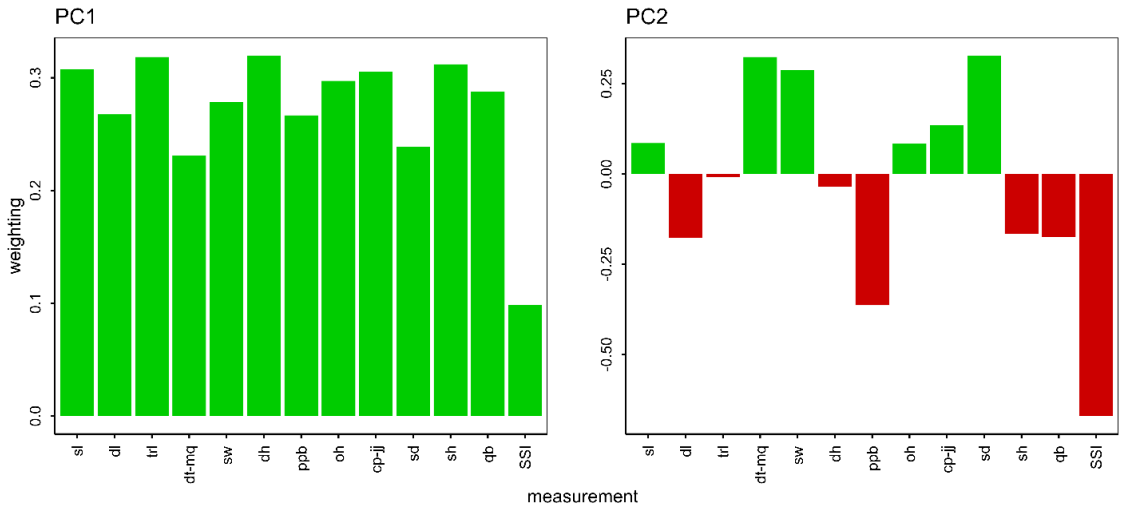

Appendix L Loadings for PCA of megaherbivores and small ornithischians for the first two PC axes of the non-size corrected dataset. Green indicates positive weightings and red indicates negative loadings. Abbreviations- sl: snout length, dl: diastema length, trl: tooth row length, dt-mq: distance from jaw joint to distal end of tooth row, sw: maximum beak width, dh: midpoint dentary height, ppb: paroccipital process breadth, oh: occiput height, cp-jj: distance from coronoid process apex to middle of jaw joint, sd: depression of snout below occlusal plane, sh: skull height, qb: quadrate breadth, SSI: snout shape index.

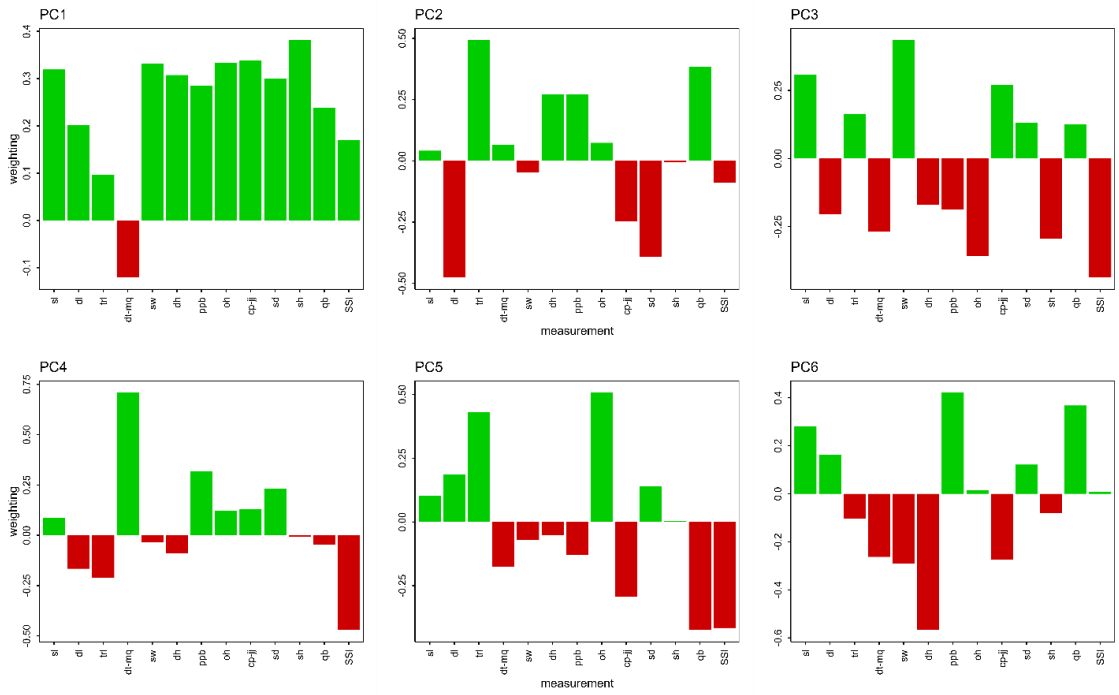

Appendix M Loadings for PCA of megaherbivores and small ornithischians for the first six PC axes of the size-corrected dataset. Green indicates positive weightings and red indicates negative loadings. Abbreviations- sl: snout length, dl: diastema length, trl: tooth row length, dt-mq: distance from jaw joint to distal end of tooth row, sw: maximum beak width, dh: midpoint dentary height, ppb: paroccipital process breadth, oh: occiput height, cp-jj: distance from coronoid process apex to middle of jaw joint, sd: depression of snout below occlusal plane, sh: skull height, qb: quadrate breadth, SSI: snout shape index.

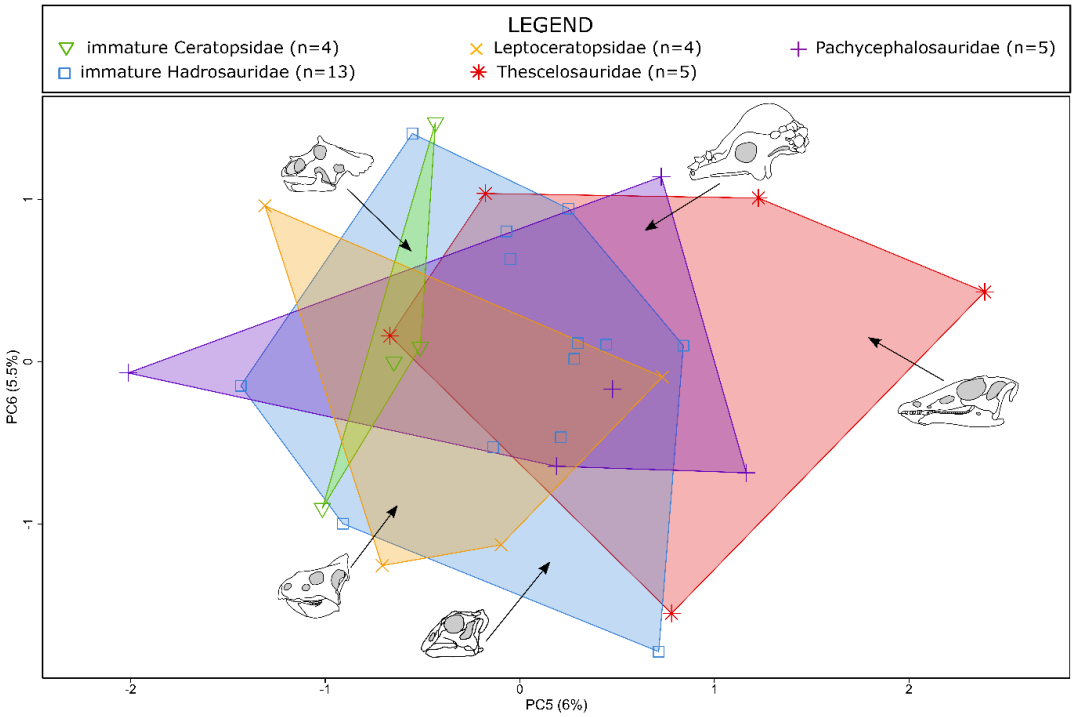

Appendix N Plot of PC6 against PC5 from principal component analysis of sized-corrected megaherbivore and small ornithischian dataset.

Appendix O Feeding height estimate data.

O.1 Raw feeding height estimate data used. Abbreviations: Fam-family, HL-humerus length, RL-radius length, UL-ulna length, MCL-metacarpal length, FL-femur length, FiL-fibula length, TL-tibia length, MTL-metatarsal length, TaL-tail length, UBL-upper body length (trunk+neck length), QFH-quadrupedal feeding height, BPH-bipedal feeding height, H-Hadrosauridae, C-Ceratopsidae, Le-Leptoceratopsidae, Th-Thescelosauridae, Pa-Pachycephalosauridae, Ha indet.-Hadrosauridae indet., La indet.-Lambeosaurinae indet., Cory- *Corythosaurus*, Lamb-*Lambeosaurus*, Para-*Parasaurolophus*, Hyp-*Hypacrosaurus*, Pro-*Prosaurolophus*, Gryp-*Gryposaurus*, Maia-*Maiasaura*, Edm-*Edmontosaurus*, Brac-*Brachyceratops*, Ava-*Avaceratops*, Cen-*Centrosaurus*, "pa"-"pachyrhinosaur", Pa-*Pachyrhinosaurus*, Sty-*Styracosaurus*, Chasm-*Chasmosaurus*, Tri-*Triceratops*, Anchi-*Anchiceratops*, Cer-*Cersinops*, Unes-*Unescoceratops*, Lepto-*Leptoceratops*, Preno-*Prenoceratops*, Mon-*Montanoceratops*, Thesc-*Thescelosaurus*, Park-*Parksosaurus*, Ory-*Oryctodromeus*, Oro-*Orodromeus*, Steg-*Stegoceras*, Pach-*Pachycephalosaurus*; *cast, if the original specimen is known the number is provided; [§]measured original and reconstructed portions of specimen; [†]composite; [††]composite mount from USNM 14765, 8023, 7951, 7953, 7957, 7958, 8076, 8077, 8078, 8079. [1]Dodson, 1986; [2]Lull and Wright, 1942; [3]Mallon et al., 2013; [4]Farke et al., 2019; [5]Ostrom, 1978; [6]Prieto-Marquez, 2014; [7]Wosik et al., 2017; [8]measurements taken using photos from M.J. Ryan. All measurements and estimated feeding heights are provided in mm. Empty cells denote missing data.

Fam	Genus	Specimen	HL	RL	UL	MCL	FL	FiL	TL	MTL	TaL	UBL	QFH	θ	BFH
H	Ha indet.	TMP 1998.058.0001	255.0	310.0	308.0		520.0	470.0	445.0	148.0	1830.0	1342.0	1138.0	0.622	1847.8
H	La indet.	UC 16624					104.0	70.0	87.0	24.0			198.0		
H	Cory	AMNH 5469					405.0		383.0	142.5			930.5		
H	Cory	CMN 8676[3]	450.0	535.0	570.0	215.0	890.0	775.0	813.0	320.0	3588.0		1985.0		
H	Cory	AMNH 5338[3]	546.0	577.0	609.0	242.0	987.0	882.0	924.0	378.0	3955.0	2635.0	2247.0	0.568	3545.9
H	Cory	TMP 1984.121.0001[3]	530.0	640.0	650.0	255.0	1040.0		980.0	349.0	4126.0		2369.0		
H	Cory	TMP 1980.023.0004[3]	546.0	616.0	671.0		1145.0		996.0	410.0	4502.0	2770.0	2551.0	0.567	3903.6
H	Cory	ROM 845[3]	530.0	640.0	695.0	270.0	1055.0	915.0	925.0	390.0	4300.0	3120.0	2360.0	0.549	3871.0
H	Cory	TMP 1980.040.0001[3]	570.0	629.0	645.0	254.0	1070.0	905.0	949.0	394.0	4233.0	3045.0	2369.0	0.560	3863.8
H	Cory	AMNH 5240[3]					1080.0	950.0	1000.0	380.0	4130.0	2956.0	2410.0	0.584	3904.2
H	Lamb	AMNH 5340[2]	305.0	320.0	350.0	151.0	590.0		550.0	210.0			1350.0		

H	Lamb	CMN 8703[3]	520.0	616.0	660.0	265.0	1020.0	940.0	1000.0	336.0	4684.0		2296.0		
H	Lamb	TMP 1982.038.0001[3]		651.0	685.0	213.0	1125.0	1012.0	1067.0	420.0	3500.0	3100.0	2557.0	0.731	4404.2
H	Lamb	TMP 1966.004.0001[3]	505.0	630.0	680.0	275.0	1063.0	976.0	1020.0	365.0	4199.0	2600.0	2404.0	0.573	3683.4
H	Lamb	ROM 1218[3]	500.0	600.0	665.0	250.0	1070.0	900.0	925.0	385.0	4120.0	2850.0	2355.0	0.572	3770.6
H	Para	UALVP 300[3]	511.0				991.0	885.0	870.0	406.0	4420.0	3016.0	2282.0	0.516	3670.8
H	Para	ROM 768[3]	495.0	490.0	540.0	185.0	1035.0		909.0	424.0	4616.0	3150.0	2368.0	0.513	3811.5
H	Para	FMNH P27393[4]					1041.5	894.0	995.2	376.0			2311.5		
H	Hyp	AMNH 28497					92.6	79.1	84.3	34.5	312.4	191.2	206.2	0.660	308.8
H	Hyp	TMP 2007.010.0001					490.0		445.0	208.0			1143.0		
H	Hyp	AMNH 5357					825.0		800.0	329.5			1954.5		
H	Hyp	TMP 1982.010.0001					890.0	758.0	787.0	285.0			1933.0		
H	Hyp	CMN 8501	541.0	619.0	620.0	240.0	1010.0	925.0	940.0	305.0	2293.0	3290.0	2240.0	0.977	4627.0
H	Hyp	USNM 7948[4]			670.0		1035.0	935.0	1000.0	400.0			2370.0		
H	Hyp	MOR 549[4]					1050.0		990.0	412.0			2452.0		
H	Pro	ROM 787[3]	535.0	475.0	545.0	230.0	975.0	835.0	850.0	320.0	3700.0	2595.0	2130.0	0.576	3427.0
H	Pro	TMP 1984.001.0001[3]	560.0	540.0	584.0	261.0	1045.0	900.0	895.0	343.0	4255.0	4650.0	2288.0	0.538	4561.0
H	Gryp	CMN 8784					506.0		495.0	148.0	1789.0	652.0	1149.0	0.642	1462.2
H	Gryp	TMP 1980.022.0001[3]	540.0	502.0	520.0	224.0	955.0	815.0	860.0	316.0	3131.0	2520.0	2086.0	0.666	3492.5
H	Gryp	AMNH 5350[3]					1140.0	930.0	1030.0	343.0	3737.0		2413.0		
H	Gryp	MCSNM 345[3]	730.0	680.0	785.0	211.0	1150.0		1080.0	330.0	3770.0	3170.0	2560.0	0.679	4358.7
H	Gryp	ROM 764[3]	600.0	560.0	615.0	220.0	1050.0	890.0	865.0	345.0	3442.0	2610.0	2285.0	0.664	3729.0
H	Maia	ROM 44864	83.0	73.0	91.0	35.0	130.0	109.5	115.0	47.5	304.0	329.0	287.0	0.944	512.7
H	Maia	ROM 44770					940.0	966.0		305.0			2211.0		
H	Edm	UCMP 128181[7]					147.0	113.0	135.9	56.6			316.6		
H	Edm	LACM 23504[6]	292.5	279.0	307.5	153.0	567.5	467.0	507.0	203.0	1739.0	1761.0	1237.5	0.712	2285.8
H	Edm	ROM 867					895.0	885.0	866.0	324.0	4731.0	2942.0	2104.0	0.445	3301.0

H	Edm	CMN 8509					925.0		757.0				1682.0			
H	Edm	USNM 2414					1002.0	860.0	870.5	319.0	4272.0	2574.0	2181.0	0.511	3345.3	
H	Edm	YPM 2182[2]	590.0	550.0	600.0	270.0	1060.0	920.0	950.0	360.0			2340.0			
H	Edm	CMN 8399	640.0		655.0	266.0	1070.0	913.0	885.0	358.0	5250.0	2792.0	2341.0	0.446	3468.3	
H	Edm	AMNH 5730[4]	501.0	440.0	500.0	220.0	1101.3	820.0	927.0	386.0			2307.3			
H	Edm	CMN 2289					1260.0	1050.0	1070.0	360.0	1151.0	1296.0	2670.0	2.320		
C	Brac	USNM ID# 289[ft]	249.5	160.0	208.0	56.5	321.5	246.0	255.0	78.0	1055.0	825.0	466.0			
C	Ava	ANSP 15800[1,4]	288.0	197.7	231.3	74.0	400.4	292.0	300.6	113.0			559.7			
C	Cen	AMNH 5351[3]	600.0	345.0	435.0	127.0	797.0	560.0	588.0	207.0			1072.0			
C	Cen	ROM 1426[3]	535.0	305.0	412.0	125.0	867.0	495.0	555.0	193.0			965.0			
C	Cen	ROM 767[3]	538.0	343.0	418.0	118.0							999.0			
C	Cen	YPM 2015[3]	592.0	297.0	439.0	120.0	788.0	519.0	545.0	190.0			1009.0			
C	Cen	AMNH 5427[3]	735.0	445.0		143.0	800.0	460.0	500.0	230.0			1323.0			
C	"pa"	TMP 2002.076.0001[3]	682.0	395.0	530.0	159.0	600.0	483.0	510.0	136.0			1236.0			
C	Pa	TMP 1993.003.0001	537.5	330.0		136.0							1003.5			
C	Sty	CMN 344[3]	575.0	378.0	483.0	130.0	818.0	577.0	626.0				1083.0			
C	Sty	AMNH 5372[3]	618.0	375.0		140.0				244.0			1133.0			
C	Chasm	CMN 2245[3]	508.0	318.0	432.0	235.0	749.0	483.0	533.0		1651.0		1061.0			
C	Chasm	ROM 839[3]	555.0	345.0	425.0	130.0	829.0		547.0	202.0			1030.0			
C	Chasm	CMN 41357[3]	600.0	526.0	409.0	136.0	767.0	489.0	555.0	150.0			1262.0			
C	Chasm	ROM 843[3]	620.0	395.0	470.0	160.0	905.0	515.0	560.0	205.0	2400.0	2190.0	1175.0			
C	Tri	MOR 2591	335.0	190.0	290.0		556.0						525.0			
C	Tri	TMP 1982.006.0001* cast of AMNH 5033	727.5	387.0		156.0							1270.5			
C	Tri	MOR 3027	728.0	385.0	500.0	173.0	1100.0						1286.0			
C	Anchi	CMN 8547	530.0	295.0	410.0	125.0							950.0			
L	Cerasinops	MOR 300[4]	260.0		206.0		348.0	324.0	341.0	171.0			843.0			

L	Unes	TMP 1995.012.0006[3]	255.0	137.0		45.0	265.0		280.0	130.0	870.0		675.0		
L	Lepto	AMNH 5205[3]	293.0	176.7	224.7		244.0		219.0				463.0		
L	Lepto	YPM PU 18133[5]					257.0		385.0	181.0			823.0		
L	Lepto	TMP 2013.024.0001	202.0		170.0	46.0	244.0	283.0		114.0	480.0	353.0	641.0	1.335	810.0
L	Lepto	CMN 8889					270.0		310.0	134.0	924.0	633.0	714.0	0.773	1086.9
L	Lepto	CMN 8887	185.0	120.0	150.0		221.0	236.0	245.0	95.0	825.0	556.0	552.0	0.669	856.6
L	Lepto	CMN 8888	215.0	140.0	175.0	39.0	280.0	251.0	265.0	92.0	1140.0	610.0	623.0	0.546	909.5
L	Preno	MNHCM #[8]	183.1	123.2	129.6	36.5	206.6	204.9	204.5	97.2	509.6	474.3	508.7	0.998	827.0
L	Mon	TMP 1982.011.0001					229.0		258.0	114.4			601.4		
L	Mon	AMNH 5464					335.0		349.0				684.0		
Th	Thesc	CMN 8537	205.0	146.0	155.0	25.0	345.0	280.0	281.0	120.0	2200.0	1020.0		0.339	1069.7
Th	Thesc	MOR 979R	319.0	212.0	210.0	30.0	465.0	395.0	450.0	168.0	1095.0	1459.5		0.939	2061.1
Th	Thesc	USNM 7757	207.0	147.0	150.0	34.0	334.5	280.5	312.0	142.0	1930.0	1039.5		0.392	1135.1
Th	Park	TMP 1980.051.0003					321.0	248.0	305.0	150.0	1648.0	939.0		0.436	1093.2
Th	Ory	MOR 1636+1642[†]	159.5	105.0	112.0	39.0	222.0	276.0	289.0	116.0	2490.0	805.0		0.247	804.3
Th	Oro	MOR 294					100.8		102.0	62.0					
Th	Oro	MOR 623					135.0	155.5	156.5	80.0					
Th	Oro	?[3]					270.0	305.0	322.0	151.0	1480.0	578.0		0.491	969.5
P	Steg	UALVP 2[3]					235.0	220.0	225.0	105.0	940.0	700.0		0.596	920.3
P	Pach	ROM 55378* cast of NSM PV 20423	222.0	148.5	151.5	30.0	430.0	376.5	394.0	145.5	1605.0	1170.0		0.593	1551.2

O.2 Maximum estimated feeding heights for five ornithischian families analyzed.

Family	Quadrupedal MFH (m)	Bipedal MFH (m)
Leptoceratopsidae	0.8	1.1
Pachycephalosauridae	n/a	1.6
Thescelosauridae	n/a	2.1
Hadrosauridae	2.7	4.6
Ceratopsidae	1.3	n/a

Appendix P Raw femoral dataset used for relative abundance analysis. Abbreviations: Grp- group, Fam/subfam- family/subfamily, FL-femur length in mm, MH-megaherbivores (Hadrosauridae and Ceratopsidae), SO-small ornithischians (Leptoceratopsidae, Pachycephalosauridae, Thescelosauridae), Ha indet.- Hadrosauridae indeterminate, La indet.- Lambeosaurinae indeterminate, Orn. indet.- Ornithischia indeterminate, Thesc indet.- Thescelosauridae indeterminate, Oro. incertae sedis- Orodrominae incertae sedis, Pachy indet.- Pachycephalosauridae indeterminate, Ce indet.- Ceratopsidae indeterminate. Taphonomic information for specimens measured in this study was taken from museum catalogue information, paleobiology databases (AMNH, CMN, ROM, TMP, USNM, YPM collection databases; Peters et al., n.d. PBDB), personal observations, and the literature (references provided in table). Note: all letters following specimen numbers are arbitrarily assigned and were used to distinguish between individual femora.

source	grp	clade	genus	Specimen #	FL	lithology	mode	Formation
original	MH	unknown	Ha/Ce indet.	TMP 1994.666.0082	325.0	unknown	unknown	unknown
original	MH	Ha	Ha indet.	CMN 58959	75.0	unknown	unknown	unknown
original	MH	Ha	Ha indet.	MOR 502	87.0	unknown	unknown	Two Medicine
original	MH	Ha	Ha indet.	MOR 972	78.0	unknown	unknown	unknown
original	MH	Ha	Ha indet.	MOR 1016	73.0	unknown	isolated	Judith River
original	MH	Ha	Ha indet.	MOR 240	370.0	unknown	unknown	unknown
original	MH	Ha	Ha indet.	TMP 1988.121.0018	84.0	sandstone	bone bed	Judith River
original	MH	Ha	Ha indet.	TMP 1990.036.0073	370.0	sandstone	unknown	Dinosaur Park
original	MH	Ha	Ha indet.	TMP 1997.012.0173	125.0	sandstone	unknown	Dinosaur Park
original	MH	Ha	Ha indet.	TMP 1990.036.0412	115.0	unknown	unknown	Dinosaur Park
original	MH	Ha	Ha indet.	TMP 2000.012.0048	107.0	unknown	unknown	Dinosaur Park
original	MH	Ha	Ha indet.	TMP 1998.093.0132	86.0	unknown	unknown	Dinosaur Park
original	MH	Ha	Ha indet.	TMP 1992.036.0921	95.0	unknown	unknown	Dinosaur Park
original	MH	Ha	Ha indet.	TMP 1988.079.0013	77.0	unknown	bone bed	Oldman
original	MH	Ha	Ha indet.	TMP 2001.012.0089	195.0	unknown	unknown	Dinosaur Park
original	MH	Ha	Ha indet.	TMP 1996.012.0175	122.0	unknown	bone bed	Dinosaur Park
original	MH	Ha	Ha indet.	TMP 1989.036.0173	127.0	unknown	bone bed	Dinosaur Park

original	MH	Ha	Ha indet.	TMP 1989.036.0415	111.0	unknown	unknown	Dinosaur Park
original	MH	Ha	Ha indet.	TMP 1997.062.0001	271.0	unknown	unknown	Oldman
original	MH	Ha	Ha indet.	TMP 1996.048.0004	88.0	mudstone	bone bed	Oldman
original	MH	Ha	Ha indet.	TMP 1996.048.0005	77.0	mudstone	bone bed	Oldman
original	MH	Ha	Ha indet.	TMP 1992.030.0019	280.0	unknown	unknown	Oldman
original	MH	Ha	Ha indet.	TMP 1983.180.0001	460.0	sandstone	bone bed	Foremost
original	MH	Ha	Ha indet.	TMP 1997.036.0128	63.0	mudstone	bone bed	Horseshoe Canyon
original	MH	Ha	Ha indet.	TMP 1997.012.0166	110.0	sandstone	unknown	Dinosaur Park
original	MH	Ha	Ha indet.	TMP 1997.057.0001	86.0	unknown	bone bed	Oldman
original	MH	Ha	Ha indet.	TMP 1997.057.0001 tray	58.0	unknown	bone bed	Oldman
original	MH	Ha	Ha indet.	TMP 1997.057.0001 tray a	83.0	unknown	bone bed	Oldman
original	MH	Ha	Ha indet.	TMP 1997.057.0001 tray e	80.0	unknown	bone bed	Oldman
original	MH	Ha	Ha indet.	TMP 1997.057.0001 tray c	86.0	unknown	bone bed	Oldman
original	MH	Ha	Ha indet.	TMP 2005.049.0084	219.0	unknown	unknown	Dinosaur Park
original	MH	Ha	Ha indet.	TMP 2007.020.0110	202.0	unknown	unknown	Dinosaur Park
original	MH	Ha	Ha indet.	TMP 1992.036.0112	95.0	unknown	bone bed	Dinosaur Park
original	MH	Ha	Ha indet.	TMP 1973.008.0360	150.0	unknown	unknown	Dinosaur Park
original	MH	Ha	Ha indet.	TMP 1992.036.0600	108.0	sandstone	bone bed	Dinosaur Park
Tanke and Surman, 2001	MH	Ha	Ha indet.	TMP 1996.012.0172	155.0	unknown	bone bed	Dinosaur Park
AMNH photos on CMN Portfolio	MH	Ha	Ha indet.	AMNH 5358 a	459.0	unknown	isolated	Two Medicine
AMNH photos on CMN Portfolio	MH	Ha	Ha indet.	AMNH 5358 b	441.0	unknown	isolated	Two Medicine
original; Gates et al., 2011	MH	Ha	*Acristavus*	MOR 1155	436.0	sandstone	unknown	Two Medicine
Farke and Yip, 2019	MH	Ha	*Edmontosaurus*	RAM 9396	277.1	sandstone	isolated	Hell Creek
Wosik et al., 2017	MH	Ha	*Edmontosaurus*	UCMP 128181	147.0	sandstone	isolated	Hell Creek
original	MH	Ha	*?Maiasaura*	MOR 1002	71.5	mudstone	bone bed	Two Medicine

original	MH	Ha	*Maiasaura*	MOR 1012*	113.0	unknown	unknown	Two Medicine
original	MH	Ha	*Maiasaura*	MOR 1136 (WCA 8.300.32)	386.0	unknown	isolated	Two Medicine
original; Varricchio, 2001	MH	Ha	*Maiasaura*	MOR 547A	455.5	unknown	bone bed	Two Medicine
original; Varricchio, 2001	MH	Ha	*Maiasaura*	MOR 547C	455.0	unknown	bone bed	Two Medicine
original; Varricchio, 2001	MH	Ha	*Maiasaura*	MOR 547D	460.0	unknown	bone bed	Two Medicine
original; Varricchio, 2001	MH	Ha	*Maiasaura*	MOR 547Q	468.0	unknown	bone bed	Two Medicine
original; Varricchio, 2001	MH	Ha	*Maiasaura*	MOR 547R	461.0	unknown	bone bed	Two Medicine
original; Varricchio, 2001	MH	Ha	*Maiasaura*	MOR 547S	465.0	unknown	bone bed	Two Medicine
Horner et al., 2000; Wosik et al., 2017	MH	Ha	*Maiasaura*	YPM-PU 22432	70.0	mudstone	bone bed	Two Medicine
Dilkes, 1993	MH	Ha	*Maiasaura*	YPM-PU 22400 A	115.6	mudstone	bone bed	Two Medicine
Dilkes, 1993	MH	Ha	*Maiasaura*	YPM-PU 22400 B	121.3	mudstone	bone bed	Two Medicine
Dilkes, 1993	MH	Ha	*Maiasaura*	YPM-PU 22400 C	124.2	mudstone	bone bed	Two Medicine
Dilkes, 1993	MH	Ha	*Maiasaura*	YPM-PU 22400 D	124.7	mudstone	bone bed	Two Medicine
Dilkes, 1993	MH	Ha	*Maiasaura*	YPM-PU 22400 E	127.5	mudstone	bone bed	Two Medicine
Dilkes, 1993	MH	Ha	*Maiasaura*	YPM-PU 22400 F	128.2	mudstone	bone bed	Two Medicine
Dilkes, 1993	MH	Ha	*Maiasaura*	YPM-PU 22400 G	130.3	mudstone	bone bed	Two Medicine
Dilkes, 1993	MH	Ha	*Maiasaura*	YPM-PU 22400 H	134.7	mudstone	bone bed	Two Medicine
original	MH	Ha	La indet.	MOR 704	70.5	unknown	bone bed	Two Medicine
original	MH	Ha	La indet.	UC 16624 (informally VP 2015.16)	104.0	sandstone	bone bed	Oldman
Farke et al., 2013	MH	Ha	*Parasaurolophus*	RAM 14000	328.9	sandstone	isolated	Kaiparowits
Farke et al., 2019	MH	Ha	*Corythosaurus*	AMNH 5469	405.0	unknown	unknown	Two Medicine
original	MH	Ha	*Hypacrosaurus*	TMP 2006.044.0012	449.0	unknown	bone bed	Horseshoe Canyon
original	MH	Ha	*Hypacrosaurus*	TMP 2007.010.0003	369.5	unknown	bone bed	Two Medicine
original	MH	Ha	*Hypacrosaurus*	AMNH 28497 (cast)	92.6	unknown	unknown	unknown
original	MH	Ha	*Hypacrosaurus*	MOR 548B	169.0	mudstone	bone bed	Two Medicine
original	MH	Ha	*Hypacrosaurus*	MOR 548H	190.0	mudstone	bone bed	Two Medicine

original	MH	Ha	*Hypacrosaurus*	MOR 548I	195.0	mudstone	bone bed	Two Medicine
original	MH	Ha	*Hypacrosaurus*	MOR 548J	205.0	mudstone	bone bed	Two Medicine
original	MH	Ha	*Hypacrosaurus*	MOR 548K	223.0	mudstone	bone bed	Two Medicine
original	MH	Ha	*Hypacrosaurus*	MOR 548L	230.0	mudstone	bone bed	Two Medicine
original	MH	Ha	*Hypacrosaurus*	MOR 548M	220.0	mudstone	bone bed	Two Medicine
original	MH	Ha	*Hypacrosaurus*	MOR 548N	160.0	mudstone	bone bed	Two Medicine
original	MH	Ha	*Hypacrosaurus*	MOR 548O	240.0	mudstone	bone bed	Two Medicine
original	MH	Ha	*Hypacrosaurus*	MOR 559	86.0	mudstone	bone bed	Two Medicine
Horner and Currie, 1994	MH	Ha	*Hypacrosaurus*	MOR 562	80.0	mudstone	isolated	Two Medicine
original	SO	unknown	Orn indet.	MOR 3039	238.0	unknown	unknown	Two Medicine
original	SO	Th	Thesc indet.	MOR 238	117.5	other	bone bed	Two Medicine
original	SO	Th	Thesc indet.	TMP 1979.011.0032	174.0	unknown	bone bed	Dinosaur Park
original	SO	Th	Thesc indet.	TMP 1990.036.0065	156.0	sandstone	unknown	Dinosaur Park
original	SO	Th	*Parksosaurus*	ROM 804	268.0	sandstone	isolated	Horseshoe Canyon
original	SO	Th	*Thescelosaurus*	CMN 8537	345.0	sandstone	isolated	Scollard
original; local from Boyd et al., 2009	SO	Th	*Thescelosaurus*	MOR 979	465.0	sandstone	isolated	Hell Creek
original	SO	Th	*Thescelosaurus*	MOR 1158	468.0	unknown	unknown	unknown
original	SO	Th	*Thescelosaurus*	MOR 1161	355.0	unknown	unknown	Hell Creek
original	SO	Th	*Thescelosaurus*	MOR 1106	450.0	unknown	unknown	unknown
original	SO	Th	*Thescelosaurus*	MOR 8123	269.0	unknown	isolated	Hell Creek
original	SO	Th	*Thescelosaurus*	USNM 7757	334.5	unknown	isolated	Lance
original	SO	Th	*Thescelosaurus*	RSM P 1225.1	303.2	sandstone	isolated	Frenchman
Brown, 2009; Boyd et al., 2009	SO	Th	*Thescelosaurus*	NCSM 15728	435.0	unknown	unknown	Hell Creek
Maidment et al., 2012	SO	Th	*Thescelosaurus*	AMNH 973	330.0	unknown	unknown	Hell Creek
Brown 2009	SO	Th	*Thescelosaurus*	RSM P 2693.3	125.0	unknown	bone bed	Frenchman
Brown 2009	SO	Th	*Thescelosaurus*	RSM P 2693.4	160.0	unknown	bone bed	Frenchman

Brown 2009	SO	Th	*Thescelosaurus*	RSM P 1990.0	260.0	unknown	bone bed	Frenchman
Brown 2009	SO	Th	*Thescelosaurus*	RSM P 2693.2	280.0	unknown	bone bed	Frenchman
Brown 2009	SO	Th	*Thescelosaurus*	CMN 22039	98.0	unknown	bone bed	Frenchman
Farke et al., 2019	SO	Th	*Thescelosaurus*	AMNH 5891	448.0	unknown	unknown	Hell Creek
AMNH, n.d.	SO	Th	*Thescelosaurus*	AMNH 5031	343.4	mudstone	isolated	Hell Creek
original	SO	Th	Oro. incertae sedis	TMP 1998.093.0014	132.0	sandstone	isolated	Dinosaur Park
original	SO	Th	Oro. incertae sedis	TMP 2008.045.0002	165.0	sandstone	isolated	Oldman
original	SO	Th	*Orodromeus*	MOR 10927	70.0	mudstone	bone bed	Two Medicine
original	SO	Th	*Orodromeus*	MOR 294	101.0	other	bone bed	Two Medicine
original	SO	Th	*Orodromeus*	MOR 623	135.0	mudstone	bone bed	Two Medicine
original	SO	Th	*Orodromeus*	MOR 1136	114.0	mudstone	bone bed	Two Medicine
original	SO	Th	*Orodromeus*	MOR 473	168.0	mudstone	isolated	Two Medicine
Horner and Weishampel, 1988	SO	Th	*Orodromeus*	YPM PU 22412	118.0	unknown	unknown	Two Medicine
Farke et al., 2019	SO	Th	*Orodromeus*	MOR 661	46.7	unknown	unknown	unknown
Farke et al., 2019	SO	Th	*Orodromeus*	MOR 685	129.3	unknown	unknown	unknown
Horner et al., 2009	SO	Th	*Orodromeus*	MOR 968-O-f-1	17.0	other	bone bed	Two Medicine
Horner et al., 2009	SO	Th	*Orodromeus*	MOR 407-F-2	75.0	other	bone bed	Two Medicine
original	SO	Th	*Oryctodromeus*	MOR 1071	126.0	unknown	bone bed	Judith River
original	SO	Th	*Oryctodromeus*	MOR cast of IMNH 44539	185.0	sandstone	isolated	Wayan
original	SO	Th	*Oryctodromeus*	MOR 1642	198.0	mudstone	isolated	Vaughn
Krumenacker, 2017	SO	Th	*Oryctodromeus*	IMNH 44920	191.0	mudstone	isolated	Wayan
Krumenacker, 2017	SO	Th	*Oryctodromeus*	IMNH 50877	202.0	mudstone	isolated	Wayan
original	SO	Pa	Pachy indet.	TMP 1992.036.0649	199.0	unknown	bone bed	Dinosaur Park
original	SO	Pa	Pachy indet.	TMP 1984.012.0004	134.0	sandstone	isolated	Horseshoe Canyon
original	SO	Pa	*Pachycephalosaurus*	ROM 55378 cast of NSM PV 20423	430.0	sandstone	isolated	Hell Creek

original	SO	Pa	*Stegoceras*	UALVP 2	217.5	sandstone	isolated	Dinosaur Park
original	SO	Le	*Leptoceratops*	CMN 8889	270.0	unknown	isolated	Scollard
original	SO	Le	*Leptoceratops*	CMN 8887	221.0	unknown	isolated	Scollard
original	SO	Le	*Leptoceratops*	CMN 8888	280.0	unknown	isolated	Scollard
original	SO	Le	*Leptoceratops*	TMP 2013.024.0001	244.0	sandstone	unknown	Willow Creek
original	SO	Le	*Leptoceratops*	TMP 2012.008.0010	288.0	mudstone	unknown	Scollard
original	SO	Le	*Leptoceratops*	TMP 2015.027.0002	290.0	sandstone	isolated	Willow Creek
Ostrom, 1978	SO	Le	*Leptoceratops*	YPM PU 18133	257.0	other	isolated	Lance
Chinnery, 2004	SO	Le	*Leptoceratops*	AMNH 5205	244.0	other	isolated	Scollard
Chinnery and Horner, 2007	SO	Le	*Cerasinops*	MOR 300	352.0	unknown	isolated	Two Medicine
photos from M.J. Ryan	SO	Le	*Prenoceratops*	MNHCM #	120.7	unknown	bone bed	Two Medicine
original	SO	Le	*Montanoceratops*	AMNH 5464	335.0	unknown	isolated	St. Mary River
Farke et al., 2019	SO	Le	*Montanoceratops*	TMP 1982.011.0001	229.0	sandstone	isolated	Willow Creek
original	SO	Le	*Unescoceratops*	TMP 1995.012.0006	265.0	sandstone	bone bed	Dinosaur Park
original	MH	Ce	Ce indet.	TMP 2008.078.0354	448.0	mudstone	bone bed	Oldman
original	MH	Ce	Ce indet.	TMP 2009.057.0067	270.0	unknown	unknown	Oldman
original	MH	Ce	Ce indet.	TMP 1982.018.0068	437.0	sandstone	isolated	Oldman
original	MH	Ce	Ce indet.	TMP 1967.020.0226	280.0	unknown	unknown	Dinosaur Park
original	MH	Ce	Ce indet.	TMP 1995.400.0144	345.0	mudstone	bone bed	Dinosaur Park
original	MH	Ce	Ce indet.	TMP 1995.400.0134	455.0	unknown	unknown	Dinosaur Park
original	MH	Ce	Ce indet.	USNM 365558	445.0	unknown	unknown	Two Medicine
original; local from Currie et al., 2016	MH	Ce	*Chasmosaurus*	UALVP 52613	231.0	sandstone	isolated	Dinosaur Park
Chinnery, 2004	MH	Ce	*Chasmosaurus*	UTEP P.37.7.111	457.0	mudstone	bone bed	Aguja
Chinnery, 2004	MH	Ce	*Chasmosaurus*	UTEP P.37.7.109	363.0	mudstone	bone bed	Aguja
original	MH	Ce	*Pachyrhinosaurus*	TMP 1987.055.0307	399.0	mudstone	bone bed	Wapiti
original	MH	Ce	*Pachyrhinosaurus*	TMP 1988.055.0210	371.0	mudstone	bone bed	Wapiti

original	MH	Ce	*Pachyrhinosaurus*	TMP 1989.055.0039	385.0	mudstone	bone bed	Wapiti
original	MH	Ce	*Pachyrhinosaurus*	TMP 1987.055.0114	402.0	mudstone	bone bed	Wapiti
original	MH	Ce	*Pachyrhinosaurus*	TMP 1988.055.0159	388.0	mudstone	bone bed	Wapiti
original	MH	Ce	*Pachyrhinosaurus*	TMP 1988.055.0071	440.0	mudstone	bone bed	Wapiti
original	MH	Ce	*Pachyrhinosaurus*	TMP 1989.055.0697	375.0	mudstone	bone bed	Wapiti
original	MH	Ce	*Pachyrhinosaurus*	TMP 1988.055.0118	280.0	mudstone	bone bed	Wapiti
original	MH	Ce	*Pachyrhinosaurus*	TMP 1989.055.0362	240.0	mudstone	bone bed	Wapiti
original	MH	Ce	*Pachyrhinosaurus*	TMP 1987.055.0005	270.0	mudstone	bone bed	Wapiti
original	MH	Ce	*Pachyrhinosaurus*	TMP 1989.055.0065	237.0	mudstone	bone bed	Wapiti
original	MH	Ce	*Pachyrhinosaurus*	TMP 1989.055.0063	385.0	mudstone	bone bed	Wapiti
original	MH	Ce	*Pachyrhinosaurus*	TMP 1987.055.0289	420.0	mudstone	bone bed	Wapiti
original	MH	Ce	*Pachyrhinosaurus*	TMP 1987.055.0225	250.0	mudstone	bone bed	Wapiti
original	MH	Ce	*Pachyrhinosaurus*	TMP 1986.055.0246	406.0	mudstone	bone bed	Wapiti
original	MH	Ce	*Pachyrhinosaurus*	TMP 1987.055.0226	366.0	mudstone	bone bed	Wapiti
original	MH	Ce	*Pachyrhinosaurus*	TMP 1989.055.1425	400.0	mudstone	bone bed	Wapiti
original	MH	Ce	*Pachyrhinosaurus*	TMP 1989.055.1574	218.0	mudstone	bone bed	Wapiti
Langston Jr., 1975	MH	Ce	*Pachyrhinosaurus*	CMN 10641	93.0	other	bone bed	St. Mary River
original	MH	Ce	*Coronosaurus*	TMP 2002.068.0078	386.0	sandstone	bone bed	Oldman
Farke et al., 2019	MH	Ce	*Centrosaurus*	TMP 1982.018.0068	440.0	unknown	bone bed	Dinosaur Park
original	MH	Ce	*Centrosaurus*	TMP 2016.045.0015	465.0	unknown	bone bed	Dinosaur Park
original	MH	Ce	*Centrosaurus*	TMP 1995.401.0008	370.0	sandstone	bone bed	Dinosaur Park
Tumarkin-Deratzian, 2009; Farke et al., 2019	MH	Ce	*Centrosaurus*	TMP 2002.068.0078	398.0	unknown	unknown	Oldman
original	MH	Ce	*Brachyceratops*	USNM 8023	331.0	unknown	unknown	Two Medicine
Chinnery, 2004	MH	Ce	*Avaceratops*	ANSP 15800	398.0	sandstone	isolated	Judith River
Rogers, 1990; Tumarkin-Deratzian, 2009	MH	Ce	*Einiosaurus*	MOR 373-7-27-6-1	446.0	mudstone	bone bed	Two Medicine

Rogers, 1992; Tumarkin-Deratzian, 2009; Reizner, 2010	MH	Ce	*Einiosaurus*	MOR 456-8-10-7-14	452.0	mudstone	bone bed	Two Medicine
Rogers, 1992; Tumarkin-Deratzian, 2009; Reizner, 2010	MH	Ce	*Einiosaurus*	MOR 456-8-10-7-32	289.0	mudstone	bone bed	Two Medicine

Appendix Q Determination of sample sizes needed for various power levels based on results from the NPMANOVA omnibus test.

Q.1 Methodology used to determine needed sample sizes to increase power for NPMANOVA test.

After running an omnibus test on the rarified dataset containing z-transformed PC scores, the model F-statistic, model degrees of freedom and residual degrees of freedom were used to calculate the partial effect size (ω^2) for the population using the "F_to_omega2()" function in the "effectsize" package (Makowski et al., 2019). The partial ω^2 effect size was used because it is a less biased measure of the standardized population effect size compared to the partial eta squared (η^2) value (Mordkoff, 2019). The "wp.kanova()" function from the "WebPower" package (Zhang and Mai, 2018) was then used to calculate the total number of samples needed for various power levels (from 10% to 100%) using the calculated effect size (partial ω^2 =0.218), a significance level (α) of 0.05, number of groups equal to 5 and the model degrees of freedom. The function then returns values for the overall sample size. To get the sample size needed for each family, the overall sample size was then rounded up to the nearest whole number and divided by 5. The required sample sizes calculated for various power levels are provided in Appendix Q.2.

Q.2 Calculated samples sizes for various power levels.

Power	Samples per group	Total sample size
10%	4	20
20%	9	45
30%	13	65
40%	17	85
50%	22	110
60%	26	130
70%	32	160
80%	39	195
90%	50	250

References

American Museum of Nature History. (2007). Paleontology collections database: https://www.amnh.org/research/paleontology/collections/search-the-database (accessed April 2020).

Arbour, V.M. and Mallon, J.C. (2017). Unusual cranial and postcranial anatomy in the archetypal ankylosaur *Ankylosaurus maniventris*. FACETS, 2, p. 764-794. DOI: 10.1139/facets-2017-0063

Arendt, J.D. and Wilson, D.S. (1997). Optimistic growth: competition and an ontogenetic diet shift select for rapid growth in pumpkinseed sunfish (*Lepomis gibbosus*). Evolution, 51(6), p. 1946-1954.

Barrett, P.M. (2005). The Diet of Ostrich Dinosaurs (Theropoda: Ornithomimosauria). Palaeontology, 48(2), p. 347-358. DOI: 10.1111/j.1475-4983.2005.00448.x

Begon, M., Townsend, C.R., Harper, J.L. (2006). Ecology: From Individuals to Ecosystems (4th ed.). Blackwell Publishing, Oxford, United Kingdom.

Bell, P.R., Currie, P.J., Russell, D.A. (2015). Large caenagnathids (Dinosauria, Oviraptorosauria) from the uppermost Cretaceous of western Canada. Cretaceous Research, 52(part A), p. 101-107. DOI: 10.1016/j.cretres.2014.09.006

Bell, P.R., Evans, D.C., Eberth, D.A., Fanti, F., Tsogtbaatar, K., Ryan, M.J. (2017). Sedimentological and taphonomic observations on the "Dragon's Tomb" *Saurolophus* (Hadrosauridae) bonebed, Nemegt Formation (Upper Cretaceous), Mongolia. Palaeogeography, Palaeoclimatology, Palaeoecology, 494, p. 75-90. DOI: 10.1016/j.palaeo.2017.11.034

Benson, R.B., Hunt, G., Carrano, M.T., Campione, N. (2017). Cope's rule and the adaptive landscape of dinosaur body size evolution. Palaeontology, 61(part 1), p. 13-48. DOI: 10.1111/pala.12329

Benyoucef, M., Läng, E., Cavin, L., Mebarki, K., Adaci, M., Bensalah, M. (2015). Overabundance of piscivorous dinosaurs (Theropoda: Spinosauridae) in the mid-Cretaceous of North Africa: The Algerian dilemma. Cretaceous Research, 55, p. 44-55. DOI: 10.1016/j.cretres.2015.02.002

Blackburn, D.C. and Moreau, C.S. (2006). Ontogenetic Diet Change in the Arthroleptid Frog *Schoutedenella xenodactyloides*. Journal of Herpetology, 40(3), p. 388-394.

Blob, R.W. and Fiorillo, A.R. (1996). The significance of vertebrate microfossil size and shape distributions for faunal abundance reconstructions: a Late Cretaceous example. Paleobiology, 22(3), p. 422-435. DOI: 10.1017/s0094837300016377

Bodmer, R.E. (1990). Ungulate Frugivores and the Browser-Grazer Continuum. Oikos, 57(3), p. 319-325. DOI:10.2307/3565960

Bowman, R.I. (1961). Morphological differentiation and adaptation in the Galapagos finches. University of California Publications in Zoology, 58, p. 1-302.

Boyd, C.A. (2014). The cranial anatomy of the neornithischian dinosaur *Thescelosaurus neglectus*. PeerJ, 2: e669. DOI: 10.7717/peerj.669

Boyd, C.A., Brown, C.M., Scheetz, R.D., Clarke, J.A. (2009). Taxonomic Revision of the Basal Neornithischian taxa *Thescelosaurus* and *Bugenasaura*. Journal of Vertebrate Paleontology, 29(3), p. 758-770.

Bramble, K., LeBlanc, A.R.H., Lamoureux, D.O., Wosik, M., Currie, P.J. (2017). Histological evidence for a dynamic dental battery in hadrosaurid dinosaurs. Scientific Reports, 7(15787), p. 1-13. DOI: 10.1038/s41598-017-16056-3

Brandt, S. (1986). Ontogenetic Shifts in Habitat, Diet, and Diel-Feeding Periodicity of Slimy Sculpin in Lake Ontario. Transactions of the American Fisheries Society, 115(5), p. 711-715.

Brett-Surman, M.K. (1989). A Revision of the Hadrosauridae (Reptilia: Ornithischia) And Their Evolution During the Campanian and Maastrichtian. [Ph.D. thesis]: George Washington University, Washington.

Brett-Surman, M.K. (1997). Ornithopods *in* Farlow, J.O. and Brett-Surman, M.K. (eds.), *The Complete Dinosaur*, Indiana University Press, Bloomington, Indiana, p. 330-346.

Bright, J.A., Marugán-Lobón, J., Cobb, S.N., Rayfield, R.J. (2016). The shapes of bird beaks are highly controlled by nondietary factors. PNAS, 113(19), p. 5352-5357. DOI: 10.1073/pnas.1602683113

ten Brink, H. and de Roos, A. (2018). Large-amplitude consumer resource cycles allow for the evolution of ontogenetic niche shifts in consumer life history. Journal of Theoretical Biology, 457, p. 237-248. DOI: 10.1016/j.jtbi.2018.08.035

Brown, C.M. (2009). *Thescelosaurus* (Dinosauria: Ornithischia) and related taxa from the Late Cretaceous of Alberta and Saskatchewan. [MSc. Thesis]: University of Calgary, Alberta.

Brown, C.M. and Vavrek, M.J. (2015). Small sample sizes in the study of ontogenetic allometry; implications for palaeobiology. PeerJ, 3:e818. DOI: 10.7717/peerj.818

Brown, C.M., Arbour, J.H., Jackson, D.A. (2012). Testing the Effect of Missing Data Estimation and Distribution in Morphometric Multivariate Data Analyses. Systematic Biology, 61(6), p. 941-954. DOI: 10.1093/sysbio/sys047

Brown, C.M., Boyd, C.A., Russell, A.P. (2011). A new basal ornithopod dinosaur (Frenchman Formation, Saskatchewan, Canada), and its implications for late Maastrichtian ornithischian diversity in North America. Zoological Journal of the Linnean Society, 163, p. 1157-1198. DOI: 10.1111/j.1096-3642.2011.00735.x

Brown, C.M., Campione, N.E., Giacomini, H.C., O'Brien, L.J., Vavrek, M.J., Evans, D.C. (2012). Ecological modelling, size distributions and taphonomic size bias in dinosaur faunas: a comment on Codron et al. (2012). Biology letters, 9(1): 20120582. DOI: 10.1098/rsbl.2012.0582.

Brown, C.M., Evans, D.C., Ryan, M.J., Russell, A.P. (2013a). New Data on the Diversity and Abundance of Small-Bodied Ornithopods (Dinosauria, Ornithischia) from the Belly River Group (Campanian) of Alberta. Journal of Vertebrate Paleontology, 33(3), p. 495-520. DOI: 10.1080/02724634.2013.746229

Brown, C.M., Evans, D.C., Campione, N.E., O'Brien, L.J., Eberth, D.A. (2013b). Evidence for taphonomic size bias in the Dinosaur Park Formation (Campanian, Alberta), a model Mesozoic terrestrial alluvial-paralic system. Palaeogeography, Palaeoclimatology, Palaeoecology, 372, p. 108-122. DOI: 10.1016/j.palaeo.2012.06.027

Brown, J.H. and Sibly, R.M. (2006). Life-history evolution under a production constraint. PNAS, 103(47), p. 17595-17599. DOI: 10.1073/pnas.0608522103

Buffetaut, E., and Suteethorn, V. (1999). The dinosaur fauna of the Sao Khua Formation of Thailand and the beginning of the Cretaceous radiation of dinosaurs in Asia. Palaeogeography, Palaeoclimatology, Palaeoecology, 150(1-2), p. 13-23. DOI: 10.1016/S0031-0182(99)00004-8

Buffetaut, E., Suteethorn, V., Khansubha, S. (2007). The ceratopsian dinosaur Psittacosaurus in the Early Cretaceous of Southeast Asia: a review of old and recent finds, *in* Tantiwanit, W. (ed.), *Proceedings of the International Conference on Geology of Thailand: Towards Sustainable Development and Sufficiency Economy*, p. 338-343.

Buffetaut, E., Suteethorn, V., Le Loeuff, J., Khansubha, S., Tong, H., Wongko, K. (2005). The Dinosaurian Fauna from the Khok Kruat Formation (Early Cretaceous) of Thailand. International Conference on Geology, Geotechnology and Mineral Resources of Indochina, 28-30, p. 575-581.

Butler, R.J., Upchurch, P., Norman, D.B. (2008). The Phylogeny of the Ornithischian Dinosaurs. Journal of Systematic Paleontology, 6(1), p. 1-40. DOI: 10.1017/S1477201907002271

Canadian Museum of Nature. (n.d.). Palaeobiology database: http://collections.nature.ca/en/Search/Index (accessed April 2020).

Campbell, J.A., Ryan, M.J. Holmes, R.B., Schröder-Adams, C.J. (2016). A Re-Evaluation of the Chasmosaurine Ceratopsid Genus *Chasmosaurus* (Dinosauria: Ornithischia) from the Upper Cretaceous (Campanian) Dinosaur Park Formation of Western Canada. PLoS ONE, 11(1): e0145805. DOI: 10.1371/journal.pone.0145805

Campione, N.E. (2019). MASSTIMATE: Body Mass Estimation Equations for Vertebrates. R package version 1.4. https://CRAN.R-project.org/package=MASSTIMATE

Campione, N.E. and Evans, D.C. (2011). Cranial Growth and Variation in *Edmontosaurus* (Dinosauria: Hadrosauridae): Implications for Latest Cretaceous Megaherbivore Diversity in North America. PLoS ONE, 6(9): e25186. DOI: 10.1371/journal.pone.0025186

Campione, N.E. and Evans, D.C. (2012). A universal scaling relationship between body mass and proximal limb bone dimensions in quadrupedal terrestrial tetrapods. BMC Biology, 10(60). DOI: 10.1186/1741-7007-10-60

Campione, N.E., Evans, D.C., Brown, C.M., Carrano, M.T. (2014). Body mass estimation in non-avian bipeds using a theoretical conversion to quadrupedal stylopodial proportions. Methods in Ecology and Evolution, 5(9). DOI: 10.1111/2041-210X.12226

Cardini, A. and Polly, P.D. (2013). Larger mammals have longer faces because of size-related constraints on skull form. Nature Communications, 4:2458. DOI: 10.1038/ncomms3458

Cardini, A., Polly, P.D., Dawson, R., Milne, N. (2015). Why the Long Face? Kangaroos and Wallabies Follow the Same 'Rule' of Cranial Evolutionary Allometry (CREA) as Placentals. Evolutionary Biology, 42, p. 169-176.

Carpenter, K. (1999). The Embryo and Hatching *in* Carpenter, K. (ed.), *Eggs, Nests and Baby Dinosaurs: A Look at Dinosaur Reproduction*, Indiana University Press, Bloomington, Indiana, p. 179-214.

Carslaw, D.C. and K. Ropkins, (2012) openair: Tools for the Analysis of Air Pollution Data. R package version 2.7-2. URL: https://CRAN.R-project.org/package=openair

Carr, T.D. (1999). Craniofacial ontogeny in Tyrannosauridae (Dinosauria, Coelurosauria). Journal of Vertebrate Paleontology, 19(3), p. 497-520. DOI: 10.1080/02724634.1999.10011161

Carrano, M.T., Janis, C.M., Seposki Jr., J.J. (1999). Hadrosaurs as ungulate parallels: Lost lifestyles and deficient data. Acta Palaeontologica Polonica, 44(3), p. 237-261.

Charig, A.J. and Milner, A.C. (1997). *Baryonyx walkeri*, a fish-eating dinosaur from the Wealden of Surrey. Bulletin of the Natural History Museum of London (Geology), 53, p. 11-70.

Chinnery, B. (2004). Morphometric analysis of evolutionary trends in the ceratopsian postcranial skeleton. Journal of Vertebrate Paleontology, 24(3), p. 591-609. DOI: 10.1671/0272-4634(2004)024[0591:MAOETI]2.0.CO;2

Chinnery, B.J. and Horner, J.R. (2007). A new neoceratopsian dinosaur linking North American and Asian taxa. Journal of Vertebrate Paleontology, 27(3), p. 625-641. DOI: 10.1671/0272-4634(2007)27[625:ANNDLN]2.0.CO;2

Chinnery-Allgeier, B.J. and Kirkland, J.I. (2010). An Update on the Paleobiogeography of Ceratopsian Dinosaurs, *in* Ryan, M.J., Chinnery-Allgeier, B.J., Eberth, D.A. (eds.), *New Perspectives on Horned Dinosaurs: The Royal Tyrell Museum Ceratopsian Symposium*, Indiana University Press, Bloomington, Indiana, p. 456-477.

Claessen, D. and Dieckmann, U. (2002). Ontogenetic niche shifts and evolutionary branching in size-structured populations. Evolutionary Ecology Research, 4, p. 189-217.

Codron, J., Botha-Brink, J., Codron, D., Huttenlocker, A.K., Angielczyk, K.D. (2016). Predator-prey interactions amongst Permo-Triassic terrestrial vertebrates as a deterministic factor influencing faunal collapse and turnover. Journal of Evolutionary Biology, 30(1), p. 40-54. DOI: 10.1111/jeb.12983

Codron, D., Carbone, C., Müller, D. W., Clauss, M. (2012). Ontogenetic niche shifts in dinosaurs influenced size, diversity and extinction in terrestrial vertebrates. Biology Letters, 8(4), p. 620-623. DOI: 10.1098/rsbl.2012.0240

Codron, D., Carbone, C., Clauss, M. (2013). Ecological Interactions in Dinosaur Communities: Influences of Small Offspring and Complex Ontogenetic Life Histories. PLoS ONE, 8(10): e77110. DOI: 10.1371/journal.pone.0077110

Coe, M.J., Dilcher, D.L., Farlow, J.O., Jarzen, D.M., Russell, D.A. (1987). Dinosaurs and land plants *in* Friis E.M., Chaloner, W.G., Crane, P. R.(eds.), *The origins of angiosperms and their biological consequences*, Cambridge University Press, Cambridge, United Kingdom, p. 225-258.

Currie, P.J., Holmes, R.B., Ryan, M.J., Coy, C. (2016). A juvenile chasmosaurine ceratopsid (Dinosauria, Ornithischia) from the Dinosaur Park Formation, Alberta, Canada. Journal of Vertebrate Paleontology: e1048348. DOI: 10.1080/02724634.2015.1048348

Currie, P.J., Langston Jr., W., Tanke, D.H. (2008). A New species of *Pachyrhinosaurus* (Dinosauria, Ceratopsidae) from the Upper Cretaceous of Alberta, Canada, *in*

Currie, P.J., Langston Jr., W., Tanke, D.H. (eds.), *A New Horned Dinosaur from an Upper Cretaceous Bone Bed in Alberta*, NRC Research Press, Ottawa, Ontario, p. 1-108. DOI: 10.1139/9780660198194

Cuthbertson, R., Tirabasso, A., Rybczynski, N., Holmes, R. (2012). Kinetic limitations of intracranial joints in *Brachylophosaurus canadensis* and *Edmontosaurus regalis* (Dinosauria: Hadrosauridae), and their implications for the chewing mechanics of hadrosaurids. The Anatomical Record Advances in Integrative Anatomy and Evolutionary Biology, 295(6), p. 968-979. DOI: 10.1002/ar.22458

Damuth, J. (1982). Analysis of the preservation of community structure in assemblages of fossil mammals. Paleobiology, 8(4), p. 434-446. DOI: 10.1017/s009483730000717x

DeSantis, L.R.G. (2016). Dental microwear textures: reconstructing diets of fossil mammals. Surface Topography: Metrology and Properties, 4(2): 023002. DOI: 10.1088/2051-672X/4/2/023002

Dilkes, D.W. (1993). Growth and locomotion in the hadrosaurian dinosaur *Maiasaura peeblesorum* from the Upper Cretaceous of Montana. [Ph.D. thesis]: University of Toronto, Ontario.

Dilkes, D.W. (2001). An ontogenetic perspective on locomotion in the Late Cretaceous dinosaur *Maiasaura peeblesorum* (Ornithischia: Hadrosauridae). Canadian Journal of Earth Sciences, 38(8), p. 1205-1227. DOI:10.1139/e01-016

Dodson, P.A. (1983). A faunal review of the Judith River (Oldman) Formation, Dinosaur Provincial Park, Alberta. Mosasaur, 1, p. 89-118.

Dodson, P. (1986). *Avaceratops lammersi*: A New Ceratopsid from the Judith River Formation of Montana. Proceedings of the Academy of Natural Sciences of Philadelphia, 138(2), p. 305-317.

Dodson, P. (1975a). Functional and ecological significance of relative growth in *Alligator*. Journal of Zoology, 175, p. 315-355. DOI: 10.1111/j.1469-7998.1975.tb01405.x

Dodson, P. (1975b). Taxonomic implications of relative growth in lambeosaurine dinosaurs. Systematic Zoology, 24(1), p. 37-54. DOI: 10.2307/2412696

Dodson, P., Behrensmeyer, A.K., Bakker, R.T., McIntosh, J.S. (1980). Taphonomy and paleoecology of the dinosaur beds of the Jurassic Morrison Formation. Paleobiology, 6(2), p. 208-232.

Dodson, P., Forster, C.A., Sampson, S.D. (2004). Ceratopsidae *in* Weishampel, D.B., Dodson, P., Osmolska, H. (eds.), *The Dinosauria* (2nd ed.), University of California Press, Berkeley and Los Angeles, California, p. 494-515.

Dompierre, H. and Churcher, C.S. (1996). Premaxillary Shape as an Indicator of the Diet of Seven Extinct Late Cenozoic New World Camels. Journal of Vertebrate Paleontology, 16(1), p. 141-148. DOI: 10.1080/02724634.1996.10011292

Durtsche, R.D. (2000). Ontogenetic plasticity of food habits in the Mexican spiny-tailed iguana, *Ctenosaura pectinata*. Oecologica, 124, p. 185-195. DOI: 10.1007/s004420050006

Drysdale, E.T., Therrien, F., Zelenitsky, D.K., Weishampel, D.B., Evans, D.C. (2019). Description of juvenile specimens of *Prosaurolophus maximus*, (Hadrosauridae, Saurolophinae) from the Upper Cretaceous Bearpaw Formation of southern

Alberta, Canada, reveals ontogenetic changes in crest morphology. Journal of Vertebrate Paleontology: e1547310. DOI: 10.1080/02724634.2018.1547310

Ebenman, B. (1992). Evolution in Organisms that Change Their Niches during the Life Cycle. The American Naturalist, 139(5), p. 990-1021. DOI: 10.1086/285370

Eberth, D.A., and Evans, D.C. International Hadrosaur Symposium: Post-Symposium Field Trip: Geology and Palaeontology of Dinosaur Provincial Park, Alberta. Royal Tyrrell Museum. URL: http://www.tyrrellmuseum.com/media/HadrSymp2011FieldGuide.pdf

Eberth, D.A., Evans, D.C., Brinkman, D.B., Therrien, F., Tanke, D.H., Russell, L.S. (2013). Dinosaur biostratigraphy of the Edmonton Group (Upper Cretaceous), Alberta, Canada: evidence for climate influence. Canadian Journal of Earth Sciences, 50(7), p.701-726. DOI:10.1139/cjes-2012-0185

Erickson, G.M., Lappin, A.K., Vliet, K.A. (2003). The ontogeny of bite-force performance in American alligator (*Alligator mississippiensis*). Journal of Zoology London, 260, p. 317-327. DOI: 10.1017/S0952836903003819

Erickson, G.M. and Zelenitsky, D.K. (2014). Osteohistology and Occlusional Morphology of *Hypacrosaurus stebingeri* Teeth throughout Ontogeny with Comments on Wear-induced Form and Function *in* Eberth, D.A. and Evans, D.C. (eds.), *Hadrosaurs*, Indiana University Press, Bloomington, Indiana, p. 422-432.

Eskew, E.A., Willson, J.D., Winne, C.T. (2008). Ambush site selection and ontogenetic shifts in foraging strategy in a semi-aquatic pit viper, the Eastern cottonmouth. Journal of Zoology, 277(2), p. 179-186. DOI: 10.1111/j.1469-7998.2008.00527.x

Evans, D.C. (2007). Ontogeny and Evolution of Lambeosaurine Dinosaurs (Ornithischia: Hadrosauridae). [Ph.D. thesis]: University of Toronto, Ontario.

Evans, D.C. (2010). Cranial anatomy and systematics of *Hypacrosaurus altispinus*, and a comparative analysis of skull growth in lambeosaurine hadrosaurids (Dinosauria: Ornithischia). Zoological Journal of the Linnean Society, 159(2), p. 398-434. DOI: 10.1111/j.1096-3642.2009.00611.x

Evans, D.C. and Reisz, R.R. (2007). Anatomy and Relationships of *Lambeosaurus magnicristatus*, a crested hadrosaurid dinosaur (Ornithischia) from the Dinosaur Park Formation, Alberta. Journal of Vertebrate Paleontology, 27(2), p. 373-393. DOI: 10.1671/0272-4634(2007)27[373:AAROLM]2.0.CO;2

Evans, D.C. and Ryan, M.J. (2015). Cranial Anatomy of *Wendiceratops pinhornensis* gen. et sp. nov., a Centrosaurine Ceratopsid (Dinosauria: Ornithischia) from the Oldman Formation (Campanian), Alberta, Canada, and the Evolution of Ceratopsid Nasal Ornamentation. PLoS ONE 10(7): e0130007. DOI: 10.1371/journal.pone.0130007

Farke, A.A., Chok, D.J., Herrero, A., Scolieri, B., Werning, S. (2013). Ontogeny in the tube-crested dinosaur *Parasaurolophus* (Hadrosauridae) and heterochrony in hadrosaurids. PeerJ, 1: e182. DOI: 10.7717/peerj.182

Farke, A.A., Maxwell, W.D., Cifelli, R.L., Wedel, M.J. (2014). A Ceratopsian Dinosaur from the Lower Cretaceous of Western North America, and the Biogeography of Neoceratopsia. PLoS ONE, 9(12): e112055. DOI: 10.1371/journal.pone.0112055

Farke, A., Wedel, M., Taylor, M. (2019). The Open Dinosaur Project (ODP): https://opendino.wordpress.com/ (accessed Feb 2020).

Farke, A.A. and Yip, E. (2019). A juvenile cf. *Edmontosaurus annectens* (Ornithischia, Hadrosauridae) femur documents a previously unreported intermediate growth stage for this taxon. Vertebrate Anatomy Morphology Palaeontology, 7, p. 59-67. ISSN: 2292-1389

Farlow, J.O., Dodson, P., Chinsamy, A. (1995). Dinosaur biology. Annual Review of Ecology and Systematics, 26, p. 445-471.

Fiorillo, A.R. (1998). Dental micro wear patters of the sauropod dinosaurs *Camarasaurus* and *Diplodocus*: Evidence for resource partitioning in the late Jurassic of North America. Historical Biology, 13(1), p. 1-16. DOI: 10.1080/08912969809386568

Fiorillo, A.R. (2011). Microwear patterns on the teeth of northern high latitude hadrosaurs with comments on microwear patterns in hadrosaurs as a function of latitude and seasonal ecological constraints. Palaeontologica Electronica, 14(3.20A), p. 1-17.

Fiorillo, A.R. and Tykoski, R.S. 2012. A new Maastrichtian species of the centrosaurine ceratopsid *Pachyrhinosaurus* from the North Slope of Alaska. Acta Palaeontologica Polonica, 57(3), p. 561-573. DOI: 10.4202/app.2011.0033

Fiorillo, A.R., McCarthy, P.J., Flaig, P.P., Brandlen, E., Norton, D.W., Zippi, P., Jacobs, L., Gangloff, R.A. (2010). Paleontology and Paleoenvironmental Interpretations of the Kikak-Tegoseak Quarry (Prince Creek Formation: Late Cretaceous), Northern Alaska: A Multi-Disciplinary Study of a High-Latitude Ceratopsian Dinosaur, *in* Ryan, M.J., Chinnery-Allgeier, B.J., Eberth, D.A. (eds.), *New Perspectives on Horned Dinosaurs: The Royal Tyrell Museum Ceratopsian Symposium*, Indiana University Press, Bloomington, Indiana, p. 456-477.

Fondevilla, V., Dalla Vecchia, F.M., Gaete R., Galobart, À., Moncunill-Sole´, B., Kohler, M. (2018). Ontogeny and taxonomy of the hadrosaur (Dinosauria, Ornithopoda) remains from Basturs Poble bonebed (late early Maastrichtian, Tremp Syncline, Spain). PLoS ONE, 13(10): e0206287. DOI: 10.1371/journal.pone.0206287

Fowler, D.W. (2017). Revised geochronology, correlation, and dinosaur stratigraphic ranges of the Santonian-Maastrichtian (Late Cretaceous) formations of the Western Interior of North America. PLoS ONE, 12(11): e0188426. DOI: 10.1371/journal.pone.0188426

Frederickson, J.A. and Tumarkin-Deratzian, A.R. (2014). Craniofacial ontogeny in *Centrosaurus apertus*. PeerJ, 2: e252. DOI: 10.7717/peerj.252

Galton, P.M. and Sues, H. (1983). New data on pachycephalosaurid dinosaurs (Reptilia: Ornithischia) from North America. Canadian Journal of Earth Sciences, 20(3), p. 462-472. DOI: 10.1139/e83-043

Gangloff, R.A. and Fiorillo, A.R. (2010). Taphonomy and paleoecology of a bonebed from the Prince Creek Formation, North Slope, Alaska. Palaios, 25, p. 299-317. DOI: 10.2110/palo.2009.p09-103r

Gaston, K.J. and Blackburn, T.M. (2000). Pattern and Process in Macroecology. Blackwell Publishing, Oxford, UK, pp. 337.

Gates, T.A. and Sampson, S.D. (2007). A new species of *Gryposaurus* (Dinosauria: Hadrosauridae) from the late Campanian Kaiparowits Formation, southern Utah, USA. Zoological Journal of the Linnean Society, 151(2), p. 351-376. DOI: 10.1111/j.1096-3642.2007.00349.x

Gates, T.A., Horner, J.R., Hanna, R.R., Nelson, C.R. (2011). New unadorned hadrosaurine hadrosaurid (Dinosauria, Ornithopoda) from the Campanian of North America. Journal of Vertebrate Paleontology, 31(4), p. 798-811. DOI:10.1080/02724634.2011.577854

Gates, T.A., Prieto- Márquez, A., Zanno, L.E. (2012). Mountain Building Triggered Late Cretaceous North American Megaherbivore Dinosaur Radiation. PLoS ONE, 7(10): e42135. DOI: 10.1371/journal.pone.0042135

Gignac, P.M. and Erickson, G.M. (2015). Ontogenetic changes in dental form and tooth pressures facilitate developmental niche shifts in American alligators. Journal of Zoology, 295(2), p. 132-142. DOI:10.1111/jzo.12187

Gilmore, C.W. (1914). A new ceratopsian dinosaur from the Upper Cretaceous of Montana, with note on *Hypacrosaurus*. Smithsonian Miscellaneous Collections, 63(3), p. 1-10.

Godfrey, S.J. and Holmes, R. (1995). Cranial morphology and systematics of *Chasmosaurus* (Dinosauria: Ceratopsidae) from the Upper Cretaceous of western Canada. Journal of Vertebrate Paleontology, 15(4), p. 726-742. DOI: 10.1080/02724634.1995.10011258

Goillot, C., Blondel, C., Peigne, S. (2009). Relationships between dental microwear and diet in Carnivora (Mammalia) – Implications for the reconstruction of the diet of extinct taxa. Palaeogeography, Palaeoclimatology, Palaeoecology, 271(1-2), p. 13-23. DOI: 10.1016/j.palaeo.2008.09.004

Goodwin, M.B. and Horner, J.R. (2010). Historical Collecting Bias and the Fossil Record of *Triceratops* in Montana, *in* Ryan, M.J., Chinnery-Allgeier, B.J., Eberth, D.A.

(eds.), *New Perspectives on Horned Dinosaurs: The Royal Tyrell Museum Ceratopsian Symposium*, Indiana University Press, Bloomington, Indiana, p. 551-563.

Goodwin, M.B., Clemens, W.A., Horner, J.R., Padian, K. (2006). The smallest known *Triceratops* skull: new observations on ceratopsid cranial anatomy and ontogeny. Journal of Vertebrate Paleontology, 26(1), p. 103-112. DOI: 10.1671/0272-4634(2006)26[103:tsktsn]2.0.co;2

Goswami, A., Flynn, J.J., Ranivoharimanana, L., Wyss, L.A. (2005). Dental microwear in Triassic amniotes: implications for paleoecology and masticatory mechanics. Journal of Vertebrate Paleontology, 25 (2), p.320-329. DOI: 10.1671/0272-4634(2005)025[0320:DMITAI]2.0.CO;2

Gould, S.J. (1966). Allometry and Size in Ontogeny and Phylogeny. Biological Reviews, 41(4), p. 587-638. DOI: 10.1111/j.1469-185x.1966.tb01624.x

Greaves, W.S. (1974). The jaw lever system in ungulates: a new model. Journal of Zoology, 184(2), p. 271-285. DOI: 10.1111/j.1469-7998.1978.tb03282.x

Greaves, W.S. (1991). The orientation of the force of the jaw muscles and the length of the mandible in mammals. Zoological Journal of the Linnean Society, 102(4), p. 367-374. DOI: 10.1111/j.1096-3642.1991.tb00006.x

Hammer, O. and Harper, D.A.T. (2006). Paleontological Data Analysis. Blackwell Publishing Ltd., Malden, Massachusetts.

Harrington, B. et al. (2004). Inkscape. URL: http://www.inkscape.org/

Hatcher, J.B., Marsh, O.C., Lull, R.S. (1907). The Ceratopsia. United States Geological Survey, Washington Government Printing Office, Washington.

Henderson, D.M. (2010). Skull shapes as indicators of niche partitioning by sympatric chasmosaurine and centrosaurine dinosaurs, *in* Ryan, M.J., Chinnery-Allgeier, B.J., Eberth, D.A. (eds), *New Perspectives on Horned Dinosaurs*, Indiana University Press, Bloomington, Indiana. p. 293-307.

Herrel, A., Joachim, R., Vanhooydonck, B., Irschick, D.J. (2006). Ecological consequences of ontogenetic changes in head shape and bite performance in the Jamaican lizard *Anolis lineatopus*. Biological Journal of the Linnean Society, 89(3), p. 443-454. DOI: 10.1111/j.1095-8312.2006.00685.x

Herring, S.W. and Teng, S. (2000). Strain in the braincase and its sutures during function. American Journal of Physical Anthropology, 112(4), p. 575-593. doi:10.1002/1096-8644(200008)112:4<575::aid-ajpa10>3.0.co;2-0

Holliday, C.M. and Witmer, L.M. (2008). Cranial kinesis in dinosaurs: Intracranial joints, protractor muscles, and their significance for cranial evolution and function in diapsids. Journal of Vertebrate Paleontology, 28, p. 1073-1088.

Holm, S. (1978). A Simple Sequentially Rejective Multiple Test Procedure. Scandinavian Journal of Statistics, 6(2), p. 65-70. DOI: 10.2307/4615733

Hone, D.W.E., Farke, A.A., Wedel, M.J. (2016). Ontogeny and the fossil record: what, if anything, is an adult dinosaur? Biology Letters, 12: 20150947. DOI: 10.1098/rsbl.2015.0947

Horner, J.R. (1983). Cranial Osteology and Morphology of the Type Specimen of *Maiasaura peeblesorum* (Ornithischia: Hadrosauridae), with Discussion of Its Phylogenetic Position. Journal of Vertebrate Paleontology, 3(1), p. 29-38.

Horner, J.R. (2000). Dinosaur Reproduction and Parenting. Annual Review of Earth and Planetary Science, 28, p. 19-45. DOI: 10.1146/annurev.earth.28.1.19

Horner, J.R. and Currie, P.J. (1994). Embryonic and neonatal morphology and ontogeny of a new species of *Hypacrosaurus* (Ornithischia, Lambeosauridae) from Montana and Alberta *in* Carpenter, K., Hirsch, K.F., Horner, J.R. (eds.), *Dinosaur eggs and babies*, Cambridge University Press, New York, New York, p. 312-336.

Horner, J.R. and Weishampel, D.A. (1988). comparative embryological study of two ornithischian dinosaurs. Nature, 332, p. 256-257. DOI: 10.1038/332256a0

Horner, J.R., Weishampel, D.B., Forster, C.A. (2004). Hadrosauridae *in* Weishampel, D.B., Dodson, P., Osmolska, H. (eds.), *The Dinosauria* (2nd ed.), University of California Press, Berkeley and Los Angeles, California, p. 438-463.

Horner, J.R. and Goodwin, M.B. (2006). Major cranial changes during *Triceratops* ontogeny. Proceedings of the Royal Society of London B: Biological Sciences, 273(1602), p. 2757-2761. DOI: 10.1098/rspb.2006.3643

Horner, J.R. and Goodwin, M.B. (2008). Ontogeny of Cranial Epi-Ossifications in *Triceratops*. Journal of Vertebrate Paleontology, 28(1), p. 134-144. DOI: 10.1671/0272-4634(2008)28[134:OOCEIT]2.0.CO;2

Horner, J. R., de Ricqlès, A., Padian, K. (2000). Long bone histology of the hadrosaurid dinosaur *Maiasaura peeblesorum*: growth dynamics and physiology based on an ontogenetic series of skeletal elements. Journal of Vertebrate Paleontology, 20(1), p. 115-129. DOI: 10.1671/0272-4634(2000)020[0115:lbhoth]2

Horner, J.R., de Ricqlès, A., Padian, K., Scheetz, R.D. (2009). Comparative long bone histology and growth of the “hypsilophodontid” dinosaurs *Orodromeus makelai*,

Dryosaurus altus, and *Tenontosaurus tillettii* (Ornithischia: Euronithopoda). Journal of Vertebrate Paleontology, 29(3), p. 734-747. DOI: 10.1671/039.029.0312

Horner, J.R., Varricchio, D.J., Goodwin, M.B. (1992). Marine transgressions and the evolution of Cretaceous dinosaurs. Nature, 358, p. 59-61. DOI: 10.1038/358059a0

Hunt, R.K. and Lehman, T.M. (2008). Attributes of the Ceratopsian Dinosaur *Torosaurus*, and New Material from the Javelina Formation (Maastrichtian) of Texas. Journal of Paleontology, 82(6), p. 1127-1138. DOI: 10.1666/06-107.1

Hunt, R. and Farke, A. (2010). Behavioral interpretations from ceratopsid bonebeds, *in* Ryan, M.J., Chinnery-Allgeier, B.J., Eberth, D.A. (eds), *New Perspectives on Horned Dinosaurs*, Indiana University Press, Bloomington, Indiana, p. 447-455

Insole, A.N. and Hutt, S. (1994). The palaeoecology of the dinosaurs of the Wessex Formation (Wealden Group, Early Cretaceous), Isle of Wight, Southern England. Zoological Journal of the Linnean Society, 112(1-2), p. 197-215. DOI: 10.1111/j.1096-3642.1994.tb00318.x

Janis, C. (1990). Correlations of cranial and dental variables with dietary preferences in mammals: A comparison of macropodoids and ungulates. Memoirs of the Queensland Museum, 28, p. 349-366.

Janis, C. (1995). Correlation between craniodental morphology and feeding behaviour in ungulates: Reciprocal illumination between living and fossil taxa, *in* Thomason, J. (ed.), *Functional morphology in vertebrate paleontology*, Cambridge University Press, Cambridge, United Kingdom, p. 76-98.

Janis, C.M. and Ehrhardt, D. (1988). Correlation of relative muzzle width and relative incisor width with dietary preference in ungulates. Zoological Journal of the Linnean Society, 92(3), p. 267-284. DOI: 10.1111/j.1096-3642.1988.tb01513.x

Jerzykiewicz, T., Currie, P.J., Eberth, D.A., Johnston, P.A., Koster, E.H., Zheng, J.J. (1993). Djadokhta Formation correlative strata in Chinese Inner Mongolia: an overview of the stratigraphy, sedimentary geology, and paleontology and comparisons with the type locality in the pre-Altai Gobi. Canadian Journal of Earth Sciences, 30(10), p. 2180-2195. DOI: 10.1139/e93-190

Jordano, P. (2000). Fruits and frugivory, *in* Fenner, M. (ed.), *Seeds: the ecology of regeneration in plant communities* (2nd ed.), CABI Publications, Willingford, United Kingdom, p. 125-166.

Jolliffe, I.T. and Cadima, J. (2016). Principal component analysis: a review and recent developments. Philosophical Transactions of the Royal Society A: Mathematical, Physical and Engineering Sciences, 374(2065): 20150202. DOI:10.1098/rsta.2015.0202

Keenan, S.W. and Scannella, J.B. (2014). Paleobiological implications of a *Triceratops* bonebed from the Hell Creek Formation, Garfield County, northeastern Montana, *in* Wilson, G.P., Clemens, W.A., Horner, J. R., Hartman, J.H. (eds.), *Through the End of the Cretaceous in the Type Locality of the Hell Creek Formation in Montana and Adjacent Areas*. Geological Society of America, 503, p. 349-364. DOI: 10.1130/2014.2503(14)

Keren-Rotem, T., Bouskila, A., Geffen, E. (2006). Ontogenetic habitat shift and risk of cannibalism in the common chameleon (*Chamaeleo chamaeleon*). Behavioral Ecology and Sociobiology, 59(6), p. 723-731. DOI: 10.1007/s00265-005-0102-z

Klingenberg, C.P. (2016). Size, shape, and form: concepts of allometry in geometric morphometrics. Developmental Genes and Evolution, 226(3). DOI: 10.1007/s00427-016-0539-2

Kobayashi, Y., Lu, J., Dong, Z., Barsbold, R., Azuma, Y., Tomida, Y. (1999). Herbivorous diet in an ornithomimid dinosaur. Nature, 402(6761), p. 480-481. DOI: 10.1038/44999

Konishi, T. (2015). Redescription of UALVP 40, and unusual specimen of *Chasmosaurus* Lambe, 1914 (Ceratopsidae: Chasmosaurinae) bearing long postorbital horns, and its implications for ontogeny and alpha taxonomy of the genus. Canadian Journal of Earth Sciences, 52(8), p. 608-619. DOI: 10.1139/cjes-2014-0167

Kozlowski, J. and Gawelczyk, A.T. (2002). Why are species' body size distributions usually skewed to the right? Functional Ecology, 16, p. 419-432.

Krumenacker, L.J. (2017). Osteology, phylogeny, taphonomy, and ontogenetic histology of *Oryctodromeus cubicularis*, from the Middle Cretaceous (Albanian-Cenomanian) of Montana and Idaho. [Ph.D. Thesis]: University of Montana, Montana.

Lakin, R.J. and Longrich, N.R. (2018). Juvenile spinosaurs (Theropoda: Spinosauridae) from the middle Cretaceous of Morocco and implications for spinosaur ecology. Cretaceous Research, 93, p. 129-142. DOI: 10.1016/j.cretres.2018.09.012

Langston Jr., W. (1975). The Ceratopsian Dinosaurs and Associated Lower Vertebrates from the St. Mary River Formation (Maestrichtian) at Scabby Butte, Southern Alberta. Canadian Journal of Earth Sciences, 12, p. 1576-1608.

Lamanna, M.C., Sues, H., Schachner, E.R., Lyson, T.R. (2014). A New Large-Bodied Oviraptorosaurian Theropod Dinosaur from the Latest Cretaceous of Western North America. PLoS ONE, 9(3): e92022. DOI: 10.1371/journal.pone.0092022

Lauters, P., Bolotsky, Y. L., Van Itterbeeck, J., Godefroit, P. (2008). Taphonomy and Age Profile of a Latest Cretaceous Dinosaur Bone Bed in Far Eastern Russia. PALAIOS, 23 (3/4), p. 153-162.

Lautenschlager, S. (2016). Reconstructing the past: methods and techniques for the digital restoration of fossils. Royal Society Open Science, 3: 160342. DOI: 10.1098/rsos.160342

LeBlanc, A.R.H., Reisz, R.R., Evans, D.C., Bailleul, A.M. (2016). Ontogeny reveals function and evolution of the hadrosaurid dental battery. BMC Evolutionary Biology, 16(152). DOI: 10.1186/s12862-016-0721-1

Lehman, T.M. (1997). Late Campanian dinosaur biogeography in the Western Interior of North America, *in* Wolberg, D.L., Stump, E., Rosenberg, G.D. (eds.), *Dinofest International: Proceedings of a symposium sponsored by Arizona State University*, Academy of Natural Sciences, Philadelphia, p. 223-240.

Lehman, T.M. (2001). Late Cretaceous dinosaur provinciality, *in* Tanke, D.H., Carpenter, K. (eds.), *Mesozoic vertebrate life*, Indiana University Press, Bloomington, Indiana, p. 310-328.

Lehman, T.M. (2006). Growth and Population Age Structure in the Horned Dinosaur *Chasmosaurus*, *in* Carpenter, K. (ed.), *Horns and Beaks: Ceratopsian and Ornithopod Dinosaurs*, Indiana University Press, Bloomington, Indiana, p. 259-318.

Levitt, C.G. (2013). Bone Histology and Growth of Chasmosaurine Ceratopsid Dinosaurs from the Late Campanian Kaiparowits Formation, Southern Utah [MSc thesis]. University of Utah, Utah.

Lewicki, P. and Hill, T. (2006). Statistics: Methods and Applications: A Comprehensive Reference for Science, Industry, and Data Mining. StatSoft Inc., Tulsa, OK. IBSN: 1-884233-59-7

Liermann, M., Steel, A., Rosing, M., Guttorp, P. (2004). Random denominators and the analysis of ratio data. Environmental and Ecological Statistics, 11(1), p. 55-71. DOI: 10.1023/B:EEST.0000011364.71236.f8

Longrich, N.R. and Field, D.J. (2012). *Torosaurus* Is Not *Triceratops*: Ontogeny in Chasmosaurine Ceratopsids as a Case Study in Dinosaur Taxonomy. PLoS ONE, 7(2): e32623. DOI: 10.1371/journal.pone.0032623

Lowi-Merri, T.M. and Evans, D.C. (2019). Cranial variation in *Gryposaurus* and biostratigraphy of hadrosaurines (Ornithischia: Hadrosauridae) from the Dinosaur Park Formation of Alberta, Canada. Canadian Journal of Earth Sciences, 0(ja). DOI: 10.1139/cjes-2019-0073

Lucas, S., Sullivan, R., Lichtig, A., Dalman, S., Jasinski, S. (2016). Late Cretaceous dinosaur biogeography and endemism in the Western Interior Basin, North America: A critical re-evaluation. Cretaceous Period Biotic Diversity and

Biogeography, New Mexico Museum of Natural History and Science Bulletin, 71, p. 195-213.

Lull, R.S. and Wright, N.E. (1942). Hadrosaurian Dinosaurs of North America. Geological Society of America special papers, 40.

Ma, W., Brusatte, S. L., Lü, J., Sakamoto, M. (2019). The skull evolution of oviraptorosaurian dinosaurs: the role of niche-partitioning in diversification. Journal of Evolutionary Biology, 33(2), p. 177-188. DOI: 10.1111/jeb.13557

Magnan, P. and FitzGerald, G. (1984). Ontogenetic changes in diel activity, food habits and spatial distribution of juvenile and adult creek chub, *Semotilus atromaculatus*. Environmental Biology of Fishes, 11(4), p. 301-307. DOI: 10.1007/BF00001377

Makowski, D., Ben-Shachar, M., Lüdecke, D. (2019). effectsize:Indices of Effect Size and Standardized Parameters. R package version 0.3.0. URL: https://CRAN.R-project.org/package=effectsize

Maidment, S.C.R., Linton, D.H., Upchurch, P., Barrett, P.M. (2012). Limb-Bone Scaling Indicates Diverse Stance and Gait in Quadrupedal Ornithischian Dinosaurs. PLoS ONE, 7(5), e36904. DOI: 10.1371/journal.pone.0036904 (supplementary information 1)

Mallon, J.C. (2019). Competition structured a Late Cretaceous megaherbivorous dinosaur assemblage. Scientific Reports, 9(15447). DOI: 10.1038/s41598-019-51709-5

Mallon, J.C. and Anderson, J.S. (2013). Skull Ecomorphology of Megaherbivorous Dinosaurs from the Dinosaur Park Formation (Upper Campanian) of Alberta, Canada. PLoS ONE, 8(7). DOI: 10.1371/journal.pone.0067182

Mallon, J.C. and Anderson, J.S. (2014a). Implications of beak morphology for the evolutionary paleoecology of megaherbivorous dinosaurs from the Dinosaur Park Formation (upper Campanian) of Alberta, Canada. Palaeogeography, Palaeoclimatology, Palaeoecology, 394, p. 29-41. DOI: 10.1016/j.palaeo.2013.11.014

Mallon, J.C. and Anderson, J.S. (2014b). The Functional and Palaeoecological Implications of Tooth Morphology and Wear for the Megaherbivorous Dinosaurs from the Dinosaur Park Formation (Upper Campanian) of Alberta, Canada. PLoS ONE, 9(6). DOI: 10.1371/journal.pone.0098605

Mallon, J.C. and Anderson, J.S. (2015). Jaw mechanics and evolutionary paleoecology of the megaherbivorous dinosaurs from the Dinosaur Park Formation (upper Campanian) of Alberta, Canada. Journal of Vertebrate Paleontology, 35(2): e904323. DOI: 10.1080/02724634.2014.904323

Mallon, J.C., Evans, D.C., Ryan, M.J., Anderson, J.S. (2012). Megaherbivorous dinosaur turnover in the Dinosaur Park Formation (upper Campanian) of Alberta, Canada. Paleogeography, Paleoclimatology, Paleoecology, 350-352, p. 124-138.

Mallon, J.C., Evans, D.C., Ryan, M.J., Anderson, J.S. (2013). Feeding height stratification among the herbivorous dinosaurs from the Dinosaur Park Formation (upper Campanian) of Alberta, Canada. BioMed Central: Ecology, 13(14), p. 1-15. DOI: 10.1186/1472-6785-13-14

Mallon, J.C., Evans, D.C., Tokaryk, T. T., Currie, M.L. (2015). First pachycephalosaurid (Dinosauria: Ornithischia) from the Frenchman Formation (upper Maastrichtian)

of Saskatchewan, Canada. Cretaceous Research, 56, p. 426-431. DOI: 10.1016/j.cretres.2015.06.005

Mallon, J.C., Ryan, M.J., Campbell, J.A. (2015). Skull ontogeny in *Arrhinoceratops brachyops* (Ornithischia: Ceratopsidae) and other horned dinosaurs. Zoological Journal of the Linnean Society, 175(4), p. 910-929. DOI: 10.1111/zoj.12294

Mallon, J.C., Ott, C.J., Larson, P.L., Iuliano, E.M., Evans, D.C. (2016). *Spiclypeus shipporum* gen. et sp. nov., a Boldly Audacious New Chasmosaurine Ceratopsid (Dinosauria: Ornithischia) from the Judith River Formation (Upper Cretaceous: Campanian) of Montana, USA. PLoS ONE, 11(5): e0154218. DOI:10.1371/journal.pone.0154218

Martin, R.E. (1999). Taphonomy: A Process Approach. Cambridge University Press, Cambridge, 524 p.

Maryanska, T., Chapman, R.E., Weishampel, D.B. (2004). Pachycephalosauria *in* Weishampel, D.B., Dodson, P., Osmolska, H. (eds.), *The Dinosauria* (2nd ed.), University of California Press, Berkeley and Los Angeles, California, p. 464-477.

Mathews, J.C., Brusatte, S.L., Williams, S.A., Henderson, M.D. (2009). The first *Triceratops* bonebed and its implications for gregarious behavior. Journal of Vertebrate Paleontology, 29(1), p. 286–290. DOI: 10.1080/02724634.2009.10010382

McDonald, A.T. (2011). A Subadult Specimen of *Rubeosaurus ovatus* (Dinosauria: Ceratopsidae), with Observations on Other Ceratopsids from the Two Medicine Formation. PLoS ONE, 6(8), e22710. DOI: 10.1371/journal.pone.0022710

McDonald, J.H. (2014). Multiple comparisons, *in* Handbook of Biological Statistics (3rd ed.). Sparky House Publishing, Baltimore, Maryland, p. 254-260.

McGarrity, C.T., Campione, N.E., Evans, D.C. (2013). Cranial anatomy and variation in *Prosaurolophus maximus* (Dinosauria: Hadrosauridae). Zoological Journal of the Linnean Society, 167, p. 531-568. DOI: 10.1111/zoj.12009.

McLeay, L.J., Page, B., Goldsworthy, S.D., Ward, T.M., Paton, D.C. (2009). Size matters: variation in the diet of chick and adult crested terns. Marine Biology, 156, p. 1765-1780. DOI: 10.1007/s00227-009-1211-4

Mendoza, M., Janis, C., Palmqvist, P. (2002). Characterizing complex craniodental patterns related to feeding behaviour in ungulates: A multivariate approach. Journal of Zoology, 258, p. 223-246.

Mendoza-Carranza, M. and Paes Vieira, J. (2009). Ontogenetic niche feeding partitioning in juvenile of white sea catfish *Genidens barbus* in estuarine environments, southern Brazil. Journal of the Marine Biological Association of the United Kingdom, 89(4), p. 839-848. DOI: 10.1017/S0025315408002403

Metzger, K.A. and Herrel, A. (2005). Correlations between lizard cranial shape and diet: A quantitative, phylogenetically informed analysis. Biological Journal of the Linnean Society, 86(4), p. 433-466. DOI: 10.1111/j.1095-8312.2005.00546.x

Mihlbachler, M.C. and Beatty, B.L. (2012). Effects of variable magnification and imaging resolution on paleodietary interpretations derived from dental microwear analysis. Palaeontologica Electronica, 15(2.25A), p. 1-14.

Mihlbachler, M.C., Beatty, B.L., Caldera-Siu, A., Chan, D., Lee, R. (2012). Error rates and observer bias in dental microwear analysis using light microscopy. Palaeontologica Electronica, 15(1), p. 1-22. DOI: 10.26879/298

Mitchell, D.R., Sherratt, E., Ledogar, J.A., Wroe, S. (2018). The biomechanics of foraging determines face length among kangaroos and their relatives. Proceedings of the Royal Society of Biology, 285: 20180845. DOI: 10.1098/rspb.2018.0845

Moore, J.R. (2012). Do Terrestrial Vertebrate Fossil Assemblages Show Consistent Taphonomic Patterns? Palaios, 27(4), p. 220-234. DOI: 10.2110/Palo.2011.P11-096r

Moore, J.R. and Norman, D.B. (2006). Quantitatively evaluating the sources of taphonomic biasing of skeletal element abundances in fossil assemblages. PALAIOS, 24, p. 591-602. DOI: 10.2110/palo.2008.p08-135r

Moore, J.R., Norman, D.B., Upchurch, P. (2007). Assessing relative abundances in fossil assemblages. Palaeogeography, Palaeoclimatology, Palaeoecology, 253(3-4), p. 317-322. DOI: 10.1016/j.palaeo.2007.06.004

Mordkoff, J.T. (2019). A Simple Method for Removing Bias From a Popular Measure of Standardized Effect Size: Adjusted Partial Eta Squared. Advances in Methods and Practices in Psychological Science: 251524591985505. DOI: 10.1177/2515245919855053

Morris, W.J. (1970). Hadrosaurian Dinosaur Bills – Morphology and Function. Contributions in Science, 193, p. 1-14.

Nakazawa, T. and Yamamura, N. (2007). Breeding migration and population stability. Population Ecology, 49(2), p. 101-113. DOI: 10.1007/s10144-006-0025-1

Nelson, S., Badgley, C., Zaken, E. (2005). Microwear in modern squirrels in relation to diet. Palaeontologica Electronica, 8(3:14A), p.1-15.

Norman, D.B. and Weishampel, D.B. (1985). Ornithopod feeding mechanisms: Their bearing on the evolution of herbivory. The American Naturalist, 126(2), p. 151-164.

Norman, D.B., Sues, H., Witmer, L.M., Coria, R.A. (2004). Basal Ornithopoda *in* Weishampel, D.B., Dodson, P., Osmolska, H. (eds.), *The Dinosauria* (2nd ed.), University of California Press, Berkeley and Los Angeles, California, p. 393-412.

O'Gorman, E. and Hone, D.W.E. (2012). Body Size Distribution of the Dinosaurs. PLoS ONE, 7(12): e51925. DOI: 10.1371/journal.pone.0051925

Oksanen, J., Guillaume Blanchet, F., Friendly, M., Kindt, R., Legendre, P., Dan McGlinn, D., Peter R. Minchin, P.R., O'Hara, R.B., Simpson, G.L., Solymos, P., Stevens, M.H.H., Szoecs, E., Wagner, H. (2019). vegan: Community Ecology Package. R package version 2.5-6. URL: https://CRAN.R-project.org/package=vegan

Ostrom, J.H. (1961). Cranial morphology of the hadrosaurian dinosaurs of North America. Bulletin of the American Museum of Natural History 122(2), p. 39-186.

Ostrom, J.H. (1964). A reconsideration of the paleoecology of hadrosaurian dinosaurs. American Journal of Science, 262(8), p. 975-997. DOI: 10.2475/ajs.262.8.975

Ostrom, J.H. (1966). Functional morphology and evolution of the ceratopsian dinosaurs. Evolution, 20(3), p. 290-308. DOI: 10.1111/j.1558-5646.1966.tb03367.x

Ostrom, J.H. (1978). *Leptoceratops gracilis* from the "Lance" Formation of Wyoming. Journal of Paleontology, 52(3), p. 697-704.

Padian, K., de Ricqles, A.J., Horner, J.R. (2001). Dinosaurian growth rates and bird origins. Nature, 412, p. 405-408. DOI: 10.1038/35086500

Peters, S.E., McClennen, M., Czaplewski, J.J., Heim, N., Jenkins, J., Syverson, V., Zaffos, A. (n.d.) The Paleobiology Database: https://paleobiodb.org/#/ (accessed April 2020).

Peters, R.H. and Wassenberg, K. (1983). The Effect of Body Size on Animal Abundance. Oecologica, 60(1), p. 89-96.

Pizzatto, L., Child, T., Shine, R. (2008). Why be diurnal? Shifts in activity time enable young cane toads to evade cannibalistic conspecifics. Behavioral Ecology, 19(5), p. 990-997. DOI: 10.1093/beheco/arn060

Platt, S.G., Rainwater, T.R., Finger, A.G., Thorbjarnarson, J.B., Anderson, T.A., McMurray, S.T. (2006). Food habits, ontogenetic dietary partitioning and observations of foraging behaviour of Morelet's crocodile (*Crocodylus moreletii*) in Northern Belize. Herpetological Journal, 16, p. 281-290.

Prieto-Márquez, A. (2014). A juvenile *Edmontosaurus* from the late Maastrichtian (Cretaceous) of North America: Implications for ontogeny and phylogenetic inference in saurolophine dinosaurs. Cretaceous Research, 50, p. 282-303. DOI: 10.1016/j.cretres.2014.05.003

Ramirez, M., Avens, L., Seminoff, J., Goshes, L., Hepell, S. (2017). Growth dynamics of juvenile loggerhead sea turtles undergoing an ontogenetic habitat shift. Oecologica, 183, p. 1087-1099. DOI: 10.1007/s00442-017-3832-5

R Core Team. (2019). R: A language and environment for statistical computing. R Foundation for Statistical Computing, Vienna, Austria. URL: https://www.R-project.org/

Reizner, J.A. (2010). An ontogenetic series and population histology of the ceratopsid dinosaur *Einiosaurus procurvicornis* [MSc. Thesis]. Montana State University, Montana.

Reilly, S.M., McBrayer, L.D., White, T.D. (2001). Prey processing in amniotes: Biomechanical and behavioral patterns of food reduction. Comparative Biochemistry and Physiology Part A, 128(3), p. 397-415. DOI: 10.1016/S1095-6433(00)00326-3

Riera, V., Oms, O., Gaete, R., Galobart, À. (2009). The end-Cretaceous dinosaur succession in Europe: The Tremp Basin record (Spain). Palaeogeography, Palaeoclimatology, Palaeoecology, 283(3-4), p. 160-171. DOI: 10.1016/j.palaeo.2009.09.018

Rivals, F. and Semprebon, G.M. (2011). Dietary plasticity in ungulates: Insight from tooth microwear analysis. Quaternary International, 245, p. 279-284. DOI: 10.1016/j.quaint.2010.08.001

Rivera-Sylva, H.E., Barrón-Ortízb, C.I., González, R.L., Rodríguez, R.L., Guzmán-Gutiérreza, J.R., Valdez, F.C., Dávila, C.D. (2019). Preliminary assessment of hadrosaur dental microwear from the Cerro del Pueblo Formation (Upper Cretaceous: Campanian) of Coahuila, northeastern Mexico. Paleontologia Mexicana, 8(1), p. 17-28.

Rogers, R.R. (1990). Taphonomy of Three Dinosaur Bone Beds in the Upper Cretaceous Two Medicine Formation of Northwestern Montana: Evidences for Drought-Related Mortality. Palaios, 5(5), p. 394-413. DOI: 10.2307/3514834

Rogers, R.R. and Kidwell, S.M. (2007). A Conceptual Framework for the Genesis and Analysis of Vertebrate Skeletal Concentrations, *in* Rogers, R.R., Eberth, D.A., Fiorilllo, A.R. (eds.), *Bonebeds: genesis, analysis and paleobiological significance*. University of Chicago Press, Chicago, Illinois, p. 1-65.

Rogers, R. R., Carrano, M. T., Curry Rogers, K. A., Perez, M., Regan, A. K. (2017). Isotaphonomy in concept and practice: an exploration of vertebrate microfossil bonebeds in the Upper Cretaceous (Campanian) Judith River Formation, north-central Montana. Paleobiology, 43(2), p. 248-273. DOI: 10.1017/pab.2016.37

Royal Ontario Museum. (n.d.). Collections database: https://collections.rom.on.ca/?_ga=2.181131809.767554998.1585921844-771259866.1566773244 (accessed April 2020).

Royal Tyrrell Museum of Palaeontology. (2020). Collections database: https://hermis.alberta.ca/rtmp/ (accessed April 2020).

RStudio Team. (2015). RStudio: Integrated Development for R. RStudio, Inc., Boston, MA. URL: http://www.rstudio.com/

Russell, D.A. and Manabe, M. (2002). Synopsis of the Hell Creek (uppermost Cretaceous) dinosaur assemblage, *in* Hartman, J.H., Johnson, K.R., Nichols, D.J. (eds.), *The Hell Creek Formation and the Cretaceous-Tertiary Boundary of the Northern Great Plains: An Integrated Continental Record of the End of the*

Cretaceous, Geological Society of America Special Paper 361, p. 169-176. DOI: 10.1130/0-8137-2361-2.169

Ryan, M.J., Russell, A.P., Eberth, D.A., Currie, P.J. (2001). The Taphonomy of a *Centrosaurus* (Ornithischia: Ceratopsidae) Bone Bed from the Dinosaur Park Formation (Upper Campanian), Alberta, Canada, with Comments on Cranial Ontogeny. PALAIOS, 16(5), p. 482-506. DOI: 10.1669/0883-1351(2001)016<0482:ttoaco>2

Ryan, M.J., Russell, A.P., Hartman, S. (2010). A New Chasmosaurine Ceratopsid from the Judith River Formation, Montana, *in* Ryan, M.J., Chinnery-Allgeier, B.J., Eberth, D.A. (eds.), *New Perspectives on Horned Dinosaurs: The Royal Tyrell Museum Ceratopsian Symposium*. Indiana University Press, Bloomington, Indiana, p. 181-188.

Ryan, M.J., Holmes, R., Mallon, J., Loewen, M., Evans, D.C. (2017). A basal ceratopsid (Centrosaurinae: Nasutoceratopsini) from the Oldman Formation (Campanian) of Alberta, Canada. Canadian Journal of Earth Sciences, 54(1), p. 1-14. DOI: 10.1139/cjes-2016-0110

Rybczynski, N., Tirabasso, A., Bloskie, P., Cuthbertson, R., Holliday, C. (2008). A three-dimensional animation model of *Edmontosaurus* (Hadrosauridae) for testing chewing hypotheses. Palaeontologica Electronica, 11(2:9A), p. 1-14.

Sampson, S.D. (1993). Cranial ornamentations in ceratopsid dinosaurs: Systematic, behavioural, and evolutionary implications. [Unpublished PhD dissertation]. University of Toronto, Ontario.

Sampson, S.D. (1995). Two new horned dinosaurs from the upper Cretaceous Two Medicine Formation of Montana; with a phylogenetic analysis of the Centrosaurinae (Ornithischia: Ceratopsidae). Journal of Vertebrate Paleontology, 15(4), p. 743-760. DOI: 10.1080/02724634.1995.10011259

Sampson, S.D. (1997). Craniofacial ontogeny in the centrosaurine dinosaurs (Ornithischia: Ceratopsidae): taxonomic and behavioural implications. Zoological Journal of the Linnean Society, 121, p. 293-337.

Sampson, S.D. (2009). Dinosaur odyssey: Fossil threads in the web of life. Berkeley, University of California Press, Berkeley and Los Angeles, California, 332 p.

Sander, P.M., Gee, C.T., Hummel, J., Clauss, M. (2010). Mesozoic plants and dinosaur herbivory, *in* Gee, C.T. (ed.), *Plants in Mesozoic time: Morphological innovations, phylogeny, ecosystems*, Indiana University Press, Bloomington, Indiana, p. 331-359.

Schneider, C.A., Rasband, W.S., Eliceiri, K.W. (2012). NIH Image to ImageJ: 25 years of image analysis. Nature methods 9(7), p. 671-675, PMID 22930834.

Schellekens, T., de Roos, A., Persson, L. (2010). Ontogenetic Diet Shifts Result in Niche Partitioning between Two Consumer Species Irrespective of Competitive Abilities. The American Naturalist, 176(3), p. 625-637. DOI: 10.1086/656488

Scherzer, B.A. and Varricchio, D.J. (2010). Taphonomy of a juvenile lambeosaurine bonebed from the Two Medicine Formation (Campanian) of Montana, United States. Palaios, 25(12), p. 780-795. DOI: 10.2110/palo.2009.p09-143r

Scott, E.E. (2015). The first monodominant bonebed from the Oldman Formation (Campanian) of Alberta [MSc. Thesis]. Case Western Reserve University, Ohio.

Semprebon, G.M., Godfrey, L.R., Solounias, N., Sutherland, M.R., Jungers, W.L. (2004). Can low-magnification stereomicroscopy reveal diet? Journal of Human Evolution, 47, p. 115-144. DOI: 10.1016/j.jhevol.2004.06.004

Semprebon, G.M., Sise, P.J., Coombs, M.C. (2010). Potential Bark and Fruit Browsing as Revealed by Stereomicrowear Analysis of the Peculiar Clawed Herbivores Known as Chalicotheres (Perissodactyla, Chalicotherioidea). Journal of Mammalian Evolution, 18(1), p. 33-55. DOI: 10.1007/s10914-010-9149-3

Siemann, E. and Brown, J.H. (1999). Gaps in mammalian body size distributions reexamined. Ecology, 80(8), p. 2788-2792.

Slowiak, J., Tereshchenko, V.S., Fostowicz-Frelik, L. (2019). Appendicular skeleton of *Protoceratops andrewsi* (Dinosauria, Ornithischia): comparative morphology, ontogenetic changes, and the implications of non-ceratopsid ceratopsian locomotion. PeerJ, 7:e7324. DOI: 10.7717/peerj.7324

Smith, F.A. and Lyons, S.K. (2011). How big should a mammal be? A macroecological look at mammalian body size over space and time. Philosophical Transactions of the Royal Society B: Biological Sciences, 366(1576), p. 2364-2378. DOI: 10.1098/rstb.2011.0067

Smith, J.B. and Dodson, P. (2003). A proposal for a standard terminology of anatomical notation and orientation in fossil vertebrate dentitions. Journal of Vertebrate Paleontology, 23(1), p. 1-12. DOI: 10.1671/0272-4634(2003)23[1:APFAST]2.0CO;2

Smithsonian National Museum of Natural History. (n.d.). Paleobiology Collections database: https://collections.nmnh.si.edu/search/paleo/ (accessed April 2020).

Solounias, N. and Semprebon, G. (2002). Advances in the Reconstruction of Ungulate Ecomorphology with Application to Early Fossil Equids. American Museum Noviates, 3366, p. 1-49.

Solounias, N., Teaford, M., Walker, A. (1988). Interpreting the diet of extinct ruminants: the case of a non-browsing giraffid. Paleobiology, 14(3), p. 287-300.

Soons, J., Herrel, A., Genbrugge, A., Aerts, P., Podos, J., Adriaens, D., de Witte, Y., Jacobs, P., Dirckx, J. (2010). Mechanical stress, fracture risk and beak evolution in Darwin's ground finches (*Geospiza*). Philosophical Transactions of the Royal Society B., 365, p. 1093-1098. DOI: 10.1098/rstb.2009.0280

Spencer, L.M. (1995). Morphological Correlates of Dietary Resource Partitioning in the African Bovidae. Journal of Mammalogy, 76(2), p.448-471.

Stacklies, W., Redestig, H., Scholz, M., Walther, D., Selbig, J. (2007). pcaMethods – a Bioconductor package providing PCA methods for incomplete data. Bioinformatics, 23, p. 1164-1167. R package version 1.80.0.

Sternberg, C.H. (1917). Hunting Horned Dinosaurs *in* Sternberg, C. H. (ed.), *Hunting Dinosaurs in the Badlands of the Red Deer River Alberta, Canada: A Sequel to the Life of a Fossil Hunter*, The World Company Press, Lawrence, Kansas, p. 78-89. https://archive.org/details/huntingdinosaurs00steruoft

Strauss, R.E., Atanassov, N.M.N., Alves, J. (2003). Evaluation of the principal-component and expectation-maximization methods for estimating missing data in morphometric studies. Journal of Vertebrate Paleontology, 23, p. 284-296. DOI: 10.1671/0272-4634(2003)023[0284:EOTPAE]2.0.CO;2

Strickson, E., Prieto-Márquez, A., Benton, M.J., Stubbs, T.L. (2016). Dynamics of dental evolution in ornithopod dinosaurs. Scientific Reports, 6: 28904. DOI: 10.1038/srep28904

Sullivan, R. (2006). A taxonomic review of the Pachycephalosauridae (Dinosauria: Ornithischia) *in* Lucas, S.G. and Sullivan, R.M. (eds), *Late Cretaceous vertebrates from the Western Interior, New Mexico*, Museum of Natural History and Science Bulletin volume 35, New Mexico, p. 345-366.

Tanke, D.H. and Brett-Surman, M.K. (2001). Evidence of Hatchling and Nestling-Size Hadrosaurs (Reptilia: Ornithischia) from Dinosaur Provincial Park (Dinosaur Park Formation: Campanian), Alberta *in* Tanke, D.H., Carpenter, K. and Skrepnick, M.W. (eds.) *Mesozoic Vertebrate Life*, Indiana University Press, Bloomington, Indiana, p. 206-218.

Teaford, M.F. (2007). What Do We Know and Not Know about Dental Microwear and Diet?, *in* Ungar, P.S. (ed.), *Evolution of the Human Diet: The Known, the Unknown, and the Unknowable*, Oxford University Press Inc., New York, New York, p. 106-149.

Trachsel, J. (2019). funfuns: Functions I Use (Title Case). R package version 0.1.1. URL: https://github.com/Jtrachsel/funfuns/

Trexler, D.L. (1995). A Detailed Description of Newly-Discovered Remains of *Maiasaura peeblesorum* (Reptilia: Ornithischia) and a Revised Diagnosis of the Genus. [Ph.D. thesis]: University of Calgary, Alberta.

Tumarkin-Deratzian, A.R. (2009). Evaluation of Long Bone Surface Textures as Ontogenetic Indicators in Centrosaurine Ceratopsids. The Anatomical Record:

Advances in Integrative Anatomy and Evolutionary Biology, 292(9), p. 1485-1500. DOI: 10.1002/ar.20972

VanBuren, C.S., Campione, N.E., Evans, D.C. (2015). Head size, weaponry, and cervical adaptation: Testing craniocervical evolutionary hypotheses in Ceratopsia. Evolution, 69(7), p. 1728-1744. DOI: 10.1111/evo.12693

van der Meij, M.A.A. and Bout, R.G. (2008). The relationship between shape of the skull and bite force in finches. Journal of Experimental Biology, 211, p. 1668-1680. DOI: 10.1242/jeb.015289

Vanderveen, E., Burns, M.E., Currie, P.J. (2014). Histologic growth dynamic study of *Edmontosaurus regalis* (Dinosauria: Hadrosauridae) from a bonebed assemblage of the Upper Cretaceous Horseshoe Canyon Formation, Edmonton, Alberta, Canada. Canadian Journal of Earth Sciences, 51, p. 1023-1033. DOI: 10.1139/cjes-2014-0064

Varricchio, D.J. (2001). Gut contents from a Cretaceous Tyrannosaurid: Implications for theropod dinosaur digestive tracts. Journal of Paleontology, 75(2), p. 401-406. DOI: 10.1017/s0022336000018199

Varricchio, D.J. (2011). A distinct dinosaur life history? Historical Biology 23 (1), p. 91-107. DOI: 10.1080/08912963.2010.500379

Varricchio, D.J. and Horner, J.R. (1993). Hadrosaurid and lambeosaurid bone beds from the Upper Cretaceous Two Medicine Formation of Montana: taphonomic and biologic implications. Canadian Journal of Earth Sciences, 30(5), p. 997-1006. DOI: 10.1139/e93-083

Varriale, F.J. (2011). Dental microwear and the evolution of mastication in the ceratopsian dinosaurs. [Unpublished PhD dissertation]. Johns Hopkins University, Maryland, 470 p.

Vickaryous, M.K., Maryanska, T., Weishampel, D.B. (2004). Ankylosauria *in* Weishampel, D.B., Dodson, P., Osmolska, H. (eds.), *The Dinosauria* (2nd ed.), University of California Press, Berkeley and Los Angeles, California, p. 363-392.

Walker, A., Hoeck, H.N., Perez, L. (1978). Microwear of Mammalian Teeth as an indicator of Diet. Science, 201(4359), p. 908-910. DOI: 10.1126/science.684415

Wang, S., Stiegler, J., Amiot, R., Wang, X., Du, G., Clark, J.M., Xu, X. (2017). Extreme Ontogenetic Changes in a Ceratosaurian Theropod. Current Biology, 27(1), p. 144-148. DOI: 10.1016/j.cub.2016.10.043

Warton, D.I., Duursma, R.A., Falster, D.S., Taskinen, S. (2012). smatr: (Standardised) Major Axis Estimation and Testing Routines. R package version 3.4-8. URL: https://CRAN.R-project.org/package=smatr

Warton, D.I., Wright, I.J., Falster, D.S., Westoby, M. (2006). Bivariate line-fitting methods for allometry. Biological Reviews, 81(2), p. 259-291. DOI: 10.1017/S1464793106007007

Weishampel, D.B. (1983). Hadrosaurid jaw mechanics. Palaeontologica Electronica Pol, 28, p. 271-280.

Weishampel, D.B. (1984). Evolution of jaw mechanics in ornithopod dinosaurs. Advances in Anatomy Embryology Cell Biology, 87, p. 1-109.

Weishampel, D.B., Norman, D.B., Grigorescu, D. (1993). *Telmatosaurus transsylvanicus* from the Late Cretaceous of Romanian: the most basal hadrosaurid dinosaur. Palaeontology, 236(2), p. 361-385.

Werner, E.E. and Gilliam J.F. (1984). The Ontogenetic Niche and Species Interactions in size-Structured Populations. Annual Review of Ecology and Systematics, 15, p. 393-425. DOI: 10.2307/2096954

Wheeler, P.E. (1978). Elaborate CNS cooling structures in large dinosaurs. Nature, 275(5679), p. 441-443. DOI: 10.1038/275441a0

White, P.D., Fastovsky, D.E., Sheehan, P.M. (1998). Taphonomy and Suggested Structure of the Dinosaurian Assemblage of the Hell Creek Formation (Maastrichtian), Eastern Montana and Western North Dakota. PALAIOS, 13(1), p. 41-51. DOI:10.2307/3515280

Wickham, H. (2011). plyr: Tools for Splitting, Applying and Combining Data. R package version 1.8.6. URL: https://CRAN.R-project.org/package=plyr

Wickham, H., François, R., Henry, L., Müller, K. (2018). dplyr: A Grammar of Data Manipulation. R package version 0.7.6. URL: https://CRAN.R-project.org/package=dplyr

Wickham, H. (2016). ggplot2: Elegant Graphics for Data Analysis. R package version 3.3.0. URL: https://CRAN.R-project.org/package=ggplot2

Williams, V.S., Barrett, P.M., Purnell, M.A. (2008). Quantitative analysis of dental microwear in hadrosaurid dinosaurs, and the implications for hypotheses of jaw mechanics and feeding. PNAS, 106(27), p. 11194-11199. DOI: 10.1073/pnas.0812631106

Williamson, T.E. and Carr, T.D. (2006). First record of a pachycephalosaurine (Ornithischia: Pachycephalosauria) from then Dinosaur Park Formation, Alberta, Canada, *in* Lucas, S.G. and Sullivan, R.M. (eds), *Late Cretaceous Vertebrates from the Western Interior*, New Mexico Museum of Natural History and Science, 35, p. 323-328.

Wilson, P.K., and Moore, J.R. (2016). Assessing the Control of Preservational Environment on Taphonomic and Ecological Patterns in an Oligocene Mammal Fauna from Badlands National Park, South Dakota. PLoS ONE, 11)(6): e0157585. DOI: 10.1371/journal.pone.0157585

Whitlock, J. (2011). Inferences of Diplodocoid (Sauropoda: Dinosauria) Feeding Behaviour from Snout Shape and Microwear Analyses. PLoS ONE 6(4): e18304. DOI: 10.1371/journal.pone.0018304

Witmer, L.M. (1995). The extant phylogenetic bracket and the importance of reconstructing soft tissues in fossils, *in* Thomason, J. (ed.), *Functional morphology in vertebrate paleontology*, Cambridge University Press, New York, New York, p. 19-33.

Woodruff, D.C., Carr, T.D., Storrs, G.W., Waskow, K., Scannella, J.B., Norden, K.K., Wilson, J.P. (2018). Smallest Diplodocid Skull Reveals Cranial Ontogeny and Growth-Related Dietary Changes in the Largest Dinosaurs. Scientific Reports, 8: 14341. DOI: 10.1038/s41598-018-32620-x

Woodward, H.N., Freedman Fowler, E.A., Farlow, J.O., Horner, J.R. (2015). *Maiasaura*, a model organism for extinct vertebrate population biology: a large sample

statistical assessment of growth dynamics and survivorship. Paleobiology, 41(4), p. 503-527. DOI: 10.1017/pab/2015.19

Wolfe, D.G. and Kirklans, J.I. (1998). *Zuniceratops christopheri* n. gen. and n. sp., a ceratopsian dinosaur from the Moreno Hill Formation (Cretaceous, Turonian) of west-central New Mexico, *in* Lucas, S.G., Kirkland, J.I., Estep, J.W. (eds.), *Low and Middle Cretaceous Terrestrial Ecosystems*, New Mexico Museum of Natural History and Science Bulletin 14, p. 303-318.

Woolley, L.A., Page, B., Slotow, R. (2011). Foraging Strategy within African Elephant Family Units: Why Body Size Matters. Biotropica, 43(4), p. 489-495. DOI: 10.1111/j.1744-7429.2010.00733.x

Wosik, M., Goodwin, M.B., Evans, D.C. (2018). A nestling-sized skeleton of *Edmontosaurus* (Ornithischia, Hadrosauridae) from the Hell Creek Formation of northeastern Montana, USA, with an analysis of ontogenetic limb allometry. Journal of Vertebrate Paleontology, 37(6), e1398168.

Xu, X. Makovicky, P.J., Wang, X., Norell, M.A., You, H. (2002). A ceratopsian dinosaur from China and the early evolution of Ceratopsia. Nature, 416(6878), p. 314-317. DOI: 10.1038/416314a

Xu, X., Wang, K., Zhao, X., Li, D. (2010). First Ceratopsid dinosaur from China and its biogeographical implications. Chinese Science Bulletin, 55(16), p. 1631-1635.

Xu, X., Zhou, Z., Sullivan, C., Wang, Y., Ren, D. (2016). An Updated Review of the Middle-Late Jurassic Yanliao Biota: Chronology, Taphonomy, Paleontology and Paleoecology. Acta Geologica Sinica - English Edition, 90(6), p. 2229-2243. DOI: 10.1111/1755-6724.13033

Yale Peabody Museum of Natural History. (2020). Collections database: https://peabody.yale.edu/collections (accessed April 2020).

You, H. and Dodson, P. (2004). Basal Ceratopsia *in* Weishampel, D.B., Dodson, P., Osmolska, H. (eds.), *The Dinosauria* (2nd ed.), University of California Press, Berkeley and Los Angeles, California, p. 478-493.

Zanno, L.E. and Makovicky, P.J. (2013). No evidence for directional evolution of body mass in herbivorous theropod dinosaurs. Proceedings of the Royal Society B, 280: 20122526. DOI: 10.1098/rspb.2012.2526

Zhang, Z. and Mai, Y. (2018). WebPower: Basic and Advanced Statistical Power Analysis. R package version 0.5.2. URL: https://CRAN.R-project.org/package=WebPower